

# **Investigation of the functional diversity of the low-molecular-weight metal species in plants**

Zur Erlangung des akademischen Grades eines

**Dr.rer.nat**

vom Fachbereich Bio- und Chemieingenieurwesen der Universität  
Dortmund  
genehmigte Dissertation

vorgelegt von

**M.Sc.Chem. Yue Xuan**

aus

ShenYang, China

Tag der mündlichen Prüfung: 30. July, 2007

1. Gutachter: PD. Dr. Jörg Ingo Baumbach

2. Gutachter: Prof. Dr. Michael Spiteller

**Dortmund 2007**

## Abstract

---

To fully understand the metal transportation and translocation system via phyto siderophores (PS) in plants, analytical tools for accurate identification and simultaneous and sensitive detection of low-molecular-weight (LMW) metal-species and their free ligands in plants are highly required.

In this PhD thesis, new methods based on capillary electrophoresis (CE) and zwitterionic hydrophilic interaction chromatography coupled to electrospray ionization mass spectrometry (ZIC-HILIC/ESI-MS) were developed to fill up the lack of analytical approaches.

A CE method (UV- and conductivity detector) was developed to separate and detect free ligands and their respective metal-complexes. For the first time, a baseline separation of PS was achieved. In addition, separation of ferric-PS-species without stability problems was realized. The CE method was applied to wheat and Arabidopsis plants and allows the characterization of changes of metal-species in a semi-quantitative way down to the  $\mu\text{mol}$ -level. To enhance detection sensitivity a new on-column photo reactor with an adjustable irradiation window was constructed. In particular, a sensitivity increase of a factor up to 6 (UV detector) and 4 (conductivity detector) was obtained for the iron-species in capillary flow injection (cFIA).

In addition, a more sensitive detection and unequivocal identification of LMW free ligands and metal-species was achieved by ZIC-HILIC/ESI-MS. The different metal-complexes and the same free ligands are baseline separated. Even when the signals are overlapping a confident identification was realized by ZIC-HILIC/ESI-MS. This was demonstrated for wheat and Arabidopsis plants.

Finally, metabolic profiling in plants was realized by coupling the separation unit to a Fourier transform ion cyclotron resonance-mass spectrometer (ESI-FTICR-MS). Here, metabolites down to the low micro molar concentration range were determined with peak intensity reproducibility better 5 %. The applicability to real plant samples was demonstrated by the analysis of a complete set of Tobacco plants.

Für ein umfassendes Verständnis der Metalltransport- und Metallverteilungsprozesse im Rahmen des Phytosiderophor (PS)-vermittelten Aufnahmesystems in Pflanzen ist die Entwicklung analytischer Methoden zur sicheren Identifizierung und empfindlichen Detektion von niedermolekularen Metallspezies und der entsprechenden freien Liganden unumgänglich.

Im Rahmen dieser Doktorarbeit wurden deshalb neue methodische Ansätze entwickelt, einerseits auf Basis der Kapillarelektrophorese (CE), andererseits auf Basis der zwitterionischen hydrophilen Wechselwirkungs-Chromatographie mit Detektion durch Elektrospray- Ionisations Massenspektrometrie (ZIC-HILIC/ESI-MS).

Die neu entwickelte CE-Methode (mit UV- und konduktometrischer Detektion) erlaubt erstmals die Basislinientrennung mehrerer PS und entsprechender Metallkomplexe. Zusätzlich ist die Trennung mehrerer Fe(III)-PS-Spezies ohne Stabilitätsprobleme möglich. Die Anwendbarkeit der CE-Methode wurde für Weizen und Arabidopsis-Pflanzenproben gezeigt. Dabei konnten Änderungen von Metallspezies in semi-quantitativer Weise bis in den mikromolaren Konzentrationsbereich verfolgt werden. Zur Steigerung der Detektionsempfindlichkeit wurde ein neuer, in der Trennkapillare integrierter Photoreaktor mit verstellbarem Detektionsfenster konzipiert und konstruiert. Damit konnte die Empfindlichkeit für Eisenspezies in der Kapillar-Fließinjektionsanalyse (cFIA) bis zu einem Faktor von 6 für die UV-Detektion, und bis zu einem Faktor von 4 für die Leitfähigkeitsdetektion gesteigert werden.

Eine noch nachweisstärkere Detektion mit der zusätzlichen Möglichkeit einer eindeutigen Identifizierung der getrennten Substanzen wurde durch die ZIC-HILIC/ESI-MS Methode erreicht. Die meisten Liganden und Metallkomplexe weisen hierbei eine Basislinientrennung auf, aber auch bei Signalüberlappungen ist die Identifizierung durch MS problemlos möglich. Auch dies wurde an Weizen- und Arabidopsisproben gezeigt.

Schließlich wurde durch Kopplung der Trennung mit einem Fourier-Transform Ionen-Cyclotron-Resonanz-Massenspektrometer (ESI-FTICR-MS) die Möglichkeit des „Metabolic Profiling“ in Pflanzen demonstriert. Es konnten Metaboliten bis in den unteren mikromolaren Konzentrationsbereich mit einer Reproduzierbarkeit besser als 5% bestimmt werden (bezogen auf Peakintensitäten). Die Anwendbarkeit auf reale Problemstellungen wurde an einem kompletten Probensatz von Tabakpflanzen gezeigt.

**Contents**

<b>1</b>	<b>Introduction</b>	<b>1</b>
1.1	Iron acquisition and translocation in plants	1
1.2	Analytical methods for detection and identification of small metal-species in plants	6
1.3	Objective of this work	7
<b>2</b>	<b>Capillary Electrophoresis (CE) with Diode Array Detector (DAD) and Capacitively Coupled Contactless Conductivity Detector (C<sup>4</sup>D)</b>	<b>8</b>
2.1	Capillary Electrophoresis	8
2.1.1	Principle of Capillary Electrophoresis	8
2.1.2	Modes of Operation	9
2.2	Capacitively Coupled Contactless Conductivity Detector (C <sup>4</sup> D)	12
2.3	Experimental	15
2.3.1	Instrumental	15
2.3.2	Solutions and Chemicals	16
2.3.3	PS, metal-PS, and Plant samples	16
2.4	Results and Discussion	18
2.4.1	Investigating of free ligands	18
2.4.2	Investigating of metal-ligands	22
2.4.3	Investigating of plant samples	29
2.4.4	Isomers separation by zwitterionic nonaqueous capillary electrophoresis (ZIC-NACE)	33
2.5	Conclusion	37
<b>3</b>	<b>Development and application of photo reactors for CE</b>	<b>39</b>
3.1	Theory of photo reactors in CE and HPLC	39
3.1.1	Commercially available reactors for HPLC	39
3.1.2	Existing photo reactors for CE	40
3.1.3	Suitability of a photo reactor for detection of metal-species	40
3.2	Experimental	42
3.2.1	Reagents, model complexes, and real plant extracts	42
3.2.2	HPLC with post-column photo reactor system	42
3.2.3	Capillary electrophoresis system	42
3.2.4	On-column CE photochemical reactor	43
3.3	Results and Discussion	44
3.3.1	HPLC Flow Injection (FIA) with online photo reactor	44
3.3.2	HPLC with post-column photo derivatization	45
3.3.3	Capillary Flow Injection (cFIA) with online photo reactor	46
3.3.4	Capillary Electrophoresis with on-column photo reactor	48
3.3.4.1	Investigation of model iron-species	48
3.3.4.2	Investigation of the relationship of the irradiation time and sensitivity	50
3.3.4.3	Application of analysis of real plant extracts	51
3.4	Conclusion	52

<b>4 High Performance Liquid Chromatography coupled to Mass Spectrometry</b> .....	<b>54</b>
4.1 High Performance Liquid Chromatography .....	54
4.1.1 Ion pair-Reversed Phase Liquid Chromatography (IP-RPLC) .....	55
4.1.2 Zwitterionic Hydrophilic Interaction Liquid Chromatography (ZIC-HILIC) .....	56
4.1.3 Zwitterionic 2-methacryloyloxyethyl phosphorylcholine hydrophilic interaction Liquid Chromatography (ZIC-MPC) .....	57
4.2 Mass Spectrometry (MS) .....	57
4.2.1 Methods of sample ionization .....	58
4.2.2 Mass Analyzer .....	58
4.2.3 Detector .....	60
4.3 Experimental .....	61
4.3.1 LC/ESI-MS for method development and optimization .....	61
4.3.1.1 LC/ESI-MS system .....	61
4.3.1.2 HPLC conditions .....	61
4.3.1.3 ESI-MS conditions .....	61
4.3.2 Plant metabolic profiling by ZIC-HILIC/ESI-FTICR-MS .....	62
4.3.2.1 LC/ESI-FTICR-MS system .....	62
4.3.2.2 HPLC conditions .....	62
4.3.2.3 ESI-FTICR MS conditions.....	62
4.3.3 Chemicals and solvents .....	63
4.3.4 PS, metal-PS standards, and Plant samples .....	63
4.3.5 Sample preparation for MS .....	63
4.4 Results and Discussion .....	64
4.4.1 Sample preparation .....	64
4.4.2 Ion-pair-Reversed phase LC (IP-RPLC) .....	67
4.4.2.1 Investigating of low-molecular-weight compounds.....	68
4.4.2.2 Investigating of plant sample.....	69
4.4.3 ZIC-HILIC/ESI-MS.....	71
4.4.3.1 Investigating of free ligands .....	73
4.4.3.2 investigating of metal-ligand complexes .....	74
4.4.3.3 Detection and identification of low-molecular-weight species in plants with on-line ESI-MS .....	75
4.4.3.4 Target analyses of important low-molecular-weight . in plant samples .....	76
4.4.3.5 Investigating of the stability of metal-ligand complexes during the separation .....	79
4.4.4 ZIC-MPC & ZIC-HILIC .....	81
4.4.4.1 Stability of ferric phytosiderophores .....	81
4.4.4.2 Comparison of the separation behavior of ZIC-MPC and ZIC-HILIC .....	82
4.4.5 Plant metabolic profiling .....	85
4.4.5.1 Metabolic profiling method .....	86
4.4.5.2 Identification of metabolites .....	90

4.4.5.3	Correlation analysis.....	98
4.5	Conclusion .....	100
<b>5</b>	<b>Conclusion and Outlook .....</b>	<b>102</b>
<b>6</b>	<b>References .....</b>	<b>105</b>
<b>7</b>	<b>Index of Abbreviations.....</b>	<b>120</b>
	<b>Appendix .....</b>	<b>i</b>
	<b>Lebenslauf.....</b>	<b>iii</b>
	<b>Acknowledgements.....</b>	<b>iv</b>

## 1 Introduction

Metals are well-known micronutrient elements for a plant's growth and survival. Copper (Cu), iron (Fe), manganese (Mn), and zinc (Zn), which come from the soil, are dissolved in water and absorbed through a plant's roots. The main function of these trace metals is the promotion of growth hormones, photosynthesis, cell development, plant metabolism, and nitrogen assimilation. These micronutrient elements occur constantly in living tissues in a small amount (varying from  $1 \times 10^{-6}$  M to less than  $1 \times 10^{-12}$  M wet wt in organ) [1]. In general, most plants grow by absorbing nutrients from the soil. Their ability to do this depends on the nature of the soil. Depending on its location, a soil contains some combination of sand, silt, clay, and organic matter. The makeup of a soil (soil texture) and its acidity (pH) determine the extent to which nutrients are available to plants. There are not always enough of these trace elements in the soil for a plant to grow healthy. For example, plants demand about  $10^{-4}$  -  $10^{-8}$  M  $\text{Fe}^{\text{III}}$  ions for normal growth, but, theoretically, only  $10^{-17}$  M are soluble at pH 7. Uptake of iron from alkaline soils is limited by the low availability of iron in the soil [2] and often results in iron deficiency, impaired growth and failure to produce seed for many crop species. Lime-induced chlorosis in calcareous soil (high pH), therefore, is a major agricultural problem resulting in reduced crop yield, because about 30 % of the world's cultivated soils are calcareous. There are similarities between mammals and plants in the absorption and transport of trace elements. The chemistry of trace element uptake from food sources in both cases is based on the thermodynamics of adsorption on charged solid surfaces embedded in a solution phase of charged ions and metal-binding ligands together with redox systems in the case of iron and some other elements. What is known about the uptake, transport and loading of the other transition elements is often analogous to iron [3]. In addition, iron deficiency is extremely widespread in humans and is also common in some farm animals. Therefore, the metal acquisition and translocation in plants systems are introduced here by taking iron as a representative example. For iron acquisition, plants adopt two strategies (termed I and II).

### 1.1 Iron acquisition and translocation in plants

**Strategy I** is an iron acquisition mechanism used by all higher plants except graminaceous monocots. Plant species show one or more of the following adaptive components. i) an iron deficiency induced enhancement of  $\text{Fe}^{3+}$  reduction to  $\text{Fe}^{2+}$  at the root surface, with preferential uptake of  $\text{Fe}^{2+}$  [4], ii)  $\text{H}^+$  extrusion, which promotes the reduction of  $\text{Fe}^{3+}$  to  $\text{Fe}^{2+}$  [5], iii) in certain cases the release of reducing and/or chelating substances by the roots [6]. This mechanism is described in Fig. 1-1. The most typical feature of strategy I is enhancement of  $\text{Fe}^{3+}$  reduction under iron-deficiency. Net  $\text{Fe}^{3+}$  reduction is strongly impaired at high pH due to inhibition of reductases and autoxidation of  $\text{Fe}^{2+}$ . As a consequence, plant species exhibiting strategy I often display chlorosis symptoms when grown on alkaline (calcareous) soils, especially at high  $\text{HCO}_3^-$  concentrations and corresponding strong pH-buffering capacities. The efficiency of this strategy depends on the supply of soluble iron (mainly iron chelates) to the reductase system.

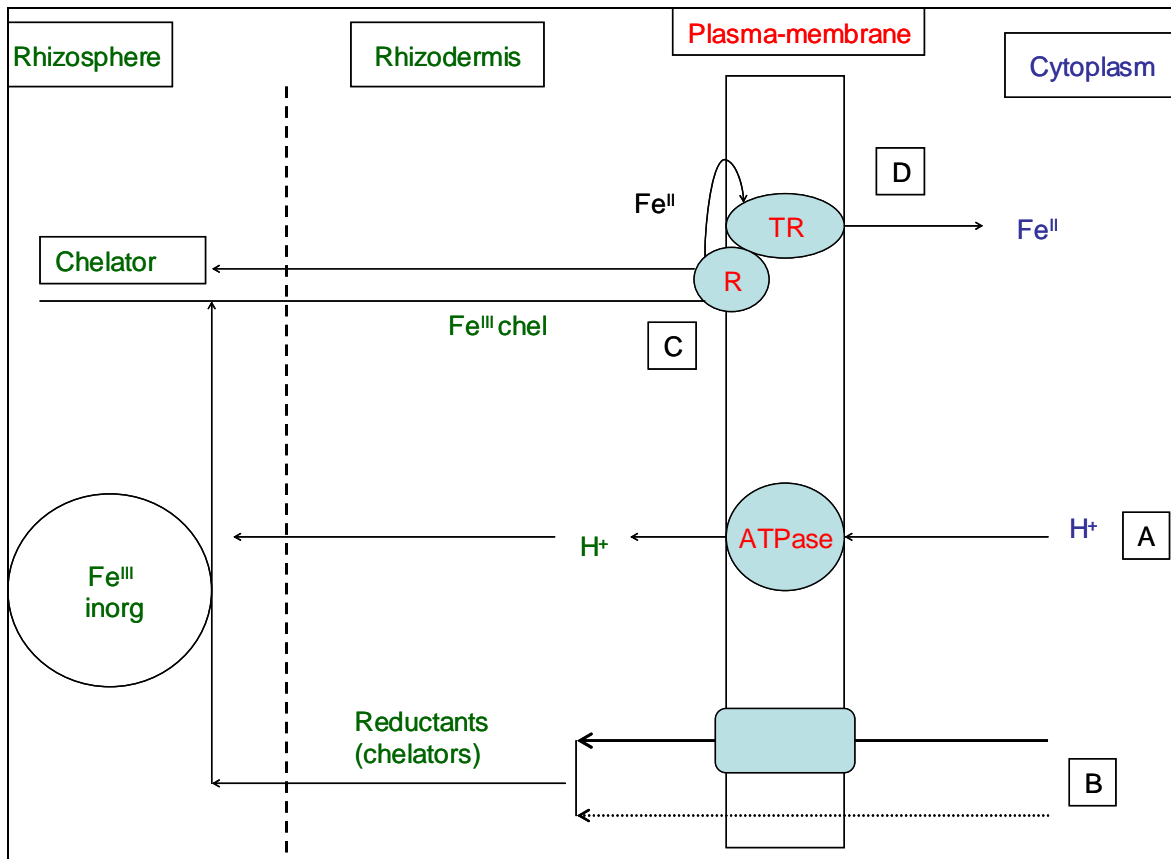


Figure 1-1. Model for iron (Fe) deficiency-induced changes in root physiology and rhizosphere chemistry associated with Fe acquisition in strategy I plants [7].

- A Stimulation of proton extrusion by enhanced activity of the plasmalemma ATPase Fe<sup>III</sup> solubilization in the rhizosphere.
- B Enhanced exudation of reductants and chelators (carboxylates, phenolics) mediated by diffusion or anion channels Fe solubilization by Fe<sup>III</sup> complexation and Fe<sup>III</sup> reduction.
- C Enhanced activity of plasma membrane (PM)-bound Fe<sup>III</sup> reductase further stimulated by rhizosphere acidification (A). Reduction (R) of Fe<sup>III</sup> chelates, liberation of Fe<sup>II</sup>.
- D Uptake of Fe<sup>II</sup> by a PM-bound Fe<sup>II</sup> transporter (TR).

**Strategy II** systems are characterized by synthesis of phytosiderophores (PS), which are hexadentate chelators with a high affinity for complexing Fe<sup>III</sup> and divalent metal ions [8]. Graminaceous monocots release these Fe-chelating substances, PS, in response to Fe-deficiency stress. These PS solubilize inorganic Fe<sup>III</sup>-compounds by chelation, and the Fe<sup>III</sup>-PS complexes are taken up through a specific transport system in the root plasma membrane proteins (Fig. 1-2). PS are capable to form stable chelates with Fe<sup>3+</sup> even at soil pH > 7. PS can also mediate the extraction of considerable amounts of Zn, Mn, Cu [9] and even Cd and Ni [10, 11] in calcareous soils, but there is only minimal competition by chelation with major soil cations such as Ca<sup>2+</sup>, Mg<sup>2+</sup>, and Al<sup>3+</sup> [12].



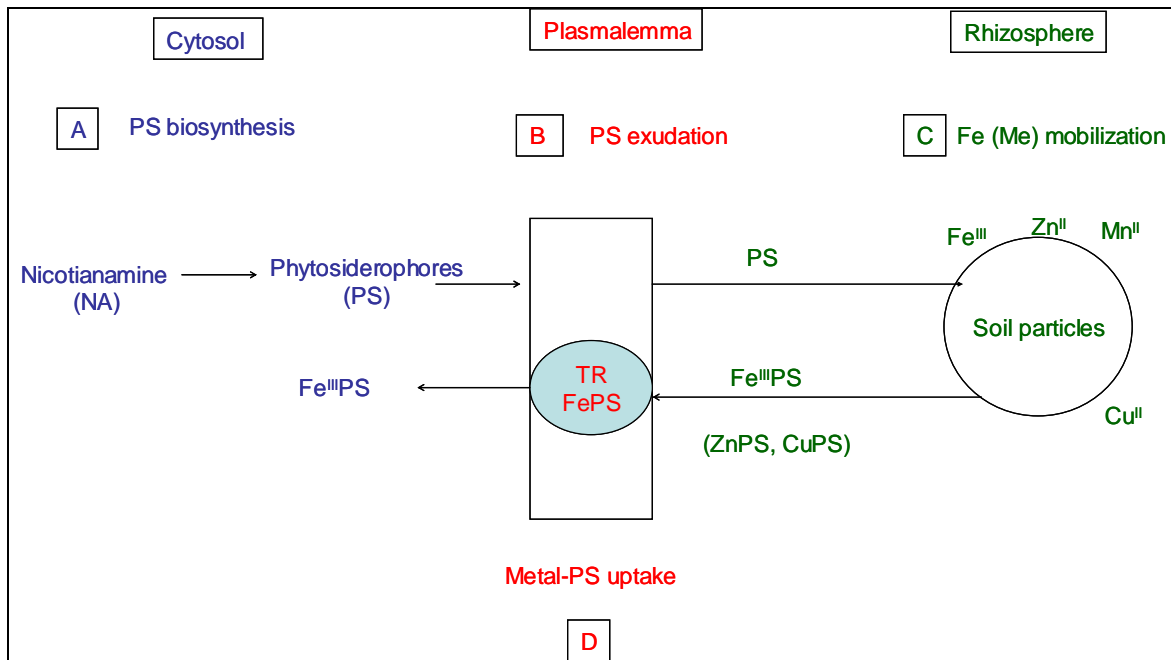


Figure 1-2. Model for root-induced mobilization of iron and other micronutrients (Zn, Mn, Cu) in the rhizosphere of graminaceous (strategy II) plants (modified after Marschner, 1995). Enhanced biosynthesis of mugineic acids (phytosiderophores, PS) in the root tissue [7].

- A Biosynthesis of PS
- B Exudation of PS anions by vesicle transport or via anion channels, charge-balanced by concomitant release of  $K^+$ .
- C PS-induced mobilization of  $Fe^{III}$  ( $Mn^{II}$ ,  $Zn^{II}$ ,  $Cu^{II}$ ) in the rhizosphere by ligand exchange.
- D Uptake of Metal-PS complexes by specific transporters (TR) in the plasma membrane.

Phytosiderophores are derived from nicotianamine (NA), which is ubiquitous in higher plants with putative functions in regulating the physiological availability of Fe and/or transport of copper and other micronutrients in the xylem [13,14]. Nicotianamine is synthesised from L-methionine via trimerization of S-adenosyl-methionine in a reaction sequence similar to ethylene biosynthesis (Yang cycle) with continuous recycling of L-methionine [15]. In graminaceous plants, PS formation proceeds by transamination and hydroxylation of nicotianamine to deoxymugineic acid (DMA). DMA is either released as PS into the rhizosphere or is converted to higher hydroxylated PS derivatives such as mugineic acid (MA), hydroxymugineic acid (HMA), 3-*epi*-hydroxymugineic acid (*epi*-HMA), distichonic acid A and avenic acid A, which were identified as PS in barely, rye and oat [16-20]. Altogether, all PS share the pathway from L-Met to DMA, although subsequent steps differ and are dependent on the plant species and cultivars. These biosynthesis pathways of nicotianamine and phytosiderophores are shown in Fig. 1-3.

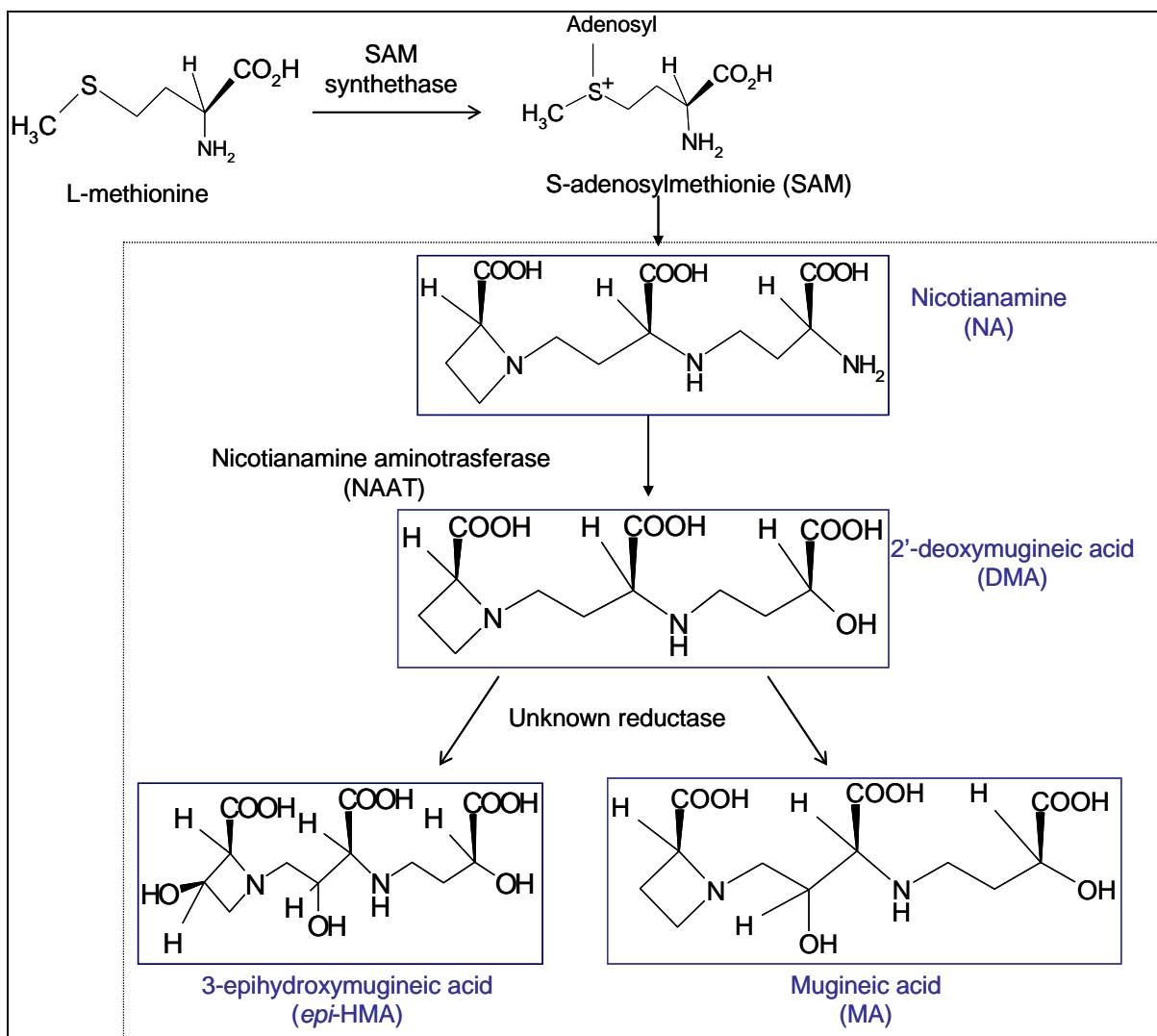


Figure 1-3. Biosynthetic pathways of mugineic acid family phytosiderophores [21].

Structurally, phytosiderophores and nicotianamine, which are non-proteinaceous amino acids, are hexadentate ligands that coordinate metal with their amino and carboxyl groups [22]. The formed metal species are low-molecular-weight (LMW) and non-covalent binding compounds, which exist only in micro molar concentration range in plants. Both nicotianamine and phytosiderophores have optimal molecular structures for complex formation with metal ions. Not only are six functional groups presents, necessary for octahedral coordination, but the distances between the groups are optimal for the formation of three 5-membered and two 6-membered chelate rings [23, 24]. The model of the  $\text{Fe}^{\text{III}}$ -MA complex is shown in Fig. 1-4.

After entering the cytosol, the behaviour of  $\text{PS-Me}^{\text{I/III}}$  ( $\text{Me}^{\text{I/III}} = \text{Ni}, \text{Cu}, \text{Zn}, \text{Fe}^{\text{II}}, \text{and Fe}^{\text{III}}$ ) complexes is still unknown, but the reduction potential suggests that Fe liberation is possible via reduction by common physiologically available reductants such as NAD(P)H, glutathione, and ascorbic acid [12]. NA chelates  $\text{Fe}^{\text{III}}$ ,  $\text{Zn}^{\text{II}}$ ,  $\text{Cu}^{\text{II}}$ , and as well  $\text{Fe}^{\text{II}}$ . The occurrence of phytosiderophores and NA in graminaceous plant species thus raises the question whether  $\text{Fe}^{\text{III}}$  undergoes a chelate exchange from phytosiderophores to NA, as proposed by von Wirén *et al.* [25]. In addition to PS and NA, many organic acids (e.g. citric acid, maleic acid, and malic acid) and amino acids (e.g. histidine) present in plants are also involved in the mechanism of metal-uptake and/or translocation [26-33]. It has already been proven that histidine is involved both in the mechanism of nickel tolerance and in the high rates of nickel transport into the

xylem required for hyperaccumulation in the shoot [26], as well citrate and histidine are the principal ligands for Cu, Ni and Zn [27]. The different levels of low-molecular-weight organic acids (oxalic, fumaric, succinic, L-malic, tartaric, citric, acetic, propionic, and butyric acids) present in the rhizosphere soil played an important role in the solubilization of particulate-bound cadmium into soil solution and its subsequent phytoaccumulation by high and low Cd accumulating cultivars [28]. Research with soybean and tomato phloem exudates indicated the association of Zn and Cu with organic acids [29]. After metal ion uptake, there may be ligand exchange with these organic compounds or/and amino acids (e.g. citric acid, histidine). All these important organic acids, amino acids, phytosiderophores, and nicotianamine, as well as their respective non-covalent metal-complexes, are low-molecular-weight (LMW) compounds with a molecular weight less than 1000 Dalton. So far, the exact mechanisms of ligand exchange and redox reactions of LMW and LMW-metal-species in plant compartments are mostly unknown [Fig. 1-4]. As a consequence of this lack of knowledge, there are many open questions, which still have to be solved for example:

- i) Which Fe-PS species are formed in the rhizosphere, if several PS are present (e.g., is there a preference of the highly hydroxylated PS for Fe complexation)? In other words: what is the biological role of PS diversity?
- ii) Which ligands are dominating the chelation of Fe and other metal ions *in planta*? In particular: What are the concentrations of LMW-metal-complexes in Xylem?
- iii) In which subcellular compartments do the LMW-metal-complexes exist, and what is the difference of these compartments with respect to metal species?
- iv) Which metal ions are actually complexed with NA *in planta*?

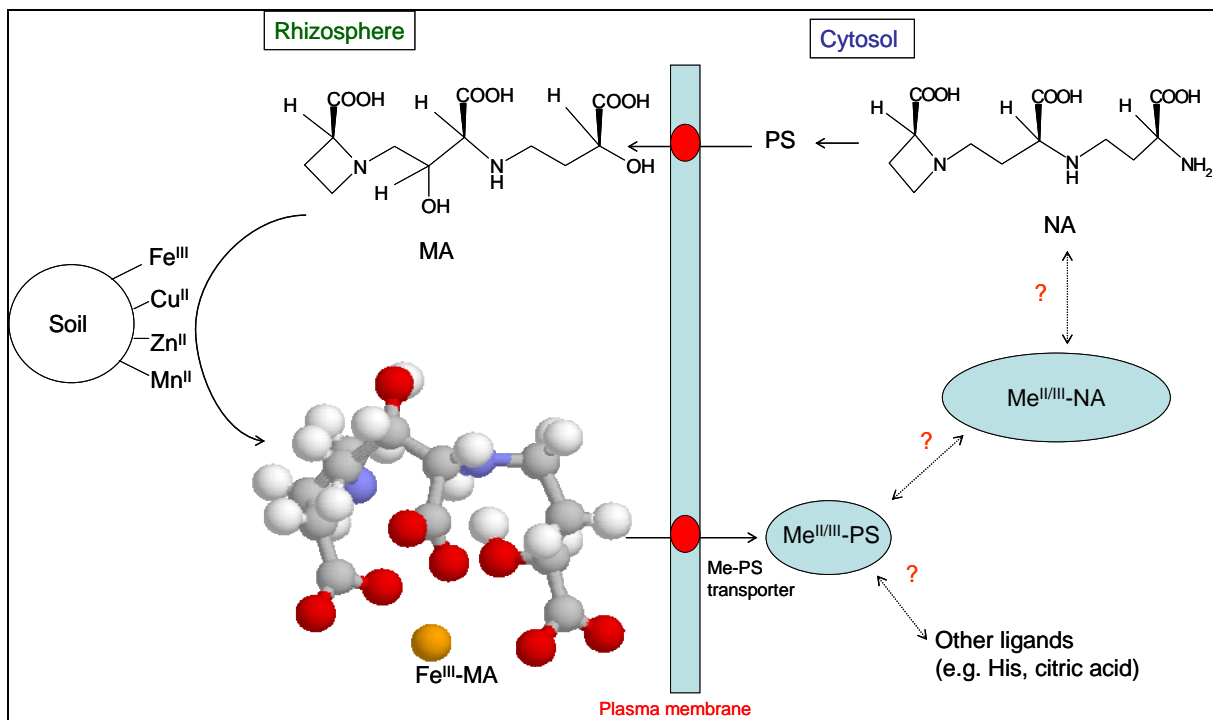


Figure 1-4. Unknown reactions: ligand exchange (between metal-PS complexes and other organic ligands, such as NA, citric acid, His); redox reactions of  $\text{Fe}^{\text{III/II}}$ , after metal-PS complexes entering the cytosol.

Since equilibria of small metal-species are “links” between inorganic species in soil (uptake) and transporters (proteins, small ligands) in cells or membranes, analytical

methods for highly sensitive and simultaneous determinations of the important LMW compounds (e.g. PS, NA, amino acids, and citric acid), and their respective metal-complexes are required to answer the above questions and investigate the mechanism of metal translocation in plants and metabolic changes of metal species *in planta*, including redox and ligand exchange equilibria [12].

## 1.2 Analytical methods for detection and identification of small metal-species in plants

Chromatographic methods analyzing various mugineic acids were introduced by paper chromatography [34] and thin-layer chromatography (TLC) [16]. However, high-performance liquid chromatography (HPLC) has been mainly applied for the determination of PS in plants using derivatization and fluorimetric detection [35-38] or photometric detection [39]. The HPLC procedures for the separation and detection of PS, which are presented by Kawai [35] and Mori [36], were modifications of the procedure developed by Ishida [40] for simultaneous fluorescence determination of primary and secondary amines. Each procedure involves three steps: i) separation of the PS on a cation-exchange column, ii) post-column derivatization with o-phthalaldehyde (OPA) following pre-treatment with NaClO, and iii) detection by fluorescence spectroscopy. The separation is based on differences in  $pK_a$  and the influence of pH on the charge of the various phytosiderophores. There are several difficulties in this procedure, e.g., poor stability of OPA derivatives, problems of Fe contamination with HPLC procedures involving the use of strong acids and low pH and the special equipment required for automated post-column derivatization. Also, the similarities in the  $pK_a$  values of the acid sites of the various PS make it difficult to obtain adequate separation by cation-exchange procedures. Another procedure involves anion-exchange at pH 10-13 rather than cation-exchange and post-column derivatization with OPA [37]. As alternative procedures for the assay of phytosiderophores, pre-column derivatization with phenylisothiocyanate (PITC) [39] or with 9-fluorenylmethyl chloroformate (FMOC) [38] followed by reversed-phase chromatography were introduced. However, it is impossible to detect metal complexes by the above-mentioned methods, which are based on the derivatization of PS. Fe-PS species have been separated by anion-exchange chromatography with NaOH gradient and pulsed amperometric detection [41, 42]; however the separation takes place in a very basic pH value, which is far from the pH of isolated plant compartments.

Alternatively, electrophoretic methods have been applied for determination of NA and other metal-binding ligands and intact metal species in plant extracts [25, 43-45]. Six nickel-complexes in the latex of a hyperaccumulating tree *Sebertia acuminata* were separated by size-exclusion chromatography (SEC) and capillary electrophoresis (CZE), and one of the nickel species with molecular mass of 360 was identified by ESI-MS as Ni-complex with NA [43, 45]. Capillary electrophoresis was also applied to determine the stability and affinity of  $Fe^{III}$ -PS species [44], as well the capability of NA chelating both  $Fe^{III}$  and  $Fe^{II}$  [25]. However, those methods were optimized to particular matrices and metal-species, and are not applicable as general methods for mixtures of metal species in plants.

A number of components, such as amino acids and phytosiderophores, directly in crude root exudates of different plant types were identified by a combination of multinuclear and 2-D NMR with GC/MS and high-resolution MS [46], however no metal species were analysed.

So far, no analytical method is available, which combines an effective separation with a highly sensitive detection and structural identification of all relevant LMW ligands and respective metal species in plants.

### 1.3 Objective of this work

The unequivocal identification (and quantification) of LMW-metal-species is a prerequisite for understanding the mechanisms and equilibria, that govern the uptake and trafficking of nutrient and trace metals in plants. This knowledge is of paramount importance not only for plant nutrition and agriculture, but also for human nutrition, toxicology, medicine, and biotechnology [47]. Therefore, analytical methods allowing simultaneous and sensitive detection and identification of the functional low-molecular-weight compounds in plants are needed.

However, the identification and quantification of metal species in plant fluids and tissues encounters several major obstacles on the level of analytical chemistry:

- i) The lack of knowledge about LMW metal species in plants. (Which species could be present?)
- ii) The unknown stability of non-covalent metal species, which are part of dynamic equilibria. (Which analytical methods can be used without disturbing these equilibria?)
- iii) The lack of pure standards for those metal species that are known (e.g. PS). This makes quantitative analyses extremely difficult.
- iv) Very low concentrations (low micro molar range) and very low sample volumes of isolated plant compartments
- v) The difficulty of identifying in one solution many metal species, which are very similar with respect to molecular weight, charge, solubility, and other physico-chemical parameters.
- vi) The absence of analytical methods, which would allow an unequivocal identification of metal species directly in complex biological matrices.

Some (but not all) of these problems can be successfully addressed by hyphenated techniques, based on the combination of a chromatographic (or electrophoretic) separation with a species-specific detection and identification system (such as ESI-MS) [48-58]. Consequently, capillary electrophoresis (CE), high performance liquid chromatography (HPLC), and electrospray ionization mass spectrometry (ESI-MS) were chosen as basic methods ("starting point") to solve the above mentioned problems.

Objective of this work is the development and critical assessment of new analytical tools for accurate identification and analysis of LMW metal-species in plants. The resulting methods should be applicable to real plant samples, allowing testing for hypotheses and answering some of the questions, which are discussed in chapter 1.1. Furthermore, the results of this work should contribute to establish a more realistic model of metal transport and translocation in plants.

## 2 Capillary Electrophoresis (CE) with Diode Array Detector (DAD) and Capacitively Coupled Contactless Conductivity Detector (C<sup>4</sup>D)

Since most of the important LMW compounds (e.g. PS, NA, amino acids, and citric acid), and their respective metal-complexes in plants are charged at physiological pH, their separation by capillary electrophoresis (CE) should be possible. As mentioned in chapter 1.2, a few capillary electrophoresis methods were applied already to determine some particular metal species in selected plant matrices [25, 43-45]. However, there is no general electrophoretic method available to separate metal-species and their free ligands in plants till now.

In this chapter, a new capillary electrophoresis method was developed to separate metal-species and their free ligands, and amino acids simultaneously (chapter 2.4.1 and 2.4.2). Different plant samples were investigated in order to test the applicability of the proposed CE method (chapter 2.4.3). Investigating real plants, wheat and Arabidopsis plants, should not only verify the presence of a certain species in an isolated plant compartments, but monitor the changes of important LMW species (free ligands and metal-species), which are directly correlated to biological processes. Since many important LMW species are similar in charge-to-size ratio, esp. for isomers, a special coated (zwitterionic coated) capillary was used to separate isomers of EDDHA-Fe<sup>III</sup> (i.e. *meso*-Fe<sup>III</sup>-EDDHA, and *rac*-Fe<sup>III</sup>-EDDHA). (chapter 2.4.4). In addition to the most commonly used UV detector, a capacitively coupled contactless conductivity detector (C<sup>4</sup>D) was used in series to offer complementary information.

### 2.1 Capillary Electrophoresis

#### 2.1.1 Principle of Capillary Electrophoresis

**Electrophoresis** is the movement of a charged molecule under the influence of an electric field. Capillary electrophoresis (CE) is electrophoresis performed in a narrow tube. Separation of ions is based on their differences in charge and size.

When an electric field is applied to the buffer-filled capillary, ions are driven to move. The electric force ( $F_E = qE$ ) imparted by the electrical field is proportional to its effective charge ( $q$ ), and the electric field strength ( $E$ ). The translational movement of the ion is opposed by a retarding frictional force ( $F_F = -6 \pi \eta r v$ ), which is proportional to the velocity of the ion ( $v$ ), solution viscosity ( $\eta$ ), and ion radius ( $r$ ). The ion almost instantly reaches a steady state velocity where the accelerating force equals the frictional force.

$$q E = 6 \pi \eta r v \quad (1)$$

The mobility ( $\mu_e$ ) of a given ion and medium, is a constant which is characteristic for that ion.

$$\mu_e = q / (6 \pi \eta r) \quad (2)$$

From equation (2), it is evident that small, highly charged species have high mobilities whereas large, less charged species have low mobilities. This relation is affected due to the formation of hydration sheaths.

A fundamental constituent of CE operation is the **electroosmotic flow (EOF)**. EOF is the bulk flow of liquid in the capillary and is a consequence of the surface charge on the interior capillary wall. The inner surface of a fused silica capillary consists of silanol groups (Si-OH), which start to become ionized to SiO<sup>-</sup> at pH > 3, and are fully ionized at about pH 9. The negatively charged surface is counterbalanced by positive ions from the buffer, forming the so-called electric double layer. Under the influence of the electric field, the positive ions in the diffuse part of the double layer migrate towards the cathode; in doing so they transport their hydration sheaths, which results in an electroosmotic flow. The EOF controls the migration time of the “running buffer” The counterions (cations, in most cases), which build up near the surface to maintain charge balance, form the double-layer and create a potential difference very close to the wall. This is known as the **zeta potential**, which is largely dependent on the electrostatic nature of the capillary surface, and to a small extent, on the ionic nature of the buffer. The magnitude of the EOF can be expressed in terms of mobility by

$$\mu_{\text{EOF}} = (\varepsilon \zeta_{\text{wall}} / \eta) \quad (3)$$

where

- $\mu_{\text{EOF}}$  = EOF “mobility”
- $\zeta_{\text{wall}}$  = zeta potential at the capillary wall
- $\varepsilon$  = dielectric constant
- $\eta$  = dynamic viscosity

**Influence of buffer pH, ionic strength, and organic modifier:** Buffer pH strongly influences the EOF. An increasing pH accelerates the EOF. In our case, a buffer pH value of 7.3 close to the intracellular pH was selected for most investigations, in order to minimize disturbances of the equilibria of the metal species and their low-molecular-weight ligands. The EOF decreases with increasing ionic strength, due to a collapse of the double layer. High ionic strength generates high current and possible Joule heating. Low ionic strength is problematic due to sample adsorption. Organic solvent in the buffer changes the zeta potential and viscosity and usually decreases the EOF. It may as well alter the selectivity (details see chapter 2.1.2 nonaqueous capillary electrophoresis (NACE)).

**Coating:** Dynamic and permanent coatings of the fused-silica capillary inner surface have been studied and applied extensively, especially for protein separations. During capillary electrophoresis separation, cations may interact with the SiO<sup>-</sup> groups, resulting in peak broadening and peak distortion, which decreases the separation efficiency. In addition, the EOF becomes unpredictable leading to poor repeatability of mobilities of analytes. Therefore, coating of the capillary inner wall is applied to suppress the EOF and decrease the wall interactions by inert siloxane bridges. In this work, a zwitterionic covalent coating was used, in order to modify the charge of the capillary inner surface, and to increase the hydrophilic interaction between the coating and the analytes (details see chapter 2.4.4).

### 2.1.2 Modes of Operation

The main separation modes used in CE are capillary zone electrophoresis (CZE), micellar electrokinetic capillary chromatography (MEKC), capillary isotachopheresis (cITP), capillary gel electrophoresis (CGE), and capillary isoelectric focusing (cIEF). MEKC needs surfactants, which interact with analytes, in the running buffer. However in our cases, a strong interaction between surfactants and our interesting metal species causes a dissociation of metal species (LMW complexes) during separation.

cITP needs a good *a priori* knowledge of the analytes for adequate choice of leading and terminating buffers. In addition, in a single cITP experiment either cations or anions can be analyzed. Therefore, cITP is not well-suited in our case. Both CGE and cIEF are extensively applied in biological sciences for macromolecules such as proteins. CGE separates analytes based on their molecular size. However, our metal-species are very similar in physico-chemical properties and similar in molecular size, which makes CGE not applicable here. cIEF separates molecules on the basis of their pI. The unknown pI value of our interesting metal-species makes the focusing difficult.

In this work, **capillary zone electrophoresis (CZE)** is applied for investigation of low-molecular-weight compounds in plants. CZE is capable to separate both cations and anions. Especially when the charge state of interesting analytes is unknown, CZE has the advantage to enable the simultaneous separation of cationic and anionic species. Consequently, CZE should be the best choice to start separating our LMW metal species in plants.

In CZE mode, sample is applied usually as a narrow zone (band), which is surrounded by the separation buffer. As an electric field is applied, each component in the sample zone migrates according to its own apparent mobility in addition to the EOF. Ideally, all sample components will eventually separate from each other to form individual zones of pure analytes in buffer. However, neutral molecules cannot be separated because they migrate together in one zone at the velocity of electroosmotic flow. The separation of charged molecules is accomplished most efficiently when differences among the apparent velocities of the components are maximized and random dispersion of the individual zones is minimized. The time required for a solute to migrate to the point of detection is called the “migration time”, and is given by the quotient of migration distance and velocity. The migration time and other experimental parameters can be used to calculate the apparent solute mobility using

$$\mu_a = l / (t E) = l L / (t V) \quad (4)$$

where:

- V = applied voltage
- l = effective capillary length (to the detector)
- L = total capillary length
- t = migration time
- E = electric field
- $\mu_a$  = apparent mobility

Electroosmotic flow migrates in the direction to cathode, where the detector is usually located. The measured mobility is called the **apparent mobility**,  $\mu_a$ . The **effective mobility**,  $\mu_e$ , can be calculated from the apparent mobility by abstracting the independently measured EOF using a neutral marker that moves at a velocity equal to the EOF.

$$\mu_a = \mu_e + \mu_{EOF} \quad (5)$$

Neutral solutes migrate in the same direction and velocity as the electroosmotic flow and are not separated. Cations and anions are separated based on differences in their apparent mobilities. For cations, which move in the same direction as the



electroosmotic flow,  $\mu_e$  and  $\mu_{EOF}$  have the same sign, that means  $\mu_a > \mu_e$ . The electrophoresis of anions, on the other hand, is in the opposite direction of electroosmosis, so for anions  $\mu_e$  and  $\mu_{EOF}$  have opposite signs. At moderate pH values (pH > 6), electroosmotic flow is generally higher than electrophoretic flow causing anions to migrate towards the cathode, which is where the detector is typically located. At lower pH, electroosmosis is weak and anions may never reach the detector unless the polarity of the instrument is reversed in order to change the location of the detector from the cathode end to the anode end of the capillary.

When the polarity of the electric field is reversed (from cathode to anode), the electroosmotic flow still is towards the cathode. In contrast to the normal polarity (towards cathode), however, the EOF is now in the direction away from the detector. Therefore, cations and neutral solutes, which both migrate towards the cathode, are never detected in the reversed mode of CE. Only anions, which migrate towards to anode, where the detector is located, are detected. The apparent mobility  $\mu_a$  of anions is the result of their electrophoretic mobility  $\mu_e$  minus EOF mobility:

$$\mu_a = \mu_e - \mu_{EOF} \quad (6)$$

**Nonaqueous capillary electrophoresis (NACE)**, which means that a high percentage of nonaqueous solvent is utilized with the technique of capillary electrophoresis, was also investigated in this work. Over the past few years, NACE has been introduced to improve selectivity in CE. Introduction of nonaqueous electrolyte solutions in CE has expanded the range of solvent parameters such as the dielectric constant, viscosity, polarity and autoprotolysis, offering new possibilities for changes in separation selectivity [59-65]. Furthermore, the ability of organic solvents to accept protons from the silanol groups of the capillary wall appears to play a crucial role in the development of electroosmotic flow. Organic solvents offer the potential for separation mechanisms based on interactions that cannot take place or are too weak to be observed in aqueous media. Hydrogen bonding and dipolar interactions are not as significant in the aqueous environments because of the strong hydrogen bonding and dipolar characteristics of water molecules that exist in large quantities. These water molecules hydrate the hydrogen bonding/dipolar moieties of the solutes and effectively reduce interactions between solutes and a hydrogen bonding/dipolar interactive additive. On the contrary, nonaqueous media have considerably weaker hydrogen/dipolar capabilities, which allow the solutes to interact through these interactions. Since some important LMW compounds, esp. for isomers, are similar in their charge to size ratios (see chapter 1.1), they may express similar mobility in capillary zone electrophoresis. Nonaqueous capillary electrophoresis was applied to improve the separation of these compounds characterized by very similar electrophoretic mobilities in CZE. In addition, structural identification of these LMW compounds in plants is not possible with UV- and conductivity detectors only, because of the limited selectivity of these detectors. In order to identify the molecular structures, a combination of CE with mass spectrometry as a structural identification detector would be necessary. For this CE-MS combination a high percentage of organic solvent (as used in NACE) is advantageous.

The electrophoretic migration of the solutes is influenced by the nature of the solvent or solvent mixture used for the electrophoresis medium in three main ways: i) The mobility may change due to changes in the size of the solvated ion. ii) The dielectric constant of the organic solvent may influence the equilibrium of the protolytic

dissociation. The higher the value of the dielectric constant, the higher the degree of ionization of acids and bases. iii) The acid-base property of the solute, expressed by its  $pK_a$  value, may change due to the differentiating effect of many organic solvents. The latter effect of the three is the most significant, as the dissociation constant,  $K_a$ , may change many orders of magnitude for different solvents. Changes in solute mobility result from differing dielectric constants and viscosities of the medium due to mixing of solvents, which can be described by the von Smoluchowski equation [66] as follows:

$$\mu_{\text{normalized}} = [\mu_{\text{solvent A}} (\epsilon/\eta)_{\text{mixture}}] / (\epsilon/\eta)_{\text{solvent A}} \quad (7)$$

where  $\mu_{\text{normalized}}$  represents the mobility of the solute ion in the solvent mixture normalized to the mobility in solvent A ( $\mu_{\text{solvent A}}$ ),  $\epsilon$  the dielectric constant and  $\eta$  the viscosity of the mixture of solvent A, respectively.

## 2.2 Capacitively Coupled Contactless Conductivity Detector (C<sup>4</sup>D)

Most commercially available CE instruments are equipped with UV-absorbance detectors. Conductivity detectors offer a different detection principle, which gives better sensitivity to non-UV-absorbing, charged analytes. In my work, I used a combination of both detectors, because most of the interesting analytes are poorly UV absorbing substances. Therefore, an advanced conductivity detector, capacitively coupled contactless conductivity detector (C<sup>4</sup>D), was applied as a second detector to complement UV detection.

In the last few years [67-69], capacitively coupled contactless conductivity detector (C<sup>4</sup>D) has become an accepted detection method in capillary electrophoresis for a variety of analytes. Advantages of this technique over optical detection modes include great flexibility in capillary handling and rather simple mechanical parts and electronics, as it can be performed in an on-capillary mode.

In conductivity detector, analyte ions displace background co-ions during electrophoretic separation equivalent to their charge. Thus, the response arises from the difference in conductivity between analytes and background electrolytes (BGEs). The most simple conductivity detector is a direct conductivity detector, whose electrodes directly are in contact with the buffer solution. However, this is difficult to realize in capillary electrophoresis. With C<sup>4</sup>D, the detection signals obtained in a longitudinal dimension along the capillary. Fig. 2-1a depicts a schematic drawing of a C<sup>4</sup>D. Two stainless steel as the electrodes are placed around a fused-silica capillary in a certain distance from each other. By applying an oscillation frequency, a capacitive transition occurs between the actuator electrode and the liquid inside the capillary. After having passed the detection gap between the electrodes, a second capacitive transition between the electrolyte and the pick-up electrode occurs. Thus, this scheme represents a series of a capacitor, an ohmic resistor, and a second capacitor (Fig. 2-1b). By using suitable amplifier electronics, conductivity changes of the electrolyte in the detection gap between the electrodes inside the capillary can be monitored. Usually, the electrodes are placed on an insulated socket to ensure a rigid construction with a constant electrode distance. The socket is then shielded by being placed in a grounded metal housing. In the simplest possible equivalent circuitry for the shielded detector cell, shown in Fig. 2-1c, the two electrodes form capacitors (C) with the inside of the capillary, which are connected by a resistor (R) formed by the electrolyte solution.  $C_0$  is the stray capacitance, which arises from direct coupling

between the electrodes if no shield is used. The application of an ac-voltage to the excitation electrode leads to an ac-current flowing through the cell, which is picked up at the second electrode. This current is then transformed back to an ac-voltage at the pick-up amplifier according to the equation:

$$V_{\text{out}} = -i * R_f \quad (8)$$

where:  $V_{\text{out}}$  = output voltage in V  
 $i$  = cell current in A  
 $R_f$  = feedback resistor value on the pick-up amplifier in  $\Omega$

The output of the pick-up amplifier is given by the following equation, which accounts for the frequency dependence of the cell impedance [61]:

$$V_{\text{out}} = - \frac{V_{\text{in}} R_f}{1 + j 2 \pi f R C_0} \frac{1}{j 2 \pi f (C + C_0) [1 + j 2 \pi f R C C_0 / (C + C_0)]} \quad (9)$$

where:  $V_{\text{out}}$  = output voltage in V  
 $V_{\text{in}}$  = input voltage in V  
 $j$  = imaginary unit  
 $f$  = frequency in Hz  
 $R_f$  = feedback resistor value on the pick-up amplifier in  $\Omega$ ,  
 $R$  = cell resistance in  $\Omega$   
 $C$  = cell capacitance in F  
 $C_0$  = stray capacitance in F

If the stray capacitance ( $C_0$ ) is absent, the equation is much simplified and corresponds to a simple, single pole high pass filter (composed of resistor and only one capacitor).

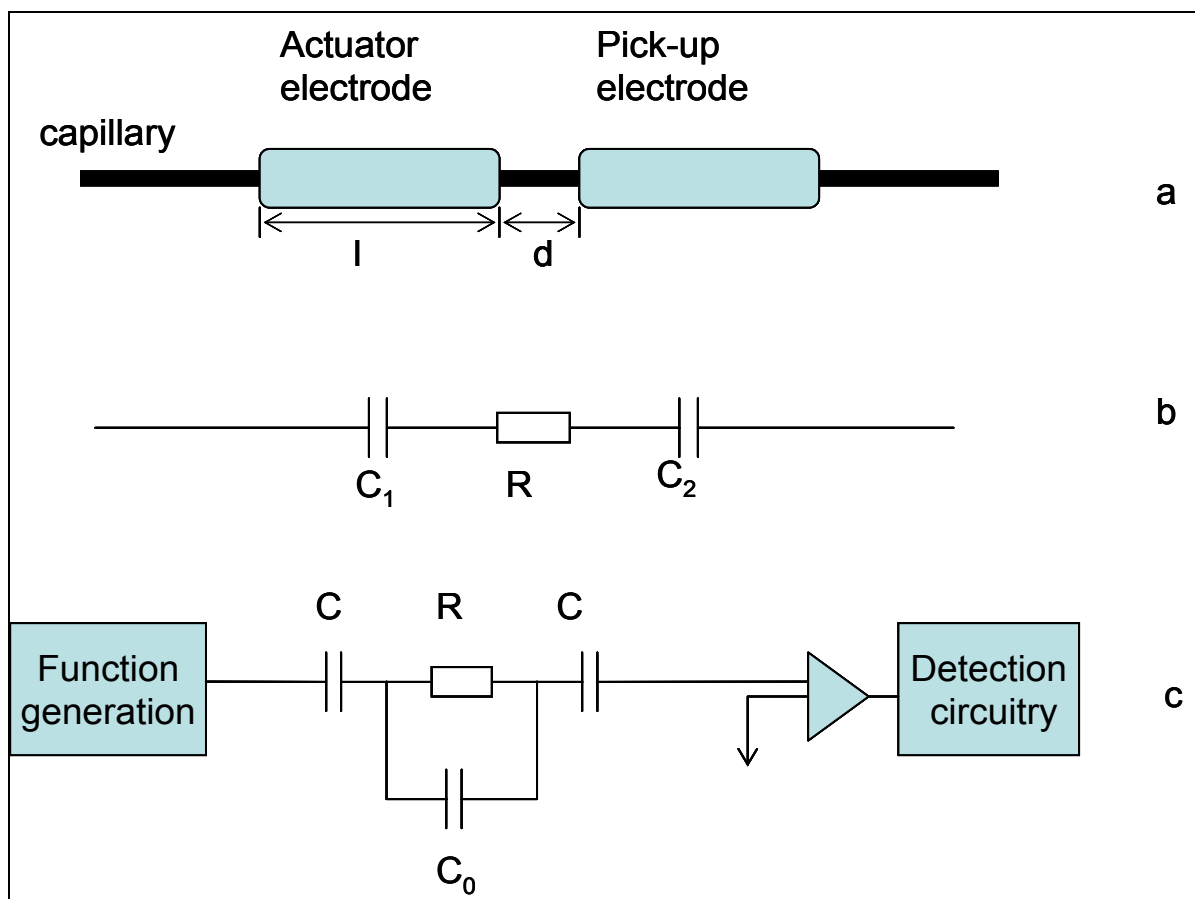


Figure 2-1. Principle of a  $C^4D$  system. (a) Schematic drawing of the sensing electrodes [70]; (b) simplified equivalent circuitry for  $C^4D$  [71]; (c) equivalent circuitry representing the  $C^4D$  cell without shielding and the pick-up amplifier [72].

## 2.3 Experimental

### 2.3.1 Instrumentation

Two different capillary electrophoresis systems (see Fig. 2-2) were applied for the investigations. Both systems were used exclusively in CZE mode.

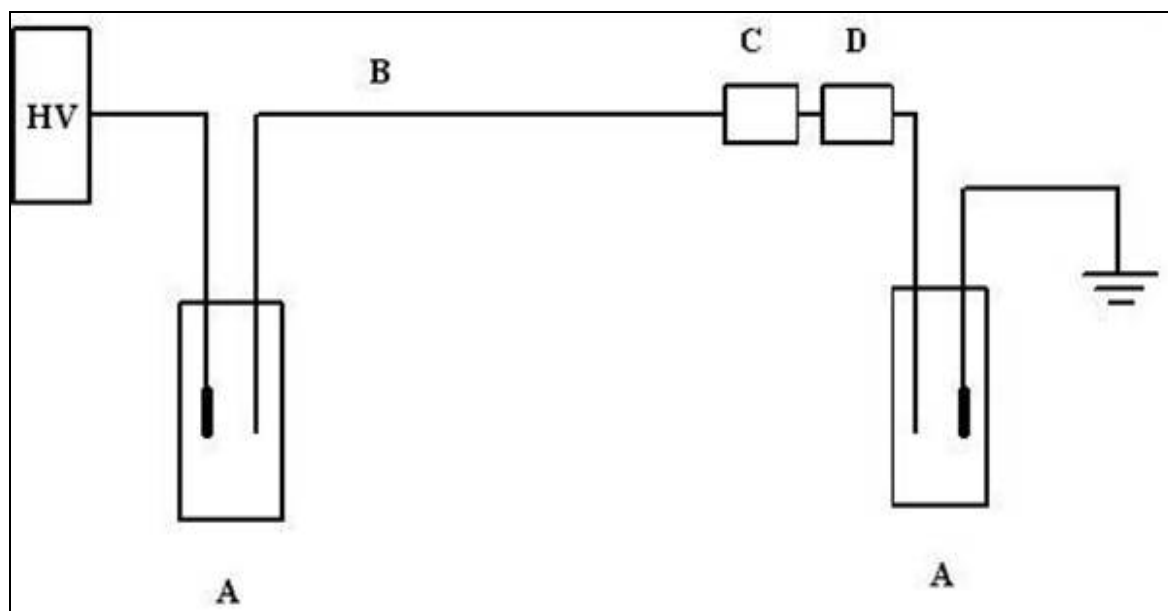


Figure 2-2. Schematic of the instrumental setup: HV, high voltage power supply; (A) buffer reservoir; (B) fused silica capillary. In CE system 1: (C) UV detector at 205 nm; (D) C<sup>4</sup>D; In CE system 2: (C) C<sup>4</sup>D; (D) DAD detector at 200 nm, 254 nm, and 280 nm with scan range from 190 - 390 nm.

#### *CE system 1:*

A Crystal 300 CE system (UNICAM, Germany) was used, equipped with a UV detector (UNICAM 4225, Germany) at 200 nm, and a TraceDec contactless conductivity detector (Innovative Sensor Technologies, Austria). All the fused silica capillaries (50  $\mu\text{m}$  i.d., 360  $\mu\text{m}$  o.d.) in this work were obtained from CS-Chromatographie Service GmbH (Langerwehe, Germany). Injection of the sample solution was performed hydrodynamically (40 mbar for 5 seconds). For capillary electrophoresis, a constant high voltage of +20 kV was applied. The capillary was rinsed with 0.1 mol L<sup>-1</sup> sodium hydroxide and deionized water for 10 min, and then equilibrated with carrier electrolytes for 30 min at the beginning of each day. Between runs the capillary was rinsed with 0.1 mol L<sup>-1</sup> sodium hydroxide for 3 min, and ultrapure water for 4 min, and then with carrier electrolytes for 5 min.

#### *CE system 2:*

All experiments with this set up were carried out at Prof. Uwe Karst's group (Institute of Inorganic and Analytical Chemistry, Münster University, Münster, Germany).

This system consisted of an Agilent CE system (Agilent Technologies Sales & Services GmbH & Co. KG, Waldbronn, Germany) with integrated Diode Array Detector (DAD), and also equipped with the TraceDec C<sup>4</sup>D (see CE system 1). The scan range of DAD was set to 190 – 390 nm, and optimum wavelengths were set to 200 nm, 254 nm, and 280 nm with a bandwidth of 4 nm. Total length of the silica capillary was 48 cm, the length to the DAD detector was 39.5 cm, and to the C<sup>4</sup>D detector 35 cm. Injection of the sample solution was performed hydrodynamically (40 mbar for 2 seconds). For capillary zone electrophoresis, a constant high voltage of +

20 kV was applied. The capillary was rinsed with 0.1 mol L<sup>-1</sup> sodium hydroxide and ultrapure water for 10 min, and then equilibrated with carrier electrolytes for 30 min at the beginning of each day. Between runs the capillary was rinsed with carrier electrolytes for 3 min.

In addition to normal (uncoated silica) capillaries, a special CE capillary was used. This zwitterionic (ZIC) capillary contains sulfobetaine-type functional groups (see Fig. 2-14) chemically bonded to the silica capillary surface. The total length of this capillary (50 μm i.d., 375 μm o.d., obtained as a kind gift from SeQuant, Umeå, Sweden) was 32 cm, the length to the DAD detector was 23.5 cm, and to the C<sup>4</sup>D detector was 19 cm. For zwitterionic capillary electrophoresis, a constant high voltage of -30 kV was applied. The ZIC capillary was rinsed with ultrapure water for 15 min, and then equilibrated with buffer for 30 min at the beginning of each day. Between runs the capillary was rinsed with buffer for 5 min.

### 2.3.2 Solutions and Chemicals

*CZE method development:* The following buffers were tested: sodium phosphate (20 mM, pH 7.5), 3-morpholino-2-hydroxypropanesulfonic acid (MOPSO) (40 mM, pH 6.9), 4-(2-hydroxyethyl)-1-piperazinethansufonic acid (HEPES) (40 mM, pH 7.5), sodium borate (20 mM, pH 9.0), and sodium acetate (20 mM, pH 4.0) were used. All buffer salts were dissolved in ultrapure water to the specified concentration and the pH was adjusted by addition of NaOH (1 M).

*CZE optimized method:* 2-morpholinoethanesulfonic acid monohydrate (MES) and 2-amino-2-hydroxymethyl-1, 3-propanediol (TRIS) were dissolved in water to 20:20 mM, and adjusted by NaOH (1 M) to pH 7.3.

*NACE method development:* Different buffer systems were investigated at pH 7.3. Ammonium acetate was dissolved in water to 50 mM, and then mixed with acetonitrile (ACN) at different ratios (2:8, 4:6, 6:4, and 8:2). MES and TRIS were dissolved in water to 50:50 mM, and then mixed with acetonitrile at different ratios (2:8, 4:6, 6:4, and 8:2). The buffer pH was adjusted to 7.3 by NaOH (1 M).

EDTA-Fe<sup>III</sup> and EDDHA-Fe<sup>III</sup> standards were prepared as follows: the stock solution of iron(III) was diluted in ultrapure water to 1 mM concentration, the resulting solution was added into the dissolved ethylenediaminetetraacetic acid (EDTA) or ethylenediaminedi(*o*-hydroxy-*p*-methylphenylacetic) acid (EDDHA) solution to form the metal-Ligand species at a ligand-to-metal ratio of 3:2. These samples were then further diluted to the proper concentration.

Chemicals are listed in the appendix.

### 2.3.3 PS, metal-PS, and Plant samples

All PS and real plant samples were isolated and purified from plant cultures at the Institute for Plant Nutrition (Hohenheim University, Stuttgart, Germany).

*DMA, MA, and epi-HMA:* The PS concentration in the purified solution was determined by HPLC [37]. The PS samples were diluted in half diluted buffer to proper concentration.

*Real plants:* Wheat plants (cv., Bezostaya) were grown in hydroponic culture following the procedure described by Rengel and Römheld [73]. Shoots and roots

were harvested separately, rinsed with ultra pure water, blotted dry between paper towels and squeezed in a hydraulic press. The obtained press sap was centrifuged at 25,000 *g* for 30 min to remove suspended particles and finally stored at -20 °C until further analysis.

*Arabidopsis thaliana* Col-0 plants were grown in hydroponic culture according to Loqué *et al.* [74] using ammonium nitrate as a nitrogen source. Plants were then exposed for 4 days to 30 µM NiCl<sub>2</sub> before being detopped. The excised stem surface was gently wiped and a flexible tube was fixed onto the cut end of the stem. Xylem sap exuded into the tube for 30 min was collected with a Pasteur pipette and stored at -20 °C until further analysis. There are always three different kinds of *Arabidopsis* samples, wild type (WT), knock out (KO), and overexpressor (OE) samples. OE samples have more amount of one membrane protein, which is responsible to transport metal or metal-species from soil to plants. On contrast, KO samples have no this membrane protein. WT samples contains normal amount of this membrane protein.

After thawing, samples were diluted 1:1 with buffer, and then filtered through 2 µm membrane filters.

NA was a kind gift from Profs. T. Kitahara and S. Mori (University of Tokyo, Japan). The purity of this chemically synthesized product was at least 95 %, as confirmed by NMR.

*Metal-PS standards* were prepared as follows: after dissolving the metal salts with ultrapure water individually, the resulting solution (1 mM) was added to the PS standard samples to form the metal-PS species at a ligand to metal ratio of 3:2. If necessary, the pH was then readjusted to the desired value. The iron(II) chloride tetrahydrate was prepared directly before sample injection to minimize the oxidation of iron(II).

## 2.4 Results and discussion

As discussed in chapter 2.1.2, capillary zone electrophoresis (CZE) was chosen as the most appropriate electrophoretic method to separate LMW metal-species and their free ligands. Different buffer systems such as phosphate, MOPSO, HEPES, borate, acetate, and MES/TRIS were investigated for the optimized separation and detection. Five amino acids (lysine, arginine, histidine, glutamine acid, and aspartic acid) include very basic amino acids (Lys and Arg) and most acidic amino acids (Glu and Asp), to scan the complete range from positively charged to negatively charged species. Inorganic buffer systems produce low UV absorbance background and therefore are advantageous for UV detection; however their high conductance level causes high background with the C<sup>4</sup>D conductivity detector. Organic buffer systems have much lower conductance comparing to inorganic buffers, but organic buffer molecules absorb UV light and cause higher UV detection background. Although phosphate (at pH 7.5) and borate (at pH 9.0) buffers enable to separate the five amino acids and rise only low background with UV detector, they cause high noisy background and unstable baseline with C<sup>4</sup>D. Acetate buffer was applied at pH 4.0, which causes a weak EOF and results in poor separation of the five amino acids, and long analysis time (> 25 min on CE system 1). In order to improve the C<sup>4</sup>D detection sensitivity, the organic buffers MOPSO (at pH 6.9), HEPES (at pH 7.5), MES/TRIS (at pH 7.3) were used. The separation of five amino acids with each of the organic buffers was similar, but only the MES/TRIS buffer allows a good detection of all five amino acids on both UV and C<sup>4</sup>D detectors (see the following chapter 2.4.1). MES/TRIS as amphoteric buffer system enables both good separation on CE and sensitive detection with C<sup>4</sup>D. The pH of different plant compartments varies in the range of about pH 4 - pH 9. However, the plant compartments applied here are prepared at pH 7.3. To keep the species in plant without change and minimize the disturbance of matrix, pH 7.3 was applied for the whole investigations. The pK<sub>a</sub> value of MES and TRIS is 6.15 and 8.30 respectively. At pH 7.3, MES is negatively charged and TRIS is positively charged. Such kind of background "ion-pairs" can be displaced by either analyte anions or cations during separation by equivalent to their charge. In addition, MES/TRIS buffer owns a good buffer capacity at pH 7.3 as well.

### 2.4.1 Investigating of free ligands

As discussed in chapter 1.1, some amino acids, esp. Histidine, are discussed as a ligand for metals [26-33]. Phytosiderophores are responsible for uptake of metal ions by forming stable complexes with them in graminaceous plants. Nicotianamine is the bioprecursor of PS in plants and exists in all higher plants and is discussed as iron transporter within plants. In order to understand what happens to PS-metal species after their uptake into the plants (see chapter 1.1), it is important and necessary to analyse free ligands in plants.

**Separation of amino acids** Five amino acids (Lys, Arg, His, Glu, and Asp) were dissolved in diluted buffer, to minimize the pH difference between sample plug and buffer system. At the same time this injection of diluted buffer serves as a marker of EOF. From Fig. 2-3, a baseline separation of the five amino acids (Asp, Glu, His, Arg, and Lys) was achieved with the proposed method. The amino acids are detectable with a concentration of 80 µM each, besides His with a concentration of 50 µM, with both UV detector and C<sup>4</sup>D detector. The detection limit of these five amino acids with C<sup>4</sup>D is 3-5×10<sup>-5</sup> M, which is relatively higher compared to 0.5-1×10<sup>-5</sup> M using lactic acid as buffer below the 2-3 pH range, as applied by Tanyanyiwa *et al.* [75]. This



higher detection limit is caused by the neutral buffer of pH 7.3. At this pH, these five amino acids are zwitterionically charged. Hence, their conductance is relative low compared to their cationic or anionic forms, which can be achieved at very low or high pH values. However, the very acidic or basic pH, which interfere the matrix and dissociate the metal-ligand complexes in plants, is not suitable for our investigations. MES/TRIS buffer absorbs UV light and causes a higher UV baseline. In additional, these five amino acids are relative poor UV absorbance. Glu and Asp produce negative signals with UV detector, but positive signals with C<sup>4</sup>D. On the contrast, Lys, Arg, and His produce positive peaks with the UV detector, but negative peaks with the C<sup>4</sup>D. A different detection sensitivity of them was observed for the two detectors. For example, Lys, which has a very poor UV absorbance, caused only a small UV signal (Peak 1), but produced a much more sensitive signal with the C<sup>4</sup>D detector. This shows the benefit of applying two completely different detectors in the system. Especially poorly UV absorbing and charged compounds are detected with better sensitivity by C<sup>4</sup>D.

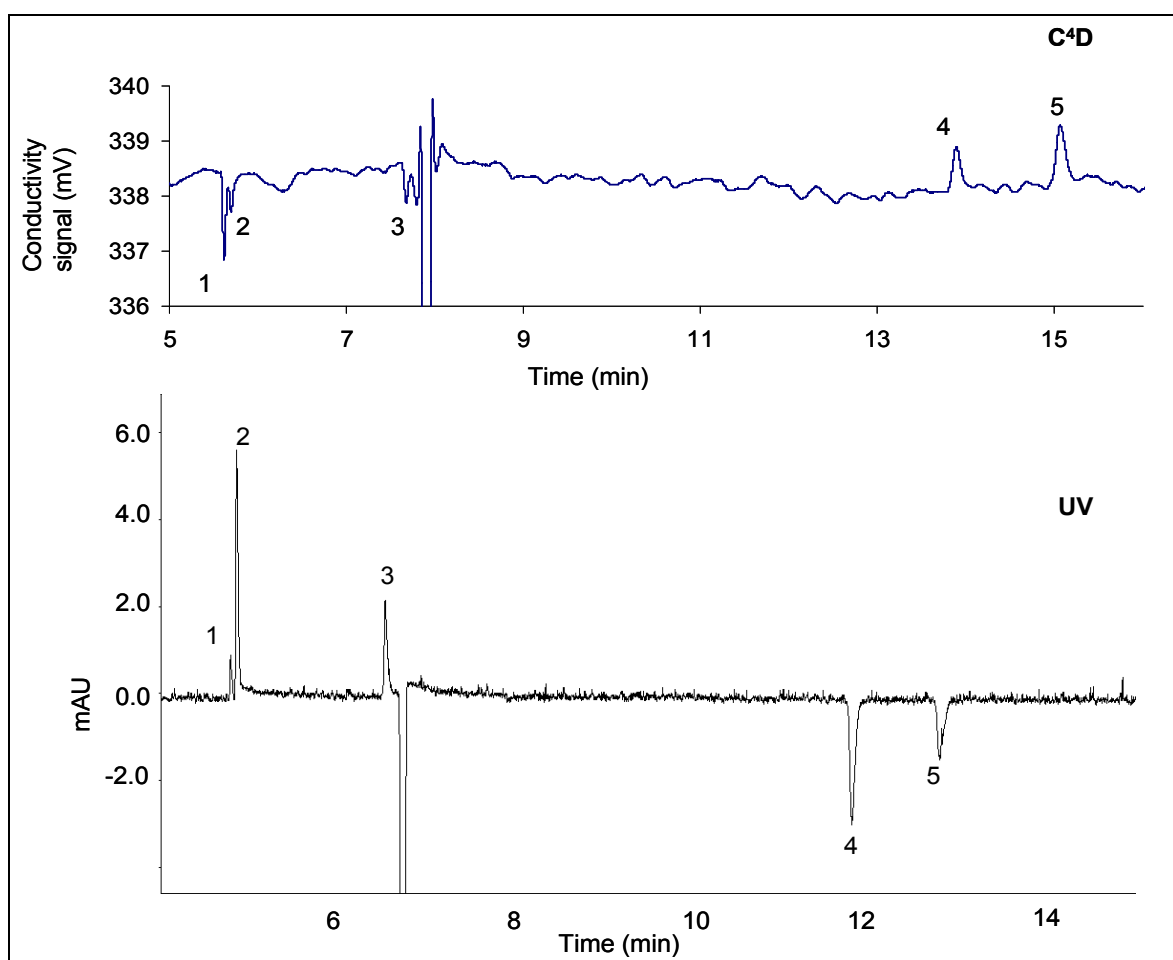


Figure 2-3. Electropherograms of amino acids obtained by UV (200 nm) and C<sup>4</sup>D detection. 20:20 mM MES/TRIS buffer, pH 7.3, 20 kV constant voltage. Hydrodynamic Injection: 40 mbar, 5 sec. 1: Lys, 2: Arg, 3: His, 4: Glu, 5: Asp. Total capillary length ( $L_{total}$ ): 81.5 cm, the length to UV detector ( $L_{UV}$ ): 48.5 cm, and the length to C<sup>4</sup>D ( $L_{C^4D}$ ): 57.5 cm. CE system 1.

Using the proposed capillary zone electrophoresis method at pH 7.3, the positively charged compounds (Lys and Arg) migrate faster than the EOF; the neutral compounds migrate together with the EOF, and the negatively charged compounds (Glu and Asp) migrate slower than the EOF. His is nearly neutral and slightly positively charged, therefore, migrates a little faster than the EOF. The most basic

amino acid, Lys, is the fastest, the most acidic amino acid, Asp, the slowest one. The effective mobilities of these five amino acids were calculated and listed in Table 2-1. The migration order, Lys < Arg < His < EOF < Glu < Asp, is based on the charge-to-size ratio of these compounds at pH 7.3, and is directly correlated to their decreasing pI values (in this order). The pI values of phytosiderophores are not exactly known, but the charge at a given pH can be estimated from the pK<sub>a</sub> values of their different functional groups, which are known, and are discussed by von Wirén *et al.* [44]. This estimation leads to the conclusion, that the electrophoretic mobilities of phytosiderophores should be in between those of the most basic amino acids ( $\mu_{\text{Lys}}$ ) and the most acidic ones ( $\mu_{\text{Asp}}$ ).

Table 2-1. Electrophoretic mobility of investigated compounds ( $\mu_e$ ), constant voltage 20 kV, buffer: MES/TRIS (20:20 mM), pH 7.3.

Cations	$\mu \times 10^{-4} (\text{cm}^2/\text{Vs})$
K <sup>+</sup>	6.21
Ca <sup>2+</sup>	4.10
Na <sup>+</sup>	3.84
Amino acids	
Lys	2.00
Arg	1.90
His	0.12
Glu	-2.14
Asp	-2.40
Synthetic chelates	
EDTA	-3.35
EDTA-Fe <sup>III</sup>	-2.52
EDDHA	-1.53
EDDHA-Fe <sup>III</sup>	-1.81
PS and metal-PS species	
NA	-0.84
DMA	-1.70
MA	-1.72
<i>epi</i> -HMA	-2.25
DMA-Fe <sup>III</sup>	-1.82
MA-Fe <sup>III</sup>	-1.80
<i>epi</i> -HMA-Fe <sup>III</sup>	-1.77
DMA-Cu <sup>II</sup>	-1.89
DMA-Zn <sup>II</sup>	-2.00
NA-Fe <sup>III</sup>	-1.92
NA-Fe <sup>II</sup>	-1.92
NA-Ni <sup>II</sup>	-1.93
NA-Cu <sup>II</sup>	-2.09
NA-Zn <sup>II</sup>	-2.00

**Separation of PS** For the first time, a baseline separation of *epi*-HMA, MA, DMA, and NA, was achieved with this method within 15 min on CE system 1 (see Fig. 2-4). The mobilities of phytosiderophores and nicotianamine were calculated and are listed in Table 2-1. As expected, the mobility of PS and NA are in between those of EOF and of Asp. The migration order of PS and NA is NA < DMA < MA < *epi*-HMA. From their chemical structures and their pK<sub>a</sub> values (listed in Table 2-2), this elution order can be explained as follows: The three carboxylic groups should be negatively charged at pH 7.3 for all four ligands. All four compounds also have two amino groups, and nicotianamine owns one more terminal amino group, which has a pK value 7.7 [76]. Because of this additional amino group NA becomes the most basic one among these four ligands, which is equivalent to the most positive charge (or least negative). Therefore, NA migrates faster than the others. One amino group of phytosiderophores is always protonated at pH 7.3 (pK between 9.5 and 10 [44]), but

the pK value of the other amino group decreases in the order of DMA > MA > *epi*-HMA, reaching 7.1 for *epi*-HMA. This means, that the positive charge goes down from NA > DMA > MA > *epi*-HMA, which agrees very well with the migration order shown in Fig. 2-4.

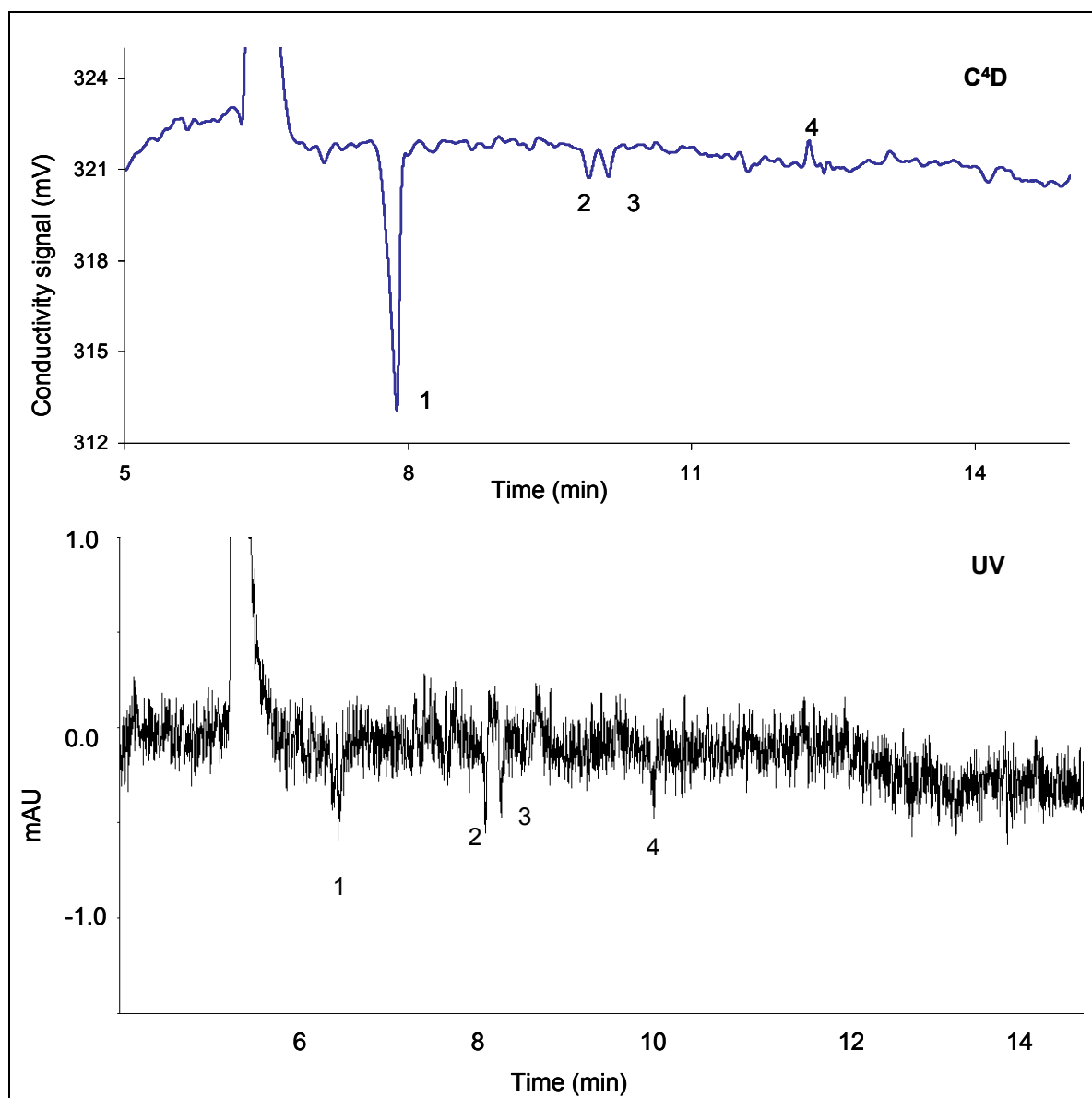


Figure 2-4. Electropherograms of PS and NA obtained by UV (200 nm) and C<sup>4</sup>D detection. 1: NA, 2: DMA, 3: MA, 4: *epi*-HMA Standard concentration: 150  $\mu$ M each in diluted buffer.  $L_{\text{total}} = 74$  cm,  $L_{\text{UV}} = 43$  cm, and  $L_{\text{C}^4\text{D}}$  is 52 cm. Other conditions see Fig. 2-3.

Table 2-2. Published pKa of EDTA, EDDHA, *rac*-EDDHA, *meso*-EDDHA, MA, DMA, *epi*-HMA, and NA.

Chelator	pKa <sub>1</sub>	pKa <sub>2</sub>	pKa <sub>3</sub>	pKa <sub>4</sub>	pKa <sub>5</sub>
EDTA <sup>c</sup>	2.24	2.93	6.01	9.85	
EDDHA <sup>d</sup>	6.32	8.64	10.24	11.68	
<i>rac</i> -EDDHA <sup>e</sup>	6.33	8.79	10.87	12.05	
<i>meso</i> -EDDHA <sup>e</sup>	6.36	8.76	10.85	11.90	
MA <sup>b</sup>	2.39	2.76	3.40	7.78	9.55
DMA <sup>a</sup>	2.35	2.74	3.20	8.25	10.00
<i>epi</i> -HMA <sup>a</sup>	2.35	2.74	3.25	7.10	9.62
NA <sup>a</sup>	2.86	6.92	9.14	10.09	

<sup>a</sup> Mutakami *et al.*, 1989 [77]; <sup>b</sup> von Wirén *et al.*, 2000 [44]; <sup>c</sup> Andereg and Ripperger *et al.*, 1989 [78]; <sup>d</sup> Frost *et al.*, 1958 [79]; <sup>e</sup> Ahrlund *et al.*, 1990 [80].

However, the UV absorbances of these compounds are very low, resulting in very small UV signals (Fig. 2-4). As a complimentary detector, C<sup>4</sup>D offers better signals of these compounds at the concentration of 150 μM (Fig. 2-4). It is worth to point out that esp. nicotianamine shows a very sensitive signal with the C<sup>4</sup>D. This is probably caused by the additional positively charged terminal amine group (Fig. 1-3).

The given results show that capillary electrophoresis offers “for the first time” a successful baseline separation of free ligands, such as NA, DMA, MA, and *epi*-HMA, within 15 min on CE system 1.

#### 2.4.2 Investigating of metal-ligands

As mentioned in chapter 1.1, metal phytosiderophores are the relevant species for iron uptake from the soil into graminaceous plants. Therefore, analytical methods for these species are highly needed to understand the metal transport and translocation system in plants. Due to the unknown pI values of PS and PS-metal species, the unknown stability of all the metal-PS species, and the low micro molar concentration range of PS-metal species in plants, a number of analytical problems may be expected. In order to better understand the separation behaviour of PS-metal species, the well-known model iron-species (EDTA-Fe<sup>III</sup> and EDDHA-Fe<sup>III</sup>) were investigated before starting the investigation of metal-PS species.

**Separation of model iron-species** To deduce the migration behaviour of PS-metal species, EDTA-Fe<sup>III</sup> and EDDHA-Fe<sup>III</sup>, as well-known iron-species, were investigated by the CZE method. Their respective free ligands, EDTA and EDDHA, are very well-known strong iron chelators. The respective synthetic metal chelates were applied for micronutrient fertilization in foliar, trunk and soil application and in hydroponic cultures [81-84]. EDTA contains 4 carboxylic acid and 2 tertiary amine groups that bind to the metal ion. EDTA forms especially strong complexes with Mn, Cu, Fe<sup>III</sup>, and Co<sup>III</sup>. Its six function groups bind with iron(III) to form the octahedral coordination of the EDTA-Fe<sup>III</sup>. EDDHA contains 2 carboxylic acid, 2 amine, and 2 phenolic functional groups, which are responsible for chelating iron. EDDHA also contains two chiral carbon centres, which produce metal-EDDHA isomers, *rac*-Fe<sup>III</sup>-EDDHA and *meso*-Fe<sup>III</sup>-EDDHA (Fig. 2-5) [23, 85].

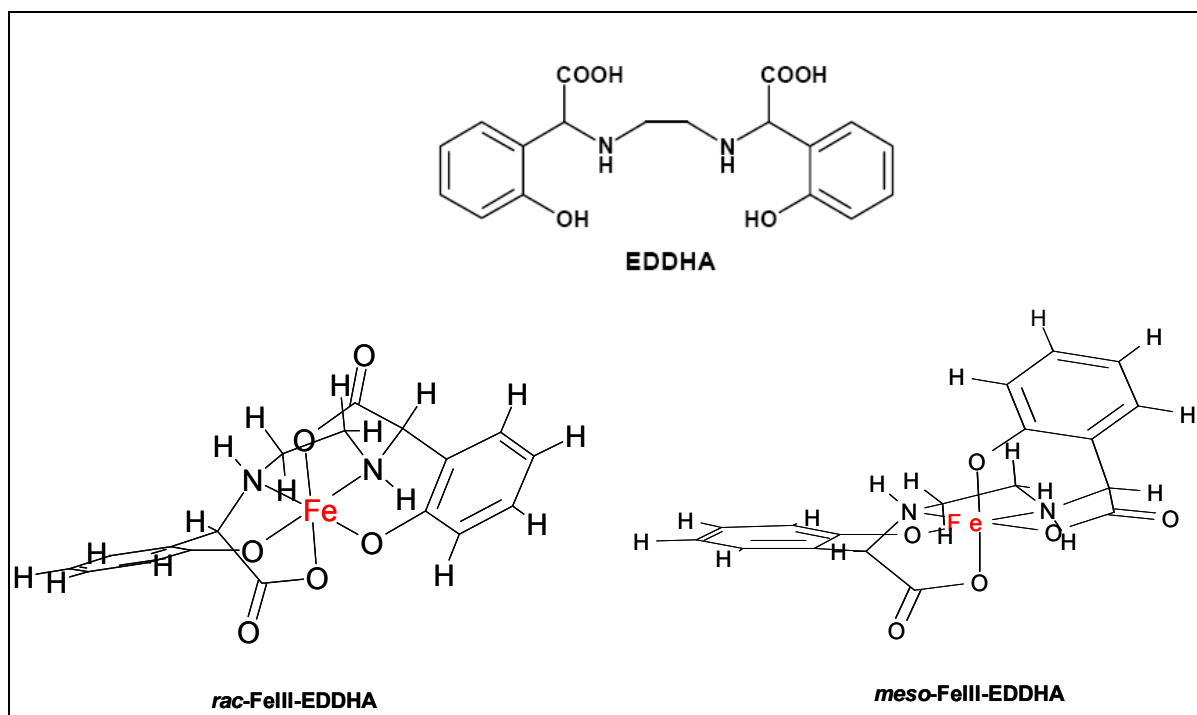
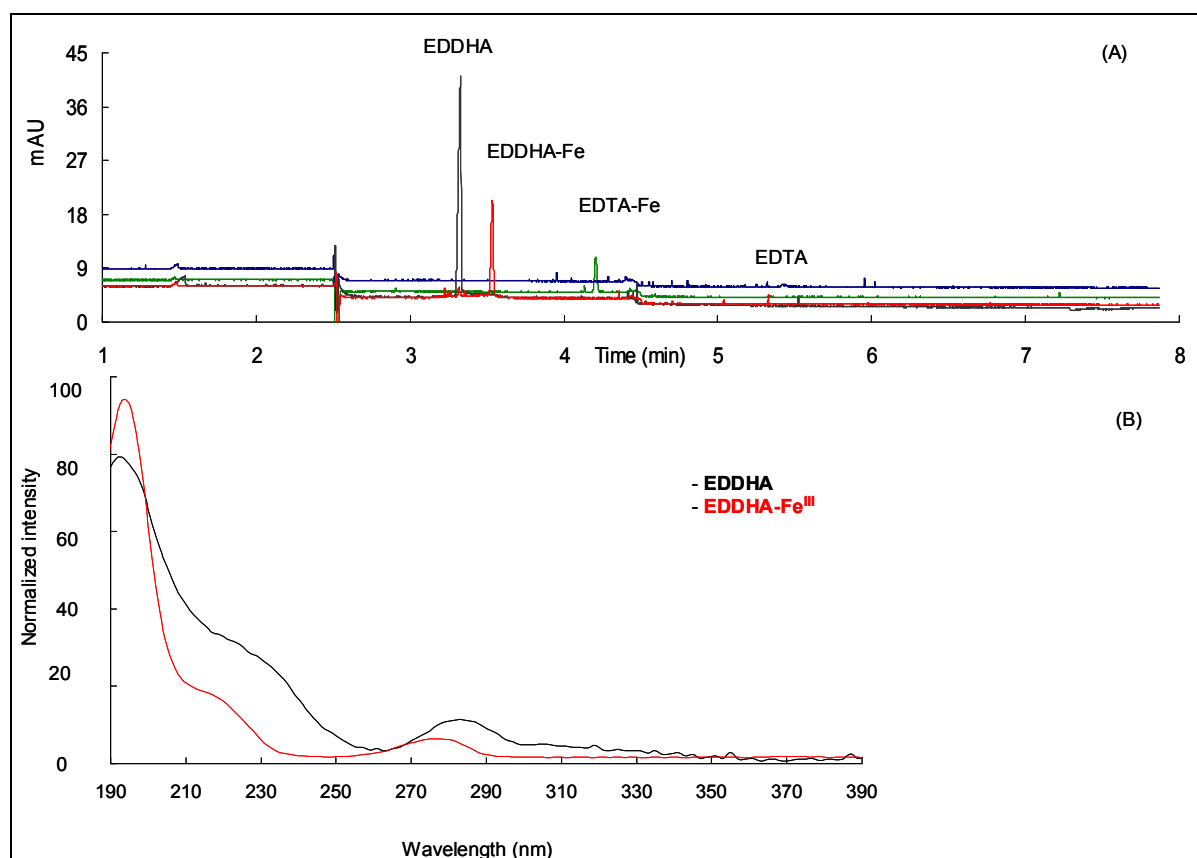
Figure 2-5. The chemical structures of EDDHA and EDDHA-Fe<sup>III</sup>.

Figure 2-6. (A) Electropherograms of EDTA, EDDHA, EDTA-Fe<sup>III</sup>, and EDDHA-Fe<sup>III</sup> obtained by UV (200 nm) and C<sup>4</sup>D detection. The concentration of EDDHA and EDTA are 150  $\mu$ M each, and EDTA-Fe<sup>III</sup> and EDDHA-Fe<sup>III</sup> are made at the concentration of 150:80  $\mu$ M (ligand: Fe<sup>3+</sup>). All solved in diluted buffer. (B) Normalized spectra of EDDHA and EDDHA-Fe<sup>III</sup> by DAD in the range of 190 - 390 nm. Injection was at 40 mbar pressure for 2 sec.  $L_{total}$  = 48cm,  $L_{UV}$  = 39.5 cm, and  $L_{C^4D}$  is 35 cm. CE system 2.

Table 2-3. Affinity constants of EDTA, EDDHA, MA, DMA, and NA for Zn, Fe<sup>II</sup>, and Fe<sup>III</sup>; Net charges of Zn- and Fe<sup>III</sup>-phytosiderophores at pH 7.0.

Chelator	Zn		Fe <sup>II</sup>	Fe <sup>III</sup>	
	Log K	Net charges	Log K	Log K	Net charges
EDTA	16.0 <sup>a</sup>	-2	14.3 <sup>a</sup>	25.1 <sup>a</sup>	-1
EDDHA				35.1 <sup>f</sup>	
<i>rac</i> -EDDHA				35.9 <sup>f</sup>	
<i>meso</i> -EDDHA <sup>f</sup>				34.2 <sup>f</sup>	
MA	12.7 <sup>b</sup>	-0.79 <sup>d</sup>	10.1 <sup>b</sup>	17.7 <sup>b</sup>	-1.1 <sup>d</sup>
DMA	12.8 <sup>b</sup>		10.4 <sup>b</sup>	18.4 <sup>b</sup>	~ -0.5 <sup>d</sup>
<i>epi</i> -HMA		-0.84 <sup>d</sup>			-1.2 <sup>d</sup>
NA	15.4 <sup>c</sup>	-0.78 <sup>d</sup>	12.8 <sup>c</sup>	20.6 <sup>e</sup>	0 <sup>d</sup>

<sup>a</sup> Smith and Martell *et al.*, 1989 [86]; <sup>b</sup> Mutakami *et al.*, 1989 [77]; <sup>c</sup> Anderegg and Ripperger *et al.*, 1989 [78]; <sup>d</sup> von Wirén *et al.*, 2000 [44]; <sup>e</sup> von Wirén *et al.*, 1999 [25]; <sup>f</sup> Yunta *et al.*, 2003 [88].

A baseline separation of these four compounds, EDDHA, EDDHA-Fe<sup>III</sup>, EDTA, and EDTA-Fe<sup>III</sup>, was obtained within 8 min by this CZE method, carried out on CE system 2 (see Fig. 2-6A). The migration order of the four compounds is EDDHA < EDDHA-Fe<sup>III</sup> < EDTA-Fe<sup>III</sup> < EDTA. Since EDTA owns four ionized carboxylic acid groups at pH 7.3, EDTA has more negative charges than the others, and thus migrates slowest. The carboxylic acid groups of EDTA coordinate the iron ion. Therefore, the negative charge of EDTA-Fe<sup>III</sup> is lower than that of the free ligand, EDTA, resulting in a faster migration of EDTA-Fe<sup>III</sup> compared to free EDTA. In contrast to this, the migration time of EDDHA-Fe<sup>III</sup> is longer than the migration time of the pure ligand EDDHA. This unusual phenomenon may be caused by the amine groups, which coordinate iron as well. The amine groups are positively charged at pH 7.3 (see Table 2-2) in the pure ligand, EDDHA. In the EDDHA-Fe<sup>III</sup> complex, these positive charges should be lower. Also the more rigid and bulky molecular structure of iron-EDDHA (compared to the free ligand) affects the charge-to-size ratio, and consequently leads to a slower migration of EDDHA-Fe<sup>III</sup> vs. free EDDHA under the given conditions. Since two different capillary electrophoresis systems were applied, the migration times of compounds are not directly comparable. Mobility, which depends only on the charge-to-size ratio of the molecule (Eq. 2), reflects much better the separation of different compounds, and also allows better comparison of the two systems. Therefore, the mobility of each ligand and metal species was calculated individually and listed in Table 2-1.

From Fig. 2-6B, the UV spectra of EDDHA and EDDHA-Fe<sup>III</sup> is shown. The maximal absorbance is at 228 nm and 280 nm with both EDDHA and iron-EDDHA. The maximal UV absorbance of EDTA-Fe<sup>III</sup> is at 254 nm (data not shown). Since our free ligands are low UV absorbance, 200 nm was applied to detect all the possible species in plants. The wavelengths of 254 nm and 280 nm were chosen to compromise the detection of these metal-PS-species, whose UV spectra are not available. EDDHA-Fe<sup>III</sup> and EDTA-Fe<sup>III</sup> were sensitively detected by UV detector, but not detected by C<sup>4</sup>D at a concentration of 150:80 μM (ligand: Fe<sup>3+</sup>). As expected, the sensitivity of UV detection is much better for EDDHA (compared to EDTA), because of the two aromatic rings in EDDHA. However, they are not well detected by C<sup>4</sup>D at a concentration of 150 μM (data not shown). Since a diode array detector is integrated in the CE system 2, spectra of the compounds are available, which helps to assign peaks to the different ligands and metal species.

**Separation of Fe<sup>III</sup>-PS species** Iron is one of the most important micronutrient elements for plants and human. Pytosiderophores are responsible for iron uptake

from soil to graminaceous plants (see chapter 1.1). Therefore, analysis of ferric phytosiderophores is helpful for plants nutrition, human nutrition, and biotechnology. Fortunately, the thermodynamic stability of ferric PS species is very high (see Table 2-3). From the separation of EDDHA-Fe<sup>III</sup>, EDTA-Fe<sup>III</sup>, and their respective free ligands (Fig. 2-6), it is to be expected that also the ferric PS species are stable enough for CE separation. DMA-Fe<sup>III</sup>, MA-Fe<sup>III</sup>, and *epi*-HMA-Fe<sup>III</sup> were therefore investigated using the same CZE method on the CE system 1. With a concentration ratio of 150:80  $\mu$ M for ligand to Fe<sup>III</sup>), they are detectable on UV detector, but not detectable on C<sup>4</sup>D. It has been determined that the phytosiderophore complexes have net charges between -1.1 and -1.2 at pH 7.0 (Table 2-3) [44]. Hence, they should be detectable by C<sup>4</sup>D. In comparison to simple inorganic ions of charge -1, however, the charge density of these ferric complexes is much less (more delocalized), and therefore the conductivity does not change very much, if buffer molecules are replaced by eluting metal species. Therefore, C<sup>4</sup>D detection sensitivity of ferric PS is worse than for PS. However, the sharp peak form and sensitive UV detection of all these Fe<sup>III</sup>-PS species indicate that Fe<sup>III</sup>-PS species are very stable during the CE separation. It is an advantage of CE over HPLC method, in which dissociation of ferric PS species happens during the separation (see chapter 4.4.3-4.4.4).

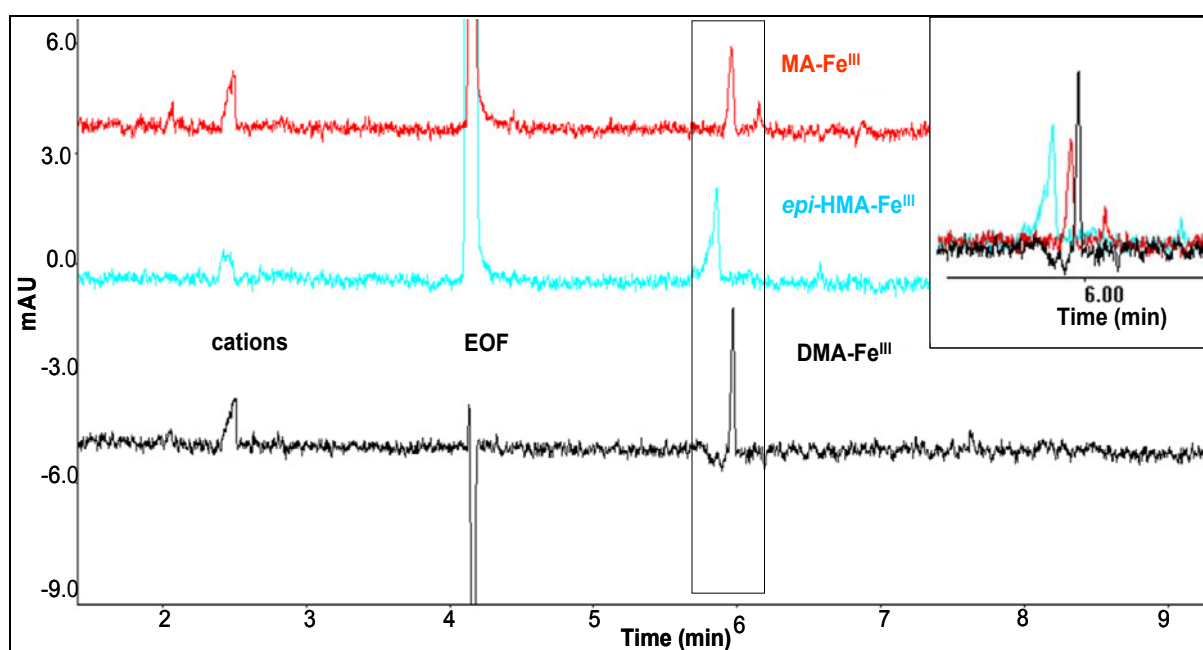


Figure 2-7. Electropherograms of Fe<sup>III</sup>-PS by UV detector at 200 nm. CE system 1. Insert electropherogram is an overlapping of the detected peaks.  $L_{\text{total}} = 72\text{cm}$ ,  $L_{\text{UV}} = 42\text{ cm}$ . All three analytes are made individually at the concentration of 150:80  $\mu$ M (ligand: metal) in diluted buffer. Other conditions see Fig. 2-3.

Since two sets of CE systems were used during the whole investigations, an accurate comparison of migration behaviour of all the species should be based on their effective mobilities. Therefore, the mobilities of ferric phytosiderophores are listed in Table 2-1. From their effective mobilities in Table 2-1 and Fig. 2-7, a slight difference in migration behaviour of the three ferric complexes are found, which is *epi*-HMA-Fe<sup>III</sup> < MA-Fe<sup>III</sup> < DMA-Fe<sup>III</sup>.  $p\text{Fe}^{3+}$  values of phytosiderophores at pH 7.0, in an order of *epi*-HMA < MA < DMA, were published by von Wiren *et al.* [25, 44, 87]. Therefore, the stability of these ferric phytosiderophores is in an order of *epi*-HMA-Fe<sup>III</sup> > MA-Fe<sup>III</sup> > DMA-Fe<sup>III</sup>, which agrees to the migration order. It indicates that more stable species migrates faster.

As shown in Table 2-1, MA-Fe<sup>III</sup> and DMA-Fe<sup>III</sup> migrate slower than their respective free ligand. However, *epi*-HMA should migrate slower than *epi*-HMA-Fe<sup>III</sup> as expected from their mobilities. This phenomenon of DMA-Fe<sup>III</sup> and MA-Fe<sup>III</sup> and their respective free ligands is similar to the migration behaviour of EDDHA-Fe<sup>III</sup> and EDDHA. There are two amino groups on all PS molecules. The amino group associated with the tertiary amino group (Fig. 1-3) is always positively charged at pH 7.3. However, at pH 7.3, -NH group of DMA and MA are positively charged, but negatively charged on *epi*-HMA, according to their respective pK<sub>a4</sub> values in Table 2-2. Except to -COOH and -OH, the -NH group on their structure goes to coordinate with metal ion. This causes a reducing of the positive charge state of DMA and MA. Therefore, DMA and MA migrate faster than their respective metal complexes. The reason for the faster migration of *epi*-HMA-Fe<sup>III</sup> vs. *epi*-HMA was already explained for the EDTA-Fe<sup>III</sup> species: the negative charge of carboxylic groups is compensated by coordination of iron, resulting in less negative charges compared to the free ligands.

**Separation of M<sup>I</sup>-DMA species** Not only iron is taken up by phyto siderophores, but other important metal ions, such as Cu and Zn, as well [9]. Therefore, it is necessary that this capillary electrophoresis method can separate and detect also these divalent metal species. DMA-Cu and DMA-Zn standards were investigated individually with this same CZE method on the CE system 2, and baseline separation was achieved within 8 min (see Fig. 2-8). Their mobilities were calculated and listed in Table 2-1. From Fig. 2-8, the migration order of them is DMA-Cu < DMA-Zn. DMA can supply up to six coordination bonds for complexation, and the distances between the groups facilitate octahedral coordination [89]. Similar to ferric-PS species, the migration order of these divalent metal-DMA species follows their stabilities listed in Table 2-3 and literature von Wirén *et al.* [25]. Since their stability order is DMA-Cu > DMA-Zn, DMA-Cu migrates earlier than DMA-Zn.

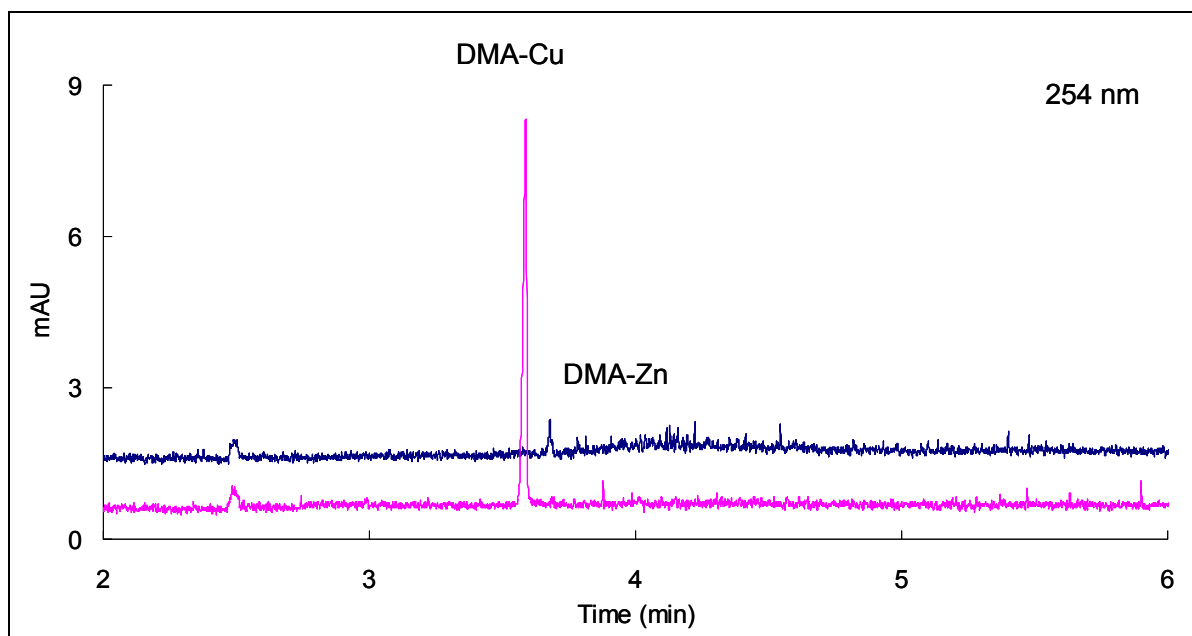


Figure 2-8. Electropherograms of DMA-Zn and DMA-Cu by DAD detector at 254 nm. CE system 2. Both DMA-Zn and DMA-Cu were made in a concentration of 150:80  $\mu$ M (ligand: metal). Other conditions see Fig. 2-6.



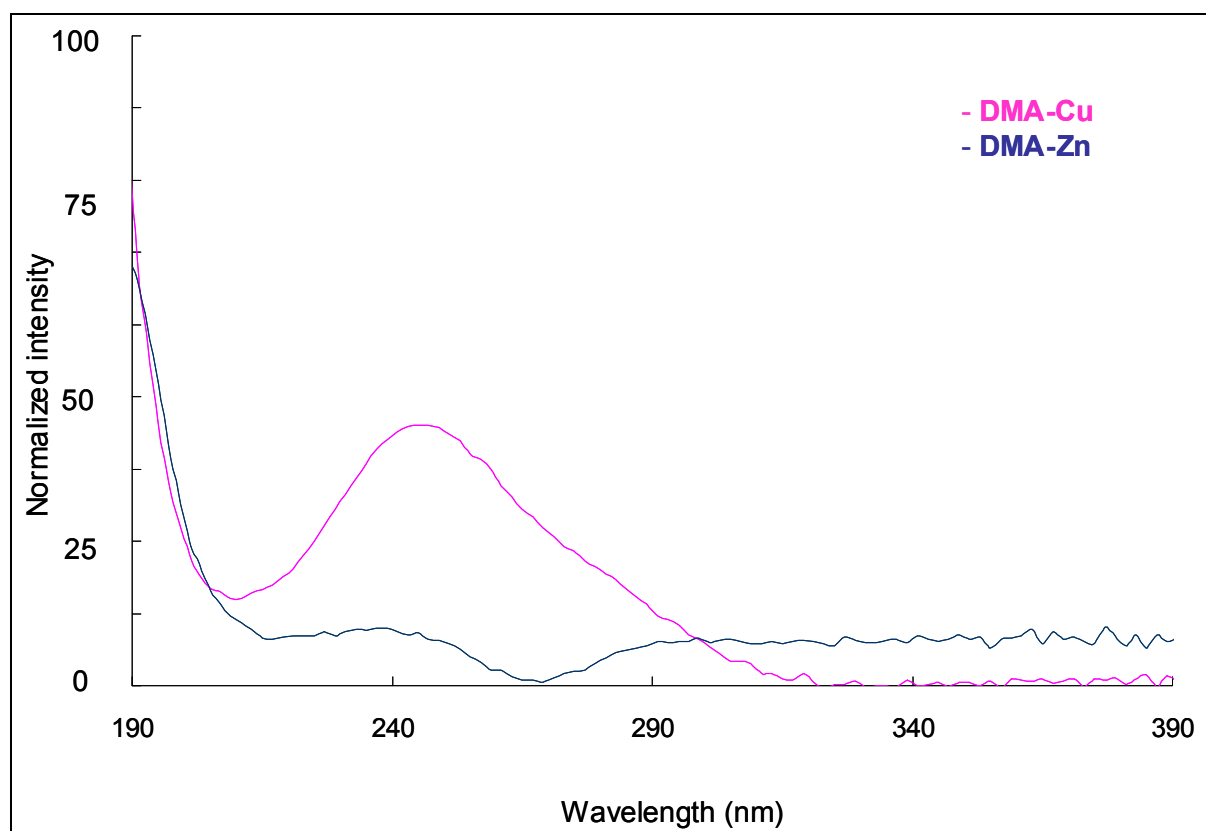


Figure 2-9. UV spectra of DMA-Cu and DMA-Zn by DAD detector with a scan range of 190-390 nm. All other conditions see Fig. 2-8.

From both Fig. 2-8 and Fig. 2-9, both of DMA-Zn and DMA-Cu with a concentration of 150:80  $\mu\text{M}$  (DMA: metal) are detectable with UV detector at 240 nm. The maximal absorbance of DMA-Cu is at 240 nm. DMA-Cu exhibits a much better absorbance in the wavelength range from 220-320 nm than DMA-Zn. Their UV spectra, which can help in identification, are different from each other. Both DMA-Cu and DMA-Zn are not detectable with  $\text{C}^4\text{D}$  with this concentration. The poor detection sensitivity with  $\text{C}^4\text{D}$  is caused by the similar reason to the ferric-PS species. The charge density of metal-species is more delocalized, and therefore the conductivity does not change very much, if buffer molecules are replaced by eluting metal species. Therefore,  $\text{C}^4\text{D}$  detection sensitivity of metal-PS species is worse than PS. Even the detection sensitivity of metal-PS with  $\text{C}^4\text{D}$  is not so good, the different UV spectrum and effective mobility of each species are sufficient for identification of them in the real plants later (see chapter 2.4.3)

**Separation of  $M^{\text{II}}$ -NA species** Nicotianamine as the precursor of phyto siderophores exists in all higher plants. NA chelates  $\text{Fe}^{\text{III}}$ ,  $\text{Zn}^{\text{II}}$ ,  $\text{Cu}^{\text{II}}$ , and as well  $\text{Fe}^{\text{II}}$ . In order to prove some hypothesis concerning NA as  $\text{Fe}^{\text{II}}$  transporter within the plants [25], it is necessary to analyse NA and its metal-species in plants. NA- $\text{Fe}^{\text{II}}$ , NA-Ni, NA-Cu, and NA-Zn were investigated individually by this CZE method on CE system 2. All of the complexes with a concentration of 150:80  $\mu\text{M}$  (NA: metal) are well detected by DAD and are detectable with  $\text{C}^4\text{D}$ , except NA-Zn, which is only detectable with  $\text{C}^4\text{D}$  (data not shown). The UV spectra of all metal-NA species (190 nm-390 nm) were measured by the DAD detector. As to be seen in Fig. 2-10, these spectra show several significant differences: NA-Ni exhibits a strong absorption at 200 nm, but no signal at all at 254 nm and 280 nm. By contrast, NA-Cu causes a very small signal at 200 nm, but strong signals at 254 nm and 280 nm. NA- $\text{Fe}^{\text{II}}$  exhibits similar absorption at the three wavelengths (200 nm, 254 nm, and 280 nm). This means, that the choice

of the detector wavelength has a very strong effect with respect to sensitivity. In particular, if no DAD is available, it is difficult to choose one wavelength for sensitive detection of all metal species. On the other hand, the differences in the spectra of metal species may help for their identification. Hence, if a combination of CE with DAD is available, an identification of the different metal-NA species is still possible – in spite of their incomplete separation. Only small negative peaks are found for these metal species using the  $C^4D$  detector (data not shown).

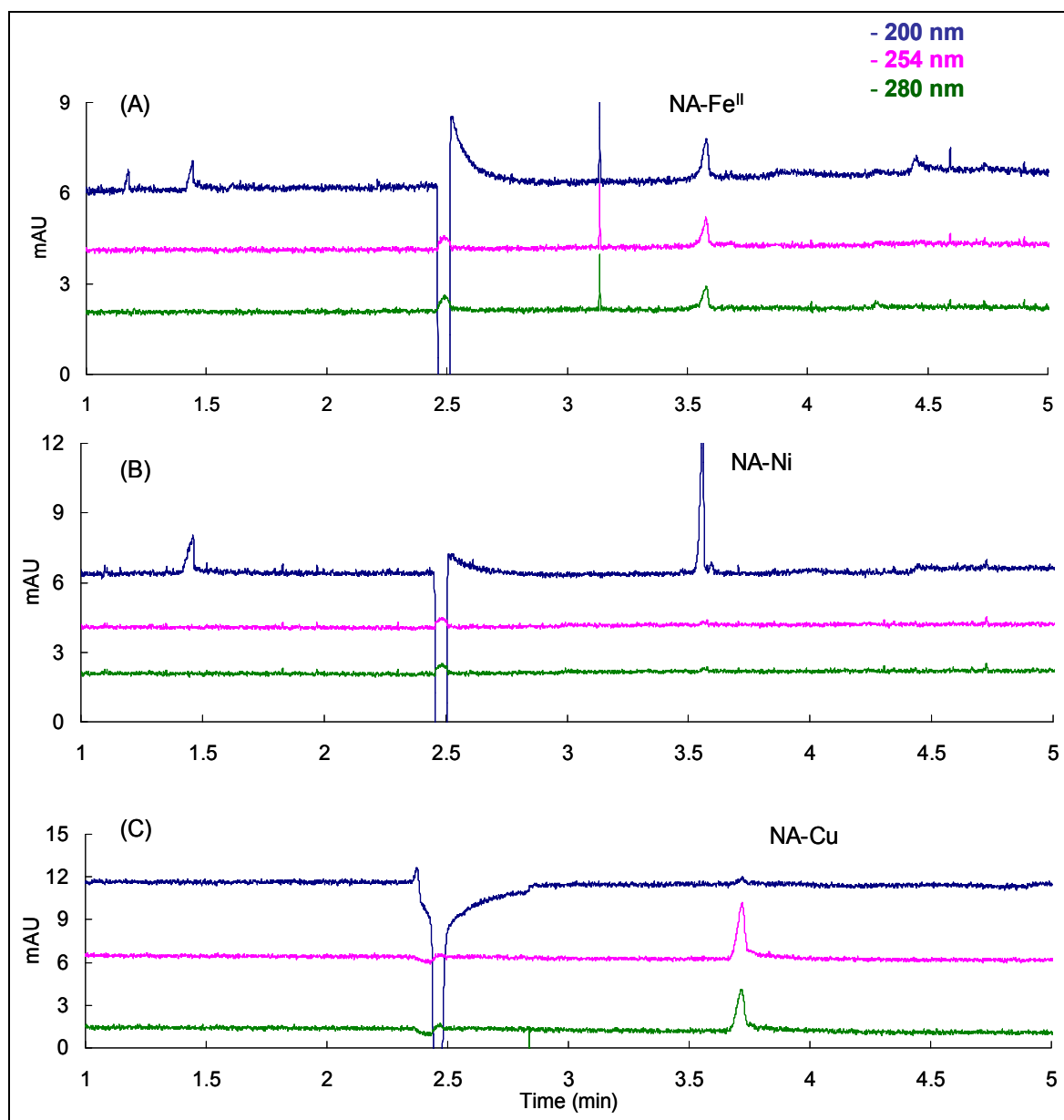


Figure 2-10. Electropherograms of NA-Cu, NA-Ni, and NA-Fe<sup>II</sup> by DAD detector at 200 nm, 254 nm, and 280 nm. CE system 2. (A) NA-Fe<sup>II</sup>, (B) NA-Ni, and (C) NA-Cu. All three NA-metal species were made in a concentration of 150:80  $\mu\text{M}$  (ligand: metal). Other conditions see Fig. 2-6.

From Table 2-1 and Fig. 2-10, NA-Cu is baseline separated from NA-Ni and NA-Fe<sup>II</sup> by the proposed CE method. Although NA-Ni and NA-Fe<sup>II</sup> are not baseline separated, according to their similar charge and geometry, their different UV spectra helps to distinguish them from each other. Moreover, all these metal-NA complexes migrate slower than the pure ligand, NA. This may be caused by a similar reason as for EDDHA and EDDHA-Fe<sup>III</sup>. That is, the positive charge (at pH 7.3) of the terminal amine group is lost by coordination with a metal ion. Hence, there are less positive

charges in a metal-NA complex compared to NA, causing a slower migration of metal-NA species. Of course, there may be additional effects due to structural differences of metal-NA and metal-PS species (e.g., change of coordination geometry in the electric field). Comparing the above described results with the chromatographic separation (in chapter 4), the CE separation of several divalent species is not as good. However, due to the measuring conditions in CE  $\text{Fe}^{\text{III}}$ -PS species can be separated without any dissociation or other analytical interferences.

### 2.4.3 Investigating of plant samples

As shown in the previous chapters, many important low-molecular-weight standards and metal complexes can be analysed by the proposed CZE method, including amino acids, phytosiderophores, nicotianamine, and their metal species. Even if some of these compounds are not baseline separated, identification still can be carried out by combining both electrophoretic mobility (listed in Table 2-1) and UV spectra of the compounds. Therefore, real plant samples were investigated by the proposed CZE method on CE system 2 (CE-DAD). The plant samples were selected with a view on a representative spectrum of ligands and metal species detectable with minimal sample preparation. Moreover, different metal species concentrations should be present, in order to test the applicability of the proposed CE method. The purpose of this part of research is not only to verify the presence of a certain species in an isolated plant compartments, but to see the changes of important LMW species (free ligands and metal-species) in response to different biological / nutritional situations.

**Wheat samples** Samples of shoot and root parts of wheat, which was cultured under iron deficiency conditions, were taken after two different times of deficiency (15 and 30 days of iron deficiency). These samples were investigated and compared to control samples, which contain no detectable iron (Fig. 2-11 and Fig. 2-12). The aim of investigating these wheat root and shoot samples is to verify the presence of a certain species, and to see the changes of these species in response to different iron deficiency conditions. In Fig. 2-11 and Fig. 2-12, the analyses of wheat shoot samples and root sample are respectively shown, including control, 15 days iron-deficiency, and 30 days iron-deficiency samples. Based on UV spectrum and mobility (as listed in Table 2-1), DMA-Zn was identified in shoot samples under iron-deficiency conditions. With increasing time of deficiency, increasing peaks for DMA-Zn ( $\mu = -1.862 \times 10^{-4} \text{ cm}^2/\text{Vs}$ ) was found at 3.79 min. The concentration changes of DMA-Zn among different samples are shown in more detail in Fig. 2-11B. Semi-quantitation was done using peak areas of DMA-Zn standard. The peak area of DMA-Zn (80  $\mu\text{M}$ ) standard was set to 100%, and the observed peak areas in real plant samples were compared to the standard. The concentration of DMA-Zn found in the shoot sample grown under 30 days iron-deficiency is about 32  $\mu\text{M}$ . All data of peak area refer to absorbance at 254 nm. The longer iron deficiency the plants under grew, more DMA-Zn was found. EDTA- $\text{Fe}^{\text{III}}$  was founded in 30days iron-deficiency sample, which is artefact coming from the nutrition solution, containing EDTA as a ligand. However, the other peaks migrating after EOF could not be identified by using only spectra and mobilities. Since no CE-MS combination was available an unequivocal identification of these species was not yet possible. With both shoot and root samples, there are many cations present in the samples that caused intense signals at 200 nm (data not shown).

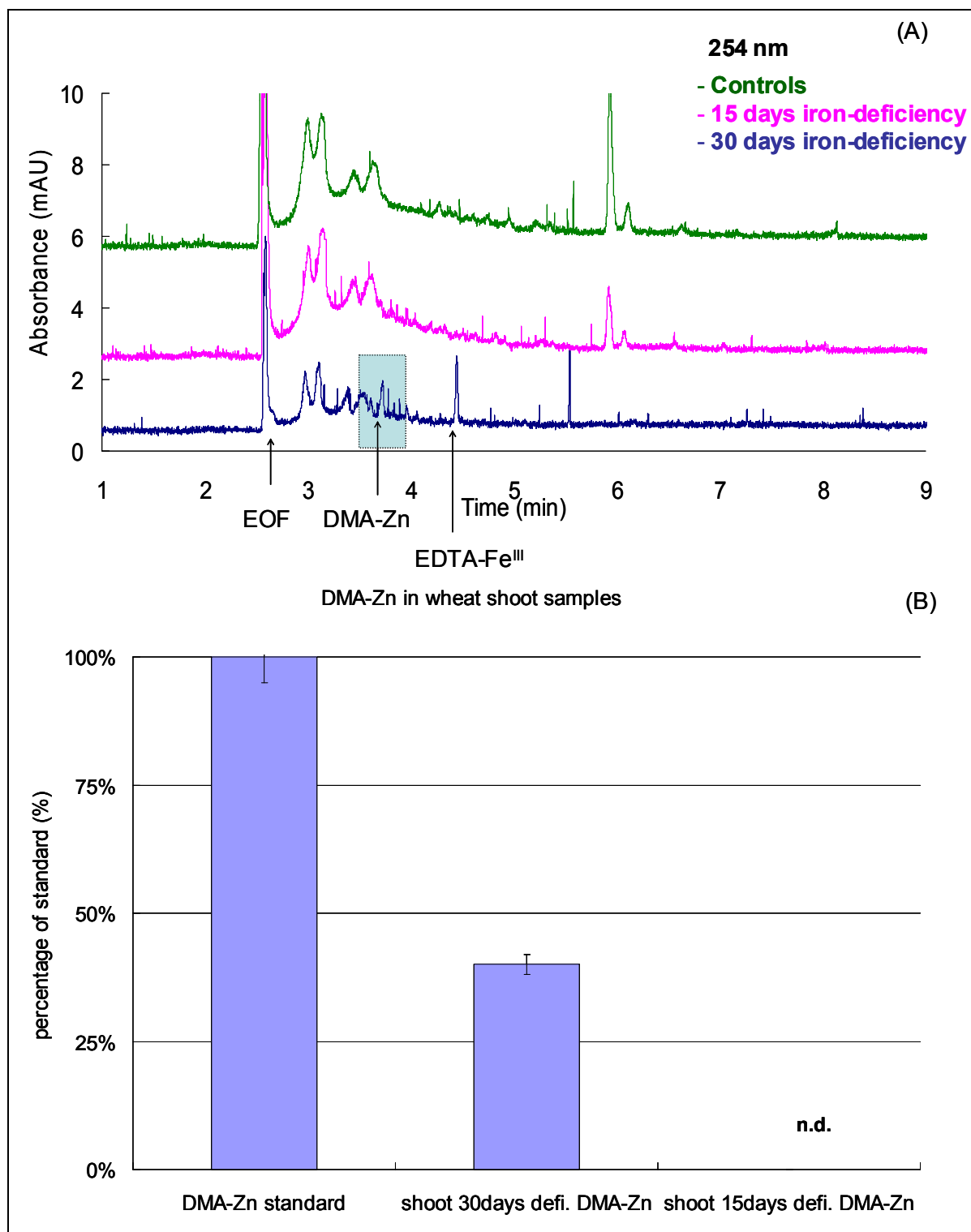


Figure 2-11. (A) Electropherograms of wheat shoot samples by DAD detector at 254 nm. Other conditions see Fig. 2-6. (B) The peak areas of DMA-Zn presenting in wheat shoot are divided by the peak area of standard. The peak area of DMA-Zn (80  $\mu$ M) as standard was set to 100%. "n.d." means not detected. Wheat shoot samples: controls; 15days iron-deficiency; 30days iron-deficiency.

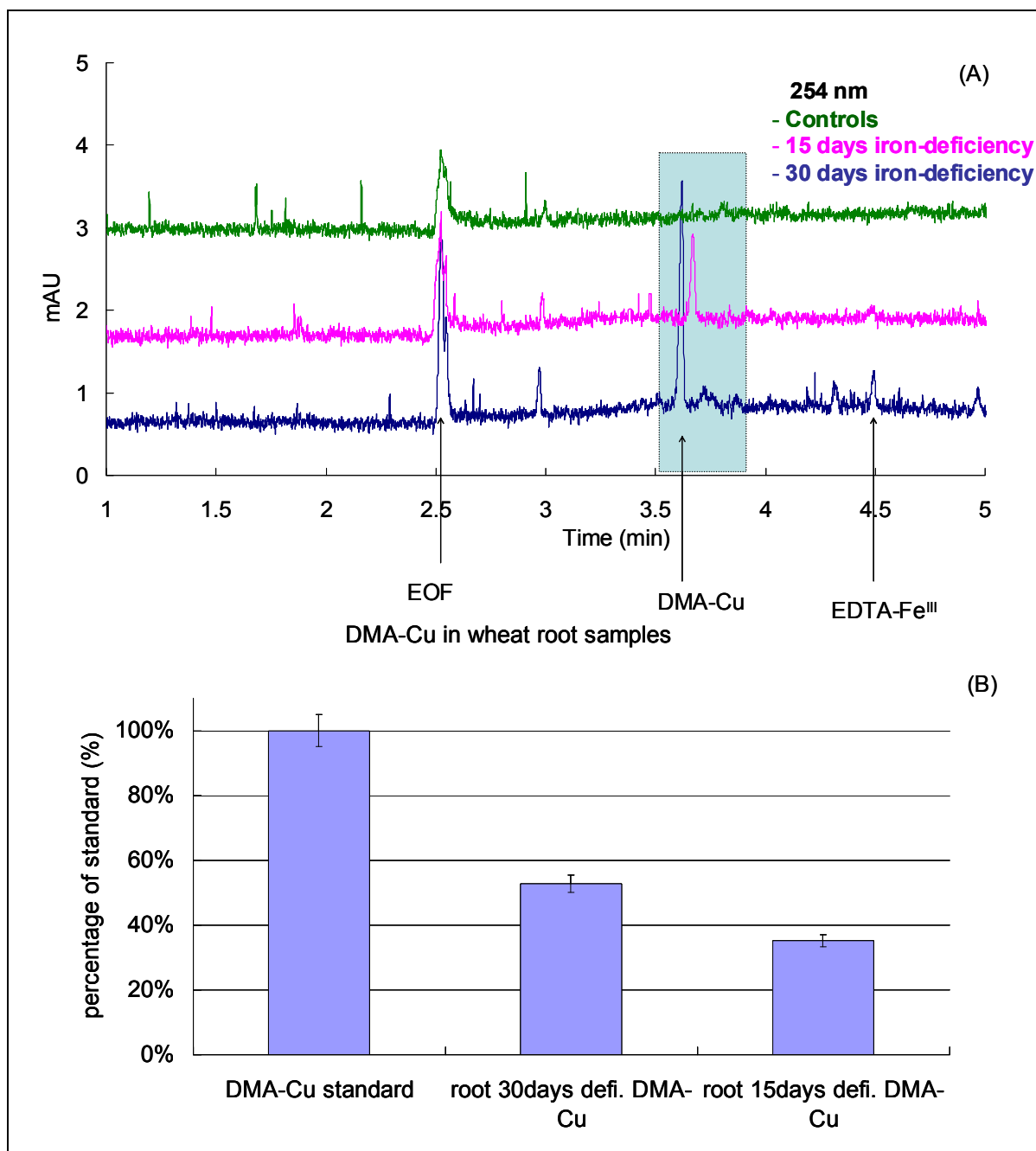


Figure 2-12. (A) Electropherograms of wheat root samples by DAD detector at 254 nm. (B) The peak areas of DMA-Cu found in wheat root are related to the peak area of standard. The peak area of DMA-Cu (80  $\mu\text{M}$ ) was set to 100%. "n.d." means not detected. Other conditions see Fig. 2-6. Wheat root samples: controls; 15days iron-deficiency; 30days iron-deficiency.

In Fig. 2-12, analyses are shown for the samples of wheat root, which were grown under iron-deficiency as well. DMA-Cu was detected and identified in iron-deficiency root samples. With increasing time of deficiency, increasing peak for DMA-Cu ( $\mu = -1.856 \times 10^{-4} \text{ cm}^2/\text{Vs}$ ) was found at 3.62 min. Similar to wheat shoot samples, there are still several unknown peaks, migrating later than EOF. EDTA-Fe<sup>III</sup> peak was found as well in this sample, according to the artefact biological sample preparation. The changes of the concentration of these identified compounds in wheat root samples are illustrated in Fig. 2-12B. The peak area of DMA-Cu standard (80  $\mu\text{M}$ ) was set to 100%. The concentration of DMA-Cu found in the wheat root sample grown under 15 days iron-deficiency is about 28  $\mu\text{M}$ , and increases to about 40  $\mu\text{M}$  in the wheat root sample grown under 30 days iron deficiency. With increasing iron deficiency

time of the root plants, more DMA-Cu was found. It means more DMA was synthesized under iron deficiency pressure by plants, in order to uptake iron. It is worthy to note that detection and identification of DMA-Cu in the wheat root samples were verified by HPLC/MS method as well (see chapter 4.4.3).

***Arabidopsis samples*** Five different cultivated *Arabidopsis* samples, which were grown under addition of nickel to the nutrient solution (see chapter 2.3.3) and differ only in their biological status (iron deficiency, knock-out or overexpressor of one membrane protein, encoding for a metal-chelate transporter), were investigated by this CZE method as well. The aim of investigating these samples is to verify the presence of a certain species, and to see the changes of these species in response to different biological status. Fig. 2-13A shows the detection of NA-Ni in 'KO-Fe+Ni' sample, which was grown in nutrient solution containing nickel but iron-deficiency and knocked-out of this membrane protein. Comparison with the spectrum and mobility to NA-Ni standard helps to the identity of this specie. This Ni-NA peak was detected in all five different cultivated samples, the semi-quantitative analysis of NA-Ni by comparing the peak area of it in different samples with the peak area of standard is shown in Fig. 2-13B. The peak area of NA-Ni standard (80  $\mu\text{M}$ ) with DAD at 200 nm was set to 100 %. The concentration of NA-Ni in wildtype (WT) sample without iron-deficiency is about 2  $\mu\text{M}$ . The concentration of NA-Ni is nearly trebled (about 5.1  $\mu\text{M}$ ) in the WT sample under iron-deficiency. The concentrations of NA-Ni in knocked-out (KO) samples with/without iron-deficiency are very similar and about 3  $\mu\text{M}$ . Identification and semi-quantitation of NA-Ni are in good agreements to the HPLC/MS method (chapter 4.4.3) of the same sample as well.

Separation and identification of cations, such as  $\text{K}^+$ ,  $\text{Ca}^{2+}$ ,  $\text{Na}^+$ , and Arg were successfully achieved by this proposed capillary electrophoresis method.  $\text{K}^+$ ,  $\text{Ca}^{2+}$ , and  $\text{Na}^+$  are well-known cations, which abound in plants. Identification of them was confirmed by investigating their respective standards. Separation and detection of inorganic cations are an advantage of CE method over HPLC as well.

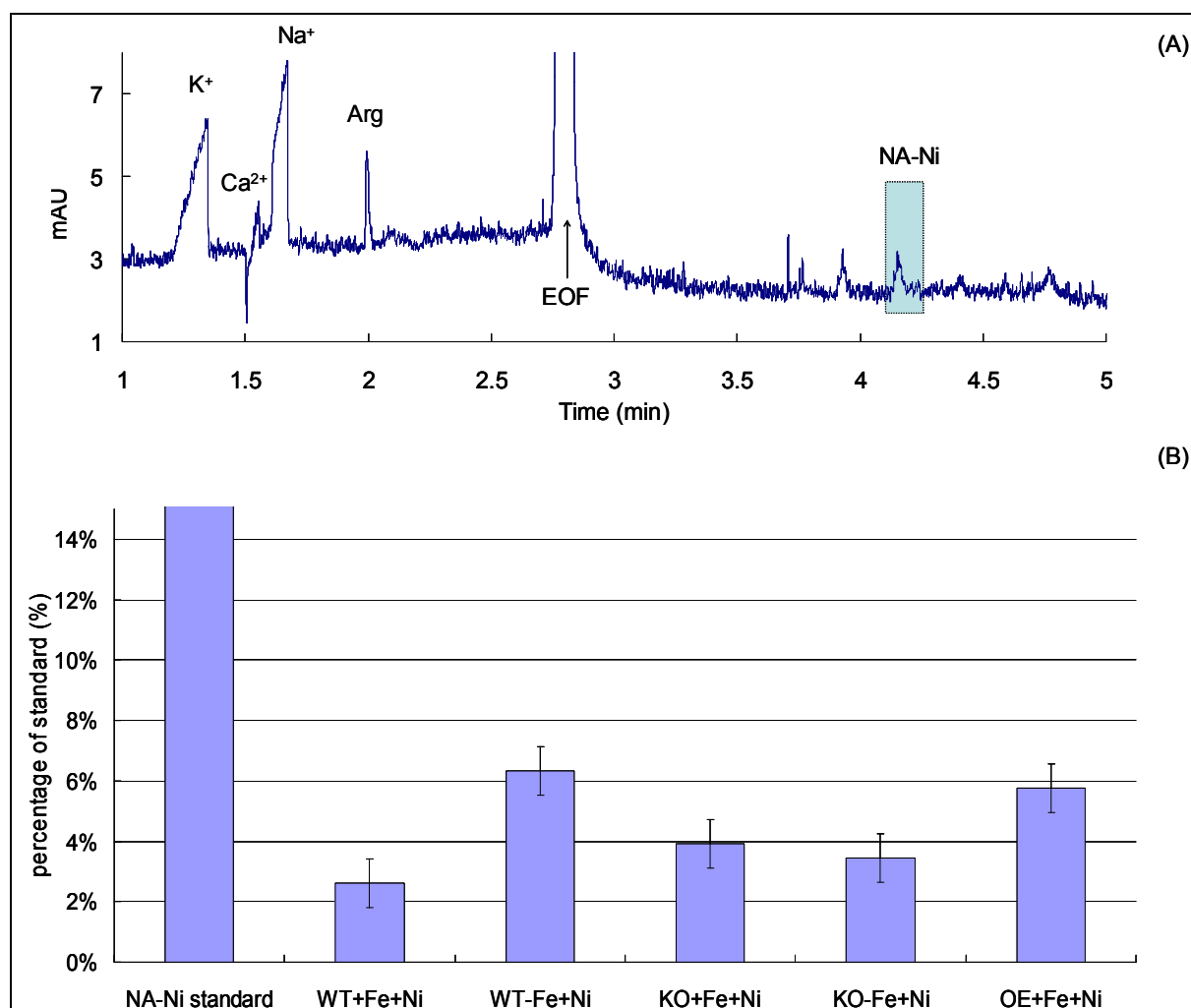


Figure 2-13. (A) Electropherograms of the xylem sap of Arabidopsis (“KO-Fe+Ni”) by DAD detector at 200 nm. (B) The peak area of NA-Ni presenting in xylem sap of Arabidopsis are divided by the peak area of respective standard. The peak area of NA-Ni (80  $\mu$ M) as standard was set to 100%. All peaks were taken with DAD at 200 nm. “WT” is wild type sample; “KO” is knock-out a membrane protein, which is responsible for transporting metal-species back to plants; “OE” is overexpressor of the same membrane protein; “+” is nutrient; “-” means deficient. Other conditions see Fig. 2-6.

The results obtained so far demonstrate, that the proposed CE method is well-suited to separate many important low-molecular-weight compounds in plants, including intact metal-species of Ni, Cu, Zn, Fe<sup>II</sup>, and Fe<sup>III</sup>. Detection of them is possible either with a diode array detector or, alternatively, with a capacitively coupled contactless conductivity detector. An identification of some of these LMW species in plants is possible based on the combination of mobility and UV spectral data. The identity and concentration changes of these species are also verified by HPLC/MS method of the same samples in the following chapter 4.4.3.

#### 2.4.4 Isomers separation by zwitterionic nonaqueous capillary electrophoresis (ZIC-NACE)

From the investigations in the previous chapters it is clear, that capillary electrophoresis is a good method to separate and detect the important ligands and metal-PS species in real plants. However, there are still some species, which are not baseline separated by the above CZE method. Esp. the isomers of Fe<sup>III</sup>-EDDHA were detected as one single peak (see Fig. 2-6). To improve the separation and detection of isomers, a novel coated capillary (zwitterionic capillary) was investigated with a high percentage of organic solvent inside buffer solution.

Zwitterionic additives are commonly used in capillary electrophoresis for separation of inorganic anions and basic proteins in the last several years [90-93]. However, interaction between analytes and additives may cause a dissociation of metal-ligand species. Therefore, a specially coated, zwitterionic capillary was investigated in order to develop a nonaqueous capillary electrophoresis method, which can be applied to improve the separation of isomers of EDDHA-Fe<sup>III</sup>, as an alternative to the “normal” CE system described in the previous chapter. Since the zwitterionic functionality is covalently attached to the inner wall of the capillary, it is permanently charged at all practically relevant pH values, but overall neutral. The separation is achieved by the influence of EOF, and weak electrostatic interactions with either positive or negative charges. It has to be noted, that detailed investigations on the behaviour of such zwitterionic capillaries under influence of an electric field are not available to date. In particular, the formation of the zeta potential and the resulting EOF could be quite different to the situation in normal CE (using silica surfaces). Theoretically, anions and cations could be attached to the zwitterionic stationary phase simultaneously, giving rise to a very complex charge layer structure at the capillary surface. Practically, however, a normal EOF is observed (towards the cathode). This is explained by the negatively charged sulfonic acid group pointing out to the solution, while the positively charged ammonium group is more hidden inside the covalent layer. Nevertheless, the EOF strength is much reduced by the presence of the quaternary ammonium group.

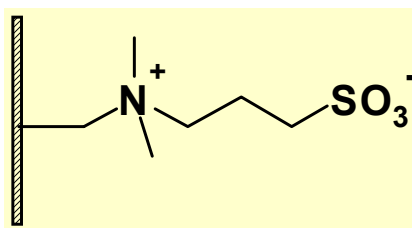


Figure 2-14. The chemical formula of the zwitterionic coating.

**Buffer and electric field** Organic solvents as additives for background electrolyte in CE are selected according to their dielectric constant, their viscosity, their UV transparency, and their capability to increase intermolecular interactions with the analytes, leading to significant changes in selectivity in analytical separations. Solvents with high dielectric constant and low viscosity are usually the most suitable for nonaqueous BGE [94]. The most commonly used solvent in NACE is acetonitrile. This solvent has a dielectric constant which places it towards the lower polarity end of organic solvents [95]. Acetonitrile is also well-known as UV transparent solvent, which offers little background and noise, if UV detection at low wavelengths is needed. Therefore, acetonitrile (ACN) was selected as organic solvent in the buffer system. To check the EOF strength, +20 kV was applied with a buffer of ammonium acetate (25 mM) and acetonitrile (v:v = 80:20) adjusted to pH 7.3 to investigate EDDHA-Fe<sup>III</sup>. But, after a separation time of 15 min. no EDDHA-Fe<sup>III</sup> could be detected. Since it is known that this species is negatively charged (see chapter 2.4.2), a reversed high voltage of -30 kV was applied to investigate EDDHA-Fe<sup>III</sup> with the same buffer. A migration time of EDDHA-Fe<sup>III</sup> was found at 3.93 min at DAD detector (data not shown). However, this buffer system offered a poor detection baseline and poor peak shape with DAD, and no detection with C<sup>4</sup>D. Therefore, a buffer consisting of MES/TRIS (50:50 mM) in acetonitrile at pH 7.3 was tested, resulting in a smooth baseline and good peak shape with DAD detector. Even the baseline with C<sup>4</sup>D is smooth, no peak of EDDHA-Fe<sup>III</sup> was detected. This may be caused by the co-elution



with a big system peak, which may be caused by the injection. This type of buffer, combined with a reversed electric field, was applied for further investigations. As already explained in chapter 2.1.2, the reversed electric field may lead to a fast and sensitive analysis of anionic species, but inevitably excludes neutral and cationic analytes from reaching the detector. For the zwitterionic capillary and anionic species, a reversed electric field is necessary, because the EOF is obviously too low (even at pH 7.3) to counterbalance the electrophoretic mobility of anions.

**Investigation of the percentage of acetonitrile** In NACE, solvating water molecules are replaced by the organic solvent used. Since the electrophoretic mobility of the ions is directly related to their solvated ionic radius (Eq. 2), the replacement of water molecules will have significant impact on solute mobility. The change of solvent properties has a significant influence on solute solvation and ion-ion interactions. The variation of the solvent can change solute migration and separation selectivity tremendously. Consequently, the mixing of solvents to varying ratios turned out to be a powerful tool for separation optimization in NACE [94].

Although a simultaneous separation of cations, neutral compounds, and anions is not possible with this method, our main target compounds, isomers of EDDHA-Fe<sup>III</sup> are negatively charged under these conditions. EDDHA and EDDHA-Fe<sup>III</sup> were investigated by different percentages of acetonitrile, namely 20 %, 40 %, 60 %, and 80 % in the buffer solution. Citric acid, Asp, and Glu, as important low-molecular-weight compounds in plants, were investigated as test substances as well. From Fig. 2-15, with increasing percentage of acetonitrile in buffer, a linear increase of the migration time of citric acid, Asp, and Glu was found. The migration times of EDDHA and EDDHA-Fe<sup>III</sup> increase with increasing concentration of acetonitrile up to 50 %. However, with higher amounts of acetonitrile, the migration times of EDDHA and EDDHA-Fe<sup>III</sup> start to decrease again. The migration time of all these compounds are listed in Table 2-4.

Table 2-4. Migration times of the analytes in Fig. 2-15.

	$t_{\text{citric acid}}$ (min)	$t_{\text{Asp}}$ (min)	$t_{\text{Glu}}$ (min)	$t_{\text{EDDHA}}$ (min)	$t_{\text{EDDHA-Fe}}$ (min)
20 % ACN	1.24	2.09	2.51	4.31	3.39
40 % ACN	1.97	2.83	3.12	6.03	4.02
60 % ACN	2.57	3.72	3.93	5.30	3.19
80 % ACN	4.02	4.61	4.71	4.35	2.59

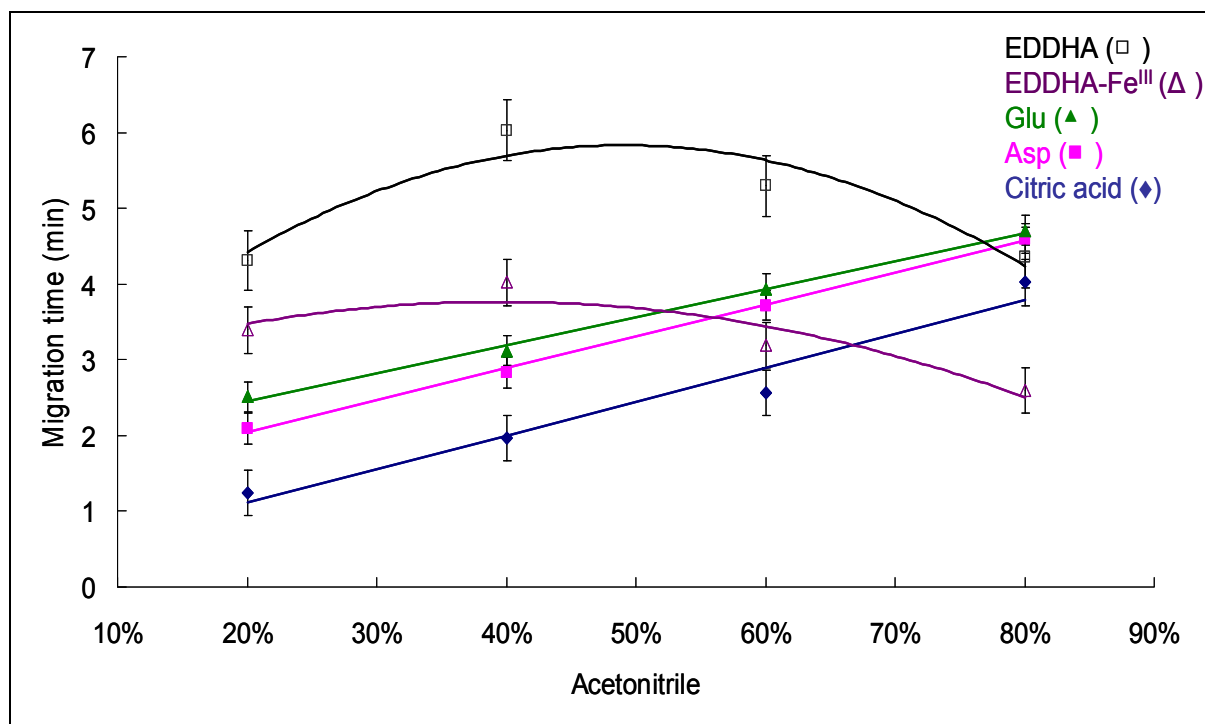


Figure 2-15. Acetonitrile concentration vs. migration time in ZIC-CE method on CE system 2: citric acid, Asp, Glu, EDDHA, and EDDHA-Fe<sup>III</sup> with 20 %, 40 %, 60 %, and 80 % acetonitrile in MES/TRIS (50:50 mM), pH 7.3, - 30 kV, Injection: 40 mbar, 2 s; DAD detector at 200 nm. The concentration of citric acid, Asp, Glu, and EDDHA are 150  $\mu$ M each, and the concentration of EDDHA-Fe<sup>III</sup> is 150:80  $\mu$ M (EDDHA: Fe<sup>3+</sup>).  $L_{\text{total}} = 48\text{cm}$ ,  $L_{\text{UV}} = 39.5\text{ cm}$ , and  $L_{\text{C}^4\text{D}}$  is 35 cm.

**Separation of isomers** To deduce the separation behaviour of PS and metal-PS, EDDHA and EDDHA-Fe<sup>III</sup> were investigated as a simple and cheap model compounds. From Fig. 2-16 it is seen, that there is no separation of the EDDHA-Fe<sup>III</sup> isomers with low concentration of acetonitrile. This situation is quite similar to that in normal CE (see chapter 2.4.2), but now the EDDHA-Fe<sup>III</sup> species migrate faster than the free ligand (due to the reversed electric field). With a concentration of acetonitrile of 60 %, however, a separation of the two EDDHA-Fe<sup>III</sup> isomers is possible. By using even higher percentages of acetonitrile, e.g. 80 %, a very good separation of them is achieved, which demonstrates the suitability of this new zwitterionic capillary for separation of isomers. From Fig. 2-16, the separated two EDDHA-Fe<sup>III</sup> isomers can be identified by two factors. One is the ratio of these two isomers peaks on UV detector. The ratio of peak 1 to peak 2 is about 4:3 on UV detector. It agrees to the ratio of *meso*-Fe<sup>III</sup>-EDDHA to *rac*-Fe<sup>III</sup>-EDDHA published by Hernandez-Apaolaza *et al.* [85]. In Fig. 2-16, peak 1 may be *meso*-Fe<sup>III</sup>-EDDHA, and peak 2 may be *rac*-Fe<sup>III</sup>-EDDHA. The other factor is the migration order of them. Even they are isomers, the charge state of these two molecules are slightly different from each other (see Table 2-2). The pK value of each functional group on *rac*-Fe<sup>III</sup>-EDDHA is higher than it on *meso*-Fe<sup>III</sup>-EDDHA. Under pH 7.3, the *rac*-Fe<sup>III</sup>-EDDHA is less negatively charged than *meso*-Fe<sup>III</sup>-EDDHA. Therefore, *rac*-Fe<sup>III</sup>-EDDHA should migrate later than *meso*-Fe<sup>III</sup>-EDDHA with this ZIC-NACE method. Consequently, peak 1 in Fig. 2-16 is *meso*-Fe<sup>III</sup>-EDDHA and peak 2 is *rac*-Fe<sup>III</sup>-EDDHA.

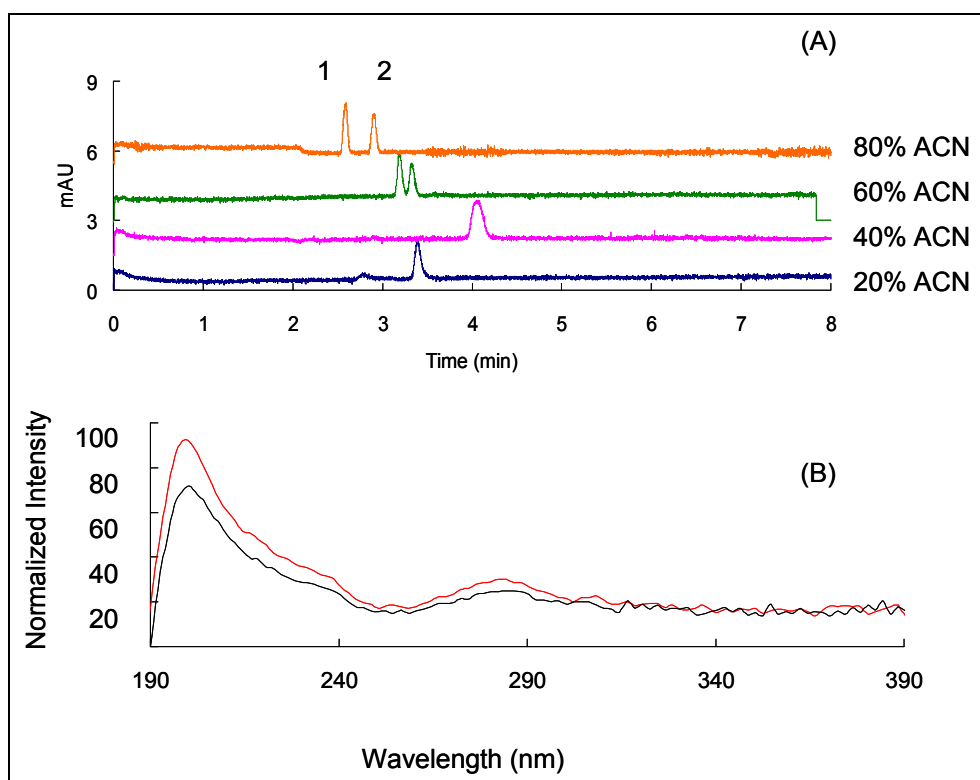


Figure 2-16. (A) Electrophoregrams of EDDHA-Fe<sup>III</sup> isomers with different percentage of acetonitrile in MES/TRIS (50:50 mM) pH 7.3 by DAD detector at 280 nm. 1: *meso*-Fe<sup>III</sup>-EDDHA, whose spectrum is (B, red curve); 2: *rac*-Fe<sup>III</sup>-EDDHA, whose spectrum is (B, black curve). Their spectra were collected with DAD from 190 nm – 390 nm. Other conditions see Fig. 2-15.

80 % acetonitrile offers a baseline separation of isomers, *rac*-Fe<sup>III</sup>-EDDHA and *meso*-Fe<sup>III</sup>-EDDHA. However with 80 % acetonitrile, the separation of amino acids and citric acid is worse than with lower percentages of acetonitrile. Considering both the separation of ligands and iron-EDDHA, the best separation is a buffer system with 60 % acetonitrile in MES/TRIS (50:50 mM). This buffer system offers the best separation efficiency not only of the ligands, but also of the iron complexes.

## 2.5 Conclusion

In this chapter, a new and effective capillary electrophoresis method, MES/TRIS (20:20 mM) as buffer, at pH 7.3, with a constant voltage 20 kV, was developed and applied to investigate the important LMW free ligands, and their metal-species, as well as real plant samples. For the first time, separation and detection of three phyto siderophores (DMA, MA, and *epi*-HMA) and NA were achieved by this proposed CE method. Also three Fe<sup>III</sup>-PS (PS = DMA, MA, and *epi*-HMA) species are separated without any stability problems, which present in HPLC. DMA-Cu and DMA-Zn are baseline separated, as well NA-Cu is baseline separated from NA-Ni and NA-Fe<sup>II</sup>. Complimentary information is obtained with DAD and C<sup>4</sup>D. Even some species are not baseline separated, such as NA-Ni and NA-Fe<sup>II</sup>, these important compounds are capable to be identified by their different DAD spectrum and effective mobility. The good applicability of this method to real plant samples was proved by investigating different kinds of plant samples, such as wheat samples and *Arabidopsis* samples. Separation and detection of DMA-Zn and DMA-Cu in wheat samples, also NA-Ni in *Arabidopsis* samples, are successfully achieved by this CZE method. The concentration changes of these detected metal-species in plants, which are correlated to biological process, can be seen simultaneously by this method. The identity and concentration changes of these present species in plants are not only

verified by electrophoretic mobility and UV spectrum of respective standard, but are also in agreement with analyses of the same samples by HPLC/MS (chapter 4.4.3.4).

A special, novel coated capillary (zwitterionic coated capillary) was used to separate isomers of Fe<sup>III</sup>-EDDHA. A buffer with 60 % acetonitrile in MES/TRIS (50:50 mM), at pH 7.3, with a constant reversed voltage of -30 kV, was found to be the optimal condition of baseline separating isomers of EDDHA-Fe<sup>III</sup>, as well some important free ligands including citric acid, Asp, and Glu. Since the LMW species presenting in low micro molar concentration range in plants, their low UV absorbance, and their low conductance, it is very attractive to improve the detection limit of DAD and C<sup>4</sup>D for these LMW species on capillary electrophoresis. Therefore, an on-column photo reactor was innovatively developed in the following research (see chapter 3).

### **3 Development and application of photo reactors for CE and HPLC**

The main conclusion from the investigation of low-molecular-weight ligands and metal species by capillary electrophoresis is (see chapter 2), that CE is very well suited for the separation of such compounds, but the detection is hampered by their low UV absorptivity, low conductance under neutral pH, and their low  $\mu\text{mol/L}$  concentration range in plants. Therefore, an enhancement of detection sensitivity and/or detection selectivity of metal-species is very attractive. Because of the well-known photochemical activity of iron-species (e.g. Fenton reaction [96-101], photo-Fenton reaction, and ligand-dependent redox-activity of Fe-species), it should be possible to exploit this photochemistry for selective signal enhancement of iron-species after chromatographic or electrophoretic separation. In this chapter, respective experiments are described and discussed, including the design and development of a new on-column photo reactor for CE (for HPLC, photochemical post-column reactors are commercially available).

#### **3.1 Photo reactors in CE and HPLC**

##### **3.1.1 Commercially available photo reactors for HPLC**

Chromatographic separation techniques belong to the most popular analytical methods, because of their wide applicability, and also because of the availability of many different detectors, enabling sensitive and selective detection of various classes of compounds (incl. metal species). However, it is not always possible to achieve the desired detection limit. In the last three decades, many applications of post-column photo reactions have been used in HPLC as a means of improving detection selectivity or sensitivity [102-111]. When light is added “as a reagent”, the procedure is called photochemical reaction or photo-derivatization. Detectors, which are commonly UV detector, fluorescence detector, and electrochemical detector, in chromatography can be used to detect the derivatization products. Photo reactors are being used currently, enabling a great variety of derivatization schemes. However, each one is suitable for a particular sample type.

The two general goals of any derivatization technique are: i) to increase detection sensitivity, normally introducing suitable chromophores or fluorophores or obtaining a different compound with higher response; and ii) to increase the selectivity, by applying a specific and selective derivatization reaction to derive only the compound or compounds of interest and to detect them selectively in a complex matrix.

There are several types of reactions that may be initiated by photochemical activation, although the application of any of them is limited to those compounds that have the right molecular structure to absorb light of enough energy and also to react appropriately. These reactions can be: oxidation and reduction, molecular rearrangements, addition and elimination, cyclization, dimerization and polymerization, etc. [112].

### 3.1.2 Existing photo reactors for CE

In comparison with the vast amount of existing applications of photo reactors in HPLC, only few applications of photo reactors have been reported for CE. Recently, the CE photochemical reaction detection (PCRD) with a laser beam for detection of substituted polycyclic aromatic hydrocarbons (PAHs) [113] and derivatized amino acids [114] significantly improved limits of detection (LODs). In the PCRD system for capillary electrochromatography from Dickson *et al.* [113], analytes are irradiated with a UV laser after separation by CE. The analytes, absorbing UV light, are promoted from ground state ( $^3\text{O}_2$ ) to an excited state ( $^1\text{O}_2$ ) which reacts rapidly with *tert*-butyl-3,4,5-trimethylpyrrolecarboxylate, which is added to the running buffer. The UV absorbance detection is based on the loss of pyrrole. The LOD is improved significantly by only a small irradiation window. However, the method is costly particularly when UV lasers are required for excitation. Moreover, these photochemical reactions are only efficient in organic solvents, limiting the range of CE separations that can be carried out when PCRD is employed.

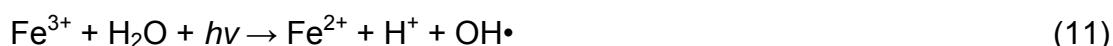
### 3.1.3 Suitability of a photo reactor for detection of metal-species

The well-known photochemical activities of iron-species: i) Fenton reaction [96-101], ii) photo-Fenton reaction, and iii) redox-activity of Fe-species, which may offer better detection sensitivity of iron species.

**Fenton reaction** Fenton's Reaction has been known since 1894 and is currently one of the most powerful oxidizing reactions available. The reaction involves hydrogen peroxide and ferrous iron catalyst (Eq. 10). The peroxide dissociates into a hydroxide ion and a hydroxyl free radical. The hydroxyl free radical is very reactive and can oxidize organic molecules efficiently. Fenton reaction has been found to be the key reaction in the oxidation of membranes [115 and 116], oxidation of amino acids [117]. Important are also some reactions where biological reduction agents are present, such as ascorbic acid or thiols [118 and 119].



**Photo-Fenton reaction** It has been known for a long time that the photochemical irradiation of ferric species leads to their reduction [120-126]. The effectivity of this reaction depends very much on the type of the ferric substance (ligand), on the irradiation wavelength used, and on the pH of the aqueous solution. The ferrous reaction product can then take part in the normal Fenton reaction.



**Redox activity of Fe-species** When a rather strong  $\text{Fe}^{2+}$  complexing agent L is present in the medium, L is able to take  $\text{Fe}^{2+}$  from the resulting  $\text{Fe}^{2+}$ -siderophore complex since siderophores usually have weak affinities for  $\text{Fe}^{2+}$  [98]. The reduction of ferric-siderophores can be driven to completion by the coupled thermodynamically

favorable complexation of  $\text{Fe}^{2+}$  by L (ligand):



Considering these above photochemical activities of iron-species, an on-column photo reactor for CE can be applied for improving the detection of those small, non-covalent iron-species in plants.

## 3.2 Experimental

### 3.2.1 Ligands, model complexes, and real plant extracts

*Ligands and metal-species:* All the ligands are dissolved in half diluted buffer (in CE) or undiluted buffer (in cFIA). Stock solutions of iron(III) (10 mg/mL diluted in HCl) and gluconic acid (50% in water) were used to prepare working standards in the micro molar concentration range by direct dilution with buffer. Iron(III) was spiked into ligand solution at ligand/iron ratio 2:1 to build up model iron complexes. Iron(II) chloride tetrahydrate was dissolved in half diluted buffer (in CE) or undiluted buffer (in cFIA) and spiked into ligand solution at ligand/iron ratio 2:1 directly before the sample injection. The purity and purchase of chemicals please see Appendix.

*Plant extracts* were obtained from the 'Institute of Plant Nutrition', Hohenheim University, Stuttgart, Germany.

All the model complexes and real plant samples were filtered by 2  $\mu\text{m}$  membrane filter.

### 3.2.2 HPLC with post-column photo reactor system

The mobile phase was 60 mM sodium phosphate buffer in acetonitrile at a ratio of 2:3 (phosphate: acetonitrile), and degassed ultrasonically. For flow injection, no analytical column was applied in the system, and the photo reactor was positioned directly behind the sample injector and in front of the diode array detector. For ZIC-HILIC chromatography, the analytical column was ZIC-HILIC (100 $\times$ 4.6 mm I.D.) positioned ahead the post-column photo reactor. The sample was eluted at a flow rate of 0.5 mL/min and detected on-line by a diode array detector (200 nm). Scan range of UV spectra was set to 200 nm and 600 nm, respectively. HPLC was performed using a Knauer gradient pump K1001 with solvent organizer K1500, solvent degasser, titanium mixing chamber and Rheodyne 9010 injection valve with 20  $\mu\text{l}$  sample loop. A photochemical reaction unit ('Beam Boost'; ICT, Frankfurt, Germany) fitted with 8 W, 254 nm UV lamp (UV Products, Cambridge, UK) was positioned behind the analytical column with 10 m reticulated Teflon tubing around the UV lamp. All capillaries and connections were made of PEEK.

### 3.2.3 Capillary electrophoresis system

All capillary flow injection and capillary electrophoresis separations were carried out on CE system 1 (see chapter 2.3). Fused silica capillaries with transparent coating (50  $\mu\text{m}$  i.d., 360  $\mu\text{m}$  o.d.) were obtained from CS-Chromatographie Service (Langerwehe, Germany). Total length was 85 cm, the length to the UV detector was 56 cm, and to the C<sup>4</sup>D detector 65 cm. Injection of the sample solution was performed hydrodynamically (40 mbar for 6 s). For capillary flow injection, a constant pressure of 500 mbar was applied instead of high voltage. For capillary electrophoresis, constant high voltage of +20 kV was applied. The capillary was rinsed with 0.1 mol/L sodium hydroxide and deionized water for 10 min, and then equilibrated with carrier electrolytes for 30 min at the beginning of each day. Between all cFIA and CE



separations the capillary was rinsed with 0.1 mol/L sodium hydroxide for 3 min, and deionized water for 4 min, and then with carrier electrolytes for 5 min.

### 3.2.4 On-column CE photo reactor

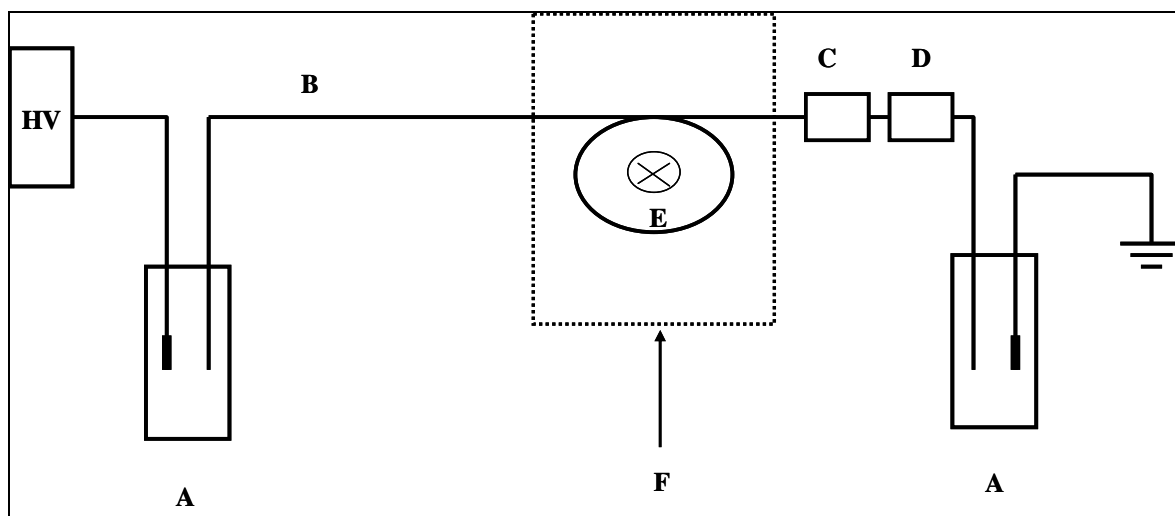


Figure 3-1. Schematic of the instrumental setup: HV, high voltage power supply; (A) buffer reservoir; (B) fused silica capillary with transparent coating; (C) UV detector at 205 nm; (D) conductivity detector; (E) Pen-Ray mercury lamp; (F) adjustable photo irradiation window compartment.

A mercury standard Pen-Ray lamp (UVP, Cambridge, UK) was applied as the on-column photo reactor (see Fig. 3-1). It was placed in the CE system directly in front of the UV detector, but optically shielded from the detector inside a cardboard made of black paper. This 'irradiation window' compartment contained the photo-accessible part of the transparent capillary, which was coiled around the lamp (only one turn) at a distance of approximately 2 cm. The lamp emits the mercury spectrum with the maximum intensity at 254 nm. The intensity of the lamp is  $2000 \mu\text{W}/\text{cm}^2$  (directly at the surface of the lamp). The length of the 'irradiation window' (i.e. the part of the transparent capillary, which is irradiated by the lamp), is easily adjustable and variable in length from 3.2 to 14 cm, e.g. by changing the radius of the coiling. The whole irradiation window compartment was flushed with a stream of nitrogen to keep it at a constant temperature.

### 3.3 Results and Discussion

From chapter 2, it can be seen that capillary electrophoresis is a powerful separation technique for LMW ligands and their metal-species in plants. However, their determinability in real plants is limited due to their low UV absorptivity, low conductance at neutral pH, and their low  $\mu\text{mol/L}$  concentration range in plants. In order to enhance the detection sensitivity and/or detection selectivity of metal-species, a photo reactor was chosen by taking advantages of photochemical activities (see chapter 3.1.3). At first, a commercially available post-column photo reactor for HPLC system was applied, to investigate the photochemical reactions of the LMW ligands and iron-species (see chapter 3.3.1). To see the influence of the sensitivity and selectivity of iron-species in capillary electrophoresis, a new on-column photo reactor was set up by using a fused silica capillary with UV-transparent coating, and a Pen-Ray mercury lamp (see Fig. 3-1). Model iron complexes, which are selected according to their well-known chelating and photochemical properties (e.g. EDTA), or according to their importance in plants (e.g. amino acids and organic acids), are investigated by both capillary flow injection (cFIA) and capillary electrophoresis (CE) to study the photoinduced sensitivity changes of iron-species. In order to find out the optimized irradiation time for later investigating real plant extracts, the relationship between irradiation time and detection sensitivity of iron-species are studied. To demonstrate the applicability of this new invented photo reactor on CE system, real plant extracts are investigated by it. UV detector and capacitively contactless conductivity detection ( $\text{C}^4\text{D}$ ) are applied in series on CE system, to monitor the changes of the UV absorbance and conductance of model-complexes and LMW species in plants by photochemical reaction.

#### 3.3.1 HPLC Flow Injection Analyses (FIA) with online photo reactor

To get a fast scanning of the photochemical activities of the LMW ligands and their metal-complexes, first investigations were carried out by flow injection analyses (FIA). In HPLC flow injection, no analytical column was applied, and the sample was injected directly into the system. After passing the photo reactor absorbance was detected on-line by a diode array detector at 205 nm. Various organic acids, amino acids, and the selected ligand-iron-species (2:1 molar ratio) were applied for flow injection analysis with the photo reactor. The absorbance of pure ligand shows no detectable difference with or without irradiation. But the absorbance of the respective iron complex was significantly enhanced under irradiation. This is shown exemplarily in Fig. 3-2A (pure ligand) and Fig. 3-2B (iron-complex) for the DAD detection of serine (Ser). It shows a very efficient and selectivity enhancement of the absorbance of serine in the presence of Fe(III). A further investigation should be an investigation of real plant sample after analytical column separation on the post-column photo reactor, in order to see effects of the real plant samples.

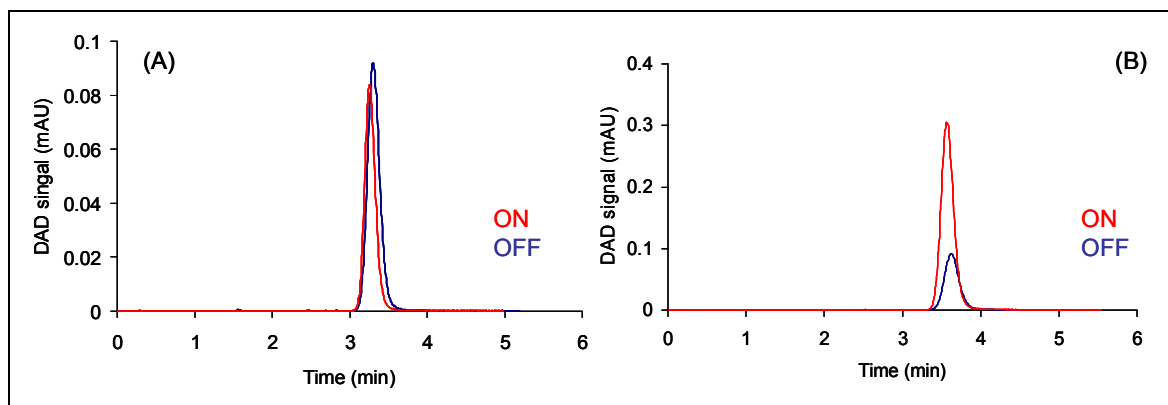


Figure 3-2. Chromatograms were obtained from DAD detector at 205 nm with FIA: (A) 200  $\mu$ M serine with photo reactor on and off; (B) serine plus iron (2:1) with photo reactor on and off. Eluent: 40 % phosphate (60 mm, pH 7.5) + 60 % acetonitrile. Injection loop was 20  $\mu$ L. Flow rate was 500  $\mu$ L/min.

### 3.3.2 HPLC with post-column photo derivatization

With fast scanning of pure ligands and their metal-species by FIA, it is clearly seen that selectively enhancements of the detection signals of metal-species were obtained on diode array detector (DAD). It is worthy to test with a set of real plant samples with this post-column photo reactor. An analytical column, zwitterionic hydrophilic interaction liquid chromatography column (ZIC-HILIC), was applied here for investigating the plant sample with a post-column photo reactor. One plant extract, which contains iron, was investigated with photo reactor “on” and “off”. From Fig. 3-3, significant changes of sensitivity were found. With photo reactor “off”, there are only several small peaks detected with DAD detector at 205 nm. The UV spectra of the sample both with photo reactor “on” and “off” were collected from 200 nm to 600 nm. When photo reactor is on, enhancement of several peaks appeared, and one new peak was detectable at 12 min. Comparing both chromatograms and spectra of this plant sample with photo reactor on and off, sensitivity of several peaks was found with photo reactor on. It seems photo reactor can be a good choice for capillary electrophoresis to improve the selectivity and sensitivity of UV and conductivity detection, as well. The details investigation of on-column photo reactor on capillary electrophoresis, therefore, was carried out in order to improve the sensitivity of iron-species in plants.

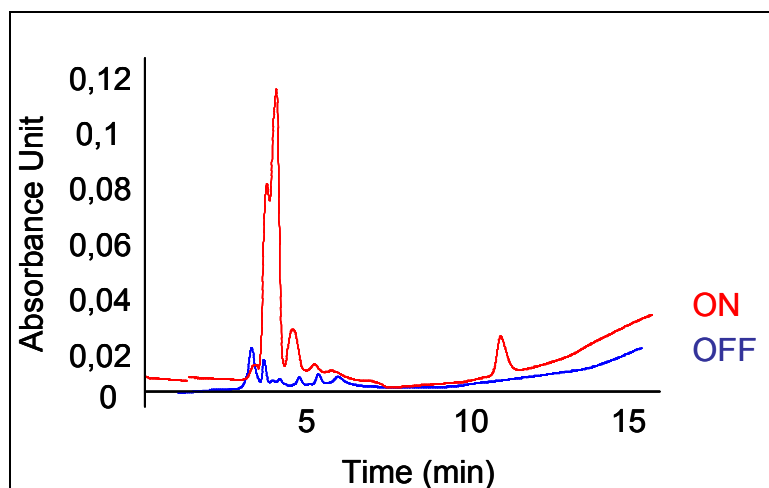


Figure 3-3. Chromatograms were obtained from DAD detector at 205 nm after separation on ZIC-HILIC column (100×4.6 mm) with photo reactor ON and OFF. The other conditions are the same as listed in Fig. 3-2.

### 3.3.3 Capillary Flow Injection (cFIA) with online photo reactor

Since significant enhancement of detection sensitivity of iron-species was observed by applying a post-column photo reactor in HPLC system, an on-column photo reactor for CE seems feasible. Therefore, a new on-column photo reactor was set up by using a fused silica capillary with UV-transparent coating, and a Pen-Ray mercury lamp (see Fig. 3-1). The proposed photo reactor illuminates some centimeters of the transparent capillary, corresponding to a volume of 100 -500 nL. The irradiation window of it is adjustable both in length and in location. To do the fast scanning of the free ligands and their metal-species, capillary flow injection (cFIA) was carried out.

In cFIA, a pressure-driven flow (500 mbar) is used to transport the analytes to the two detectors, instead of high voltage in CE. With the 50  $\mu\text{m}$  i.d. capillary, this is equivalent to a flow-rate of 23 cm/min (= 0.45  $\mu\text{L}/\text{min}$ ), and to a photo irradiation time of approximately 0.6 min with a 14 cm long photo irradiation window. Clearly, there are no separations in cFIA, but this method is ideally suited for screening purposes. Here, the injected samples are screened for the presence of photoactive compounds, provided that the photo reaction leads to a change in absorbance (UV detector) and/or conductivity (conductivity detector). The photoactivity was tested for the ligand itself and for the respective ligand-iron-species (2:1 molar ratio) by comparing the detector signals with photo reactor 'off' and 'on'. Some tests were also done with different ligand/iron ratios, ranging from 1:1 up to 4:1. For some iron-ligand systems (e.g. iron-EDTA), equimolar concentrations were advantageous in terms of sensitivity, while for other systems (e.g. iron plus amino acids) an excess of ligand resulted in better sensitivity. The latter may be explained by a more effective complex formation at excess of ligand for the amino acid complexes of iron, which are only moderately stable. For the iron-EDTA system, an excess of ligand is not necessary to form a stable complex. However, the dependence of photoactivity on ligand concentration was not investigated in detail, because the mechanism may be very complex, depending also on pH, redox potential of the respective iron-species, etc. As a

compromise, which resulted in increased sensitivity for all investigated iron-ligand systems, a 2:1 excess of ligand was used for further studies. For both, UV detection and conductivity detection, the sensitivity of the pure ligand shows no detectable variation with photo reactor on and off, but after formation of the respective iron complex, the signal is significantly enhanced with the photo reactor switched on. This is shown exemplarily in Fig. 3-4A (pure ligand) and Fig. 3-4B (iron-complex) for the conductivity detection of gluconic acid. A very similar behavior is observed for other ligands and their iron complexes, e.g. amino acids (Asp, Ser), organic acids (gluconic acid, oxalic acid) and EDTA. The signal enhancement factors for the respective iron species are shown in Table 3-1. As expected, the magnitude of the effect depends on the type of iron-species and on the type of detector. For the pure ligands, no change is observed. Hence, the photo reaction is selective for the iron-species, provided that no other photoactive metal species are present. For plants, this assumption should be fairly well met, because most metals, that are known to effectively induce photo reactions (e.g. cobalt(III)- or uranyl-complexes), are only present at trace levels, which are orders of magnitude lower compared to the micro molar iron concentration.

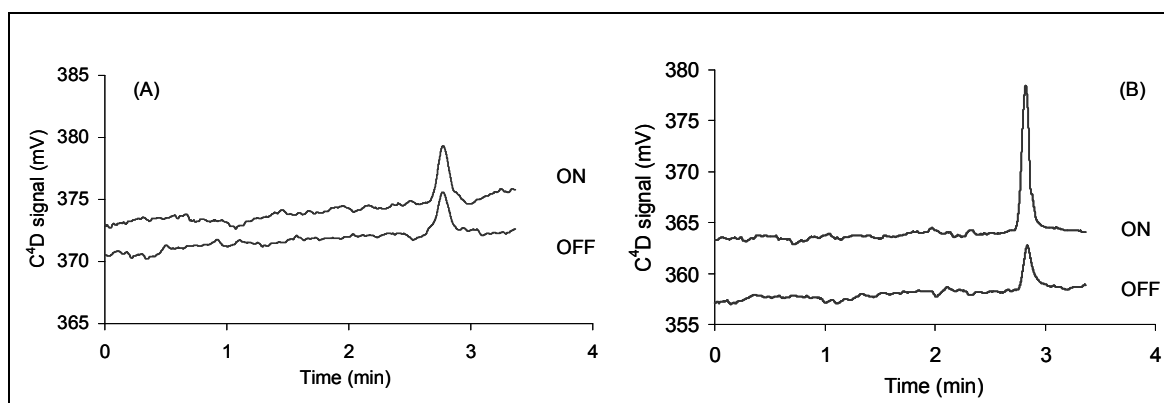


Figure 3-4. Electropherograms were obtained from photo reaction and conductivity detector with cFIA: (A) 200 µmol/L gluconic acid with photo reactor ON and OFF; (B) gluconic acid plus iron (2:1), with photo reactor ON and OFF. Phosphate buffer (10 mM, pH 7.5), injection is performed by 40 mbar pressure for 6 s. The flow injection pressure is 500 mbar.

Table 3-1. The enhancement factor of iron-species with photo reaction in capillary flow injection system, with a photo irradiation time of 0.6 min

Ligand-Fe (2:1)	Enhancement factor with UV detector	Enhancement factor with C <sup>4</sup> D
Oxalic acid-Fe	6	2.7
Gluconic acid-Fe	3	3.5
EDTA-Fe	4	1.5
Asp-Fe	4	2.0
Ser-Fe	4	1.6

However, it should be kept in mind that the selectivity of the photo reactor is not simply given by the presence of iron, but is given by the presence of a certain class of iron-species (i.e. photoactive iron-species). General structural requirements for such iron-species and mechanistical details of the respective photo reactions are known

from investigations of the (photo-) Fenton reaction [96-99], and will not be recapitulated here. Briefly, the two most important requirements are: (i) the species must have the right chemical structure to absorb light of enough energy to react; and that (ii) a suitable redox system is formed (ferrous and ferric complexes of the respective ligand) for interaction with oxygen species that are present in the respective system. Obviously, the first requirement plays a pivotal role for the plant ligands, which exhibit only very low UV absorbances before binding of iron, and thus are not photoactive. After complexation with iron, the absorbance spectrum and also the redox chemistry is completely changed, resulting in the photoactivity of the species. The selective detection of photoactive iron-species may be very attractive as a means to detect Fenton-active species that are closely related to oxidative damage in plants [23]

### **3.3.4 Capillary Electrophoresis with on-column photo reactor**

From the precious chapter 3.3.3, this new constructed on-column photo reactor does significantly enhance the sensitivity of iron-species with both UV detector and conductivity detector in cFIA investigations. Therefore, model iron species were investigated by capillary electrophoresis with this photo reactor “on” and “off” in the following chapter.

#### **3.3.4.1 Investigation of model iron-species**

In capillary electrophoresis, a high voltage of +20 kV (~235 V/cm) was used for separation. All other experimental parameters, including type of capillary, buffer, and type and concentration of model iron-species were unaltered. With a 14 cm photo irradiation window, the signal of iron-species vanished completely from both UV and C<sup>4</sup>D detectors. This is shown in Fig. 3-5 for the Fe<sup>III</sup>-complex of the phyto siderophore, DMA, a very stable iron-complex of 1:1 stoichiometry [23]. The pure ligand without iron was also investigated, but no effects were observed with the photo reactor switched on (results not shown). While the latter result agrees with the results of the cFIA experiments, the results for iron-species in CE are completely different from the respective cFIA measurements, that mean decreasing detector signals during irradiation). This behaviour was also observed for several other model iron-species; but with different kinetics in each case. Details of the kinetics of the decrease are discussed in chapter 3.3.4.2.

The mechanism, which causes the different results of CE and cFIA, is not yet clear. The only difference between cFIA and CE is the additional electric field in CE, which influences the zeta potential and the double layer on the capillary wall. One possible explanation for the observed effect in CE would be a different charge state and orientation of molecules, especially iron-species, induced by the electric field. The UV light also interacts with the buffer molecules in the double layer, and thus has an influence on separation parameters. In particular, this is important for organic (i.e. UV-absorbing) buffers, such as MES/TRIS at pH 7.5, which we used as alternative for the phosphate buffer. An elucidation of the complete mechanism of the photo reaction, e.g. by mass spectrometric analysis of the reaction products, is beyond the scope of

this paper, but most probably the mechanism will have some similarity to the well-known photo-Fenton degradation [127-130]. In this photo-Fenton reaction, free radicals, which are strong oxidants for organic compounds, are produced. As a consequence, the sample compounds may be oxidized by those radicals.

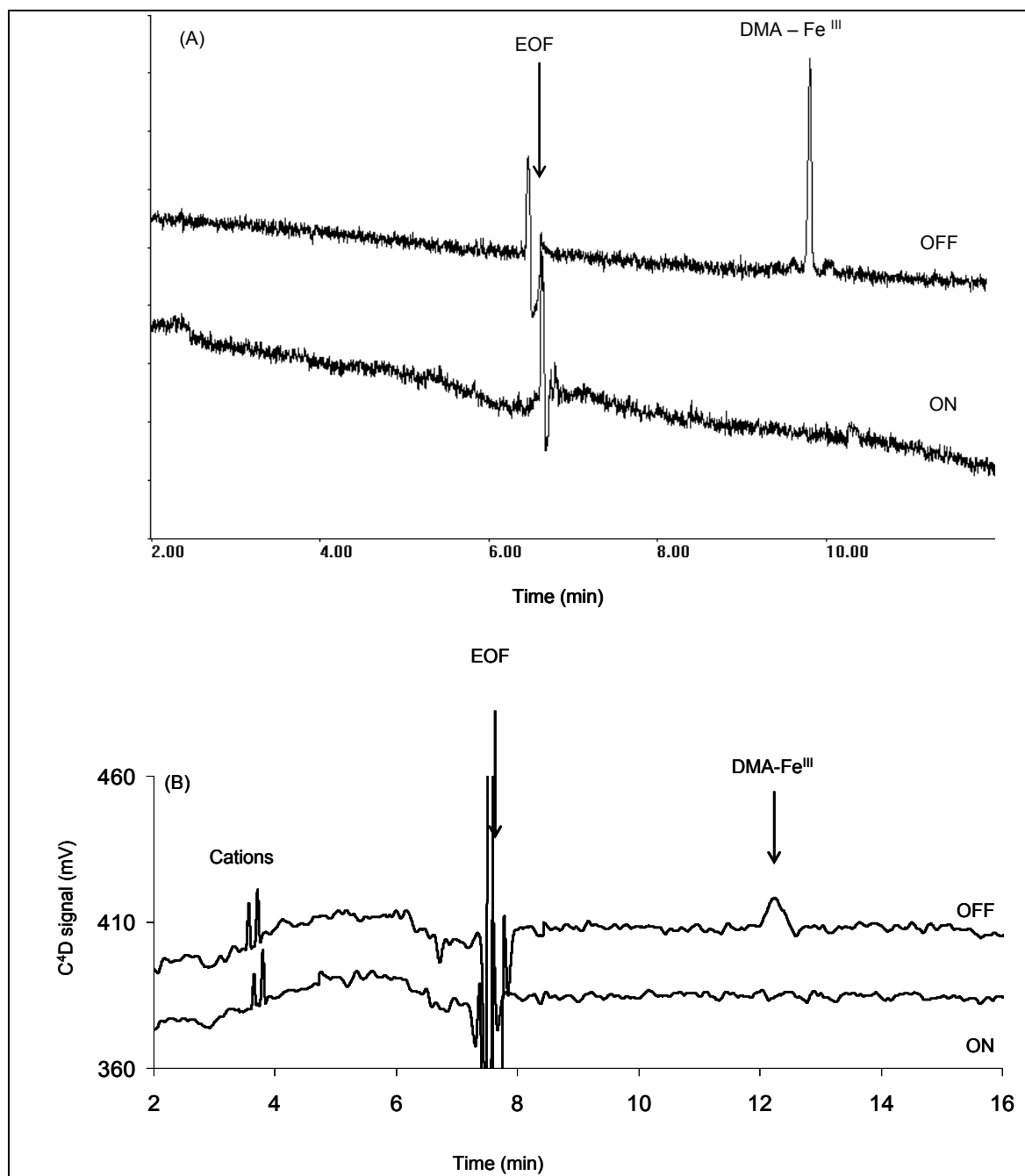


Figure 3-5. Electropherograms obtained using photo reactor (with a photo irradiation window of 6.3 cm) and UV detector at 205 nm (A) and conductivity detector (B). Phosphate buffer 10 mM, pH 7.5, 20 kV, injection: 40 mbar 6 s. Sample is 200  $\mu\text{mol/L}$  of DMA-Fe<sup>III</sup>.

The effect of the photo reaction in CE to iron-species (decrease of signals) is a disadvantage in terms of sensitivity, but not in terms of selectivity, because iron species are selectively degraded. This will be discussed later for real plant samples (see chapter 3.3.4.3). The different effects in cFIA and CE may be looked upon even

as an advantage, because there should be only few compounds that exhibit such converse effects in the two analytical techniques. Before investigating of the real plants, understanding of the relationship of the irradiation time/volume/length and sensitivity helps to optimize the photo irradiation window length to the specific analyte and sample matrix.

### 3.3.4.2 Investigation of the relationship of the irradiation time and sensitivity

The relationship of the irradiation time, which relates to irradiation window length and irradiation volume, and sensitivity of iron species was investigated by using EDTA-Fe<sup>III</sup> as model standard. To determine the effect of photo irradiation time on the detection sensitivity, electropherograms were run with different photo irradiation window length (14, 8.8, 6.3, 3.3 cm), corresponding to photo irradiation times of approximately 138, 89, 62 and 30 s, respectively (listed in Table 3-2). The photo irradiation times were calculated using the linear velocity of the analyte peak [EDTA-Fe<sup>III</sup>] and the photo irradiation window length. Fig. 3-6 shows the respective electropherograms for UV-detection (A), and conductivity detection (B). In both cases, the initial EDTA-Fe<sup>III</sup> peak (I) the relation of signal decrease to irradiation time (window length) is similar for both detection methods (Fig. 3-6C). Note, that in C<sup>4</sup>D the EDTA-Fe<sup>III</sup> gives rise to a negative peak, which is due to the relative contributions to conductivity of iron-species and buffer, respectively. While the initial peak (I) decreases, some unknown positive peaks are observed with both detectors. Clearly, these peaks are related to the photo reaction products, but different products are detected by the two different detectors. This is shown in Fig. 3-6D. For short irradiation time up to 30 s (irradiation window length up to 3.3 cm), the UV signal increases, showing the formation of new UV absorbing compounds. With the following decrease of the UV signal, a signal appears in the conductivity detection mode, which increases continuously up to 136 s irradiation time. With the beginning of the photo-degradation, intermediate products are formed with good UV absorbance, which then are converted into nonabsorbing compounds detectable via C<sup>4</sup>D. The results shown in Fig. 3-6 demonstrate the advantage of complementary information by using two different detectors though photochemical reaction mechanisms can vary for the different Fe-Ligand complexes. The determination of the individual decay process offers the possibility to optimize the photo irradiation window length for the specific analyte and sample matrix. For the real plant extracts under investigation, a photo irradiation window length of 6.3 cm was chosen, which provides a decreasing effect on the iron-species, which lies in between totally vanishing of species (14 cm) and no effect (0 cm).

Table 3-2. Irradiation times (window length) vs. Sensitivity of EDTA-Fe<sup>III</sup>

Irradiation length (cm)	Irradiation time (sec)	UV (% of original signal)	C <sup>4</sup> D (% of original signal)
0	0	100	100
3.3	30	50	67
6.3	62	33	46
8.8	89	15	30
14.0	138	5	10



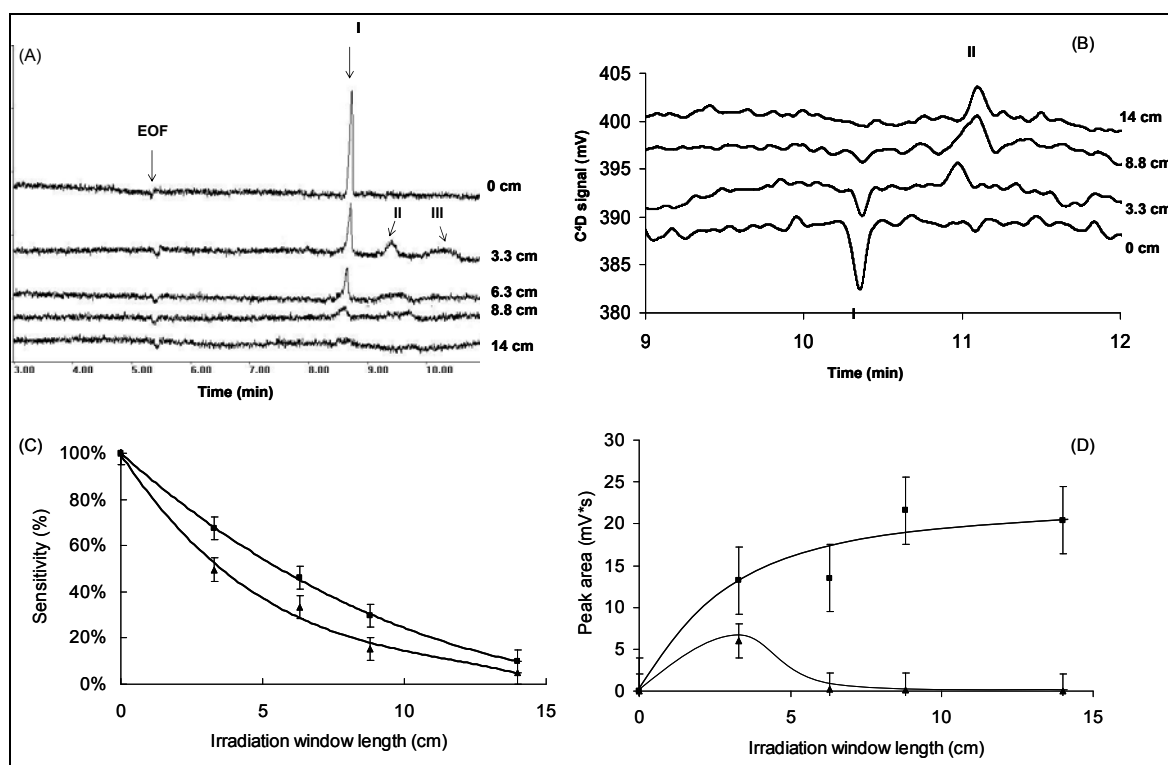


Figure 3-6. Photo irradiation time (irradiation window length) vs. sensitivity: 150  $\mu\text{mol/L}$  EDTA-Fe<sup>III</sup> with different lengths of irradiation window 0, 3.3, 6.3, 8.8 and 14 cm in UV detection (A) and in conductivity detection (B). Peak I is EDTA-Fe<sup>III</sup>, peaks II and III are photo irradiation products; (C) irradiation window length vs. EDTA-Fe<sup>III</sup> sensitivity; (D) irradiation window length vs. sensitivity of photo reaction product. Phosphate buffer 10 mM, pH 7.5, 20 kV, injection: 40 mbar 6 s; (filled triangles), UV detection Signal II; (filled squares), C<sup>4</sup>D detection.

### 3.3.4.3 Application of analysis of real plant extracts

The electropherogram of an extract of an iron deficient wheat root sample irradiated under optimized conditions (window length: 6.3 cm; irradiation time: 62 s) is shown in Fig. 3-7. Only the migration time range of the electropherogram from 6 to 12 min is shown for UV detection, corresponding to the time range of 7-18 min for conductivity detection (due to the distance between the two detectors). It could be shown that this part of the electropherogram is characteristic for most amino acids, phytosiderophores, nicotianamine and their respective iron-species, which are expected to play a major role in iron transport in plants. For example, peak (I) in Fig. 3-7 is the Fe-NA peak, which disappeared completely after irradiation. The other peaks, which vanish completely (IV-VII in Fig. 3-7), are most likely also iron-species, because most ligands that migrate within this range of time (amino acids, phytosiderophores, etc.) have been tested separately and did not show any photoactivity without iron, as have been found in separate investigations. Moreover, the formation of photoactive species with other metals is rather unlikely, because of their lower concentration. However, the respective structures of iron-species have not been identified yet. From the electrophoretic mobilities and from comparison with model species, they should be closely related to phytosiderophores (mugineic acid and hydroxylated derivatives) or some more acidic amino acids. Some peaks are not much changed (II and III in Fig.

3-7) and consequently can be assigned to ligands without iron. A new peak is also observed by the conductivity detection (Fig. 3-7B, see arrow), which is probably due to the formation of a photo reaction product; similar to the EDTA-Fe<sup>III</sup> photo reaction system (Fig. 3-6). The most important result of this experiment is the detection of several iron-species (about 5 different peaks in the CE) by the selectivity photo reaction. Taking into account the vast amount of organic species present in a plant extract, application of this on-column photo reactor is important to get an idea, where to look for the important iron-species.

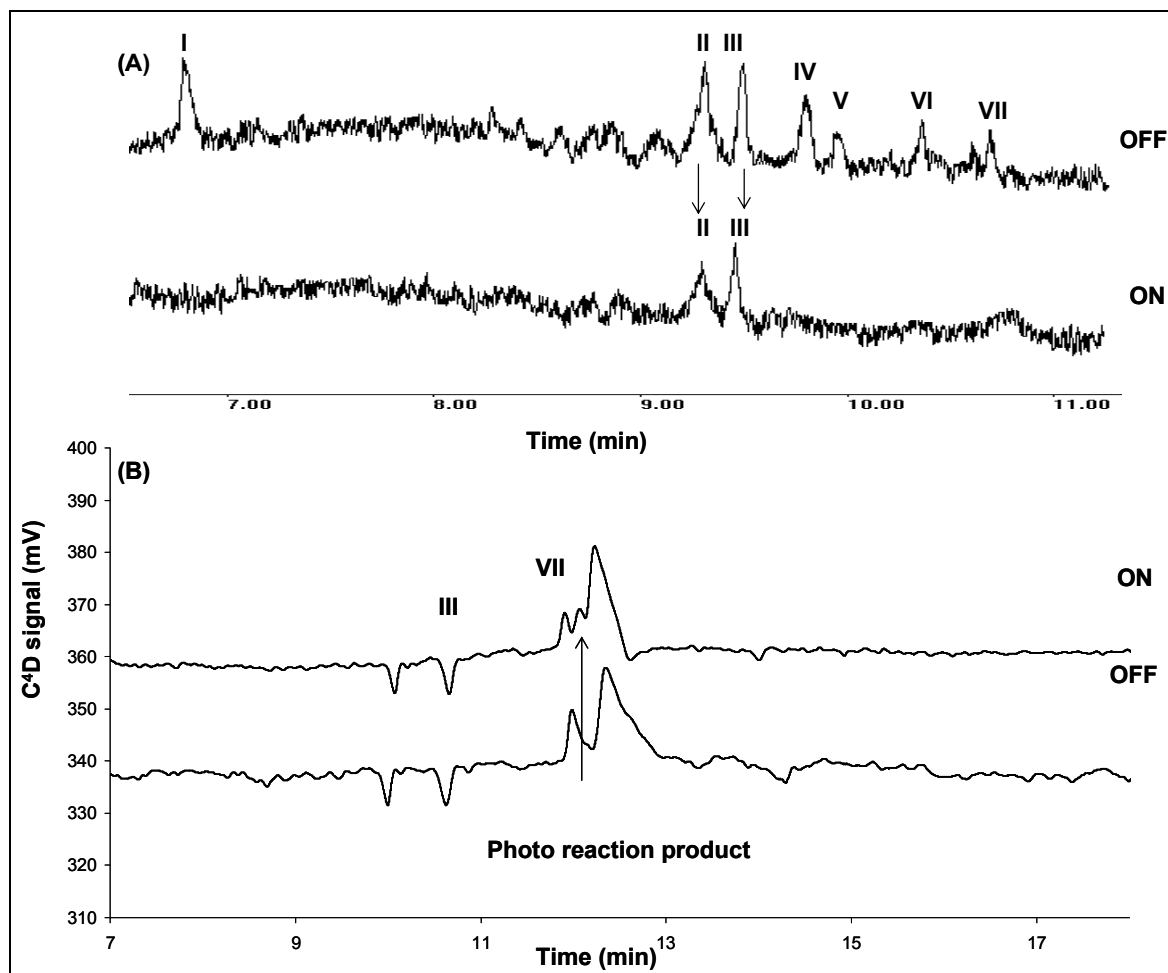


Figure 3-7. Electropherograms obtained using photo reactor (with a photo irradiation window 6.3 cm) and UV detector at 205 nm (A) and conductivity detector (B). Phosphate buffer 10 mM, pH 7.5, 20 kV, injection: 40 mbar 6 s.

### 3.4 Conclusion

Capillary electrophoresis methods (see chapter 2) are well suited for separating LMW species in plants. However, most of these LMW species are poor UV absorbance and metal-PS are not well detected by conductivity detector. In order to improve the absorbance and conductivity detection for small metal-species, a new on-column photo reactor was developed and investigated not for all species in a complex matrix of plant extracts, but for the most important iron ligand species. That means the reactor should provide a selective photochemical reaction of these compounds and

their identification within an electropherogram of plant extracts. To understand the feasibility of photo reaction, a commercially available post-column photo reactor for HPLC was investigated first. Both sensitivity and selectivity were enhanced for iron-species using a diode array detector in FIA and HPLC. The detection sensitivity of iron-species in plants was significantly enhanced by this post-column photo reactor. This principle was adapted for cFIA and CE using an adjustable photo irradiation window, with an irradiation volume between 100 and 500 nL). This allows a variation of the irradiation time and a certain control of the photochemical reaction (degradation kinetics). It could be shown, that pure ligands are not affected by photo reaction. The photochemical reaction of iron species was observed by UV absorbance detection and contactless conductivity detection, with model iron-species and plant extracts. In CE, the iron-species are degraded by photo reaction. The kinetic vary with the complex ligand offers the possibility of ligand identification. Additional information about the iron species are given by their reaction products of the photochemical degradation process. Due to different sensitivities of the used detectors (UV and conductivity) for degradation products complementary information improve the selectivity. By combination of cFIA and CE with the photo reactor, an even better interpretation of electropherograms concerning iron-species can be obtained and allows selective detecting of iron-species in plants without using CE-MS system.

## 4 High Performance Liquid Chromatography coupled to Mass Spectrometry

Liquid chromatography-mass spectrometry (LC/MS) is an analytical technique that combines the separation capabilities of liquid chromatography (HPLC) with the mass analysis capabilities of mass spectrometry. LC/MS is a powerful technique used for many applications, because of its high sensitivity and specificity. Generally its application is oriented towards the specific detection and identification of non-volatile (polar) chemicals in a complex mixture. However, a method for the simultaneous separation and mass spectrometric identification of all relevant PS and metal-PS complexes in plants was not yet available. Since the species of interest in plants are polar, low-molecular-weight substances, which are present at low micro molar concentrations in a complex matrix, a very efficient separation technique (such as HPLC) is needed to separate the target species from the plant matrix, which is present in excess and may interfere with sensitive mass spectrometric detection and identification. ESI-MS was applied as standard detection, because it is essential to obtain structural information of the metal-species in plants, which are only partly known.

### 4.1 High Performance Liquid Chromatography

HPLC is used to separate components of a mixture by using a variety of chemical interactions between analytes, dissolved in the liquid “mobile phase”, and the “stationary phase”. In isocratic HPLC the analyte is forced through a column of the stationary phase by introducing a liquid at constant mobile phase. Solvents used include any miscible combination of water and/or various organic liquids (the most common solvent mixtures are methanol/water and acetonitrile/water). Water usually contains buffers or salts to assist in the separation of the analytes. A further refinement to HPLC has been to vary the mobile phase composition during the analysis; this is known as gradient elution. The gradient separates the analyte mixtures as a function of how well the changing solvent mobilizes the analyte. The choice of solvents, additives and gradient depends on the nature of the stationary phase and the analyte. There are several types of HPLC, the most important one is reversed phase liquid chromatography (RPLC), others are normal phase liquid chromatography (NPLC), size exclusion chromatography (SEC), and ion-exchange chromatography (IEC).

In a first attempt to separate the small plant substances, RPLC was applied. This technique combines a non-polar stationary phase with a polar mobile phase. Some applications of RPLC for small, polar analytes are known (e.g., amino acids [131-133], organic acids [134, 135], phenolic substances [136, 137]). However, these methods are not directly applicable to the analysis of metal-species, because the high pH is not good for the stability of metal-species. Moreover, our target analytes (small metal-species and ligands) are very polar compounds, which exhibit no retention on reversed-phase column. They all eluted together around the dead volume, and no separation could be achieved. One Synergy C18 column was tested at the beginning to separate polar amino acids (aspartic acid, glutamine acid, histidine, lysine, and arginine). However, no satisfactory separation could be achieved at pH 7.3, which is close to the pH in plant compartments and minimizes the disturbance of metal species. Normal phase liquid chromatography separates compounds based on their polarity, using a highly polar stationary phase and (usually) a non-polar mobile phase. Therefore, in principle, this technique could give a good retention of our analytes of

interest. However, the polarities of some important metal species are very similar. For example complexes of different divalent metal ions with the same ligand are often very similar in charge, size, and geometry. As a consequence, a good separation based on the polarities of species is hard to achieve by NPLC. In ion-exchange chromatography, retention is based on the electrostatic interactions between charged analytes and charged sites on the stationary phase. However, ion-exchange chromatography may need unfavorable pH and high concentrations of buffer or salt. This is a disadvantage esp. for on-line mass spectrometric identification, but also for the stability of metal-species, which may be dissociated by pH-shifts or by strong interactions with the stationary phase.

A much “softer” type of ionic interactions (as compared to IEC) is the basis of ion-pair chromatography (IPC). This chromatographic technique is very similar to RPLC, but with the presence of an ion-pairing reagent in the mobile phase, which interacts with the analytes and thus modifies their retention. Ion-pairing is most commonly used to perform separations of ionic compounds on reversed phase columns. IP-RPLC has been applied already for investigating biological samples, including metal-complexes [85, 144, and 145] and amino acids [146-148], in the last several years. A method for the determination of five inorganic and organic Se species in human urine by reversed-phase liquid chromatography with mixed ion-pair reagents coupled with inductively coupled plasma mass spectrometry (HPLC/ICP-MS) is described by Zheng et al. [144]. HPLC ion-pair chromatographic methods to identify and quantify iron chelates [145] and iron-EDDHA isomers [85] have been reported. Underivatized amino acids are separated by ion-pair reversed-phase HPLC [146-149]. Ion-pairing seems to be a powerful tool that changes or enhances selectivity of ionic compounds to help separate interest of species in plants. Therefore, IP-RPLC was carried out to separate these LMW metal-species in plants (chapter 4.4.2).

In addition to ion-pair chromatography, which is described in the following paragraph, two novel separation techniques were developed, in order to allow the separation of small plant substances and respective metal-species. These techniques are “zwitterionic hydrophilic interaction liquid chromatography” (ZIC-HILIC), and the closely related ZIC-MPC-HILIC (MPC standing for 2-methacryloyloxyethyl phosphorylcholine). Both techniques combine at least two different modes of separation: (zwitter-)ionic interactions, and hydrophilic interactions. Several applications of HILIC for the investigation of polar compounds [139, 140], mixed-mode HILIC/anion-cation exchange chromatography for small molecules [141], and mixed mode HILIC/cation-exchange chromatography for peptides [142] were published in the last few years. Recently, a combination of size-exclusion chromatography and hydrophilic interaction liquid chromatography (HILIC) has been proposed for the separation/purification of such nickel species in the metal hyperaccumulator plant [143]. In this work, nickel complexes with malate, citrate, histidine, NA, and EDTA (originating from the hydroponic growth solution) were identified by mass spectrometry. These applications indicate that a charged HILIC stationary phase may be a good choice for separation of phytosiderophores and their metal complexes, which are very polar, hydrophilic, and exist as zwitterions in solution. Therefore, both ZIC-HILIC (chapter 4.4.3) and ZIC-MPC-HILIC (chapter 4.4.4) coupled to mass spectrometry were carried out to analyses the important LMW species in plants.

#### **4.1.1 Ion pair – Reversed Phase Liquid Chromatography (IP-RPLC)**

The use of ion-pair reagents as mobile phase additives allows the separation of ionic

and highly polar substances on reversed phase HPLC columns. Ion-pair reagents are non-polar ionic compounds with the opposite charge of the sample analytes. This allows them to bind to both the ionic sample analytes and a reversed-phase column packing. These reagents are comprised of an alkyl chain with an ionizable terminus (Fig. 4-1A). When used with common hydrophobic HPLC phases in the reversed-phase mode, ion pair reagents can be used to selectively increase the retention of charged analytes (Fig. 4-1B). The quaternary amine ion pair reagent is comprised of quaternary alkyltriethylamines that can be used for the resolution of negatively charged species (i.e. the species of interest).

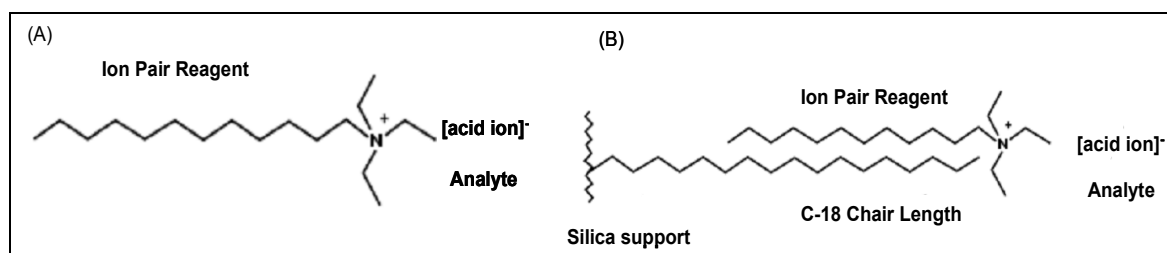


Figure 4-1. (A) quaternary amine ion pair reagent; (B) quaternary amine ion pair reagent interacting with C-18 support.

To choose the proper reagent, alkyl chain lengths must be taken into consideration. The chain lengths enable selective separation of the analyte. The longer the chain, the more hydrophobic the counterion, the greater the retention. Since the species of interest are mostly very polar compounds, longer alkyl chain will be a benefit to make a longer retention on the reversed phase column. However, the longer the alkyl chain, the lower the volatility, and therefore stronger ion suppression of ESI mass signal. Taken together both considerations, tetrabutyl ammonium (TBA) was applied as ion pair reagents for the investigation. As an alternative counterion, tributyle amine, which is higher volatile, but shorter alkyl chain, than TBA, was investigated as well.

#### 4.1.2 Zwitterionic Hydrophilic Interaction Liquid Chromatography (ZIC-HILIC)

Hydrophilic interaction liquid chromatography (HILIC) was originally introduced to describe separations based on solute hydrophilicity [76]. Under HILIC conditions, a water-enriched liquid layer is established within the stationary phase, and the eluent typically contains a high percentage of organic modifiers. In contrast to RPLC, solutes are eluted in order of increasing hydrophilicity (decreasing hydrophobicity). The separation is achieved by partitioning of analytes from the eluent into the hydrophilic environment at the stationary phase, a process that typically is exothermic. Hence, both hydrogen bonding, the extent of which depends on the acidity or basicity of the solutes, and dipole–dipole interactions, which depend on the dipole moments and polarizability of the solutes, are factors governing retention. If a charged stationary phase is used, the retention will also be influenced by electrostatic (ionic) interactions. In this application, a zwitterionic hydrophilic stationary phase (see Fig. 2-14) exhibits weak electrostatic interactions with either positive or negative charges. It should be noted, that the zwitterionic stationary phase has the negatively charged sulfonic acid group pointing out to the mobile phase and the positively charged quaternary ammonium group more ‘hidden’ inside the alkyl chain. In case of analysis compounds, which have the similar hydrophilic ability but different charge states, a higher retention times for the compounds carrying more charged groups, a higher retention times for positively charged analytes, and shorter retention times for negatively charged analytes should be achieved by this zwitterionic charged stationary phase. Shortly, the

separation is achieved by a hydrophilic partitioning and weak electrostatic interactions with either positive or negative charges.

#### 4.1.3 Zwitterionic 2-methacryloyloxyethyl phosphorylcholine hydrophilic interaction Liquid Chromatography (ZIC-MPC)

In contrary to the charge arrangement of the stationary phase of ZIC-HILIC (chapter 4.1.2), ZIC-MPC has a stationary phase, in which the positively charged quarternary ammonium groups are pointing out to the mobile phase, and the negatively charged phosphoric acid groups are hiding inside the alkyl chain. Under pH 7, the surface charge (zeta potential) of ZIC-MPC (phosphorylcholine functional group) is  $-16.7 \pm 1.1$  mV, while that of ZIC-HILIC (sulfobetaine functional group) is  $-16$  mV at the same test conditions [138]. It means that the phosphorylcholine functionality has a slightly negative surface charge in a wide pH range (similar to the sulfobetaine type structure), although their spatial charge arrangement is reversed to sulfobetaine groups on the ZIC-HILIC column. Hydrophilic interaction liquid chromatography is still the main separation parameter with ZIC-MPC column. The separation is based on both hydrophilic interaction and zwitterionic interaction between stationary phase and analytes. Since both exhibits hydrophilic interactions, the only difference between ZIC-MPC and ZIC-HILIC is the zwitterionic interaction among the stationary phase and analytes.

It is worth to point out that the weak electrostatic interaction of ZIC-HILIC and ZIC-MPC stationary phase allows using low buffer concentrations, which is a clear advantage for mass spectrometry, and it reduces the risk of metal complex dissociation by strong interaction with the stationary phase during separation. In addition, typical eluents for HILIC consist of high percentage organic solvent (methanol, acetonitrile) in water or a volatile buffer. Hence, these zwitterionic hydrophilic interaction liquid chromatography techniques are mass spectrometry friendly and should be well-suited for the separation of PS and their metal complexes.

## 4.2 Mass Spectrometry (MS)

Electrospray ionization-mass spectrometry (ESI-MS) after chromatographic separation was widely applied to detect and identify low-molecular-weight compounds in a complex matrix, such as amino acids [149-152], organic acids [153, 154], phenols [155, 156]. As well, ESI-MS was applied to the speciation of different  $\text{Fe}^{\text{III}}$ -chelate complexes [157-160]. Even a direct analysis of NA and DMA complexes with  $\text{Fe}^{\text{II}}$  and  $\text{Fe}^{\text{III}}$  in one solution without separation is possible using nano-electrospray ionization Fourier transform ion cyclotron resonance mass spectrometry (nano-ESI-FTICR-MS) [161]. The advantage of the latter technique is the high mass resolution combined with accurate mass information, which allows identifying metal-PS-species with very similar masses. For example, the mass difference of the  $\text{Fe}^{\text{II}}$ -NA complex (measured as  $[\text{NA-3H+Fe}^{\text{II}}]^-$ ) and the  $\text{Fe}^{\text{III}}$ -DMA complex (measured as  $[\text{M-4H+Fe}^{\text{III}}]^-$ ) is only 0.0239 amu. With standard resolution ESI-MS equipment, as is used normally in HPLC/MS, it would be impossible to resolve these species. Hence, chromatographic separation of the species is necessary for unequivocal identification. An advantage of HPLC/MS over direct FTICR-MS is the separation of the target species from the plant matrix, which is present in excess and may interfere with sensitive mass spectrometric detection and identification. In my work, two sets of electrospray ionization-mass spectrometer, Finnigan LCQ (from ThermoQuest, San Jose, CA, USA) and Finnigan LTQ-FT systems (from ThermoElectron, Bremen, Germany) were used after LC separation to sensitively detect and accurately identify the LMW species in plants.

Therefore, the following discussion of mass spectrometer mainly focuses on these two systems.

Mass spectrometers can be divided into three fundamental parts, namely the ionization source, the analyzer, and the detector. The sample has to be introduced into the ionization source of the instrument. Once inside the ionization source, the sample molecules are ionized. These ions are extracted into the analyzer region of the mass spectrometer where they are separated according to mass-to-charge ratios ( $m/z$ ). The separated ions are detected and this signal sent to a data system where the  $m/z$  ratios are stored together with their relative abundance for presentation in the format of a  $m/z$  spectrum.

#### 4.2.1 Methods of sample ionization

The ionization methods to be used should depend on the type of sample under investigation. The most common and probably most suitable ionization modes are ESI and APCI for the analysis of metabolites. APCI is useful for generating ions from less polar molecules, but may induce fragmentation. This complicates the mass spectrum. In this work, electrospray ionization (ESI) was applied because it can run ionize very polar compounds. Another advantage of applying ESI is that little fragments of ions produced during ionization.

**Electrospray Ionization (ESI)** is one of the atmospheric pressure ionization (API) techniques and is well-suited to the analysis of polar molecules ranging from less than 100 Da to more than 1,000,000 Da in molecular mass. During standard electrospray ionization, the sample is dissolved in a polar, volatile solvent and pumped through a narrow, stainless steel capillary at a flow rate between 1 – 1000  $\mu\text{L}/\text{min}$ . A high voltage of 3 or 4 kV is applied to the tip of the capillary, which is situated within the ionization source of the mass spectrometer, and as a consequence of this strong electric field, the sample emerging from the tip is dispersed into an aerosol of highly charged droplets, a process that is aided by a co-axially introduced nebulizing gas flowing around the outside of the capillary. This gas, usually nitrogen, helps to direct the spray emerging from the capillary tip towards the mass spectrometer. The charged droplets diminish in size by solvent evaporation, assisted by heated capillary (in both Finnigan LCQ and Finnigan LTQ-FT systems). Eventually charged sample ions, free from solvent, are released from the droplets, some of which pass through a sampling cone or orifice into an intermediate vacuum region, and from there through a small aperture into the analyzer of the mass spectrometer, which is held under high vacuum. The lens voltages are optimized individually for each sample.

#### 4.2.2 Mass analyzer

The main function of the mass analyzer is to separate the ions formed in the ionization source of the mass spectrometer according to their mass-to-charge ( $m/z$ ) ratios. There are a number of different mass analyzers currently available, the better known of which include magnetic sectors, linear quadrupoles, time-of-flight (TOF) analyzers, quadrupole ion traps (QIT), and Fourier-transform ion-cyclotron resonance (FTICR).

**Quadrupole ion trap (QIT)** In LCQ system, a quadrupole ion trap consists of a cylindrical ring electrode with holes at one end for introducing ions or electrons into the trap, while the bottom end-cap contains holes for ions ejected towards the electron multiplier. Ions that are generated in an external ion source are stored in the trap. In LTQ-FT system, a linear ion trap was applied in front of Fourier-transform



ion-cyclotron resonance (FTICR) cell. A linear quadrupole ion trap is similar to a QIT, but traps ions in a 2D quadrupole field, instead of a 3D quadrupole field as in a QIT.

**Tandem MS (MS/MS) and MS<sup>n</sup>** Tandem MS involves multiple stages of mass spectrometric analysis carried out by various events occurring between each stage. In case of two stages, it is known as tandem MS or MS/MS. In case of more than two stages, it is known as MS<sup>n</sup>, in which precursor ions are isolated for further fragmentations. Mass analysis of the fragments provides information on the structure of the precursor ion. There are several different methods available for the fragmentation, including collision induced dissociation (CID), electron capture dissociation (ECD), electron transfer dissociation (ETD), infrared multiphoton dissociation (IRMPD), and blackbody infrared radiative dissociation (BIRD). The CID technique was the fragmentation method used with the linear ion trap on LTQ-FT system. The precursor ions isolated in ion trap and collided by neutral gas molecules (helium). During the collision, some kinetic energy converts into internal energy, breaking the chemical bonds and yielding fragments. During plant metabolic profiling in this work, MS<sup>2</sup> and MS<sup>3</sup> were carried out to give sets of complementary fragments, offering the possibility of to derive the molecular structure for an unknown metabolite.

QIT mass spectrometry is a sensitive and versatile instrument, which is capable of identifying both large and small molecules and determining their molecular structure. It is a robust system and designed to interface with atmospheric pressure ionization techniques that are optimal for the analysis of biomolecules. Unit mass resolution is maintained over the 2,000 Dalton mass range with a mass accuracy of 0.015%. Therefore, QIT mass spectrometry (Finnigan LCQ), was applied for LC/MS method to do “target analysis” of known species (chapter 4.4.1- chapter 4.4.4). However, in cases when ions are very similar m/z, for example [NA-3H+Zn<sup>II</sup>]<sup>+</sup> (m/z = 364.0487046) and [DMA-3H+Cu<sup>II</sup>]<sup>+</sup> (m/z = 364.0331742) with a mass difference = 0.0145 amu, only high resolution mass spectrometry allows an unequivocal identification of these ions. In addition, to identify many unknown metabolites in one single chromatographic run, FTICR-MS serves as the most selective technique of MS with highest mass resolution, providing precision of mass measurement to enable metabolomic analyses. Therefore, a FTICR-MS, Finnigan LTQ-FT mass spectrometry, was applied after HPLC separation to investigate plant metabolic profiling (see chapter 4.4.5).

**Fourier-transform ion-cyclotron resonance (FTICR)** In a Fourier-transform ion-cyclotron resonance mass spectrometer (FTICR-MS) the mass analysis is performed in a cubic cell placed in a strong magnetic field B. The cell consists of two opposite trapping plates, two opposite excitation plates and two opposite receiver plates. An ion of mass m, velocity v and with z elementary charges presents in such a cell a circle of radius r, perpendicular to the magnetic field. The cyclotron frequency  $\omega_c$ , which is inversely proportional to the m/z value, is given by:

$$\omega_c = 2 \pi f = v/r = B z / m \quad (14)$$

where f is the frequency in Hertz. When the ions, trapped in their cyclotron motion in the cell, are excited by means of a radio-frequency (RF) pulse, the radius of the circle is increased and ions of one m/z value start moving in phase. The coherent movement of the ions generates an image current in the receiver plates. As the coherency is disturbed in time, the image current signal is decaying as well. The time-domain signal from the receiver plates contains all frequency information of the moving ions. By

applying Fourier transformation, the time-domain signal can be transformed into a frequency-domain signal that subsequently can be transformed in a regular mass spectrum by application of Eq. 14. Because each ion is counted more than once, FTICR-MS has the advantage of high sensitivity and high resolution and mass accuracy.

### 4.2.3 Detector

The detector monitors the ion current, amplifies it and the signal is then transmitted to the data system where it is recorded in the form of mass spectra. The  $m/z$  values of the ions are plotted against their intensities to show the number of the components in the sample, the molecular mass of each component, and the relative abundance of the various components in the sample. The type of detector must be chosen to suit the type of analyzer; the more common ones are the photomultiplier, the electron multiplier, and the micro-channel plate detectors.

In electron multiplier detectors, a conversion dynode is used to convert either positive or negative ions into electrons. These electrons are amplified by a cascade effect in a horn shape device, to produce current. This type of detector is widely used in quadrupole ion trap instruments.

In FTICR-MS, the detector consists of a pair of metal surfaces within the mass analyzer/ion trap region which the ions only pass near as they oscillate. No direct current (DC) but a weak alternating current (AC) image current is produced in a circuit between the electrodes. Detection of the frequency of the image current is converted to a mass spectrum by Fourier transform.

## 4.3 Experimental

### 4.3.1 LC/ESI-MS for method development and optimization

#### 4.3.1.1 LC/ESI-MS system

The HPLC system consisted of a Finnigan TSP P4000 HPLC pump, an online Finnigan TSP SCM1000 degasser and a Finnigan TSP AS3000 auto sampler (all ThermoQuest, San Jose, CA, USA). The ESI-MS instrument was quadrupole ion trap mass spectrometer, Finnigan LCQ DECA (ThermoQuest, San Jose, CA, USA). The system was operated under the Xcalibur software (version 1.2 SP1, Thermo Finnigan). Injection volume was set to 5  $\mu$ L, and flow rate was 0.15 mL/min for all the investigations.

#### 4.3.1.2 HPLC conditions

*ZIC-HILIC*: Separations were performed using a ZIC-HILIC column (150 mm $\times$ 1.0 mm I.D.) equipped with guard column (14 mm $\times$ 1.0 mm I.D., SeQuant, Umeå, Sweden). To investigate PS and metal-PS complexes, the following gradient was applied. Solvent A: 10 mM ammonium acetate/acetonitrile (10 + 90) at pH 7.3. Solvent B: 30 mM ammonium acetate/acetonitrile (80 + 20) at pH 7.3. The gradient was mixed from solvent A and B: 0-3 min, 100 % A; 3-33 min, linear gradient to 30 % A + 70 % B. From 33 to 40 min, a column clean-up was performed using isocratic 30 % A and 70 % B. Then the column was re-equilibrated using a linear gradient down to 100 % A and holding this concentration until 60 min. A fast isocratic separation was used, employing 10 mM ammonium acetate/acetonitrile (20 + 80, pH 7.3).

*ZIC-MPC*: a ZIC-MPC column (150 mm $\times$ 1.0 mm I.D.) equipped with guard column (14 mm $\times$ 1.0 mm I.D., SeQuant, Umeå, Sweden) was investigated with the same test condition as ZIC-HILIC method above.

*IP-RPLC*: a LUNA C18(2) column (150 mm $\times$ 2.0 mm I.D) was equipped with a LUNA C18(2) guard column (4.0 $\times$ 2.0 mm I.D., Phenomenex Inc., Aschaffenburg, Germany). Tetrabutyl ammonium acetate (TBA acetate) was applied as ion pair reagent. Isocratic elution with buffer (0.2 mM TBA acetate/ACN (80 + 20), pH 7.3) was applied. A short alkyl chain compounds, tributylamine with acetic acid as count ions, was applied as well. Isocratic elution profile with buffer (0.2 mM tributyleamine/ACN (80 + 20), pH 7.3) was carried out.

*Precautions*: Both in ZIC-HILIC and ZIC-MPC investigations, the re-equilibration time should be kept at least for 30 min, in order to obtain reproducible retention times. Also metal, especially iron, contamination of the column affects the retention times and resolution of phytosiderophores. Therefore, the guard column and analytical column should be regenerated periodically with 10 column volumes of 10 mM EDTA, followed by 20 column volumes of 100 mM ammonium acetate to remove the EDTA, then by 20 column volumes of deionized water to remove salt contamination, finally by 30 column volumes of solvent A.

#### 4.3.1.3 ESI-MS conditions

*ESI-MS*: Detection was carried out by ESI-MS in the negative ionization mode. Capillary spray voltage was set to 4.5 kV, the temperature of the heated transfer capillary was maintained at 350  $^{\circ}$ C, and tube lens voltage was 20 V. Full scan mass

spectra were acquired in the mass range  $m/z$  100-700 using five micro scans.

### 4.3.2 Plant metabolic profiling

#### 4.3.2.1 LC/ESI-FTICR-MS system

The Surveyor HPLC system consisted of a pump, an online degasser and a autosampler (all ThermoElectron, Bremen, Germany). All LC/ESI-FTICR-MS experiments were carried out using a LTQ-FT FTICR mass spectrometer (ThermoElectron, Bremen Germany), equipped with a 7.0 Tesla actively shielded superconducting magnet and ESI source. The system was operated under the Xcalibur software (Version 1.4).

#### 4.3.2.2 HPLC conditions

*ZIC-HILIC:* The separation column, guard column, solvent A and solvent B are all the same as in ZIC-HILIC part of chapter 4.3.1.2. The gradient was mixed from solvent A and B: 0 - 4 min, 100 % A; 4 - 40 min, linear gradient to 25 % A + 75 % B. From 40 to 50 min, a column clean-up was performed using isocratic 25 % A and 75 % B. The injection volume was set to 5  $\mu$ L. The flow rate was 75  $\mu$ L/min. Temperature of the column oven and the sample tray was set to 30 °C and 15 °C, respectively.

*Cleaning and re-equilibrated process:* A cleaning and re-equilibrated wash process was applied in between each two plant samples measurements with a full loop injection of water. Isocratic 10 % A + 90 % B was applied for cleaning for 10 min at flow rate 100  $\mu$ L/min, followed by applying 100 % A to re-equilibrate the column for 20 min at flow rate 75  $\mu$ L/min.

#### 4.3.2.3 ESI-FTICR-MS conditions

*ESI-FTICR MS:* The instrument was operated in negative ionization mode. Ion transmission into the linear trap and signal intensity was automatically optimized for maximum ion signal of the NA-Fe<sup>II</sup> complex. The parameters were: source voltage 2.8 kV, capillary voltage 18 V, capillary temperature 300°C, and tube lens voltage 85 V. The targets for the full scan linear trap and FTICR cell were  $3 \times 10^4$ , and  $1 \times 10^6$ , respectively. Full-scan FTICR mass spectra in the mass range  $m/z$  80-800 were acquired using single micro scan.

*Reproducibility test and semi-quantitation:* The resolving power of the FTICR mass analyzer was set to 50,000, FWHM is 400. Full scan mass spectra were acquired in the mass range  $m/z$  80-800 using single micro scan. Centroid data were collected. This condition was applied to all the plant samples and each sample was repeatedly measured 3 times.

*Identification by the data dependent MS<sup>n</sup> measurement* was programmed. In this case, we can find metabolites by scanning the mass chromatogram, then subsequent CID fragmentation in the linear ion trap of the 3 most intensive signals with dynamic exclusion. The complete set of Tobacco plants was investigated by the data dependent MS<sup>3</sup> once in order to get structurally identification information of the intensive ions in plants. The detail scan events are: first full scan of 80-800 Da with a resolution 25,000, then the most intensive ion was selected with resolution 50,000 and mass window 10 amu. Fragmentation of selected ion was then carried out with relative collision energy 35 % to obtain MS<sup>2</sup> and MS<sup>3</sup> information in the linear trap. For full ion scan and selected ion scan (SIM) profile data were collected. For ion trap

fragmentation, centroid data were collected.

### 4.3.3 Chemical and solvents

All chemicals and solvents are listed in Appendix.

### 4.3.4 PS, metal-PS standards, and Plant samples

All PS and real plant samples were isolated and purified from plant cultures at the Institute for Plant Nutrition (Hohenheim University, Stuttgart, Germany).

*NA, PS, and metal-PS standards* see chapter 2.3.3.

*Real plants:* Wheat plants (cv., Bezostaya) and *Arabidopsis thaliana* Col-0 plants (see chapter 2.3.3) were applied for target analysis in chapter 4.4.2-4.4.4. Wheat root exudates, xylem exudates of maize under iron-deficiency, and xylem exudates of maize under normal iron nutrition were applied to investigate sample preparation method for MS. The sample preparation of xylem exudates of maize is the same as wheat plants in chapter 2.3.3. One complete set of Tobacco plants is grown under over expressed of nicotianamine synthase (NAS) in hydroponic culture according to Loqué *et al.* [74]. Four different sample groups are inside this set of Tobacco plants. Group-I was wildtype (WT) sample grown in a nutrition solution with 50  $\mu\text{M}$   $\text{Fe}^{3+}$ . Group-II was wildtype (WT) sample grown in a nutrition solution with 5  $\mu\text{M}$   $\text{Fe}^{3+}$ . Group-III and Group-IV were overexpressor of NAS and grown in 5  $\mu\text{M}$   $\text{Fe}^{3+}$  solution. The leave of Tobacco were rolled together, and then pressed. The pressed juice was collected with a Pasteur pipette and stored at  $-20\text{ }^{\circ}\text{C}$  until further analysis for plant metabolic profiling. There are four different sample groups in this set of Tobacco plants.

### 4.3.5 Sample preparation for MS

Sample preparation is an important procedure in chemical analysis, in order to remove the interfering matrix constituents, such as proteins. Therefore, a pre-separation of the LMW metal-species and important ligands from these interfering compounds is necessary. To keep LMW metal-species unchanged, the pH of the matrix should be kept constant. Three different sample preparation methods were tested by using wheat root exudates, xylem exudates of maize under iron-deficiency, and xylem exudates of maize under normal iron nutrition.

- i) *Filtration:* The plant samples were 1:1 diluted with solvent A, and then filtered through syringe filter with 0.2  $\mu\text{m}$  Nylon membranes (Whatman, Germany), and collected as **fraction-1**.
- ii) *Centrifugal ultrafiltration:* The plant samples were 1:1 diluted with solvent A, and then ultrafiltered through 10 KDa Ultracel YM-10 membrane filter (Millipore, Schwalbach, Germany) by Hettich EBA 3S centrifuge rotor (Hettich AG, Büch, Switzerland) at 5000 g for 60 min. The collected fraction by this method is called **fraction-2**.
- iii) *Solid phase extraction (SPE):* The adsorbent C-18 (uncapped particles 100 mg) was activated and conditioned first with 0.5 mL methanol, and then 0.5 mL ammonium acetate buffer (10mM, pH 7.3). After loading the sample onto the column, two kinds of fractions were prepared in parallel. One fraction was obtained by applying vacuum to directly elute the polar compounds and collect this elution fraction, namely **fraction-3**. The other fraction was prepared by using 0.3 mL ammonium acetate buffer (10 mM, pH 7.3) to wash out the polar compounds and collect this as wash fraction, namely **fraction-4**.

#### 4.4 Results and Discussion

Before starting this work, a method for the simultaneous separation and mass spectrometric identification of all relevant PS and metal-PS complexes in plants was not yet available. In addition, no literatures of metabolic profiling method of seeing the changes of both ligand pools and metal-species in plants can be followed. To make up these lack, the HPLC/ESI-MS methods were developed and optimized to simultaneously separate and detect all PS, metal-PS, and other important species in plants. Two important aims are supposed to be achieved by the optimized HPLC/MS method. One is “target analysis” of the well known LMW species, such as amino acids, PS, organic acids, and their metal species in plants. The other aim is to investigate the plant metabolic profile, esp. for the changes of metal-species and ligand pools in plants. Based on both “targeted analysis” and (non-targeted) metabolic profiling, a better understanding of metal transportation/translocation mechanisms in plants should be possible, and also a testing of related hypotheses (verification, falsification) should be possible.

As discussed in chapter 4.1, three different LC separation techniques, IP-RPLC, ZIC-HILIC, and ZIC-MPC, were expected to give a good separation of our polar and charged LMW species in plants. These LC methods online coupled to electrospray mass spectrometry, therefore, were investigated. The negative ionization mode was applied due to the structure of the metal-PS-complexes in solution, which are negatively charged 1:1 metal:ligand complexes in the case of divalent ions ( $Zn^{II}$ ,  $Cu^{II}$ ,  $Ni^{II}$ , and  $Fe^{II}$ ) at pH 7.3, whereas some  $Fe^{III}$ -PS may exist also as neutral species. These species are detected as  $[M-3H+Me^{II}]^{-}$  species and as  $[M-4H+Fe^{III}]^{-}$  species, respectively. Also the free ligands MA, DMA, *epi*-HMA, and nicotianamine (NA), are detectable in the negative ionization mode as  $[M-H]^{-}$  species in the  $\mu\text{mol/L}$  range, which is the relevant concentration range in real plant samples. The best HPLC/MS method is able to minimize the dissociation of metal species, give the best separation of LMW species, and allow the best detection sensitivity of both ligands and metal-species. In additional, the best method is capable to do both “target analysis” and “plant metabolic profiling”. To accurately identify the unknown metabolites in plants, Fourier-transform ion-cyclotron resonance mass spectrometry (FTICR-MS) was carried out for metabolic profiling investigations, instead of quadrupole ion trap mass spectrometry after LC separation.

Before optimization of HPLC separation and ESI-MS detection, sample preparation techniques were investigated first. This must be done, in order to remove high amounts of proteins, inorganic salts, non-polar compounds, and phenols, which would complicate the chromatograms and mass spectra, and contaminate the electrospray ionization interface. As described in chapter 4.3.5, three different sample preparation techniques were investigated: filtration, centrifugal ultrafiltration, and solid phase extraction (SPE) are the most commonly used sample preparation techniques, and carried out to remove the interfering matrix substances. As well, the sample must be properly prepared in solution for subsequent HPLC analysis.

##### 4.4.1 Sample preparation for MS

Wheat root exudates, which contain almost all of interesting species, such as DMA, DMA-metal, and citric acid, was tested by these three sample preparation methods, in order to see the changes of these important LMW species. To prove the applicability of this sample preparation method to different plants, another two different plant

samples, xylem exudates from maize under iron-deficiency or normal iron nutrition, were investigated as well. After the sample preparation process, a sample, which is “cleaner” without losing of interesting analytes, was expected.

Filtration method is carried out because most macromolecules and proteins are precipitated by adding addition water-miscible organic solvents. Therefore, solvent-A containing 90 % acetonitrile was added into the plant sample. Then this plant sample, in which most small molecules of interest are retained, was filtered by syringe filter to remove the sedimentations or particles. To remove macromolecules, centrifugal ultrafiltration is commonly applied in the biological field. In our case, centrifugal ultrafiltration (10 KDa membrane filter) was used at 5000 g for 60 min to remove the macromolecules and proteins from these plant samples. Since most of our interesting substances are polar compounds, solid phase extraction (SPE) with C-18 particles was carried out to remove the nonpolar compounds. At the same time, also proteins and phenolic compounds are removed by adsorption to the C18 material. There are mainly three kinds of SPE stationary phases, reversed phase, normal phase, and ion exchange. In our cases, the analytes are very polar and hydrophilic, which causes too strong retention on normal phase. Ion exchange SPE needs to treat the samples in either alkaline or acidic pH range, which may causes metal-species pH-shift or dissociation and disturb matrix. Therefore, reversed phase material C-18 was chosen to remove the interfering substance without changing pH. After the sample was loaded onto the column, two elution processes were carried out for collecting fractions. The first one uses a direct elution by applying vacuum. Because the plant samples are stored in water solution, polar compounds should elute out under vacuum pressure together the water composition. However, there are still some interests compounds remain on the C18 column. In order to minimize the loss of interest compounds, 0.3 mL ammonium acetate was used to wash out polar compounds. The collected elution here is called fraction-4. Comparing to the second SPE process, the first SPE method needs less the sample preparation time and limits sample dilution. The second SPE method is taking advantage of reducing the loss of interest polar compounds. After both SPE elution process, the interesting analytes are diluted in aqueous solution, which is a disadvantage for the later HILIC measurements. On contrast, samples are dissolved in high percentage of organic solvent after filtration and centrifugal ultrafiltration sample preparation.

The three sample preparation techniques were applied in parallel to these plant samples, and four fractions (1-4) were collected. All the fractions were separated by ZIC-HILIC gradient elution, and detected by online ESI-MS. The detail of investigation with this ZIC-HILIC/ESI-MS method is introduced in the following chapter 4.4.3. A comparison of the results enables to find out the optimized sample preparation method. From Fig. 4-2, total ion chromatograms (TICs) observed from fraction 1, 2, 3, and 4 were similar to each other (Fig. 4-2). Two major peaks at 14.19 min and 17.95 min ( $\pm 0.3$  min) were found in all four fractions with similar intensity. However, the peak at 4.90 min ( $\pm 0.3$  min) becomes much less in fraction 3 and 4. It means this peak may be caused by some nonpolar compound, which is retained on the SPE reversed phase packing without eluting. A closer look into the mass spectrum of the peak at 4.9 min revealed a  $m/z$  of 317.9, which is in the mass range of possible nickel-His species ( $m/z = 300 - 370$ ). Clearly, a loss of such small metal species during sample preparation must be avoided, and therefore the SPE method was not appropriate for further application to plant samples.

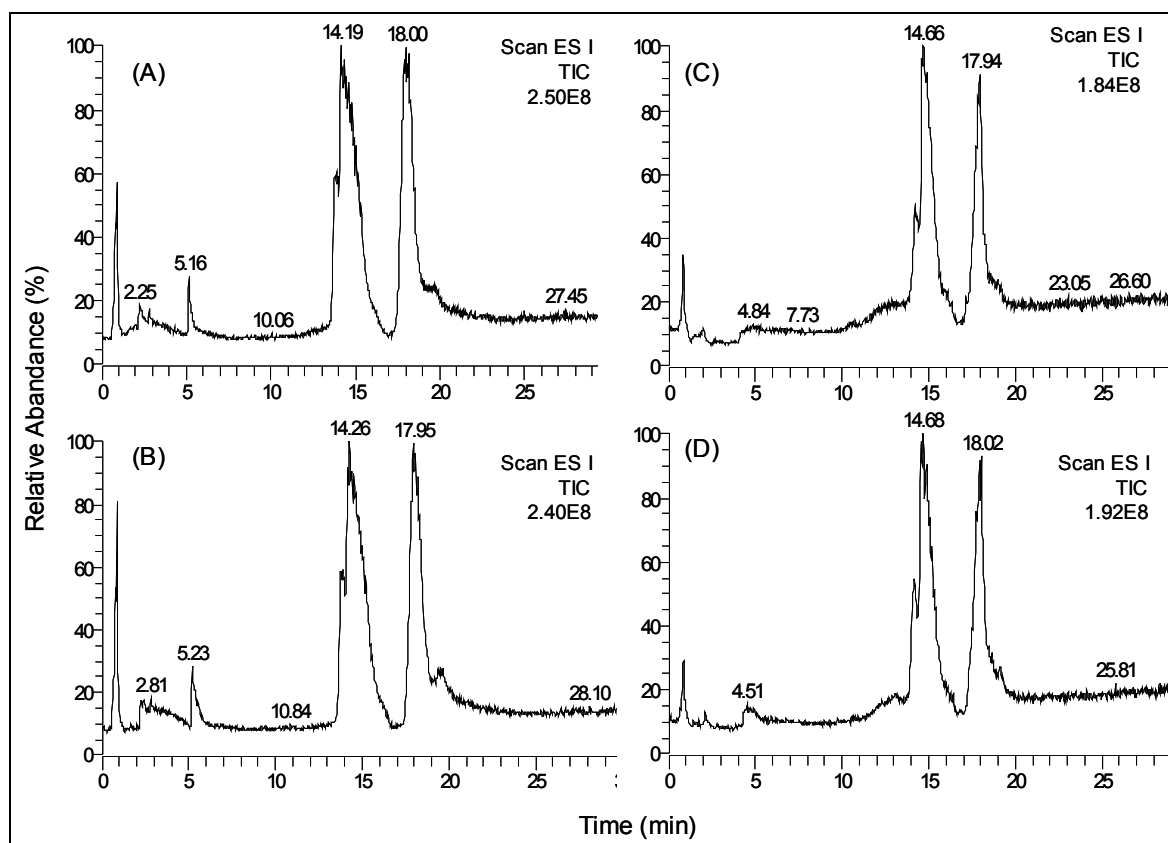


Figure 4-2. Wheat root exudates were analyzed after different sample preparation techniques. Fractions 1 (A), Fraction 2 (B), Fraction 3 (C), and Fraction 4 (D) were analyzed by on a ZIC-HILIC column with gradient elution and ESI-MS detection in the mass range  $m/z$  150-700 with negative ionization mode, individually. *Conditions*: 0-3 min 100 % eluent A (10 mM ammonium acetate + 90 % acetonitrile, pH 7.3), 3-33 min linear gradient to 30 % eluent A and 70 % eluent B (30 mM ammonium acetate + 20 % acetonitrile, pH 7.3); flow rate: 0.15 mL/min; injection volume: 5  $\mu$ L.

In order to get more detailed information on the compounds that are retained in the different sample preparation techniques, reconstructed ion chromatograms of  $m/z$  303, 356, 365, and 191 ( $\pm 0.3$  amu), were selected from the TICs (A-D). The signal of  $m/z$  303 is expected for DMA,  $m/z$  356 is expected DMA-Fe<sup>III</sup>,  $m/z$  191 is expected citric acid, and  $m/z$  365 is expected DMA-Zn<sup>II</sup>. Identification of these compounds was obtained by comparing the retention time and isotope pattern to the standard and calculated mass spectrum (details will be discussed in the following chapter 4.4.3). After different sample preparation techniques, different intensities of these species were found (shown in Fig. 4-3). The intensity of these compounds in fraction-1 was set to 100 %. The intensities of DMA in fraction-1 and -2 are very similar and much higher than in fraction-3 and -4, meaning that DMA is partially lost during SPE. The intensity of DMA-Fe<sup>III</sup> and DMA-Zn<sup>II</sup> becomes much reduced in fraction-2, -3, and -4 compared to fraction-1, indicating partial losing of this metal species during ultrafiltration and SPE. From Fig. 4-3, the intensity of citric acid was reduced in fraction 2, and no detection of citric acid was found in fraction 3 and 4. It means that SPE preparation techniques are not suitable for citric acid, which is an important free ligand in plants.



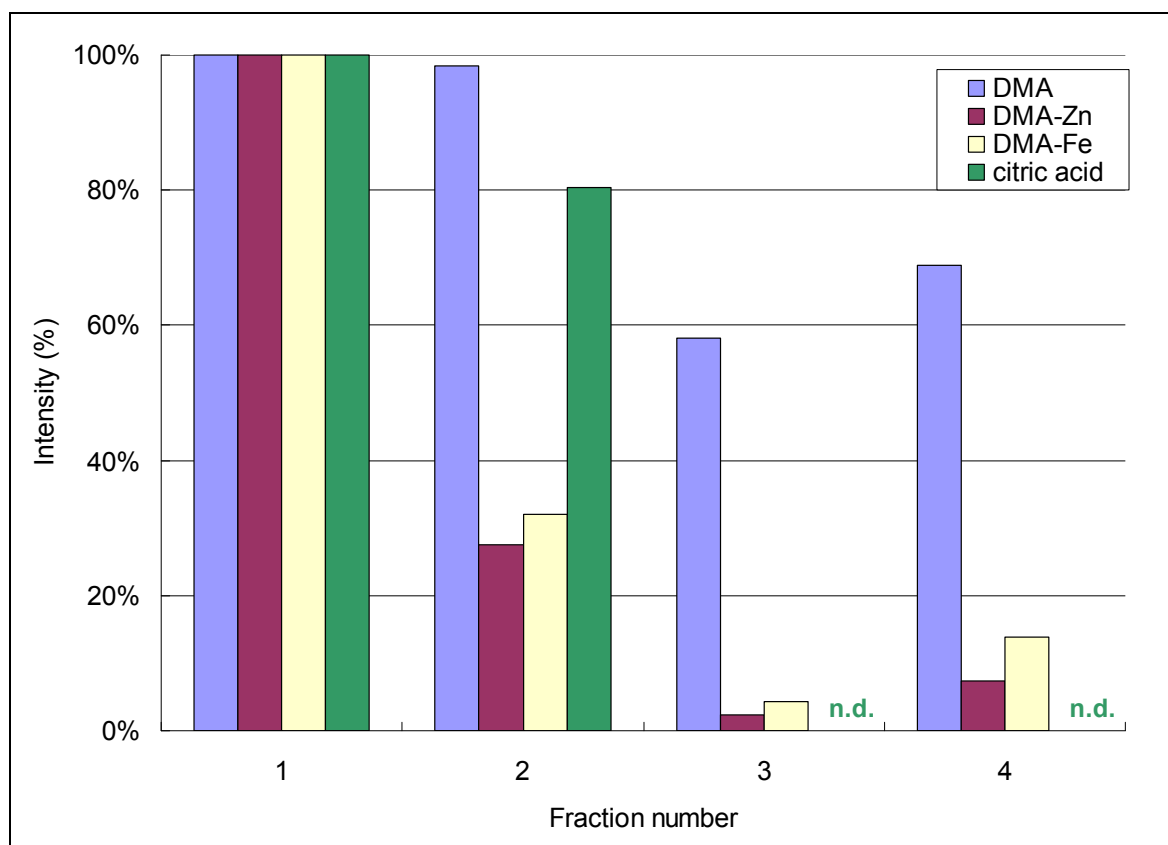


Figure 4-3. After sample preparation of root exudates sample from *Besostaja* and analyzed by ZIC-HILIC/ESI-MS method, the peak intensity of DMA and DMA-Fe<sup>III</sup> were observed in fraction (1-4). Conditions see Fig. 4-1.

Therefore, SPE is not suitable for both ligands and metal species, and ultrafiltration is suitable for metal-species. In order to keep all the important species in the solution for further analysis, the first sample preparation method, filtration (see chapter 4.3.5), is the best method, which minimizes the loss of important species and needs the shortest preparation time. Another two different plant samples, xylem exudates from maize under iron-deficiency, and xylem exudates from maize under normal iron nutrition, were investigated as well, in order to check the applicability of the sample preparation method to different plants. A similar influence of these three sample preparation techniques on the metal species was found, as for the wheat root exudates (data not shown). This confirms the suitability of the simplest sample preparation technique (precipitation/filtration) for different cultivated plant samples. In addition, after filtration process, prepared sample was dissolved in a high percentage of acetonitrile solution, which is suitable for the subsequent HILIC separation starting with a high percentage of acetonitrile in solution. Therefore, plant samples are all prepared by this method for further investigations.

#### 4.4.2 Ion-pair - Reversed phase LC (IP-RPLC)

As discussed in chapter 4.1.1, tetrabutyl ammonium (TBA) was applied as ion pair reagent for the investigation. Since TBA suppresses the mass signal, the concentration of it should be kept as low as possible. TBA with a concentration of 0.2 mM was found as the minimum amount for a proper separation of LMW compounds. When the concentration of TBA is lower than 0.2 mM, the separation of LMW species is hardly achieved, and also the reproducibility of retention time is not good. Acetonitrile was applied as organic solvent in this investigation. A high percentage of water in the mobile phase helps to achieve good separation of polar compounds.

However, too much water (high concentration of TBA) and too little acetonitrile will decrease the mass spectrometric detection sensitivity, and may even completely inhibit the detection. Increasing the percentage of acetonitrile can increase the detection sensitivity, but may cause a worse separation. To compromise these two parameters, 20 % acetonitrile was applied for the investigations.

#### 4.4.2.1 Investigating of low-molecular-weight compounds

Separation of model iron-species: In order to monitor the separation behavior of PS-metal species, EDTA-Fe<sup>III</sup> and EDDHA-Fe<sup>III</sup> as the well-known model iron species were separated on a C18 column with an isocratic elution, using TBA/ACN (80 + 20) at a flow rate of 0.15 mL/min. The retention times of them are listed in Table 4-1. EDTA-Fe<sup>III</sup> eluted at 8.8 min. Isomers of iron-EDDHA can even be baseline separated and elute out at 13.3 min and 24.7 min, respectively. These model iron-species are baseline separated by this method.

Separation of free ligands: Amino acids are important LMW species in plants, and phytosiderophores are non-protein amino acids. Five very polar amino acids, Lys, Arg, His, Glu, and Asp, were investigated by the same IP-RPLC method, in order to monitor the separation behavior of phytosiderophores. Under pH 7.3, Lys and Arg as the basic amino acids are positively charged and repulsed by the positively charged tetrabutyl ammonium group. Therefore, they have no retention on the C18 column and elute out at 1.9 min and 2.0 min, respectively. On the contrary, the negatively charged Asp and Glu interact with the positively charged tetrabutyl ammonium group, resulting in a relatively longer retention time, 5.6 min and 5.7 min, respectively. Histidine has a charge state in between Glu and Arg, and thus elutes in between these two compounds at 2.4 min. Citric acid, as one of the most important ligands in plants, was investigated as well. However, it has nearly no retention with C18 column and elutes out at 1.9 min. The dead volume time of this method is 1.9 min. It means no separation of citric acid, Lys, and Arg by this IP-RPLC method.

Table 4-1. Retention times and observed m/z values of low-molecular-weight compounds with IP-RP LC/ESI-MS method. Conditions see chapter 4.3.1 IP-RP LC.

Species	t <sub>R</sub> (min)	Observed m/z
[Lys-H] <sup>-</sup>	1.9	145.2
[Arg-H] <sup>-</sup>	2.0	173.1
[His-H] <sup>-</sup>	2.4	154.1
[Glu-H] <sup>-</sup>	5.6	146.1
[Asp-H] <sup>-</sup>	5.7	132.1
[citric acid-H] <sup>-</sup>	1.9	191.1
[EDDHA-4H+Fe <sup>III</sup> ] <sup>-</sup>	13.3	412.0
	24.5	412.0
[DMA-H] <sup>-</sup>	2.6	303.1
[DMA-3H+Zn] <sup>-</sup>	6.7	365.1
[EDTA-4H+Fe <sup>III</sup> ] <sup>-</sup>	8.8	344.1

Since metal-ligand complexes are less polar than the pure ligands according to using carboxyl and hydroxyl groups to complexate metal ions, they should have longer retention time than their free ligands on C18 column. In order to check the applicability of this method with real plant samples, a wheat root sample under iron-deficiency, which contains DMA, DMA-Zn, and citric acid, was investigated by this IP-RPLC/ESI-MS method. This same sample was investigated by CE (chapter 2.4.3), as well by the following chapter ZIC-HILIC/ESI-MS method (chapter 4.4.3.4).

#### 4.4.2.2 Investigating of plant sample

This ion-pair method shows a baseline separation of EDTA-Fe<sup>III</sup> and isomers of EDDHA-Fe<sup>III</sup>, however no good separation of acidic amino acids and citric acid. In order to check for separation efficiency for real plant samples, an iron-deficient wheat root sample, which was investigated as well by the following ZIC-HILIC/ESI-MS method (chapter 4.4.3), was investigated by IP-RPLC/ESI-MS.

As shown in Fig. 4-4A, two peaks were observed by extracting the total ion chromatogram with  $m/z$  of 303.1 ( $\pm 0.3$  amu), which is expected of DMA. By comparing the observed mass spectrum of each peak to the calculated mass spectrum of DMA, the peak at 2.6 min is unequivocally identified as DMA. The first peak, which is contained by the system peak, elute at the dead volume time. From Fig. 4-4B,  $m/z$  of 191.1 ( $\pm 0.3$  amu), which is expected of citric acid, was extracted from the total ion chromatogram of the wheat root sample, which grown under iron-deficiency. One sharp peak with  $m/z$  191.0 was found at 1.9 min, which agrees to the retention time of citric acid standard. By comparing the observed mass spectrum to the calculated mass spectrum of citric acid (the insert), good agreement was observed with the measured mass spectrum and the calculated isotope pattern. Therefore, unequivocal identification of citric acid in wheat sample can be concluded. As shown in Fig. 4-4C, the  $m/z$  of 365.0 ( $\pm 0.3$  amu), which is expected to be DMA-Zn<sup>II</sup>, was extracted from the total ion chromatogram. A broad peak was found at 6.7 min. By looking into its mass spectrum carefully (the insert), its isotope pattern is characteristic of DMA-Zn<sup>II</sup>. The broad peak form should be caused by dissociation of DMA-Zn<sup>II</sup> during separation, since PS-Zn<sup>II</sup> is relatively less stable than other divalent metal-PS species (see Table 2-3). From its observed mass spectrum (insert), many background signals, which disturb the detection sensitivity, are in the mass range 374-371 amu. Citric acid, DMA, and DMA-Zn<sup>II</sup> in real plant sample were separated and identified by this IP-RPLC/ESI-MS method within 10 min.

In additional to DMA, DMA-Zn and citric acid, DMA-Fe<sup>III</sup> and histidine were detected in the same wheat root sample by the following ZIC-HILIC method (see chapter 4.4.3.3). However, [DMA-4H+Fe<sup>III</sup>]<sup>-</sup> ( $m/z$  356.0) and [His-H]<sup>-</sup> ( $m/z$  154.1) were not found by this IP-RPLC method. This may be caused by dissociation of ferric-DMA during separation or a suppression of the mass signal from TBA causing a big mass signal at  $m/z$  360.1 in negatively mode. To check this, EDTA (50  $\mu$ M) was injected onto the C18 column after measuring the wheat root sample. Neither [EDTA-4H+Fe<sup>III</sup>]<sup>-</sup> ( $m/z$  344.1) peak, nor [EDTA-H]<sup>-</sup> ( $m/z$  291.1) peak, was found. This means, that the reason for not detecting ferric DMA lies in the bad detection sensitivity due to the presence of the ion-pair reagent, suppressing the mass spectrometric signal.

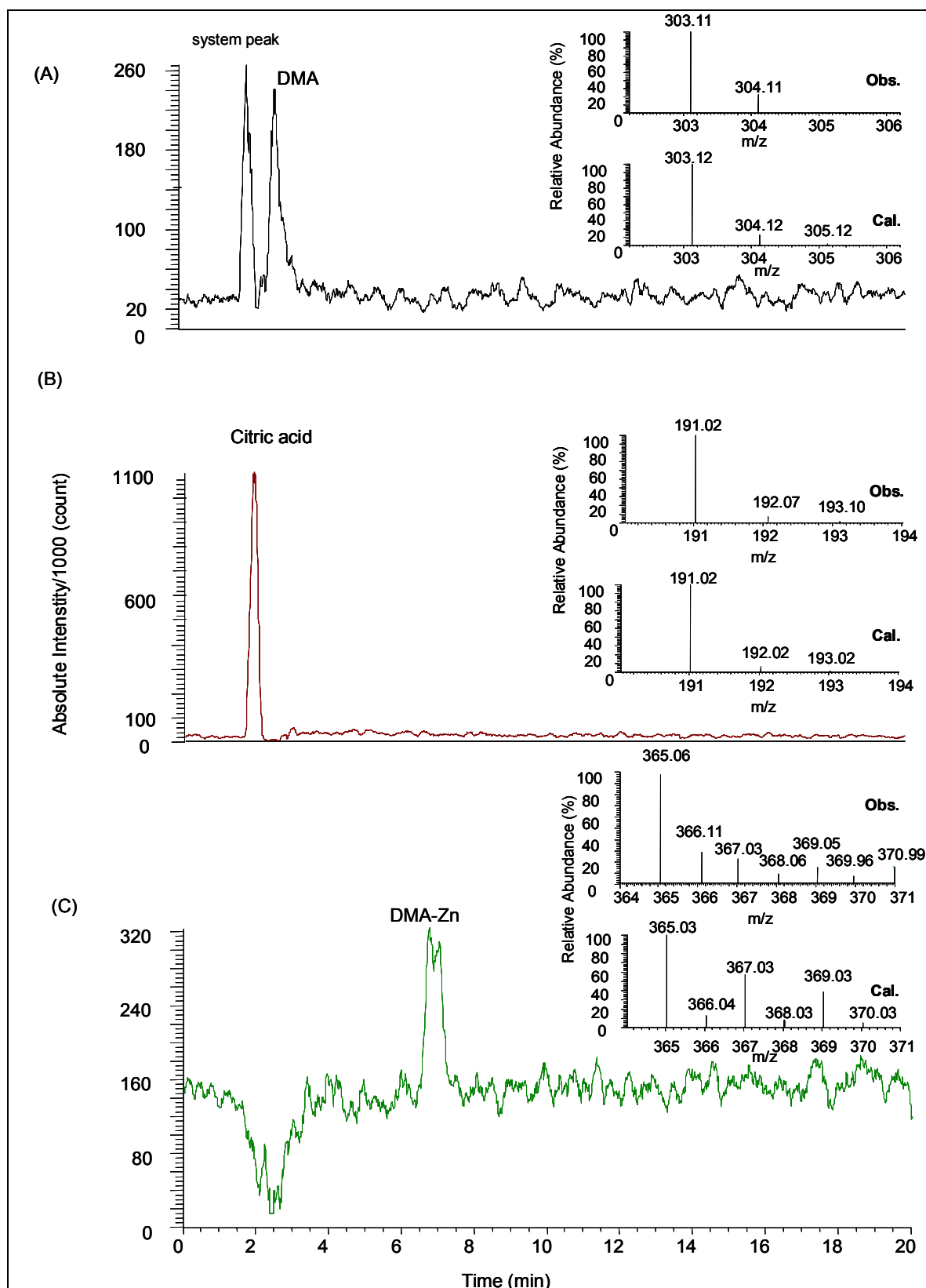


Figure 4-4. Reconstructed ion chromatograms of m/z 303 (A), 191 (B), and 365 (C) with a mass tolerance  $\pm 0.3$  amu are shown. The m/z of 191 is expected for citric acid in plant samples, m/z 303 is expected for DMA, m/z 365 is expected DMA-Zn. Insert spectra are the observed mass spectrum (Obs.) and calculated mass spectrum (Cal.) of respective peak. *Isocratic conditions*: 0 - 15 min buffer (0.2 mM TBA acetate/ACN (80 + 20), pH 7.3), flow rate: 0.15 mL/min. Sample is press sap of iron-deficient wheat root sample after 30 days of iron deficiency displayed is extracted mass chromatograms.

Although this IP-RPLC/ ESI-MS method is capable to separate some important

low-molecular-weight species in plants within a short time (about 10 min), it is not sensitive enough for some species, e.g. DMA-Fe<sup>III</sup>. The application of the ion-pair reagent, TBA, suppresses the mass spectrometric signal too much. Tributylamine, which is better volatile, was applied as a substitute of TBA to minimize the ion suppress. However, the purity of tributylamine is a key parameter. The impurities in the tributylamine cause ghost peaks especially during gradient elution profile. Therefore, IP-RPLC/ESI-MS was not carried out further. The ZIC-HILIC method, which is discussed in the next chapter, takes advantage of low salt concentration in the elution system, which is much better suited for mass spectrometry. As well a strong retention of polar and charged compounds is expected on the ZIC-HILIC column. Therefore, the ZIC-HILIC column was investigated for separation of LMW species with ESI-MS detection.

#### 4.4.3 ZIC-HILIC/ESI-MS

As described in chapter 4.1.2, zwitterionic hydrophilic interaction stationary phase takes simultaneous advantage of both the zwitterionic charged character of phytosiderophores and their hydrophilic properties, e.g. by additional hydroxyl-groups. This allows obtaining considerable high retention times for the more hydrophilic and charged analytes (e.g., free ligands), and to separate the less charged metal-ligand complexes from the free ligands. As already mentioned, this general retention characteristics are reversed with respect to RP-LC, where all PS and metal-PS species exhibit only very weak interaction with the stationary phase and are eluted near the void volume. The chromatographic behavior of the four free ligands (DMA, MA, *epi*-HMA, and NA), and that of the respective metal complexes of PS (including NA) with copper, zinc, nickel, Fe<sup>II</sup> and Fe<sup>III</sup>, is shown in Fig. 4-5 and listed in Table 4-2. Each chromatogram corresponds to the injection of one individual standard solution. Other important low-molecular-weight compounds, such as amino acids and citric acid, are investigated as well on this ZIC-HILIC column. A gradient elution with increasing water and buffer concentration was used at a pH of 7.3, which is close to the intracellular pH in plants. Ammonium acetate was chosen as buffer salt, because it is well tolerated by the ESI source in the subsequent detection step. Based on the hydrophilicity and the charge state of the analytes, a sufficient separation of most species was achieved within 25 min (see Table 4-2).

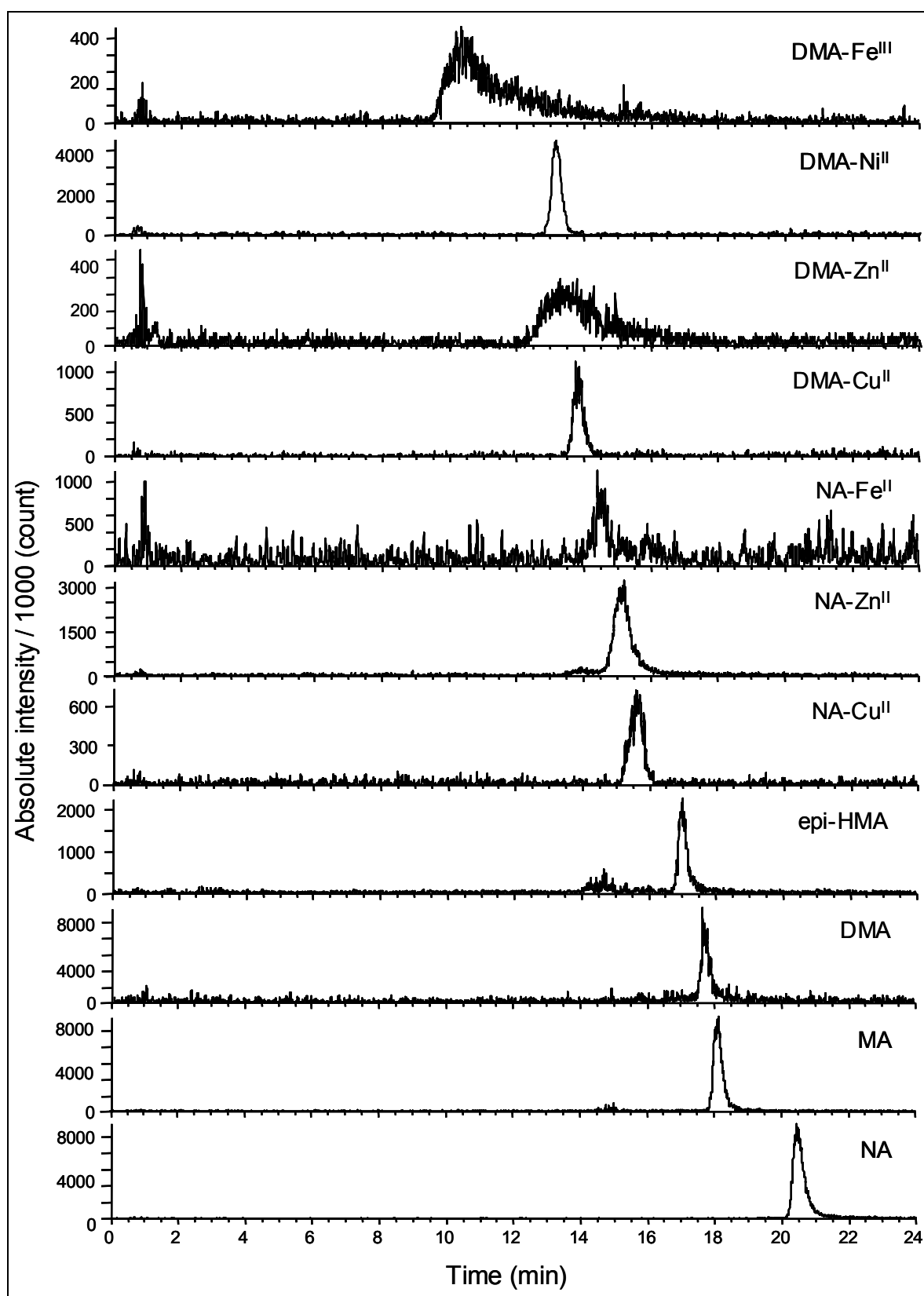


Figure 4-5. Retention of phytosiderophores and metal-phytosiderophore complexes on a ZIC-HILIC column with gradient elution and ESI-MS detection in the mass range  $m/z$  150–700 with negative ionization mode. Displayed are extracted mass chromatograms, using the  $m/z$  ( $\pm 0.3$  amu) of each species (see Table 4-2). *Conditions*: 0–3 min 100 % eluent A (10 mM ammonium acetate + 90 % acetonitrile, pH 7.3), 3–33 min linear gradient to 30 % eluent A and 70 % eluent B (30mM ammonium acetate + 20 % acetonitrile, pH 7.3); flow rate: 0.15 mL/min; injection volume: 5  $\mu$ L. NA, DMA, MA, and *epi*-HMA are 80  $\mu$ M, and all the metal phytosiderophores are in a concentration of ligand:metal = 60:40  $\mu$ M.

Table 4-2. Retention times ( $t_R$ ) and observed and calculated  $m/z$  of PS, amino acids, citric acid, EDTA, EDDHA, EDTA-Fe<sup>III</sup>, EDDHA-Fe<sup>III</sup>, and metal-PS found in standards, using the ZIC-HILIC gradient separation method and ESI-MS detection in the negative ionization mode.

Species	$t_R$ (min)	$m/z$ (observed)	$m/z$ (calculated)
[EDDHA-4H+Fe <sup>III</sup> ] <sup>-</sup>	2.4	412.0	412.1
	2.7	412.0	412.1
[EDDHA-H] <sup>-</sup>	4.0	359.0	359.1
[MA-4H+Fe <sup>III</sup> ] <sup>-</sup>	9.2	372.0	372.0
[DMA-4H+Fe <sup>III</sup> ] <sup>-</sup>	10.9	356.0	356.0
[ <i>epi</i> -HMA-4H+Fe <sup>III</sup> ] <sup>-</sup>	11.6	382.1	382.0
[MA-3H+Zn <sup>II</sup> ] <sup>-</sup>	12.4	381.1	381.1
[MA-3H+Ni <sup>II</sup> ] <sup>-</sup>	12.7	375.1	375.1
[MA-3H+Cu <sup>II</sup> ] <sup>-</sup>	12.9	380.0	380.1
[DMA-3H+Ni <sup>II</sup> ] <sup>-</sup>	13.1	359.0	359.0
[EDTA-1H] <sup>-</sup>	13.3	291.1	291.2
[DMA-3H+Zn <sup>II</sup> ] <sup>-</sup>	13.3	365.1	365.0
[ <i>epi</i> -HMA-3H+Zn <sup>II</sup> ] <sup>-</sup>	13.6	397.1	397.1
[ <i>epi</i> -HMA-3H+Ni <sup>II</sup> ] <sup>-</sup>	13.7	391.1	391.1
[DMA-3H+Cu <sup>II</sup> ] <sup>-</sup>	13.8	364.1	364.0
[ <i>epi</i> -HMA-3H+Cu <sup>II</sup> ] <sup>-</sup>	13.9	396.0	396.1
[NA-3H+Fe <sup>III</sup> ] <sup>-</sup>	14.2	355.1	355.0
[His-H] <sup>-</sup>	14.3	154.2	154.1
[Glu-H] <sup>-</sup>	14.9	146.1	146.0
[Asp-H] <sup>-</sup>	15.0	132.1	132.0
[NA-3H+Zn <sup>II</sup> ] <sup>-</sup>	15.2	364.1	364.0
[NA-3H+Ni <sup>II</sup> ] <sup>-</sup>	15.5	358.1	358.1
[NA-3H+Cu <sup>II</sup> ] <sup>-</sup>	15.8	363.0	363.0
[citric acid-H] <sup>-</sup>	16.8	191.0	191.1
[ <i>epi</i> -HMA-H] <sup>-</sup>	17.0	335.1	335.1
[DMA-H] <sup>-</sup>	17.7	303.1	303.1
[MA-H] <sup>-</sup>	18.1	319.1	319.1
[NA-H] <sup>-</sup>	20.5	302.1	302.1
[EDTA-4H+Fe <sup>III</sup> ] <sup>-</sup>	24.7	344.0	344.0
[Arg-H] <sup>-</sup>	22.8	173.0	173.0
[Lys-H] <sup>-</sup>	23.9	145.1	145.2

#### 4.4.3.1 Investigating of free ligands

**Amino acids** are very important LMW compounds in plants, esp. His. It has already been proven that histidine is involved both in the mechanism of nickel tolerance and in the high rates of nickel transport into the xylem required for hyperaccumulation in the shoot [26], as well citrate and histidine are the principal ligands for Cu, Ni and Zn [27]. In addition, amino acids are similar to phytosiderophores. Therefore, five amino acids (Lys, Arg, His, Glu, and Asp), which are polar and zwitterionic charged under pH 7.3, were investigated with the ZIC-HILIC/ESI-MS method for method development and optimization. The separation of these amino acids is based on both hydrophilic interaction and zwitterionic interaction between stationary phase and zwitterionic compounds. The five amino acids are all charged under pH 7.3, except to His, which is nearly neutral. Therefore, His is least charged and interacts least with the charged stationary phase, and then elutes first. The acidic amino acids, Glu and Asp, are negatively charged. On the contrary, Lys and Arg are basic amino acids and positively charged under these conditions. The interaction between positively charged amino acids and the negatively charged sulfonic acid group is stronger than the interaction between the negatively charged amino acids and the 'hidden' positively charged ammonium group. All together, the elution sequence of the five amino acids is His < Asp < Glu < Arg < Lys. The respective retention time and  $m/z$  value are listed in Table 4-1. As one of the most important plant metabolites, **citric acid** was investigated with the same method. A peak of  $m/z$  (191.1) was found with citric acid standard at 16.8

min (see Table 4-2).

The elution order of **phytosiderophores** (including NA) is governed by two main principles. One is the number and nature of charged groups, i.e. three carboxylic groups for all ligands, and two amino groups for the PS ligands, while NA has three amino groups (see Fig. 1-3). The other is the number of hydroxyl groups, which is increasing (from 0 to 3) in the order NA < DMA < MA < *epi*-HMA. Increasing the number of hydroxyl groups should lead to stronger hydrophilicity of the compound and thus, stronger retention on the HILIC column, resulting in an elution order of NA < DMA < MA < *epi*-HMA. Obviously, this order is not in agreement with Fig. 4-5, only the relative order of DMA and MA is explained. The reason for this discrepancy is that the charge state of the molecules has been neglected. In principle, pK values for the carboxylic acid and amino groups of the four ligands are available [in Table 2-2], but it is difficult to calculate exact values for the separation conditions. However, the relative influence of negative and positive charges can be discussed for the four ligands. Firstly, the three carboxylic groups should be negatively charged at pH 7.3 for all ligands, and one of the amino groups of PS and NA (the most basic one) is always protonated (pK between 9 and 10 [44, 87]). However, the pK value of the second amino group of PS is more and more reduced with an increase of the number of hydroxyl groups, reaching a value of 7.1 for *epi*-HMA [44]. For NA, a third (terminal) amino group is present, with a reported pK of 7.7 [87]. This means, that the contribution of positive charges goes down from NA > DMA > MA > *epi*-HMA, while the number of negative charges is not changing in this series. As an increase of charged groups on an analyte should lead to stronger interaction with the zwitterionic stationary phase, the elution order, as estimated from charge state, is *epi*-HMA < MA < DMA < NA. This series reflects the elution order of Fig. 4-5 much better than the above discussed order due to the hydroxyl groups, but it can be seen from the elution order of MA and DMA that both principles contribute to the overall retention mechanism. It should be noted, that the zwitterionic stationary phase has the negatively charged sulfonic acid group pointing out to the mobile phase and the positively charged quarternary ammonium group more 'hidden' inside the alkyl chain. Hence, the attractive interaction of any positive charge of the analyte with the sulfonic acid group of the zwitterionic stationary phase is stronger than the respective interaction between a negative charge of the analyte with the positively charged group of the zwitterionic stationary phase. Similarly, negatively charged analytes are more strongly repelled by the sulfonic acid groups than are the positively charged analytes by the 'hidden' ammonium groups. Altogether, this leads to higher retention times for positively charged analytes, and shorter retention times for negatively charged analytes. This explains the longest retention time of NA. The retention time and m/z value of the investigated PS are listed in Table 4-2.

#### 4.4.3.2 Investigating of metal-ligand complexes

**PS and PS-metal:** All metal-ligand complexes elute earlier than the respective free ligands, as depicted in Fig. 4-5 and Table 4-2. This is in accordance with theory, because the negative charge of the 1:1 metal complexes is generally lower, compared to the free ligands. Both NA and PS can supply up to six coordination points for complexation, and the distances between the groups facilitate octahedral coordination [23, 78]. The divalent metals (Zn, Cu, Ni, Fe<sup>II</sup>) are compensating two negative charges, and Fe<sup>III</sup> even one more. Hence, metal-ligand species have shorter retention times compared to pure ligands, and Fe<sup>III</sup> species elute earlier than respective Fe<sup>II</sup>-species. The slightly different retention times of different divalent metals with one ligand are



probably explained by slightly different charge states through interaction with the carboxyl and amino groups. At pH 7.3 all the divalent PS and Fe<sup>III</sup>-DMA complexes have a net charge of -1; but Fe<sup>III</sup>-NA has a net charge of zero [25]. The lack of charge on Fe<sup>III</sup>-NA is due to the compensation of the negative charges of the carboxylate groups by the Fe<sup>III</sup>. In the case of PS, the additional negative charge is due to the deprotonation of the terminal OH group in presence of Fe<sup>III</sup> [89]. The final elution sequence of all species is listed in Table 4-2.

**Same metal-different ligand species:** From the data presented in Fig. 4-5 and Table 4-2, it is clearly seen that the uncomplexed ligands DMA, MA, *epi*-HMA, and NA and the respective complexes of one metal are baseline separated. For example, Ni<sup>II</sup>-MA (12.7 min), Ni<sup>II</sup>-DMA (13.1 min), Ni<sup>II</sup>-*epi*-HMA (13.7 min), and Ni<sup>II</sup>-NA (15.5 min) are baseline separated. The similar separation efficiency was achieved with Zn<sup>II</sup>-PS and Fe<sup>III</sup>-PS (PS = MA, *epi*-HMA, and NA) as well. Cu<sup>II</sup>-DMA (13.8 min), Cu<sup>II</sup>-MA (12.9 min), and Cu<sup>II</sup>-NA (15.8 min), are baseline separated. Although Cu<sup>II</sup>-*epi*-HMA (13.9 min) and Cu<sup>II</sup>-DMA (13.8 min) elute at similar retention time and their chromatographic peaks are partially overlapping, their *m/z* value difference is 36 amu, which allows unequivocal identification of them. **Same ligand-different metal species:** Baseline separation of the species of different metal species of one single ligand was achieved. As shown in Fig. 4-5 and Table 4-2, for example, DMA-Fe<sup>III</sup> (10.9 min), DMA-Cu<sup>II</sup> (13.8 min), and DMA-Zn<sup>II</sup> (13.3 min) are baseline separated. Although DMA-Ni<sup>II</sup> (13.1 min) and DMA-Zn<sup>II</sup> (13.3 min) are partially chromatographic overlapped, unequivocal identification was achieved by their distinct mass spectra. Similar separation efficiency of different metal species complexing with each other free ligand was achieved as well, e.g. MA-Me, *epi*-HMA-Me, NA-Me (Me = Ni<sup>II</sup>, Cu<sup>II</sup>, Zn<sup>II</sup>, and Fe<sup>III</sup>). This is an advantage over CE, which can not baseline separate all these investigated metal-species.

**Metal-species with overlapping mass spectra:** As mentioned in chapter 4.2, some complexes have very similar *m/z* values, namely the Fe<sup>II</sup>-NA and Fe<sup>III</sup>-DMA species. On the ZIC-HILIC column, a baseline of Fe<sup>II</sup>-NA (*t<sub>R</sub>* = 14.2 min) and Fe<sup>III</sup>-DMA (*t<sub>R</sub>* = 10.4 min) is achieved. A baseline separation is also obtained for Zn-NA (*t<sub>R</sub>* = 15.2 min) and Cu-DMA (*t<sub>R</sub>* = 13.8 min), which have overlapping mass spectra. It is really important, that the metal-species having overlapping mass spectra are baseline separated from each other. Only in case of achieving such separation, an unequivocally identification could be realised by ZIC-HILIC/ESI-MS.

The variation of the retention times is < 3 %, and the retention times of individually injected standards do not differ significantly from those of respective species in mixtures or real plant samples (see chapter 4.4.3.3). Also listed in this table are the *m/z* values (theoretical and measured), which are used for the detection of all species. The combination of mass spectrometric and retention time data allows an unequivocal identification of all target compounds.

#### 4.4.3.3 Detection and identification of low-molecular-weight species in plants with on-line ESI-MS

For element specific detection of metal phytosiderophore complexes, AAS and ICP-MS have been applied [42, 45]. For analyses of plant material, however, complete information on the molecular identity of metal complexes is needed. Identification of PS and metal-PS species is straight forward by comparison with respective standards containing only one of the mugineic acids or metal-PS complexes. The negative ionization mode was applied due to the structure of the

metal-PS-complexes in solution, which are negatively charged 1:1 [metal: ligand] complexes in the case of divalent ions ( $Zn^{II}$ ,  $Cu^{II}$ ,  $Ni^{II}$ , and  $Fe^{II}$ ) at pH 7.3. Also  $Fe^{III}$ -DMA is negatively charged at pH 7.3, but  $Fe^{III}$ -NA exists as neutral species and was not detectable with appropriate sensitivity by ESI-MS (data not shown). *In planta*, the concentration of PS and metal-PS complexes is in the micro molar concentration range [38, 41]. To assess the applicability of the method to analyze real plant samples, micro molar concentrations of PS and metal-PS complexes were investigated. The small signal for  $Fe^{II}$ -NA is due to instability of this compound (dissociation, oxidation) during chromatographic separation, and is not caused by low ionization efficiency of the ESI process. This will be shown in chapter 4.4.3.5. The distinctive mass spectra, in conjunction with the retention time differences, enable unambiguous identification of all target analytes, in this case.

**Calibration curve and linearity of ESI-MS:** The linearity of ESI-MS detection was demonstrated by determination of EDDHA. Since the amounts of standard phytosiderophores are very limited, EDDHA, which is structurally and also physiologically similar to phytosiderophores, was applied to determine the linear mass spectrometric quantification range with the proposed method. EDDHA contains two chiral carbon centers, which produce  $Fe^{III}$ -EDDHA isomers [85, 88, and 162]. Moreover, it was one of the important synthetic metal chelates applied for micronutrient fertilization in foliar, trunk and soil application and in hydroponic cultures. EDDHA and  $Fe^{III}$ -EDDHA were analysed by the proposed ZIC-HILIC/ ESI-MS method. The retention times (see Table 4-2) are shorter than the retention times of PS and metal-PS species, because of the two phenol groups, which are relatively unpolar. Therefore, EDDHA is less hydrophilic than PS and NA and elutes earlier. Similar to PS, the respective  $Fe^{III}$ -EDDHA complexes eluted earlier than the pure ligand EDDHA, due to the involvement of several charged groups in the coordination with Fe. The separation of the two isomers of  $Fe^{III}$ -EDDHA (*rac*- and *meso*-forms), which was reported using ion-pair chromatography [85, 88], is also possible using our proposed method (see Table 4-2). This indicates that the zwitterionic hydrophilic stationary phase is also well-suited for isomer separation. To investigate the linearity of our method, EDDHA was applied as standard for obtaining a calibration curve. A linear range of quantification was found between 5 and 100  $\mu$ M with a correlation coefficient of the linear regression of  $> 0.99$ . This corresponds to injected amounts of 9 - 180 ng EDDHA (25-500 pmol). 5  $\mu$ M (9 ng) is the limit of quantification (signal to noise ratio  $> 10$ ). The detection limit is 2  $\mu$ M (3.6 ng), as estimated from a signal to noise ratio  $> 3$  at the respective *m/z*.

#### 4.4.3.4 Target analyses of important low-molecular-weight species in plant samples

In order to check the applicability of the proposed ZIC-HILIC/ESI-MS method, several plant samples were analysed. **Arabidopsis plants**, which are grown under iron-deficiency and differ only in their nutrient status (with or without nickel-nutrient), were investigated. One example of wildtype (WT) with nickel-nutrient and iron-deficiency, namely "WT-Fe+Ni", was shown in Fig. 4-6. For comparison, the chromatograms of a Ni-NA standard (32 + 80  $\mu$ M) and one wildtype (WT) Arabidopsis sample, which is grown without nickel-nutrient and with iron-deficiency, namely "WT-Fe-Ni", are also shown. The respective mass spectrum of the Ni-NA peak ( $[M-3H+Ni]^-$ , *m/z* 358.1), which is found at 15.4 min, is shown as inset to Fig. 4-6. Comparison with the theoretical mass spectrum (isotopic pattern), and also with the retention time of the standard (Fig. 4-5) confirmed the identity of this species. As

expected, there is no NA-Ni was detected in this “WT-Fe-Ni” sample. By comparing the peak areas of NA-Ni in “WT-Fe+Ni” sample and in standard, the concentration of NA-Ni was around 5  $\mu\text{M}$  in “WT-Fe+Ni” sample. It proves that the detection sensitivity of ESI-MS is sufficient to detect low micro molar concentrations, which is the concentration range of most important LMW species in plants. It also proves this method can monitor the concentration changes of metal-species in plants. It is worthy to point out that the identity and semi-quantitation of NA-Ni were in good agreement with analyses of the same *Arabidopsis* plant by CE method (see chapter 2.4.3).

As an advantage over CE, this developed ZIC-HILIC/ESI-MS method can simultaneously detect and identify the important free ligands in plants, such as citric acid and histidine. Citric acid ( $m/z = 191.1$ ) and histidine ( $m/z = 154.0$ ) were found in the sample as well. Concentration changes are easily seen for these potential ligands with this method. This will be discussed below.

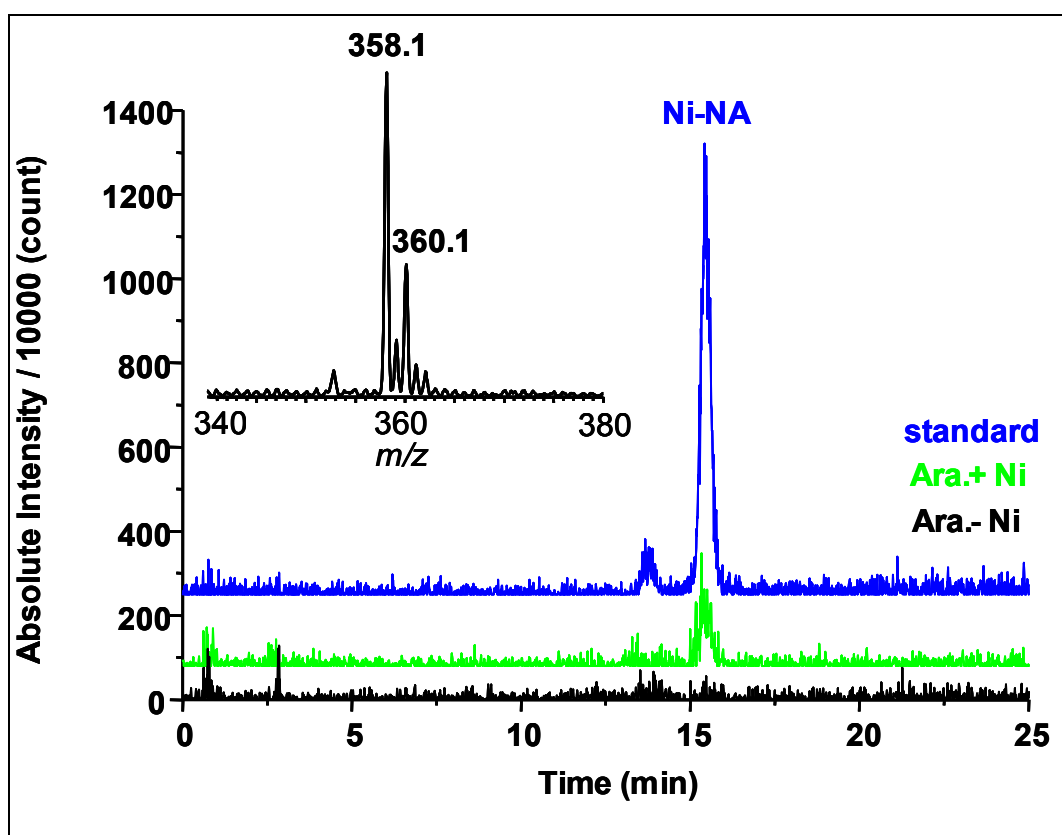


Figure 4-6. Analysis of the Ni-NA in xylem sap of *Arabidopsis* (grown with/without Ni-nutrient solution) by ZIC-HILIC/ESI-MS. Std: standard (80  $\mu\text{M}$  NA plus 32  $\mu\text{M}$  Ni); Ara.+Ni: Xylem sap of *Arabidopsis* grown under Ni-nutrient solution; Ara.-Ni: Xylem sap of *Arabidopsis* grown without Ni-nutrient solution; displayed are extracted mass chromatograms at  $m/z$  358.1 ( $\pm 0.3$  amu); Inset: Mass spectrum ( $m/z$  340-380) extracted from the NA-Ni peak at 15.4 min. Conditions see Fig. 4-5.

In Fig. 4-7A and B, analyses are shown for a sample of **wheat root**, which was grown under different time period of Fe-deficiency. With increasing time of deficiency, increasing peaks for Zn-DMA ( $m/z$  365.1), and Cu-DMA ( $m/z$  363.9) are found at 13.5 min, and 14.0 min, respectively. Comparison with the mass spectra, which are shown as insets to the figures, confirmed the identity of the species. The increasing concentration of Zn-DMA and Cu-DMA is because of the increased synthesis of DMA under iron-deficiency stress. A small peak of  $\text{Fe}^{\text{III}}$ -DMA ( $m/z$  356.0) was also found in the samples, but with very low intensity (due to the Fe deficiency status). Comparing to the results with CE analysing the same wheat root samples, the similar

concentration changes of DMA-Cu under different period of iron-deficiency was found. It demonstrates both CE and HPLC/MS method verify the identification and concentration changes of important species in plants. DMA-Fe<sup>III</sup> and DMA-Zn are only detected and identified by HPLC/MS, but not by CE method. It shows the advantages of this developed HPLC/MS method that it is much more sensitive and capable to identify partially co-elute species.

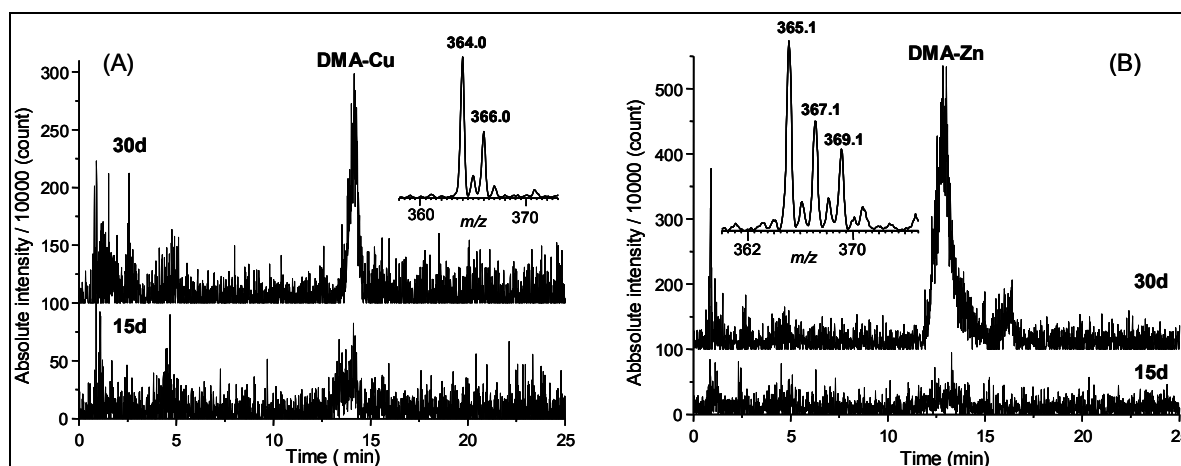


Figure 4-7. (A) Detection of Cu-DMA in press sap of iron-deficient wheat root. 15d, sample after 15 days of iron deficiency; 30d, sample after 30 days of iron deficiency; displayed are extracted mass chromatograms at  $m/z$  364.0 ( $\pm 0.3$  amu); Inset: Mass spectrum ( $m/z$  358-373) extracted from the DMA-Cu peak at 14.2 min. (B) Detection of Zn-DMA in press sap of iron-deficient wheat root. 15d, sample after 15 days of iron deficiency; 30d, sample after 30 days of iron deficiency; displayed are extracted mass chromatograms at  $m/z$  365.0 ( $\pm 0.3$  amu); Inset: Mass spectrum ( $m/z$  360-375) extracted from the DMA-Zn peak at 13.1 min. Conditions see Fig. 4-5.

Another advantage of the developed method is the simultaneous detection of other compounds in the plant samples, in addition to the PS species. Several peaks are well separated and some of them are easily identified by comparison with individual standards. For example, as shown in Fig. 4-8A, citric acid ( $m/z$  191.0) was detected in the Arabidopsis plants, which are grown with/without Ni-nutrient solution. The concentration of citric acid changes with different cultivated environment. In the wheat samples grown under different period of iron-deficiency, citric acid ( $m/z$  191.0) and histidine ( $m/z$  154.2) were detected at retention time 17.4 min and 14.8 min, respectively. From Fig. 4-8B, it can be seen that longer iron-deficiency the plant sample is, more citric acid presents. Both citric acid and histidine are well known ligands in plants, but respective metal-species of these ligands were not yet detected. The simultaneous separation and identification of several compounds, which are discussed as potential ligands in plants, enable the method to investigate metabolic profiling of the ligand pool, being available for metal complexation.

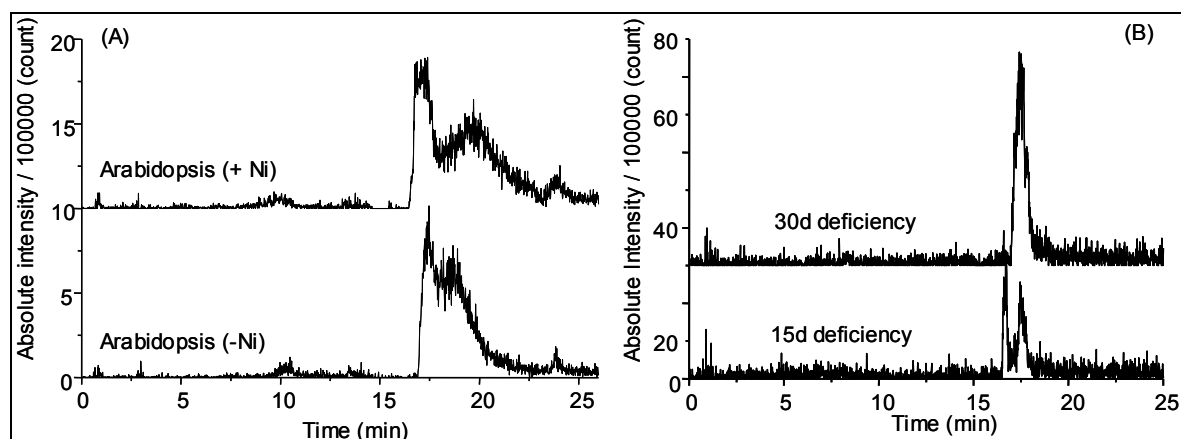


Figure 4-8. (A) Detection of citric acid in the same *Arabidopsis* samples in Fig. 4-6. Arabidopsis (+Ni): Arabidopsis sample grown with nickel-nutrient; Arabidopsis (-Ni): Arabidopsis sample grown without nickel-nutrient; displayed are extracted mass chromatograms at  $m/z$  191.0 ( $\pm 0.3$  amu); (B) Detection of citric acid in the same wheat root samples in Fig. 4-7; displayed are extracted mass chromatograms at  $m/z$  191.0 ( $\pm 0.3$  amu); 30d deficiency: 30 days iron-deficiency; 15d deficiency: 15 days iron-deficiency. Conditions see Fig. 4-5.

#### 4.4.3.5 Investigating of the stability of metal-ligand complexes during the separation

During chromatographic separation, dissociation of metal-PS complexes may appear. With ferrous complexes, oxidation may also occur during the separation. Those reactions can cause column contamination, poorly reproducible retention times, and even may lead to systematic errors in the analysis of plant samples. Therefore, it is essential to check whether any metal contamination of the column occurs. For this purpose, EDTA (20  $\mu$ M) was injected after each run of metal-phytosiderophore samples. In case of no dissociation (and no metal contamination of the column), a peak of the pure ligand EDTA ( $[M-H]^-$ ,  $m/z$  290.9) is detected at 13.3 min. This behavior was observed in the case of EDTA measurements after the runs of  $Me^{II}$ -DMA and  $Me^{II}$ -NA ( $Me^{II} = Cu^{II}$ ,  $Ni^{II}$ , and  $Zn^{II}$ ); only the EDTA peak was found in the chromatograms. That indicates that those divalent PS complexes, except ferrous complexes, are stable during the separation. But after injection of EDTA directly after the run of  $Fe^{III}$ -DMA, a peak of  $[EDTA-4H+Fe^{III}]^-$  ( $m/z$  344.0) appeared instead of  $[EDTA-H]^-$  at a retention time of 21.7 min, indicating partial dissociation of  $Fe^{III}$ -DMA during the separation. Also, the broad and tailing peak profile (see Fig. 4-5) of  $Fe^{III}$ -DMA is an indication of the dissociation during the separation. The degree of dissociation was estimated to be 15-20 %, based on the amount of Fe, which was recovered by the cleaning procedure after injecting the  $Fe^{III}$ -DMA standard. When dissociation of metal complexes was observed, a cleaning process was performed to wash out all the residual metal out of the column (see chapter 4.3.1.2). In spite of the partial dissociation of  $Fe^{III}$ -DMA on the column, the sensitivity is still good enough to detect  $Fe^{III}$ -DMA in (non-deficient) plant samples. PS complexes of other metals are little dissociated during the separation (< 5 %), giving very good sensitivity and peak profiles.

It is well known that ferrous compounds are usually unstable in aerobic environment and quickly oxidize to ferric compounds. Therefore, it is important to investigate whether any oxidation of ferrous phytosiderophore complexes happens during the separation. When  $Fe^{II}$ -DMA was investigated (data not shown), there was no  $[DMA-3H+Fe^{II}]^-$  ( $m/z$  357.0), instead a  $Fe^{III}$ -DMA peak eluted around 11 min with  $m/z$  value of 356.0. Hence,  $Fe^{II}$ -DMA oxidized to  $Fe^{III}$ -DMA during the separation, or

maybe was partly oxidized already before the injection.  $\text{Fe}^{\text{II}}\text{-NA}$  was also investigated by the same gradient method, and at a retention time of 14.2 min a small  $[\text{NA-3H+Fe}^{\text{II}}]^-$  peak with a  $m/z$  value of 356.1 was found (see Fig. 4-5). Although, the ferrous NA peak is detectable, the sensitivity is far too poor by comparing to the other divalent NA complexes. To check whether dissociation or oxidation of  $\text{Fe}^{\text{II}}\text{-NA}$  occurs during the separation, different mobile phase elution profiles were used to change the elution speed of  $\text{Fe}^{\text{II}}\text{-NA}$  complex. A mobile phase consisting of 20 % ammonium acetate (10 mM) + 80 % acetonitrile, pH 7.3, was applied for stronger elution strength than solvent A, which was used in the beginning of the standard gradient. The same concentration of  $\text{Fe}^{\text{II}}\text{-NA}$  sample was investigated with the isocratic elution profile and the gradient one. With this isocratic elution,  $\text{Fe}^{\text{II}}\text{-NA}$  ( $m/z$  356.1) eluted at 1.4 min with a sharp and sensitive peak profile (see Fig. 4-9). Moreover, the isotopic pattern of the mass spectrum is in good agreement with the theoretical spectrum (see inset to Fig. 4-9). Compared to the gradient elution, where  $\text{Fe}^{\text{II}}\text{-NA}$  eluted at 14.4 min, this is a drastic decrease of separation time. The decrease of retention time is the main reason for the increase in stability of the  $\text{Fe}^{\text{II}}\text{-NA}$  species. From this it can be concluded, that the instability of  $\text{Fe}^{\text{II}}\text{-NA}$  is mainly due to kinetic instability of this species, and not due to oxidation. It has already been proved that Fe complexes of NA are relatively poor Fenton reagents, as measured by their ability to mediate  $\text{H}_2\text{O}_2$ -dependent oxidation of deoxyribose [25]. This suggests that NA could have an important role in scavenging Fe and protecting the cell from oxidative damage.

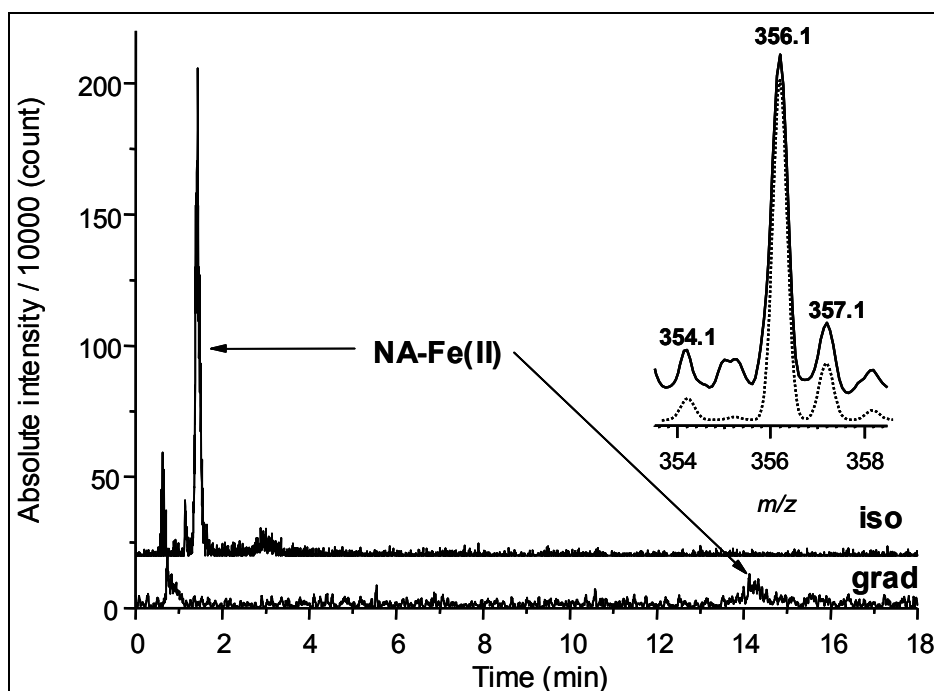


Figure 4-9. Isocratic vs. gradient chromatography of  $\text{Fe}^{\text{II}}\text{-NA}$  by ZIC-HILIC/ESI-MS. Iso: isocratic separation (10 mM ammonium acetate + 80 % acetonitrile, pH 7.3; flow rate 0.15 mL/min); grad: gradient separation (for details see Fig. 4-5); displayed are extracted mass chromatograms at  $m/z = 355 (\pm 0.3 \text{ amu})$ ; the analyte was mixed from 100  $\mu\text{M}$  NA + 40  $\mu\text{M}$   $\text{Fe}^{\text{II}}$  + 40  $\mu\text{M}$   $\text{Fe}^{\text{III}}$ ; Inset: observed mass spectrum ( $m/z$  353.5-358.5) extracted from the  $\text{NA-Fe}^{\text{II}}$  peak at 1.4 min. Also shown is the calculated mass spectrum (isotope pattern) of this species (dotted line).

The fast isocratic separation method for  $\text{Fe}^{\text{II}}\text{-NA}$  can even be used to separate  $\text{Fe}^{\text{II}}\text{-NA}$  and  $\text{Fe}^{\text{III}}\text{-NA}$ . If a mixture of  $\text{Fe}^{\text{III}}\text{-NA}$  and  $\text{Fe}^{\text{II}}\text{-NA}$  is injected and separated by the isocratic method, a peak of mass 355.1 was found at 0.81 min for  $\text{Fe}^{\text{III}}\text{-NA}$ , which is well separated from the peak of  $\text{Fe}^{\text{II}}\text{-NA}$  (at 1.4 min). This proves that a separation of mixtures of ferrous and ferric complexes is possible within 2 min. However, this

method is not recommended for application of complex plant samples, because the  $\text{Fe}^{\text{III}}$ -NA is eluted very close to the void volume, and the identification would be hampered by coelution of many other compounds. Moreover, this fast separation does not allow a separation of all metal-PS-species simultaneously. If equilibria involving ferrous and ferric complexes of phyto siderophores must be analyzed with high accuracy, the use of high resolution MS [161] is a better alternative to separation based analysis.

Till now, sufficient separation of LMW species in plants is achieved in 25 min, sensitive detection of known LMW species in plants is possible at low micro molar concentrations, and unequivocal identification of LMW species in plants is obtained based on both retention time and isotope pattern of mass spectrum, by using the optimized ZIC-HILIC/ESI-MS method. Even DMA- $\text{Fe}^{\text{III}}$  dissociates during separation, detection of DMA- $\text{Fe}^{\text{III}}$  is possible in the real plants. A possible explanation of this instability could be the strong interaction of iron species with the negatively charged sulfonic acid group of the ZIC-HILIC material. In order to test this hypothesis, another zwitterionic charged HILIC column (ZIC-MPC) was investigated, in which the sulfonic acid group is replaced by a phosphonic acid group. Moreover, in ZIC-MPC the polarity is reversed, i.e. the negatively charged group is more hidden inside the material and thus should exhibit only weak interactions with metal complexes.

#### 4.4.4 ZIC-MPC & ZIC-HILIC

As described in chapter 4.4.3.5., ferric phyto siderophore complexes are partially dissociating during separation on ZIC-HILIC column, which may be due to interaction with sulfonic acid groups. In order to decrease this dissociation of ferric-PS species, a different HILIC column, ZIC-MPC, was investigated. With ZIC-MPC, a phosphorylcholine group is covalently bonded to the stationary phase. While the hydrophilic interaction mechanism should be similar for both HILIC stationary phases, the major difference of the separation behavior between ZIC-MPC and ZIC-HILIC is the zwitterionic charge arrangement. On ZIC-MPC column, the positively charged quaternary amine group is pointing out to the mobile phase and the negatively charged phosphoric acid group is hiding inside the alkyl chain. The stationary phase with phosphorylcholine functionality has a net negative surface charge in wide pH range, although their spatial charge arrangement is in favor of giving positive charge [138]. However, the surface charges differ between the stationary phase having sulfobetaine and phosphorylcholine functional groups [138, 163], in which the zeta-potential of both functional groups were measured. The stability of ferric phyto siderophores on the ZIC-MPC column was investigated. To make a comparison of the separation efficiency of the important LMW species in plants between ZIC-MPC and ZIC-HILIC, all the pure ligands, metal-ligand species, and real plant samples, which were investigated in chapter 4.4.3, were also investigated on ZIC-MPC column with the same elution gradient profile and ESI-MS conditions as on ZIC-HILIC.

##### 4.4.4.1 Stability of ferric phyto siderophores

Stability of ferric phyto siderophores was investigated with the same method as on ZIC-HILIC column (chapter 4.4.3.5). A dissociation of ferric-PS is as well happening with ZIC-MPC column, according to injection of EDTA (20  $\mu\text{M}$ ) after the measurement of metal-PS. Quite similar results as for the ZIC-HILIC column were found on the ZIC-MPC column as well for divalent PS complexes, except ferrous complexes, which are stable during the separation. Since EDTA- $\text{Fe}^{\text{III}}$  was found upon injection of EDTA after the measurement of ferric-PS, it is clear that dissociation of ferric PS takes place

also on ZIC-MPC. The broad and tailing peak profile of Fe<sup>III</sup>-DMA is also found on the ZIC-MPC column (similar to ZIC-HILIC), which confirms the dissociation during the separation. The degree of dissociation was estimated to be 12-18 % (15-20 % with ZIC-HILIC column), based on the amount of Fe, which was recovered by the cleaning procedure after injecting the Fe<sup>III</sup>-DMA standard. This means that the reversed polarity of ZIC-MPC and the substitution of sulfonic acid by phosphoric acid groups do not result in less dissociation of the ferric-PS complexes. One explanation may be the net negative charge state of both stationary phases, interacting still strongly with iron ions.

#### 4.4.4.2 Comparison of the separation behavior of ZIC-MPC and ZIC-HILIC

In order to see whether ZIC-MPC gives better separation efficiency, amino acids, citric acid, EDTA, EDDHA, phytosiderophores, nicotianamine, including respective metal-ligand species were investigated on ZIC-MPC column with the same concentration as ZIC-HILIC column. Also same plant samples were investigated on both columns.

**Amino acids** To compare the separation behavior between ZIC-MPC and ZIC-HILIC, the same five polar and zwitterionic charged amino acids (Lys, Arg, His, Glu, and Asp) were investigated by ZIC-MPC method. A similar separation behavior was achieved on ZIC-MPC with the same gradient profile and ESI-MS conditions, as compared to ZIC-HILIC. A comparison of these ligands retention behavior is listed in Table 4-3. They elute in the same sequence as on ZIC-HILIC column. Histidine, which is nearly neutral at pH 7.3, elutes first, because of the weakest zwitterionic interactions with the charged stationary phase. Asp and Glu are negatively charged and elute directly after His. The retention times of these two, compared to ZIC-HILIC, are later on ZIC-MPC. This phenomenon is caused by the stronger ionic interaction between the negatively charged Asp and Glu and the positively charged amine end-group of the stationary phase. Lys and Arg are positively charged and elute last. Lys and Arg elute earlier on ZIC-MPC column than on ZIC-HILIC, which is caused by the stronger electrostatic repulsion between positively charged Lys and Arg and positively charged quaternary amine end-groups. The general elution order of amino acids is not changed, because of the net negatively charged ZIC-MPC stationary phase. However, due to the above mentioned effects, the amino acids are 'pushed together', which leads to a decrease of separation efficiency of amino acids on ZIC-MPC (as compared to ZIC-HILIC).

Table 4-3. Comparison of the retention behavior of LMW compounds on ZIC-HILIC column and ZIC-MPC column. Separation and detection conditions are shown in Fig. 4-5.

Species	Retention time on ZIC-HILIC column $t_R$ (min)	Retention time on ZIC-MPC column $t_R$ (min)
[EDDHA-4H+Fe <sup>III</sup> ] <sup>-</sup>	2.4	0.9
	2.7	1.9
[EDDHA-H] <sup>-</sup>	4.0	7.9
[DMA-4H+Fe <sup>III</sup> ] <sup>-</sup>	10.9	8.4
[MA-3H+Ni <sup>II</sup> ] <sup>-</sup>	12.7	13.4
[DMA-3H+Ni <sup>II</sup> ] <sup>-</sup>	13.1	13.4
[EDTA-H] <sup>-</sup>	13.3	18.2
[epi-HMA-3H+Ni <sup>II</sup> ] <sup>-</sup>	13.7	15.0
[His-H] <sup>-</sup>	14.3	14.5
[Glu-H] <sup>-</sup>	15.0	15.8
[Asp-H] <sup>-</sup>	14.9	15.7
[NA-3H+Ni <sup>II</sup> ] <sup>-</sup>	15.5	15.0
[citric acid-H] <sup>-</sup>	16.8	17.1
[epi-HMA-H] <sup>-</sup>	17.0	15.0



Species	Retention time on ZIC-HILIC column $t_R$ (min)	Retention time on ZIC-MPC column $t_R$ (min)
[DMA-H] <sup>-</sup>	17.7	17.7
[MA-H] <sup>-</sup>	18.1	17.8
[NA-H] <sup>-</sup>	20.5	19.8
[Arg-H] <sup>-</sup>	22.8	21.4
[Lys-H] <sup>-</sup>	23.9	21.8
[EDTA-4H+Fe <sup>III</sup> ] <sup>-</sup>	24.7	25.4

**Citric acid, EDTA, and EDDHA** exhibit longer retention on the ZIC-MPC column than on the ZIC-HILIC column. Since their negative charges interact stronger with the positively charged amine group, hence, they elute later.

**Phytosiderophores**, including *epi*-HMA, MA, DMA, and NA, elute in the same order on ZIC-MPC column as on ZIC-HILIC column. Similar to amino acids, poor separation efficiency was found with MA, DMA, and NA on ZIC-MPC column as well. A direct comparison of elution behavior of PS (including NA) on both ZIC-MPC and ZIC-HILIC columns is shown in Fig. 4-10. All phytosiderophores elute earlier on the ZIC-MPC column than they do on the ZIC-HILIC column. This is because they are all zwitterionic charged compounds at pH 7.3. The electrostatic repulsive interaction between their positively charged amine groups with the positively charge quaternary amine end-groups on ZIC-MPC is greater than with the ZIC-HILIC stationary phase, in which the positively charged quaternary amine groups are hidden inside the alkyl chain. No changed elution order is caused by both the hydrophilic interaction and the net negatively charged zwitterionic stationary phase. This whole electrostatic interaction among charged analytes and zwitterionic charged stationary phase produces smaller separation efficiency on ZIC-MPC column. It can be directly seen from the retention time listed in Table 4-3 and Fig. 4-10. For our interesting ligands, ZIC-MPC column gives worse separation efficiency than ZIC-HILIC column.

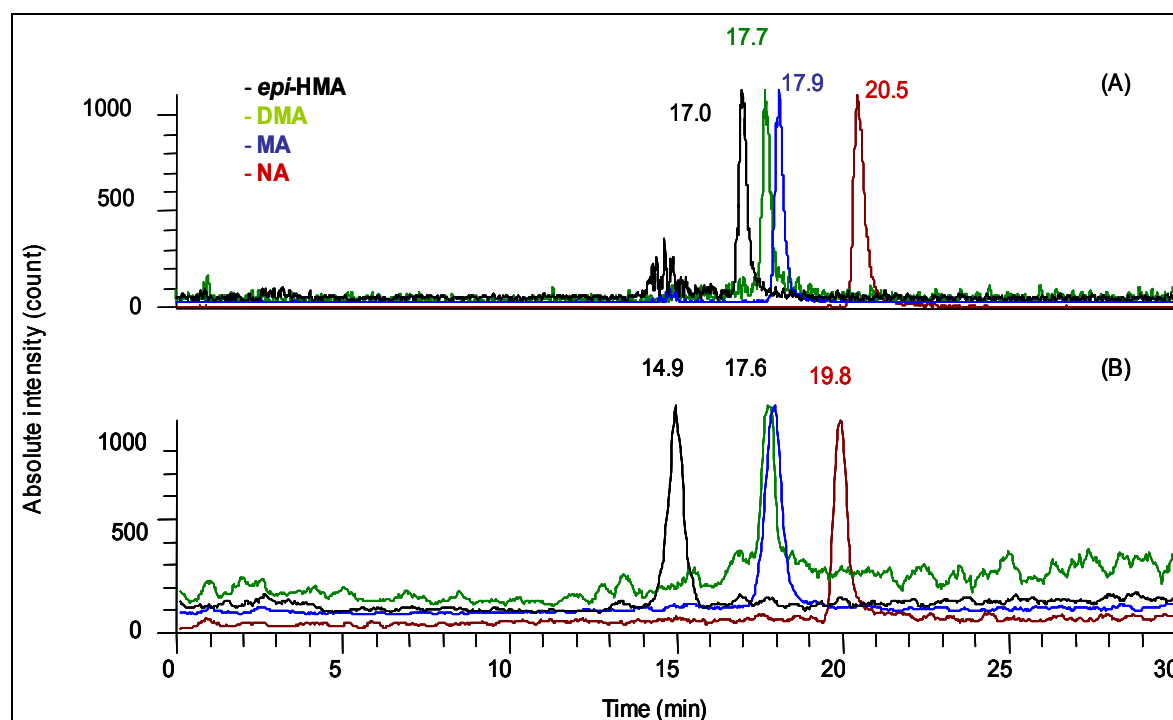


Figure 4-10. Reconstructed ion chromatograms of  $m/z$  335 ( $\pm 0.3$  amu) *epi*-HMA; 303 ( $\pm 0.3$  amu) DMA; 319 ( $\pm 0.3$  amu) MA; and 302 ( $\pm 0.3$  amu) NA. Chromatograms in (A) were analyzed on ZIC-HILIC column; chromatograms in (B) were analyzed on ZIC-MPC column. Conditions see Fig. 4-5.

**Nickel-PS complexes** are investigated in order to see the separation behavior on the ZIC-MPC column. From Table 4-3, Ni<sup>II</sup>-PS complexes, except to Ni<sup>II</sup>-NA, elute later on ZIC-MPC column than on ZIC-HILIC column. The retention order of these nickel-PS complexes on ZIC-MPC column is the same as on ZIC-HILIC column. The nickel-PS complexes have lower negatively charged state than their respective ligands, however they are all negatively charged at these conditions. The total net charge state of the stationary phase both of ZIC-MPC and ZIC-HILIC is negative. The positive charge group of ZIC-MPC stationary phase is pointing out, but negative charge group of ZIC-HILIC is pointing out. The total net negative charge state of the ZIC-HILIC is stronger than it of ZIC-MPC. Therefore, a stronger retention of these negatively charged compounds on ZIC-MPC column comparing to ZIC-HILIC column.

However, the situation of Ni<sup>II</sup>-NA is different because of the respective ligand, NA. NA owns the most charged groups on its structure comparing to the other phytosiderophores at pH 7.3. More charged groups mean more interaction between compound and zwitterionic charged stationary phase. Therefore, the six function groups on NA are all charged interacting strongest with both ZIC-MPC and ZIC-HILIC column. The number of negatively charged groups on all the phytosiderophores including NA is the same due to they all have three carboxylic acid groups. NA has most positively charged groups comparing to the other phytosiderophores. When its charged functional groups goes for coordinating metal ions, the number of charged groups reduces. Comparing to the other PS, the total positively charged groups of NA reduces most. Therefore, decreasing positive charges of nickel-NA results a weaker electrostatic interactions with the weaker negatively charged stationary phase of ZIC-MPC column comparing to ZIC-HILIC column. The weaker electrostatic interaction causes the less retention of NA-Ni on ZIC-MPC column.

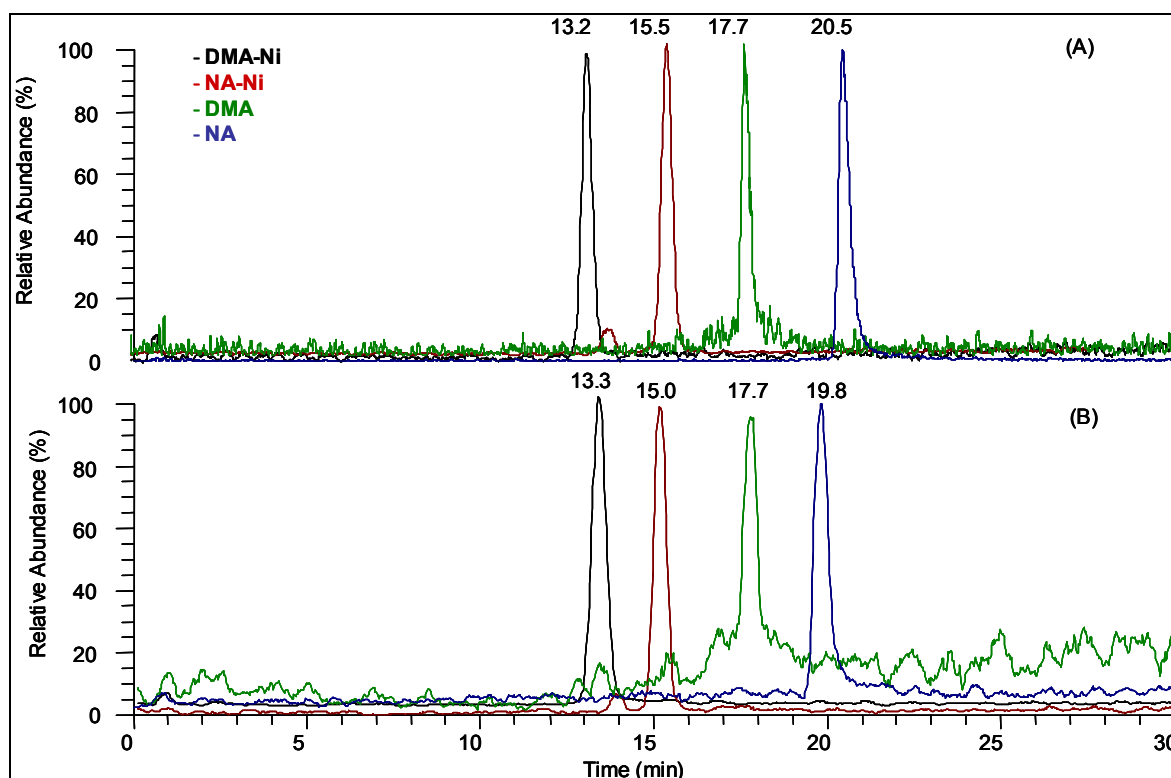


Figure 4-11. Reconstructed ion chromatograms of  $m/z$  359 ( $\pm 0.3$  amu) DMA-Ni; 358 ( $\pm 0.3$  amu) NA-Ni; 303 ( $\pm 0.3$  amu) DMA; and 302 ( $\pm 0.3$  amu) NA. Chromatograms were analyzed on ZIC-HILIC column (A), and on ZIC-MPC column (B), respectively. Conditions see Fig. 4-5.

**Separation of metal-PS and PS** From the Table 4-3 and Fig. 4-11, pure ligands elute earlier, but metal-species elute later on ZIC-MPC column comparing to ZIC-HILIC column. In Fig. 4-11, separation of DMA, NA and their respective nickel complexes is possible on both ZIC-HILIC and ZIC-MPC column. All these peaks are more closed eluted on ZIC-MPC column. Therefore, closely less separation efficiency of phytosiderophores and their metal-PS complexes is observed on ZIC-MPC column compared to it of ZIC-HILIC column.

Based on both hydrophilic interaction and zwitterionic interaction between stationary phase and analytes, separation of the important LMW species in plants is possible on ZIC-MPC column. However, comparing to ZIC-HILIC, worse separation efficiency was found with the ZIC-MPC column. Similar dissociation of ferric complexes was found on the ZIC-MPC column as well. Hence, the ZIC-HILIC column exhibits obviously better separation properties for our analytes. Although ferric-PS dissociate during separation with ZIC-HILIC, the sensitivity of ferric complexes is still good enough to be detected. The ZIC-HILIC/ESI-MS method enables to see changes of ligand pools, such as changes of citric acid, or histidine. Therefore, it is suitable for use as a plant metabolic profiling method. However, in order to detect and identify a metabolic profile of plants, a described mass spectrometer providing higher mass resolution and accurate  $m/z$  value is needed.

#### 4.4.5 Plant metabolic profiling

Metabolomics is defined as the study of the entire metabolite pool in a biological system. Metabolic profiling, as a method for direct monitoring of changes of metabolite pools in a biological system, provides a powerful tool for gaining insight into functional biology. A snapshot of the level of numerous small molecules within a cell or a biofluid, and how those levels change under different conditions, is complementary to gene expression and proteomic studies. Metabolic profiling is actively being applied to studies of drug toxicity, drug efficacy and model organisms, as well as humans and plants. In our case, the metabolic profile of plants can be affected by many parameters, such as environmental conditions, stage of growth, nutritional status, interaction with other species and genetic make-up. Graminaceous plants, such as maize, barley, and wheat, that are produced for animal feeds or human consumption can undergo subtle changes in their metabolic profile which often are unnoticed if the metabolites are present in small amounts or are undetected by standard analytical methods. Therefore, in this chapter, one analytical method, ZIC-HILIC/ESI-FTICR-MS, was applied to monitor the metabolic profile of plants. However, there are several major difficulties to do the plant metabolic profiling investigation.

- i) The huge number of metabolites in one solution. It is very hard or impossible to baseline separate all of them by a single chromatographic run within a reasonable time. Co-elution of several compounds happens during one single chromatographic separation run. This complicates the mass spectrum of the peaks, esp. for these compounds of similar  $m/z$  value.
- ii) Low micro molar concentration range in plant samples adds the difficulty to detection and identification.
- iii) Complete information on the identity of all metabolites in plants is missing. Till now, there is no literature that is capable to list all the possible metabolites in plants.
- iv) For metal species in plants, the available information is even less. This refers to the knowledge of chemical structures and concentrations, as well as to other important information, such as  $pK$  and  $pI$  values of metal species in complicate

biological matrices. Only a few references for a few special metal species are available [43-45].

- v) No effective data evaluation software for metabolic profiling is available. Thousands of mass spectra obtained in one chromatographic run need lots of analysis time and are difficult to be handled manually.

From the previous investigations (chapter 4.4.2 – 4.4.4), the best separation and identification of LMW ligands and their respective metal complexes in plants was achieved by ZIC-HILIC/ESI-MS. This method is capable to see the changes of important metabolites, such as citric acid, histidine. Therefore, it is useful as a method for plant metabolic profiling.

In cases when metabolites are present in very low micro molar concentration range, or if coelution of the species with similar  $m/z$  values ( $< 1$  amu) is observed, quadrupole mass spectrometry, as a low resolution mass spectrometry, is not sufficient to identify unknown species. FTICR-MS has been applied already to phenotyping of plants, where the ripening process in strawberries and transgenic mutant tobacco plant was investigated [65]. A direct injection ESI-FTMS analysis has been reported, applied to yeast cultures [50]. Therefore, the performance characteristics of FTICR-MS are ideally suited for the type of complex mixtures encountered in high throughput metabolomics applications. ESI-FTICR-MS was tested here as a plant metabolic profiling method, to determine as many as possible unknown metabolites. Negatively ionization mode was still used for further investigations. The ZIC-HILIC separation method was slightly changed, according to the requirements of FTICR-MS (see chapter 4.3.2).

To demonstrate the applicability of this metabolic profile method, one complete set of real plant samples, Tobacco plants, was investigated. This set of Tobacco plants was prepared under over expressed of NA-Synthase (NAS) (see Fig. 1-3), and owns four different nutrient sample groups. NAS is an enzyme and responsible for biosynthesis NA. It means more NAS synthesized by this set of Tobacco plants. Therefore, nicotianamine is expected in this Tobacco samples. There are four different nutrient sample groups of this set of Tobacco plants, and so called **Group-I, -II, -III, and -IV (see chapter 4.3.4)**. Each group contains four parallel extracted and prepared samples, called here Sample 1-4 for Group-I, Sample 5-8 in Group-II, Sample 9-12 in Group-III, and Sample 13-16 in Group-IV. The changes of metabolites in different sample groups in response to their different nutrient status enable the comparison among these four sample groups. The aim of this chapter is to

- i) Detect and identify the potential metabolites as many as possible in this set of Tobacco plants.
- ii) Find out the correlation metabolites changes among different sample groups of this set of Tobacco plants in response to their different nutrition situation.

#### 4.4.5.1 Metabolic Profiling method

A good metabolic profile method can offer an overview of the samples. Not only “target analysis” of known compounds is important, the changes of metal-species and related ligand pools are even more important to see. A key parameter of a good metabolic profile method is its reproducibility. Only when peak area and retention time are reproducible, experiment results are comparable. To check the quantitative reproducibility of this method, internal standard was applied.

**Internal standard** is a chemical substance that is added in a constant amount to samples, the blank and calibration standards in a chemical analysis. However, in metabolomics analyses, there are no many isotope-labeled internal standards commercially available. Abundance of phosphate and other inorganic salt in plant samples may contaminate the separation LC column or electrospray interface. These contaminations may cause many system errors, such as losses of important chromatographic peaks, variation of retention time, unreliable peak area, ghost unknown peaks, and high background noise. Therefore, taurine, 2-aminoethanesulfonic acid, was applied here as internal standard to check the systematic variance, correct the loss of analyte during sample inlet, and to monitor the separation and detection reproducibility. Taurine is a substance found in high abundance in the tissues of many animals, but not in plants. It is a derivative of the sulphur-containing (sulfhydryl) amino acid, and chemical structure close to our interests. Taurine was applied to each sample solution with a concentration of 30  $\mu\text{M}$  as the internal standard. A detection of taurine with  $m/z$  124.0689 amu was found at retention time 10.9 min  $\pm$  0.5 min. A reproducibility of peak area and retention time was > 98 %.

**Calibration curve and linearity of ESI-FTICR-MS:** Effective quantitation of many metabolites in a complex matrix represents the most difficult technical challenge for high throughput metabolic studies. Standard curves cannot be constructed for so many analytes simultaneously. Asp, Glu, His, Arg, and Lys were used to check the linearity of ESI-FTICR-MS detection. A linear range of quantification was found between 1 and 50  $\mu\text{M}$  with a correlation coefficient of the linear regression of > 0.99 of each compound (Fig. 4-12). This corresponds to injected amounts of amino acids (0.5-50  $\mu\text{mol}$ ). 1  $\mu\text{M}$  is the limit of quantification (signal to noise ratio > 10). The detection limit is 0.5  $\mu\text{M}$ , as estimated from a signal to noise ratio > 3 at the respective  $m/z$ . Comparing the peak area of the analytes in real samples to the calibration curve, the concentration of these five amino acids is capable to be calculated. However, the exactly quantification of each metabolite is very difficult to obtain. Instead of the exactly quantification information, correlation analyses among the diverse plant samples are more interesting here (see chapter 4.4.5.3). A good linearity of detection, which limits the systematic error and keeps the correlation analyses accurately, was achieved here.

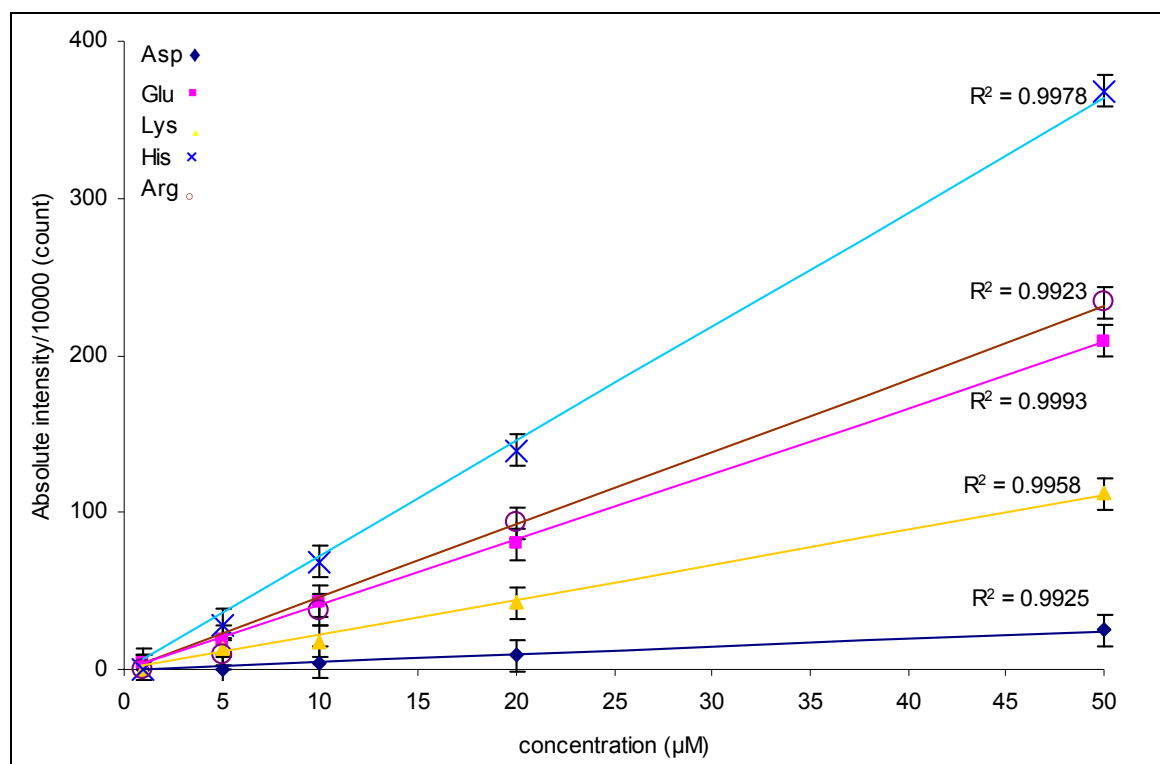


Figure 4-12. Calibration curves of Asp, Glu, His, Lys, and Arg with ZIC-HILIC/ESI-FTICR-MS method. Correlation coefficient of the linear regression of each compound is marked as  $R^2$ . Conditions: 0-4 min 100 % eluent A (10 mM ammonium acetate + 90 % acetonitrile, pH 7.3), 4-40 min linear gradient to 25 % eluent A and 75 % eluent B (30mM ammonium acetate + 20 % acetonitrile, pH 7.3); flow rate: 75  $\mu$ L/min; injection volume: 5  $\mu$ L. Full-scan FTICR mass spectra in the mass range  $m/z$  80-800 were acquired using single micro scan. Resolution was set to 50,000.

**Reproducibility:** Only a good reproducibility of retention time and peak intensity can offer the meaningful and reliable metabolites information. To keep the HPLC/MS system performing reproducible, a re-equilibrated and cleaning procedure (see chapter 4.3.2.2) was applied in between each single chromatographic run. As mentioned above, there are four different cultivated sample groups (Group I-IV) of this set of Tobacco plants. Each group contains four parallel extracted and prepared samples (sample 1-16). These samples in the same group are isolated under same conditions and from the sample plants. However, the concentration of the metabolites found in these four samples from one sample group is variance around 10-30 % from each other. This variation is caused by biological variation and sampling, and impossible to be totally avoided. The method reproducibility was tested by investigating each sample for at least three times. Systematic variation in average values less than  $\pm 0.5$  min with retention time and 5 % with peak area for all the metabolites are found in Tobacco sample-11 (see Table 4-4).

Table 4-4. The average retention time  $t_R$  and peak area of the identified metabolites in Tobacco plant sample-11. The sample was measured three times by ZIC-HILIC/ESI-FTICR-MS method.

Metabolites	$t_R$ (min)	Peak area (count)
Serine	$17.55 \pm 0.4$	$9.28 \pm 0.68e^4$
Proline	$9.01 \pm 0.2$	$5.44 \pm 0.25e^5$
Threonine	$13.68 \pm 0.5$	$2.15 \pm 0.01e^5$
Leucine	$4.44 \pm 0.1$	$1.42 \pm 0.04e^5$
Asparagine	$16.23 \pm 0.5$	$1.22 \pm 0.04e^5$
Aspartic acid	$21.12 \pm 0.3$	$1.61 \pm 0.02e^4$
Glutamic acid	$20.92 \pm 0.2$	$1.61 \pm 0.03e^5$
Glutamine	$16.98 \pm 0.3$	$5.09 \pm 0.11e^6$

Metabolites	$t_R$ (min)	Peak area (count)
Lysine	$32.12 \pm 0.2$	$1.00 \pm 0.03e^5$
Histidine	$18.89 \pm 0.4$	$7.96 \pm 0.19e^4$
Phenylalanine	$3.85 \pm 0.1$	$1.56 \pm 0.04e^6$
Arginine	$31.00 \pm 0.2$	$2.21 \pm 0.05e^5$
Tryptophane	$4.55 \pm 0.1$	$5.44 \pm 0.12e^5$
$\gamma$ -Aminobutyric acid	$19.88 \pm 0.3$	$2.00 \pm 0.12e^5$
Citrate	$24.20 \pm 0.5$	$1.07 \pm 0.01e^8$
Ascorbate	$17.15 \pm 0.5$	$3.87 \pm 0.11e^5$
Maleate	$20.45 \pm 0.3$	$5.89 \pm 0.23e^5$
Malate	$20.40 \pm 0.3$	$1.01 \pm 0.04e^7$
Succinate	$11.01 \pm 0.1$	$4.57 \pm 0.11e^7$
NA	$22.15 \pm 0.2$	$6.27 \pm 0.30e^4$

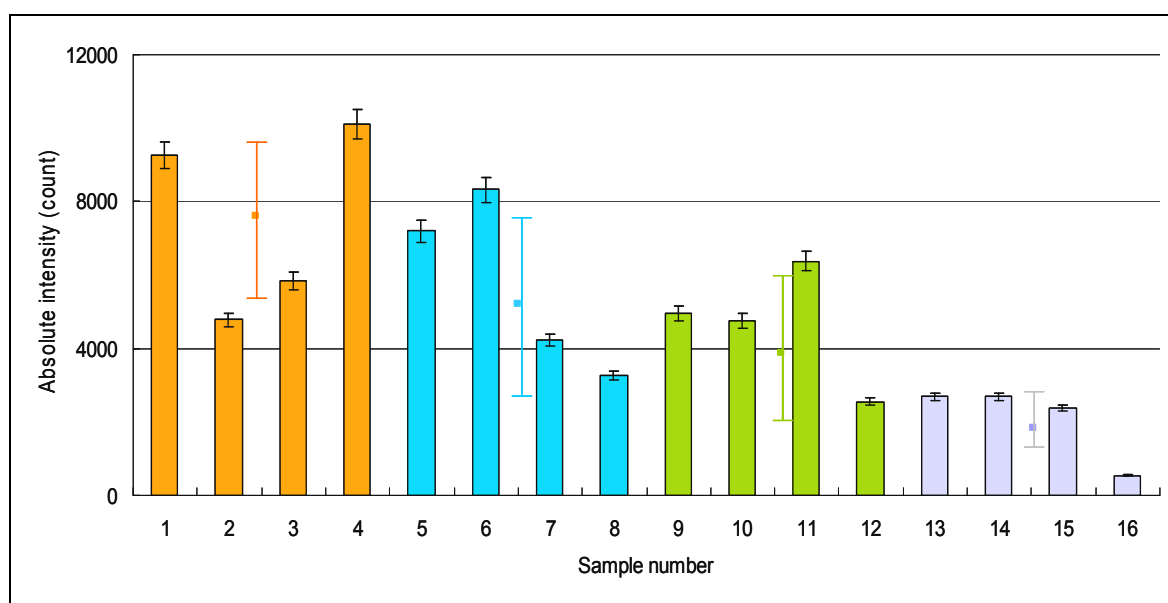


Figure 4-13. Asp was determined in extracts from four individual Tobacco groups. Sample 1-4 are from Group-I; Sample 5-8 are from Group-II; Sample 9-12 are from Group-III; and sample 13-16 are from Group-IV. The square is the average value of the parallel extracted four samples in each group. Conditions see Fig. 4-12.

One example for the variance is demonstrated for Asp, which is detected and identified in all Tobacco plants (Fig. 4-13). The peak intensity of Asp found in all these sixteen samples is shown with a systematic variation of 2 %. The mean value of each group is marked as a square and biological variance is marked as an error bar. In Group-I, sample 1 and sample 4 contains similar amount of Asp, which is around 30 % more Asp than in sample 2 and 3. In Group-II, both sample 5 and 6 have around 30 % more Asp than in sample 7 and 8. The amount of Asp from sample to sample in both Group-III and Group-IV vary not as much as in the other two sample groups. However, sample 16 owns the least amount of Asp in all the sixteen samples. The amount of Asp decreases from Group-I to Group-IV. Obviously, the biological variance is much more than the systematic bias, which is between 10-20 % according to different sample groups.

The sampling variance and biological variance are not possible to avoided responding to the complicate biological treatments. This method has a much less systematic variance than the biological variance and sampling variance, offering good reliability for metabolites correlation analyses. Good reproducibility of this method enables to see the concentration changes of the metabolites in plants (see chapter 4.4.5.3).

#### 4.4.5.2 Identification of metabolites

Separation and detection a wide range of hydrophilic metabolites, such as amino acids, organic acids, sugar, and sugar phosphates, were achieved within a single chromatographic run by the developed metabolic profiling method. The task of metabolic profiling is to identify as many as possible metabolites here. To achieve this aim, several steps were carried out to deal with the chromatograms and mass spectra data, which are obtained by investigating plant samples by the method:

- Step 1: A list of metabolites, such as amino acids, organic acids, PS, and metal-species, sugar and sugar phosphate, which are expected and very likely to be in plants [51, 54-56], was made firstly. Metabolites belonging to different classes were listed out in Table 4-5.
- Step 2: Calculating the exact  $m/z$  value of these metabolites in the list with a mass accuracy of 0.0001 amu. The exact  $m/z$  value then was used to extract chromatogram from the total ion chromatogram with a mass tolerance 20 ppm. Consequently, a reconstructed ion chromatogram (RIC) is obtained. In case none peak in RIC, which means no present of this compound in this sample or the concentration of this compounds is lower than the LOD. In case one or more peaks in RIC, the following steps are carried out.
- Step 3: Find out the observed  $m/z$  value of these peaks in RIC from step 2 respectively. A molecular formula can be deduced by using the observed  $m/z$  value in mass spectrum. In additional, the observed isotope pattern mass spectrum should agree to the calculated one. However, unequivocal identification of this molecular formula still requires fragmentation.
- Step 4: To unequivocally identify the molecular formula, fragments of the molecule obtained in data dependent  $MS^n$  method (see chapter 4.3.2.3) have to be checked. When these fragments agree with the molecular structure, in most cases, an unequivocal identification has been achieved.

By means of above identification method, fourteen amino acids, six organic acids, five sugars, two sugar phosphates, and nicotianamine were detected and identified in Tobacco plants by a single chromatographic run, listed in Table 4-5.

Table 4-5. The calculated  $m/z$  values of metabolites that are expected in plants. The observed  $m/z$  values were based on the detection and identification of metabolites in Tobacco plants by ZIC-HILIC/ESI-FTICR-MS in negative ionization with in full scan mode. "n. d." means not detected in Tobacco plants.

Metabolites	Class	Retention time (min)	Obs. $m/z$	Cal. $m/z$
Alanine	Amino acids		<i>n.d.</i>	88.0404
Serine		17.1	104.0349	104.0353
Proline		8.8	114.0556	114.0560
Valine			<i>n.d.</i>	116.0717
Threonine		12.7	118.0510	118.0509
Cysteine			<i>n.d.</i>	120.0124
Isoleucine			<i>n.d.</i>	130.0873
Leucine		4.0	130.0870	130.0873
Asparagine		15.7	131.0457	131.0462
Aspartic acid		21.1	132.0297	132.0302
Glutamic acid		20.7	146.0453	146.0459
Glutamine		16.8	145.0612	145.0619
Lysine		32.1	145.0975	145.0982
Methionine			<i>n.d.</i>	148.0437
Histidine	18.9	154.0617	154.0622	
Phenylalanine	3.9	164.0712	164.0717	
Arginine	31.0	173.1036	173.1044	
Tyrosine		<i>n.d.</i>	180.0666	



## 4 High Performance Liquid Chromatography coupled to Mass Spectrometry

Metabolites	Class	Retention time (min)	Obs. m/z	Cal. m/z
Tryptophane		4.5	203.0818	203.0826
$\gamma$ -aminobutyric acid		18.7	102.0558	102.0561
Citrate	Organic acids	23.9	191.0187	191.0197
Ascorbate		16.9	175.0242	175.0248
Maleate		20.4	115.0032	115.0037
Malate		20.4	133.0137	133.0142
Tartarate			<i>n.d.</i>	149.0092
Succinate		9.3	117.0189	117.0193
Gluconate		16.1	195.0503	195.0510
a		Sugars	9.7	179.0556
b	7.6		179.0556	179.0561
c	5.6		179.0558	179.0561
d	15.9		179.0557	179.0561
glycerol			<i>n.d.</i>	91.0401
mannitol			<i>n.d.</i>	181.0717
Sucrose	13.0		341.1085	341.1089
Gluconate-6-P	Sugar phosphates		18.2	275.0177
fructose-6-P		26.2	259.0221	259.0224
ethanolamine phosphate			<i>n.d.</i>	140.0118
DMA	PSs		<i>n.d.</i>	303.1198
<i>epi</i> -HMA			<i>n.d.</i>	319.1147
MA			<i>n.d.</i>	335.1096
NA		22.0	302.1358	302.1358
NA-Fe <sup>II</sup>	Metal-species		<i>n.d.</i>	356.0546
NA-Ni			<i>n.d.</i>	358.0546
NA-Cu			<i>n.d.</i>	363.0496
NA-Zn			<i>n.d.</i>	364.0486
NA-Mn			<i>n.d.</i>	355.0576
DMA-Fe <sup>III</sup>			<i>n.d.</i>	356.0308
DMA-Ni			<i>n.d.</i>	359.0386
DMA-Cu			<i>n.d.</i>	364.0336
DMA-Zn			<i>n.d.</i>	365.0326
DMA-Mn			<i>n.d.</i>	356.0416
<i>epi</i> -HMA-Fe <sup>III</sup>			<i>n.d.</i>	372.0257
<i>epi</i> -HMA-Ni			<i>n.d.</i>	375.0335
<i>epi</i> -HMA-Cu			<i>n.d.</i>	380.0285
<i>epi</i> -HMA-Zn			<i>n.d.</i>	381.0275
<i>epi</i> -HMA-Mn			<i>n.d.</i>	372.0365
MA-Fe <sup>III</sup>			<i>n.d.</i>	388.0206
MA-Ni			<i>n.d.</i>	391.0284
MA-Cu			<i>n.d.</i>	396.0234
MA-Mn			<i>n.d.</i>	388.0314
MA-Zn			<i>n.d.</i>	397.0224
His-Fe <sup>III</sup>			<i>n.d.</i>	206.9731
His-Ni			<i>n.d.</i>	209.9810
His-Cu			<i>n.d.</i>	214.9760
His-Zn			<i>n.d.</i>	215.9750
His-Mn			<i>n.d.</i>	206.9840
2His-Fe <sup>III</sup>			<i>n.d.</i>	362.0427
2His-Ni			<i>n.d.</i>	365.0505
2His-Cu			<i>n.d.</i>	370.0455
2His-Mn			<i>n.d.</i>	362.0535
2His-Zn			<i>n.d.</i>	371.0445
citrate-Fe <sup>III</sup>			<i>n.d.</i>	243.9307
citrate-Ni			<i>n.d.</i>	246.9385
citrate-Zn		<i>n.d.</i>	252.9325	
citrate-Cu		<i>n.d.</i>	251.9335	
citrate-Mn		<i>n.d.</i>	243.9415	

Metabolites	Class	Retention time (min)	Obs. m/z	Cal. m/z
2citrate-Mn			<i>n.d.</i>	435.9685
2citrate-Zn			<i>n.d.</i>	444.9595
2citrate-Cu			<i>n.d.</i>	443.9605
2citrate-Ni			<i>n.d.</i>	438.9655
2citrate-Fe <sup>III</sup>			<i>n.d.</i>	435.9577

Unequivocal identification of metabolites is based on their observed m/z value (mass error < 1 ppm under simultaneously ion selection (SIM) mode), mass spectrum isotope pattern (agree to the calculated one), and fragmentation. Examples of unequivocal identification of Asp, ascorbate, and nicotianamine were shown in Fig. 4-14, 4-15, and 4-16, respectively. Reconstructed ion chromatograms of the exactly calculated m/z values of Asp, ascorbate, and NA (see Table 4-5) were selected of the total ion chromatograms with a mass error of 20 ppm, respectively. With Fig. 4-14 and Fig. 4-15, there is only one peak appearing in respective RIC. However, there are three peaks shown in the RIC of Fig. 4-16. By calculating the formula of the observed m/z, C<sub>4</sub>H<sub>7</sub>O<sub>4</sub>N<sub>1</sub> was obtained from the Fig. 4-14, and C<sub>6</sub>H<sub>8</sub>O<sub>6</sub> was obtained from the Fig. 4-15. These two formulas agree to the chemical formula of Asp and ascorbate with a mass error less than 1 ppm under SIM mode, respectively. With Fig. 4-16, the spectrum of each peak in RIC was evaluated thoroughly. A good agreement both with C<sub>12</sub>H<sub>21</sub>O<sub>6</sub>N<sub>3</sub> ( $\Delta m < 1$  ppm) and retention time ( $\pm 0.3$  min) was found with the major peak, which is nicotianamine. A further confirmation of the chemical structures of these compounds can be addressed by their fragmentation information. The fragments of Asp, ascorbate, and nicotianamine were identified and listed in Table 4-6, respectively.

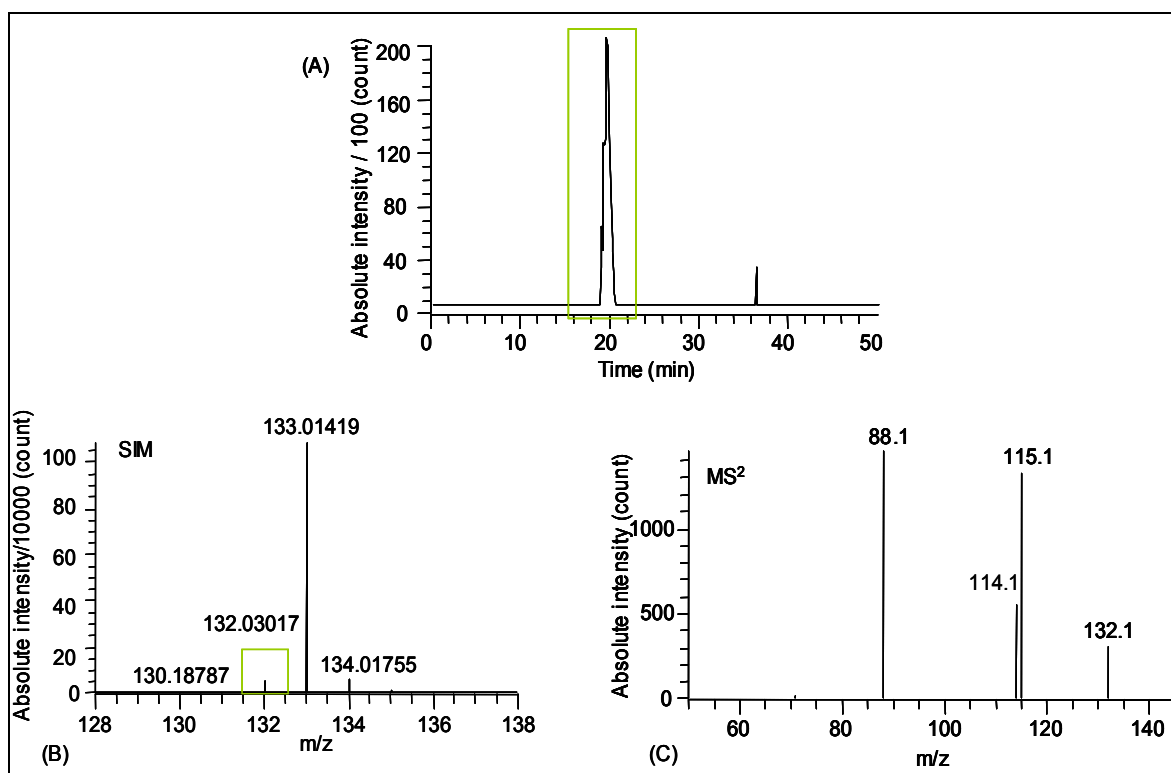


Figure 4-14. Detection and identification of Asp in Tobacco plants. (A) Reconstructed ion chromatogram of m/z = 132.0302 (20 ppm). (B) Selected ion monitoring (SIM) of mass range 128-138. (C) MS/MS fragmentation of m/z of 132.03. Full ion scan of 80-800 Da with a resolution 25,000, the most intensive ion was isolated by a resolution 50,000. Then it was fragmented with relative collision energy 35 % to obtain MS<sup>2</sup> and MS<sup>3</sup> information in the linear trap. Separation conditions see Fig. 4-12.

Table 4-6 The CID data during fragmentation of Asp, ascorbate, nicotianamine in the mass spectra in Fig. 4-14, -15, -16 was interpreted here.

Compounds	Fragments m/z	Lost fragment m/z	Identity of lost fragments
Asp	115.1	17	NH <sub>3</sub>
	114.1	18	H <sub>2</sub> O
	88.1	44	CO <sub>2</sub>
Ascorbate	157.0	18	H <sub>2</sub> O
	115.1	60	HO-CH=CH-OH
	87.0	78	H <sub>2</sub> O HO-CH=CH-OH
NA	284.1	18	H <sub>2</sub> O
	258.2	44	CO <sub>2</sub>
	209.2	93	H <sub>2</sub> O HOOCCH <sub>2</sub> NH <sub>2</sub>
	187.9	115	HOOCCH(CH <sub>2</sub> ) <sub>2</sub> NCH <sub>3</sub>
	132.1	170	CO <sub>2</sub> CH=CHN(CHCOOH)(CH <sub>2</sub> ) <sub>2</sub>
	143.1	159	CO <sub>2</sub> HOOCCH(CH <sub>2</sub> ) <sub>2</sub> NCH <sub>3</sub>
	116.1	176	CH=CHCOOH HOOCCH(CH <sub>2</sub> ) <sub>2</sub> NCH <sub>3</sub>

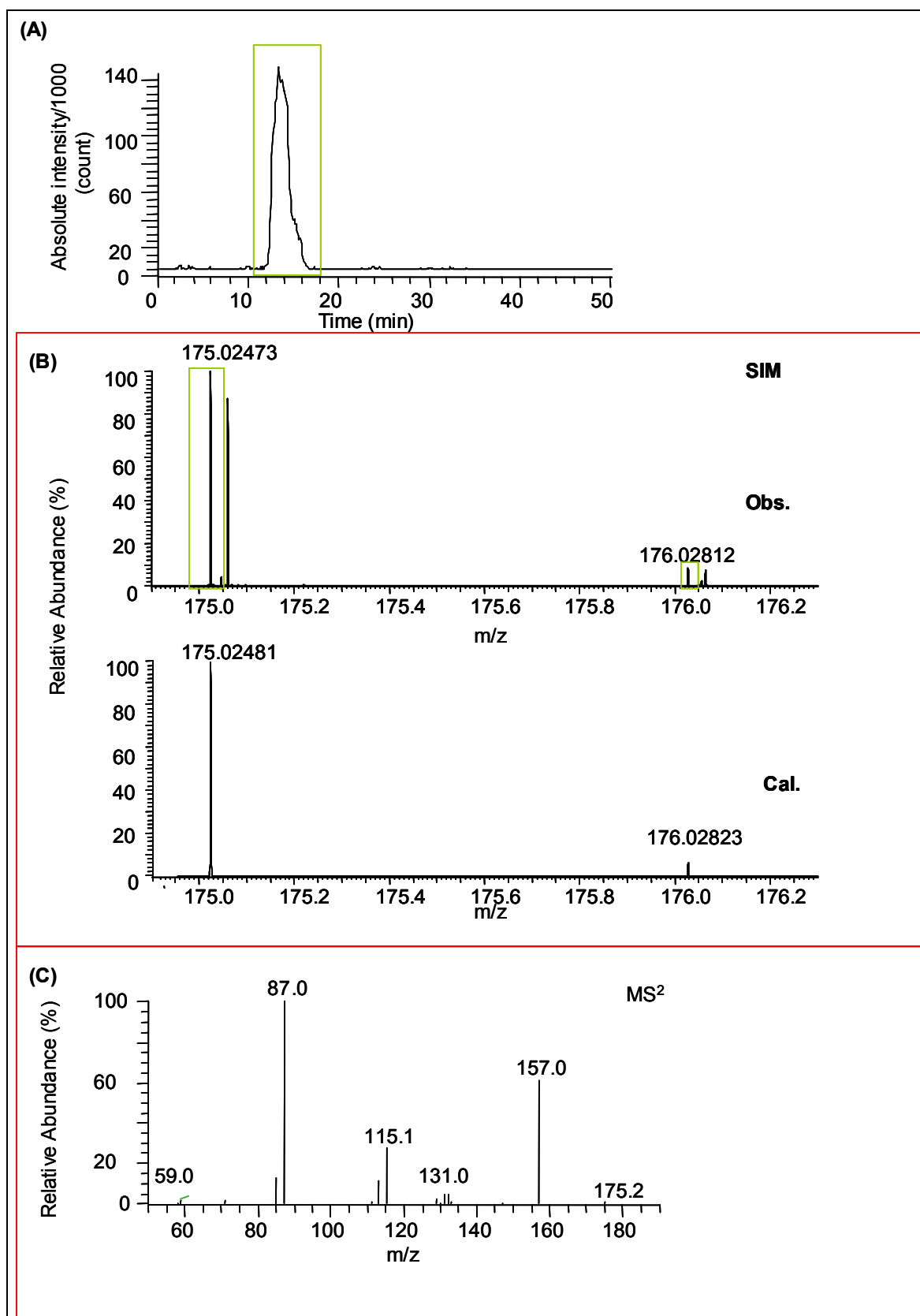


Figure 4-15. Detection and identification of ascorbate in Tobacco plants. (A) Reconstructed ion chromatogram of  $m/z = 175.0248$  (20 ppm). (B) SIM of mass range 174.9-176.2. The observed spectrum (Obs.) and the calculated spectrum (Cal.) show a well agreement to each other. (C) MS/MS fragmentation of  $m/z$  of 175.02. Conditions see Fig. 4-14.

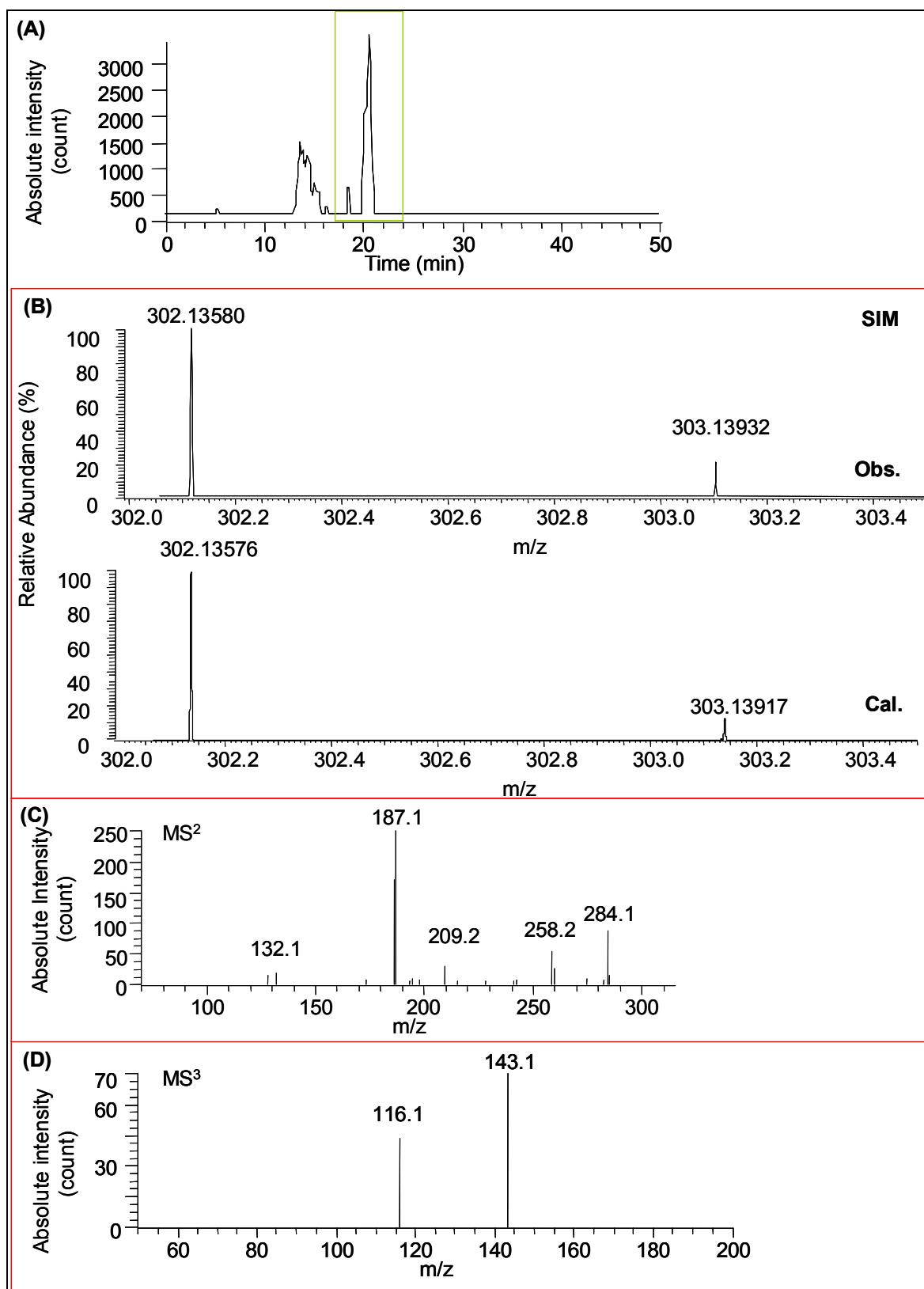


Figure 4-16. Detection and identification of nicotianamine in Tobacco plants. (A) Reconstructed ion chromatogram of  $m/z = 302.1358$  (20 ppm). (B) SIM of mass range 302.0-303.5. Observed mass spectrum (Obs.) and calculated mass spectrum (Cal.). (C) MS/MS fragmentation of  $m/z$  of 302.14. (D) MS<sup>3</sup> fragmentation of  $m/z$  of 187.1. Conditions see Fig. 4-14.

FTICR-MS allows identification of metabolites on the basis of their accurate mass, and their fragments, and their isotope pattern. Most of the metabolites in Table 4-5 are identified by this typical low ppm mass accuracy, their fragments, and isotope pattern

obtained by FTICR-MS. However, structural isomers, owning identical  $m/z$  values and sharing the same formula, need further structural elucidation and identification. This may be achieved by  $MS^n$  measurements and individual standard measurement.

**Proposed metabolites:** Amino acids, organic acids, and phytosiderophores, sugar substances in Tobacco plants were detected and separated by the proposed ZIC-HILIC/ESI-FTICR-MS method. Sugar substances are well-known metabolites, which abound in plants [29, 46, and 164]. According to these literatures, fructose, galactose, glucose, inositol, and sucrose present with a remarkable level in plants. Fig. 4-17 shows the chromatogram of the accurate mass (179.05611 amu) filtering of full scan MS data with 20 ppm and fragmentations of mass 179.05606 amu (observed) in negative ionization mode in sample 11. Four peaks, which mean there are at least four compounds having identical  $m/z$  in this sample, were found. A formula of  $C_6H_{12}O_6$  was calculated from  $m/z$  of 179.05606 at negative mode. This formula agrees very well with the several sugar compounds listed in literatures [46, 164] such as galactose, glucose, fructose, and inositol, mass error is less than 1 ppm with SIM mode. The SIM mass spectra of these four peaks in Fig. 4-17 are identical. And their mass spectrum isotope pattern well agrees to the calculated one, which is shown as insert in Fig. 4-17. These four compounds are very likely sugar substances. A further proof of these four peaks, were obtained by fragmentation of them using CID. The respective fragments of these four peaks are shown in Fig. 4-17 and listed in Table 4-7 with identity of the lost fragments. According to their fragments, the first and second fragments to lose are water molecules, which are caused by multi OH groups on the chemical structure, which agree to the structure of sugar substances. However, unequivocal identification is difficult for structurally isomeric compounds, which are identical mass-to-charge ratio and produce similar fragments during CID, by  $MS^n$  alone. To do the unequivocal identification of these isomers, NMR exhibits more advantages over MS. However, the information from  $MS^n$  experiments can significantly speed the structure determination process by NMR.

Table 4-7. The CID data during fragmentation of four peaks with an identical  $m/z$  179.0561 in the mass spectra in Fig. 4-16 was interpreted here.

Chemical structures	Fragments $m/z$	Lost fragment $m/z$	Identity of lost fragments
peak (a)	161.0	18	$H_2O$
	143.1	36	$2H_2O$
peak (b)	161.0	18	$H_2O$
	143.1	36	$2H_2O$
peak (c)	161.0	18	$H_2O$
	143.1	36	$2H_2O$
peak (d)	161.0	18	$H_2O$
	125.0	54	$3H_2O$

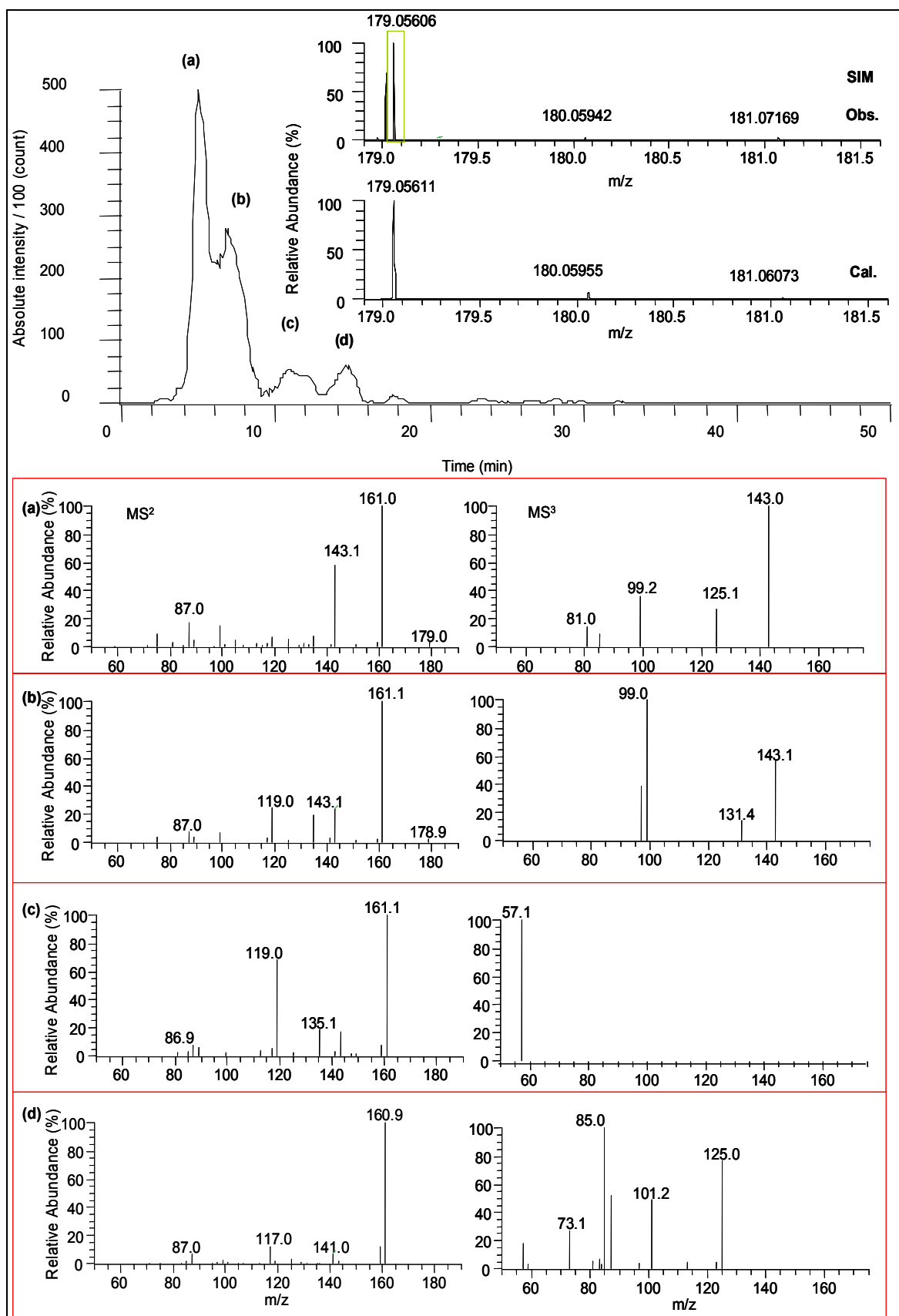


Figure 4-17. Detection and fragmentation of sugar substances in Tobacco plants, sample number 11, by ZIC-HILIC/ESI-FTICR-MS. The upper chromatogram is accurate mass filtering of full scan MS data  $m/z$  179.0561 (20 ppm) with four peak (a), (b), (c), and (d), which is identical; Inset, mass spectrum ( $m/z$  178.9-181.5) extracted from a detection zoom of these sugar peaks from 5-15 min. (a) fragments of  $m/z$  179.06 at 5.58 min; (b) fragments of  $m/z$  179.06 at 7.60 min; (c) fragments of  $m/z$  179.06 at 9.67 min; (d) fragments of  $m/z$  179.06 at 15.87 min. Conditions see Fig. 4-14.

#### 4.4.5.3 Correlation analysis

Effectively quantification of many metabolites in a complex matrix is very difficult for high-throughput metabolomics studies. Studies the variance of the concentration of metabolites are more amenable to our ZIC-HILIC/ESI-MS method, and do not require quantitation. The changes of metabolites, esp. for the metal species related ligand pools, are much more important than quantitation.

**Correlation analysis of Tobacco samples** This set of Tobacco plant samples, which are overexpressor of NAS, was grown nutrition solution in different concentration of  $\text{Fe}^{3+}$ . Samples in Group-I were grown in a nutrition solution with  $50 \mu\text{M Fe}^{3+}$ . However, the samples in the other Groups (II, III, and IV) were grown in nutrition solution with only  $5 \mu\text{M Fe}^{3+}$ . Therefore, an higher concentration of iron(III) was expected in the samples in Group-I than the others.

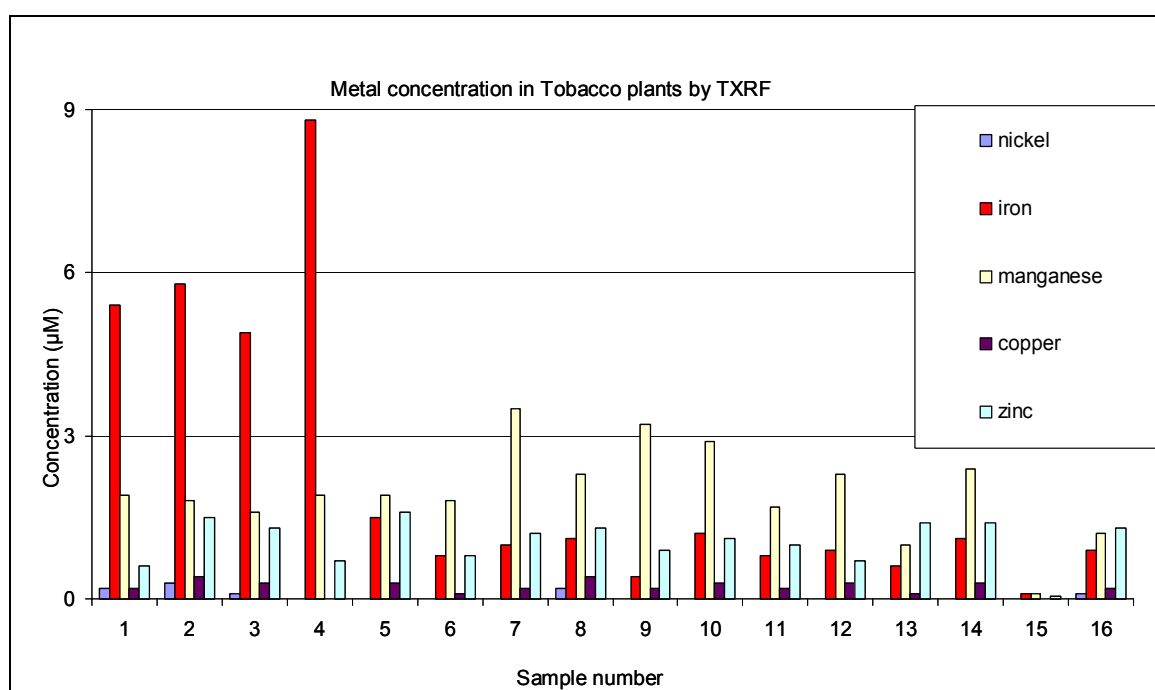


Figure 4-18. The metal element concentration in Tobacco leaves were measured by TXRF.

The element concentration in these samples was measured by total reflection x-ray fluorescence (TXRF), which is done by Mr. von Bohlen at our institute, and shown in Fig. 4-18. TXRF is applied to measure the elements concentration of our plant samples, because it needs only small amount of sample ( $10 \mu\text{L}$ ) and possible to do multi-element analysis in one measurement. The detection limit of TXRF was  $0.1 \mu\text{M}$  for all the metal elements. As shown in Fig. 4-18, samples of Group-I indeed have more iron than the other samples. This agrees well to the sample preparation. Iron, manganese and zinc are all detected in all the samples. However, these trace elements are all in very low concentration range (less than  $9 \mu\text{M}$ ). Copper and nickel are much less concentrated in these Tobacco samples. Nickel is only detected in sample 1, 2, 3, 8 and 16. Copper was not detected in sample 4 and 15.  $\text{NA-Fe}^{\text{III}}$  and/or  $\text{NA-Fe}^{\text{II}}$  are expected in Tobacco samples, esp. with the samples in group-I, because there is high concentration of iron existing in Group-I samples, However, no detection of iron-NA species was achieved by this ZIC-HILIC/ESI-FTICR-MS method. This may be caused by the kinetic unstable of  $\text{NA-Fe}^{\text{II}}$  during the separation (see chapter 4.4.3.5).  $\text{NA-Fe}^{\text{III}}$  exists as neutral complex in our condition, no good detection of it



can be achieved by mass spectrometry. In addition, the concentration of the trace metal ions is very low in the Tobacco samples. The metal-species, which are unknown stoichiometry, exist in an even lower concentration range (less than 9  $\mu\text{M}$  with iron-species, less than 3  $\mu\text{M}$  with the other metal-species). Therefore, so low concentration of metal-species is difficult to be detected.

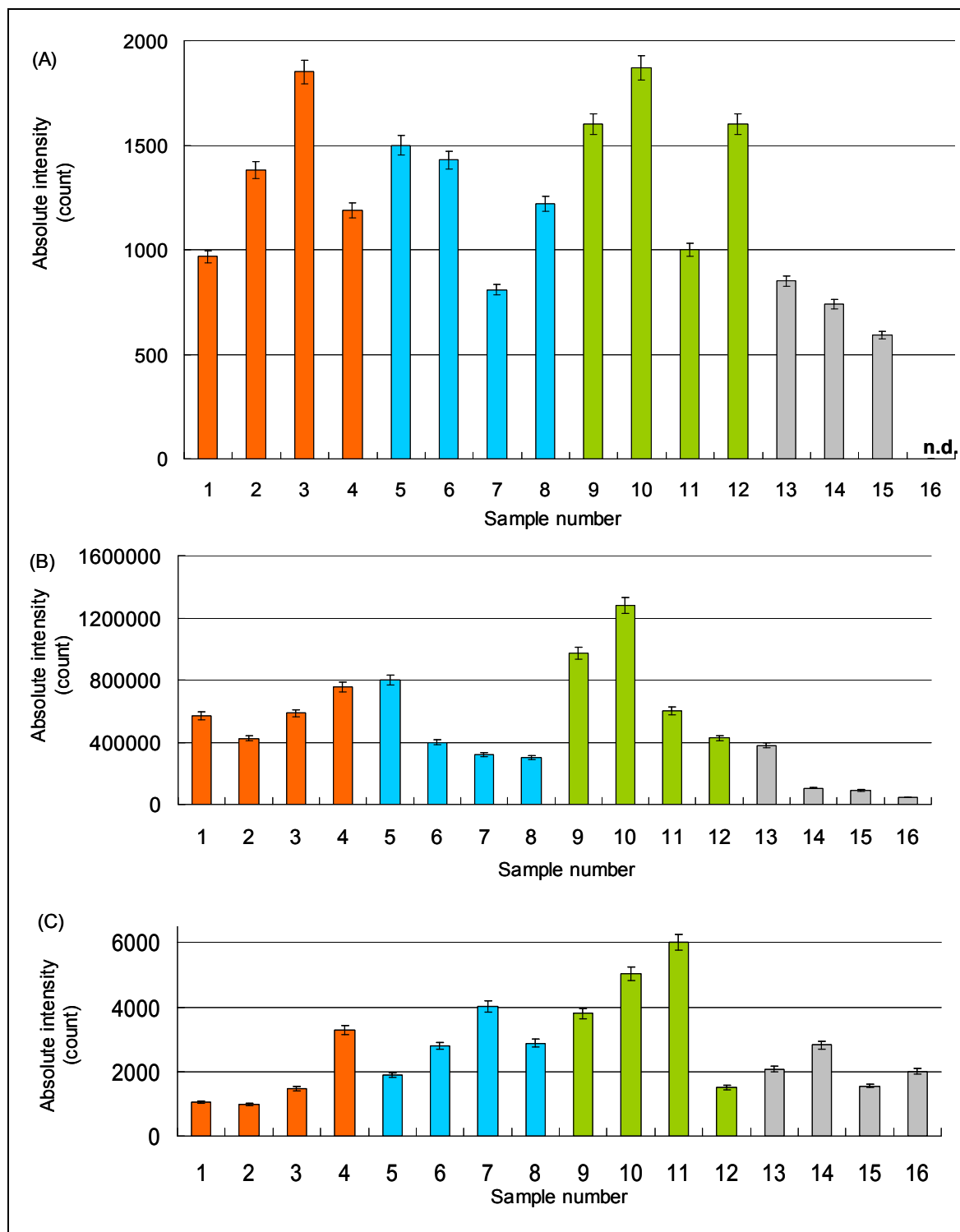


Figure 4-19. Nicotianamine (A), citric acid (B), and histidine (C) were determined in Tobacco plants by ZIC-HILIC/ESI-FTICR-MS method. Sample 1-4 are from Group-I; Sample 5-8 are from Group-II; Sample 9-12 are from Group-III; and sample 13-16 are from Group-IV. Conditions see Fig. 4-12.

Important ligands, such as NA, citrate, and His were detected and the concentration

changes of these important ligands can be seen by the measurements (see Fig. 4-19). Since this set of Tobacco sample was grown under over expressed of NAS, which is an enzyme and responsible for biosynthesis of NA. Therefore, determination of NA was expected in these plants. As expected, NA was detected in all sixteen samples of four different groups (see Fig. 4-19). Citric acid and histidine were simultaneously determined in these samples as well. As shown in Fig. 4-19, samples of Group-IV contain relative less NA than the other sample Groups (I-III). The same case was found with citric acid as well. On contrast, samples of Group-I contain least histidine among all the sample groups. Obviously, samples of Group-III contain more NA, citric acid, and histidine than the other sample Groups.

These examples of monitoring the concentration variances of NA, citric acid, and histidine in different sample groups of Tobacco demonstrate a good applicability of this metabolic profiling method. All these concentration changes of these ligand pools are directly correlated to biological processes and enable to offer important biological information.

#### 4.5 Conclusion

In this chapter, HPLC/MS method developed to analyse LMW metal-species and free ligands in plants was described. Three different HPLC separation methods including ion-pair reversed phase liquid chromatography (IP-RPLC), zwitterionic hydrophilic interaction liquid chromatography (ZIC-HILIC), and zwitterionic 2-methacryloyloxyethyl phosphorylcholine hydrophilic interaction liquid chromatography (ZIC-MPC), were developed by online coupling to electrospray ionization mass spectrometry.

Sufficient separation, sensitive detection, and unequivocal identification of these important LMW free ligands and metal-species in plants were for the first time achieved by this proposed novel ZIC-HILIC/ESI-MS method within 25 min. The metal-species having overlapping mass spectra, e.g. Zn-NA ( $t_R = 15.2$  min) and Cu<sup>II</sup>-DMA ( $t_R = 13.8$  min), or Fe<sup>II</sup>-NA ( $t_R = 14.2$  min) and Fe<sup>III</sup>-DMA ( $t_R = 10.4$  min), were baseline separated from each other. Only in case of baseline separation of these species having overlapping mass spectra, unequivocal identification of them is realised. The species of different metals (Cu<sup>II</sup>, Ni<sup>II</sup>, Zn<sup>II</sup>, and Fe<sup>III</sup>) respectively complexing the same free ligand (DMA, MA, *epi*-HMA, and NA) are baseline separated. On the other hand, the free ligands and their respective complexes of one metal are also baseline separated. Although, zinc-PS and nickel-PS have similar retention times and chromatographic peaks are partially overlapped, unequivocal identification was achieved by their distinct mass spectra. Cu<sup>II</sup>-DMA and Cu<sup>II</sup>-*epi*-HMA are also partially chromatographic overlapped, unequivocal identification of them can be achieved by their distinct mass spectra. It is an advantage of HPLC over CE method that most of different metal-species are baseline separated. Different plant samples, which differ in their biological / nutrient status, were investigated by this method. Important LMW metal-species and free ligands, e.g. NA-Ni, DMA-Zn, DMA-Cu, DMA-Fe<sup>III</sup>, DMA, His, and citric acid, were simultaneously separated and detected in these real plant samples. The changes of these metal-species and ligand pools can be seen by this method. The identity and concentration changes of these species in plants are verified not only by this HPLC/MS (retention time and mass spectra) method, but also by CE of the same samples (chapter 2.4.3).

Metabolic profiling of plants is investigated by a further optimized ZIC-HILIC with a

high resolution mass spectrometry, FTICR-MS. One complete set of Tobacco sample, which contains four different nutrient sample groups, was investigated by this ZIC-HILIC/ESI-FTICR-MS method. A good reproducibility of this method was shown by a systematic variation in average values less than  $\pm 0.5$  min with retention time and 5 % with peak area for all the metabolites found in all the samples. In one single chromatographic run, many metabolites were separated and detected in this set of Tobacco plants. Accurate mass, isotope pattern, fragmentation, and retention time enable unequivocal identification of most metabolites, except of structural isomers. The variances of the metabolites among different sample groups can be monitored by this metabolic profiling method. These variances are directly correlated to biological processes and offering important biological information. All these achievements demonstrate the applicability of this developed method for metabolite profiling.

## 5 Conclusion and Outlook

The original lack of analytical approaches holds back the procedure of fully understanding of the metal transport and translocation systems in plants. In this PhD thesis, new capillary electrophoretic (CE) and a novel zwitterionic hydrophilic interaction chromatography coupled to electrospray ionization mass spectrometry method (ZIC-HILIC/ESI-MS) were successfully developed to fill up the lack of analytical approaches.

The major results are:

- i) A new capillary electrophoresis method, which contains MES/TRIS (20:20 mM) buffer at pH 7.3, allows baseline separation of the important LMW ligands (DMA, MA, *epi*-HMA, and NA) for the first time. Diode array detector (DAD) and capacitively coupled contactless conductivity detector (C<sup>4</sup>D) were applied in series to complement the information of interesting analytes. Separation of ferric-PS species was achieved by this CE method without any stability problem, which is an advantage over HPLC separation. Another advantage of this proposed CE method is simultaneously separating and detecting inorganic cations, such as K<sup>+</sup>, Ca<sup>2+</sup>, and Na<sup>+</sup>, which are abundant in plants. Different kinds of plants were investigated by this proposed CE method. DMA-Zn, DMA-Cu, and NA-Ni are successfully separated and detected in these real plant samples. The changes of these detected species can be monitored by this CE method as well.
- ii) A special novel coated (zwitterionic coated) capillary was used to improve the separation of isomers of Fe<sup>III</sup>-EDDHA. Baseline separation of Asp, Glu, citric acid, and isomers of Fe-EDDHA can be achieved within 8 min.
- iii) In order to enhance the sensitivity and selectivity of iron-species in plants on UV and C<sup>4</sup>D detectors, an on-column photo reactor was innovatively developed for CE. Significant influences on the detection of iron-species were achieved by applying this photo reactor. In capillary flow injection with photo reactor, an enhancement of the detector signal of iron-species was achieved up to a factor of 6 with UV, and up to a factor of 4 with C<sup>4</sup>D. Similar enhancement effects were also observed in HPLC. A selective decrease of the detection signal of iron-species was found in capillary electrophoresis with photo reactor. This can be used for a fast scanning for iron-species.
- iv) A novel ZIC-HILIC/ESI-MS method was developed to simultaneously separate, sensitively detect, and unequivocally identify LMW ligands and metal-species in plants within 25 min. The species of the same PS (DMA, MA, *epi*-HMA, and NA) complexing with different metal, e.g. Cu<sup>II</sup>, Zn<sup>II</sup>, and Fe<sup>III</sup>, are baseline separated. On the other hand, the free ligands (DMA, MA, *epi*-HMA and NA) and their respective complexes of one metal are baseline separated as well. Although PS-Zn<sup>II</sup> and PS-Ni<sup>II</sup>, as well as Cu<sup>II</sup>-DMA and Cu<sup>II</sup>-*epi*-HMA, are partially chromatographic overlapped, unequivocal identification of them can be achieved by their distinct mass spectra, which is an advantage over CE method. Mass spectrometry offers the structure information of metal-species and agrees

to the 1:1 stoichiometry of metal-PS. The metal-species having overlapping mass spectra, e.g.  $\text{Zn}^{\text{II}}$ -NA and  $\text{Cu}^{\text{II}}$ -DMA, or  $\text{Fe}^{\text{II}}$ -NA and  $\text{Fe}^{\text{III}}$ -DMA, were baseline separated from each other. This baseline separation of species having overlapping mass spectra is essential to realise unequivocal identification of them. Wheat and Arabidopsis samples were investigated by this method. Important LMW metal-species and free ligands, e.g.  $\text{NA-Ni}^{\text{II}}$ ,  $\text{DMA-Zn}^{\text{II}}$ ,  $\text{DMA-Cu}^{\text{II}}$ ,  $\text{DMA-Fe}^{\text{III}}$ , DMA, His, and citric acid, were simultaneously separated and detected in these real plant samples. Concentration changes of metabolic ligands and metal species are detected by this method, and can be correlated to the biological status of the plant (e.g., iron-deficiency, trace metal supply via nutrient solution, etc.).

- v) The ZIC-HILIC/ESI-MS method was also demonstrated as an adequate method for plant metabolic profiling, which can detect changes of ligand pools and other metabolites in plants. Fourier transform ion cyclotron resonance mass spectrometry (FTICR-MS), as a high resolution mass spectrometry technique, was applied for this purpose after ZIC-HILIC separation. One complete set of Tobacco samples containing different cultivated sample groups were investigated by this metabolic profiling method. Retention time, isotope pattern, accurate  $m/z$ , and  $\text{MS}^n$  fragmentation enable identification of most metabolites in plants, except to structural isomers. Correlation analysis among different sample groups can be achieved based on the very good reproducibility (system variance of retention time  $< \pm 0.5$  min and of peak intensity  $< 5$  %) and high sensitivity (limit of quantification is  $1 \mu\text{M}$ ) of this method.
- vi) All the different analytical approaches developed in this work, including CE, NACE, ZIC-HILIC/ESI-MS, ZIC-HILIC/ESI-FTICR-MS, and on-line photo reactor for CE, offer complementary information of metabolites in plants. Various plant samples investigated by them provide new and valuable information, which helps to modify existing hypotheses about metal-transport and translocation systems in plants.

For the first time it was shown for wheat and Arabidopsis plants that the identity and the concentration changes of species under consideration are verified and compared. Both HPLC/MS and CE method developed was applied to wheat and Arabidopsis plants and allows a characterization of changes of metal-species in a semi-quantitative way down to the  $\mu\text{mol}$ -level.

Summarizing, the major advantage of the ZIC-HILIC/ESI-MS method is the realization of the separation and identification of all relevant PS species in a single run and the applicability shown for real plant samples. Both enhance the state-of-the-art of analytical methods to be available for further biological applications. Thus, the results presented fill up the lack of analytical approaches.

Generally, all important LMW metal-species and free ligands in plants could be analyzed. Therefore, the results support and contribute directly to a better

understanding of the metal transport and translocation systems in plants. Mature analytical methods for separation, detection, and identification of LMW metal-species and their free ligands in plants are achieved. For a full understanding of the metal-transport systems and related equilibria in plants the next steps to be considered are:

- CE- and HPLC-based separations should be extended to, and validated for further classes of ligands and metal-species,
- Mass spectrometric detection and identification methodology should be further developed to all present plant metabolites.
- Other analytical methods, such as NMR or HPLC-NMR, should be included in metabolic profiling studies for identification of stereoisomers.

## 6 References

- [1] Prasad, A.S., Oberleas, D., Rajasekaran, G., *Essential Micronutrient Elements Biochemistry and Changes in Liver Disorders*. Am. J. Clin. Nutr., 1970. **23**: 581-591.
- [2] Lindsay, W.L., *Zinc in Soils and Plant Nutrition*. Adv. Agron., 1972. **24**: 147-186.
- [3] Graham, R.D., Stangoulis, J.C.R., *Trace element uptake and distribution in plants*. J. Nutr., 2003. **133**: 1502S-1505S.
- [4] Chaney, R.L., Brown, J.C., Tiffin, L.O., *Obligatory Reduction of Ferric Chelates in Iron Uptake by Soybeans*. Plant Physiol., 1972. **50**: 208-213.
- [5] Römheld, V., Muller, C., Marschner, H., *Localization and Capacity of Proton Pumps in Roots of Intact Sunflower Plants*. Plant Physiol., 1984. **76(3)**: 603-606.
- [6] Hether, N.H., Olsen, R.A., Jackson, L.L., *Chemical identification of iron reductants exuded by plant roots*. J. Plant Nutr., 1984. **7**: 667-676.
- [7] Neumann, G., Römheld, V., *The release of root exudates as affected by the plant physiological status*. In: *The Rhizosphere: Biochemistry and organic substances at the soil-plant interface*. Pinton, R., Varanini, Z., Nannipieri, Z., (eds.). Marcel Dekker, New York 2000.
- [8] Mori, S., *Iron acquisition by plants*. Curr. Opin. Plant Biol., 1999. **2**: 250-253.
- [9] Treeby, M., Marschner, H., Römheld, V., *Mobilization of iron and other micronutrient cations from a calcareous soil by plant-borne, microbial, and synthetic metal chelators*. Plant and Soil, 1988. **114**: 217-226.
- [10] Awad, F., Römheld, V., *Mobilization of heavy metals from contaminated calcareous soils by plant born, microbial and synthetic chelates and their uptake by wheat plants*. J. Plant Nutr., 2000. **23**: 1847-1855.
- [11] Ma, J.F., Nomoto, K., *Effective regulation of iron acquisition in graminaceous plants. The role of mugineic acids as phytosiderophores*. Physiol. Plant., 1996. **97**: 609-617.
- [12] Shenker, M., Fan, T.W.M., Crowley, D.E., *Phytosiderophores Influence on Cadmium Mobilization and Uptake by Wheat and Barley Plants*. J. Environ. Qual., 2001. **30**: 2091-2098.

- [13] Petersen, W., Böttger, M., *Contribution of organic acids to the acidification in the rhizosphere of maize seedlings*. Plant and Soil, 1991. **132**: 159-163.
- [14] Pich, A., Scholz, G., Stephan, U.W., *Iron-dependent changes of heavy metals, nicotianamine, and citrate in different plant organs and in the xylem exudates of two tomato genotypes. Nicotianamine as possible copper translocator*. Plant and Soil, 1994. **165**: 189-196.
- [15] Ma, J.F., Shinada, T., Matsuda, T., Nomoto, K., *Biosynthesis of phytosiderophores, mugineic acids, associated with methionine cycling*. J. Biol. Chem., 1995. **270**: 16549-16554.
- [16] Kawai, S., Tagaki, S., Sato, Y., *Mugineic acid-family phytosiderophores in root secretions of barley, corn and sorghum varieties*. J. Plant Nutr., 1988. **11**: 633-642.
- [17] Shojima, S., Nishizawa, N.K., Mori, S., *Establishment of a Cell-Free System for the Biosynthesis of Nicotianamine*. Plant Cell Physiol., 1989, **30(5)**: 673-677
- [18] Shojima, S., Nishizawa, N. K., Fushiya, S., Nozoe, S., Irifune, T., Mori, S. *Biosynthesis of phytosiderophores: In vitro biosynthesis of 2'-deoxymugineic acid from L-methionine and nicotianamine*. Plant Physiol., 1990. **93**: 1497-1503.
- [19] Mori, S., Nishizawa, N., *Methionine as a Dominant Precursor of Phytosiderophores in Gramineae Plants*. Plant Cell Physiol., 1987, **28(6)**: 1081-1092.
- [20] Ma, J.F., Nomoto, K., *Two Related Biosynthetic Pathways of Mugineic Acids in Gramineous Plants*. Plant Physiol., 1993, **102**: 373-378.
- [21] Higuchi, K., Suzuki, K., Nakanishi, H., Yamaguchi, H., Nishizawa, N.K., Mori, S., *Cloning of nicotianamine synthase genes, novel genes involved in the biosynthesis of phytosiderophores*. Plant Physiol., 1999, **119**: 471-479.
- [22] Mino, Y., Ishida, T., Ota, N., Inoue, M., Nomoto, K., Takemoto, T., Tanaka, H., Sugiura Y., *Mugineic acid-iron (III) complex: characterization for absorption and transport of iron in gramineous plants*. J. Am. Chem. Soc. 1983. **105**: 4671-4676.
- [23] Ripperger, H., Schreiber, K., *Nicotianamine and analogous amino acids, endogenous iron carriers in higher plants*. Heterocycles, 1982. **17**: 447-461.
- [24] Budesinsky, M., Budzikiewicz, H., Prochazka, Z., Ripperger, H., Römer, A.,



- Scholz, G., Schreiber, K., *Nicotianamine, a possible phytosiderophore of general occurrence*. Photochemistry, 1980. **19**: 2295-2297.
- [25] Von Wirén, N., Klair, S., Bansal, S., Briat, J.F., Khodr, H., Shioiri, T., Leigh, R.A., Hider, R.C., *Nicotianamine chelates both Fe-III and Fe-II. Implications for metal transport in plants*. Plant Physiol., 1999. **119**: 1107-1114.
- [26] Krämer, U., Cotter-Howells, J.D., Charnock, J.M., Baker, A.J.M., Smith, J.A.C., *Free histidine as a metal chelator in plants that accumulate nickel*. Letters to Nature, 1996. **379**: 635-638.
- [27] Rauser, W.E., *Structure and function of metal chelators produced by plants*. Cell Biochem Biophys., 1999, **31**: 19-48.
- [28] Cieśliński, G., Van Rees, K.C.J., Szmigielska, A.M., Krishnamurti, G.S.R., Huang, P.M., *Low-molecular-weight organic acids in rhizosphere soils of durum wheat and their effect on cadmium bioaccumulation*. Plant and Soil, 1998. **203**: 109-117.
- [29] Walker, C.D., Welch, R.M., *Low molecular weight complexes of zinc and other trace metals in lettuce leaf*. J. Agric. Food Chem., 1987. **35**: 721-727.
- [30] Jones, D.L., Edwards, A.C., Donachie, K., Darrah, P.R., *Role of proteinaceous amino acids released in root exudates in nutrient acquisition from the rhizosphere*. Plant and Soil, 1994. **158**: 183-192.
- [31] Bienfait, H.F., Scheffers, M.R., *Some properties of ferric citrate relevant to the iron nutrition of plants*. Plant and Soil, 1992. **143**: 141-144.
- [32] White, M.C., Decker, A.M., Chaney, R.L., *Metal complexation in xylem fluid: I. Chemical composition of tomato and soybean stem exudates*. Plant Physiol., 1981. **67**: 292-300.
- [33] Mench, M., Morel, J.L., Guckert, A., Guillet, B., *Metal binding with root exudates of low molecular weight*. J. Soil Sci., 1988. **39**: 521-527.
- [34] Takagi, S. *Production of phytosiderophores*. Eds. Barton LL, Hemming B C. Iron Chelation in Plants and Soil Microorganisms. San Diego: Academic Press, 1993. p. 111-131.
- [35] Kawai, S., Sato, Y., Takagi, S., *Separation and determination of mugineic acid and its analogues by high-performance liquid chromatography*. J. Chromatogr., 1987. **391(1)**: 325-327.

- [36] Mori, S., Nishizawa, N., Kawai, S., Sato, Y., Takagi, S., *Dynamic state of mugineic acid and analogous phytosiderophores in Fe-deficient barley*. J. Plant Nutr., 1987. **10**: 1003-1011.
- [37] Neumann, G., Haake, C., Römheld, V., *Improved HPLC method for determination of phytosiderophores in root washings and tissue extracts*. J. Plant Nutr., 1999. **22**: 1389-1402.
- [38] Wheal, M.S., Helle, L.I., Norvell, W.A., Welch, R.M., *Reversed-phase liquid chromatographic determination of phytometallophores from Strategy II Fe-uptake species by 9-fluorenylmethyl chloroformate fluorescence*. J. Chromatogr. A, 2002. **942(1-2)**: 177-183.
- [39] Howe, J.A., Choi, Y.H., Loeppert, R.H., Senseman, S., Juo, A.S.R., *Column chromatography and verification of phytosiderophores by PITC derivation and UV detection*. J. Chromatogr., 1999. **841(2)**: 155-164.
- [40] Ishida, Y., Fujita, T., Asai, K., *New detection and separation method for amino acids by high-performance liquid chromatography*. J. Chromatogr., 1981. **204**: 143-148.
- [41] Weber, G., Neumann, G., Haake, C., Römheld, V., *Determination of phytosiderophores by anion-exchange chromatography with pulsed amperometric detection*. J. Chromatogr. A, 2001. **928(2)**: 171-175.
- [42] Weber, G., Neumann, G., Römheld, V., *Speciation of iron coordinated by phytosiderophores by use of HPLC with pulsed amperometric detection and AAS*. Anal. Bioanal. Chem., 2002. **373**: 767-771.
- [43] Vacchina, V., Mari, S., Czernic, P., Marquès, L., Pianelli, K., Schaumlöffel, D., Lebrun, M., Łobiński, R., *Speciation of nickel in a hyperaccumulating plant by high-performance liquid chromatography-inductively coupled plasma mass spectroscopy and electrospray MS/MS assisted by cloning using yeast complementation*. Anal. Chem., 2003. **75**: 2740-2745.
- [44] Von Wirén, N., Khodr, H., Hider, R.C., *Hydroxylated Phytosiderophore Species Possess an Enhanced Chelate Stability and Affinity for Iron(III)*. Plant Physiol. 2000. **124(3)**: 1149-1158.
- [45] Schaumlöffel, D., Ouerdane, L., Bouyssièrè, B., Łobiński, R., *Speciation analysis of nickel in the latex of a hyperaccumulating tree *Sebertia acuminata* by HPLC and CZE with ICP MS and electrospray MS-MS detection*. J. Anal. At. Spectrom., 2003. **18**: 120-127.

- [46] Fan, T.W.M., Lane, A.N., Shenker, M., Bartley, J.P., Crowley, D., Higashi, R.M., *Comprehensive chemical profiling of gramineous plant root exudates using high-resolution NMR and MS*. *Phytochemistry*, 2001, **57**: 209-221.
- [47] Welch, R.M., *The impact of mineral nutrients in food crops on global human health*. *Plant and Soil*, 2002, **247**: 83-90.
- [48] Bantan, T., Milacic R., Mitrovic, B., Pihlar, B., *Investigation of low molecular weight Al complexes in human serum by fast protein liquid chromatography (FPLC)-ETAAS and electrospray (ES)-MS-MS techniques*. *J. Anal. At. Spectrom.*, 1999, **14(11)**: 1743-1748.
- [49] Bantan, T., Milacic, R., Mitrovic, B., Pihlar, B., *Combination of various analytical techniques for speciation of low molecular weight aluminium complexes in plant sap*. *Fresenius J. Anal. Chem.*, 1999, **365(6)**: 545-552.
- [50] Casiot, C., Vacchina, V., Chassaingne, H., Szpunar, J., Potin-Gautier, M., Łobinski, R., *An approach to the identification of selenium species in yeast extracts using pneumatically-assisted electrospray tandem mass spectrometry*. *Anal. Commun.*, 1999, **36(3)**: 77-80.
- [51] Kotrebai, M., Bird, S.M., Tyson, J.F., Block, E., Uden, P.C., *Characterization of selenium species in biological extracts by enhanced ion-pair liquid chromatography with inductively coupled plasma-mass spectrometry and by referenced electrospray ionization-mass spectrometry*. *Spectrochim. Acta, Part B*, 1999, **54(11)**: 1573-1591.
- [52] Kotrebai, M., Tyson, J.F., Block, E., Uden, P.C., *High-performance liquid chromatography of selenium compounds utilizing perfluorinated carboxylic acid ion-pairing agents and inductively coupled plasma and electrospray ionization mass spectrometric detection*. *J. Chromatogr. A*, 2000, **866(1)**: 51-63.
- [53] McSheehy, S., Yang, W., Pannier, F., Szpunar, J., Łobinski, R., Auger, J., Potin-Gautier, M., *Speciation analysis of selenium in garlic by two-dimensional high-performance liquid chromatography with parallel inductively coupled plasma mass spectrometric and electrospray tandem mass spectrometric detection*. *Anal. Chim. Acta.*, 2000, **421(2)**: 147-153.
- [54] Montes-Bayon, M., LeDuc, D.L., Terry, N., Caruso, J.A., *Selenium speciation in wild-type and genetically modified Se accumulating plants with HPLC separation and ICP-MS/ESI-MS*. *J. Anal. At. Spectrom.*, 2002, **17(8)**: 872-879.

- [55] McSheehy, S., Pohl, P., Lobinski, R., Szpunar, J., *Complementarity of multidimensional HPLC-ICP-MS and electrospray MS-MS for speciation analysis for arsenic in algae*. J. Anal. At. Spectrom., 2001, **440(1)**: 3-16.
- [56] Madsen, A.D., Goessler, W., Pedersen, S.N., Francesconi, K.A., *Characterization of an algal extract by HPLC-ICP-MS and LC-electrospray MS for use in arsenosugar speciation studies*. J. Anal. At. Spectrom., 2000, **15 (6)**: 657-662.
- [57] Van Hulle, M., Zhang, C., Zhang, X., Cornelis, R., *Arsenic speciation in Chinese seaweeds using HPLC-ICP-MS and HPLC-ES-MS*. Analyst, 2002, **127**: 634-640.
- [58] Vacchina, V., Lobinski, R., Oven, M., Zenk, M.H., *Signal identification in size-exclusion HPLC-ICP-MS chromatograms of plant extracts by electrospray tandem mass spectrometry (ES MS/MS)*. J. Anal. At. Spectrom., 2000, **15**: 529-534.
- [59] Bjørnsdottir, I., Hansen, S., Terabe S., *Chiral separation in non-aqueous media by capillary electrophoresis using the ion-pair principle*. J. Chromatogr. A, 1996, **745**: 37-44.
- [60] Riekkola, M.L., Wiedmer, S. K., Valko, I.E., *Selectivity in capillary electrophoresis in the presence of micelles, chiral selectors and non-aqueous media*. J. Chromatogr. A, 1997, **792(1-2)**: 13-35.
- [61] Altria, K.D., Bryant, S.M., *Highly selective and efficient separations of a wide range of acidic species in capillary electrophoresis employing non-aqueous media*. Chromatographia, 1997, **46**: 122-130.
- [62] Karbaum, A., Jira, T., *Nonaqueous capillary electrophoresis: Application possibilities and suitability of various solvents for the separation of basic analytes*. Electrophoresis, 1999, **20**: 3396-3401.
- [63] Riekkola, M.L., Jussila, M., Porras, S.P., *Non-aqueous capillary electrophoresis*. J. Chromatogr. A, 2000, **892(1-2)**: 155-170.
- [64] Wang, F., Khaledi, M.G., *Enantiomeric separations by nonaqueous capillary electrophoresis*. J. Chromatogr. A, 2000, **875(1-2)**: 277-293.
- [65] Steiner, F., Hassel, M., *Nonaqueous capillary electrophoresis: a versatile completion of electrophoretic separation techniques*. Electrophoresis, 2000, **21 (18)**: 3994-4016.
- [66] Shaw, D., *Introduction to Colloid and Surface Chemistry*, 3<sup>rd</sup> Ed., Butterworth,

- London, 1980.
- [67] Kuban, P., Kuban, P., Kuban, V., *Simultaneous determination of inorganic and organic anions, alkali, alkaline earth and transition metal cations by capillary electrophoresis with contactless conductometric detection*. *Electrophoresis*, 2002, **23**: 3725-34.
- [68] Coufal, P., Zuska, J., Van de Goor, T., Smith, V., Gas, B., *Separation of twenty underivatized essential amino acids by capillary zone electrophoresis with contactless conductivity detection*. *Electrophoresis*, 2003, **24(4)**: 671-677.
- [69] Baltussen, E., Guijt, R.M., Van der Steen, G., Laugere, F., Baltussen, S., Van Dedem, Gijs W. K., *Considerations on contactless conductivity detection in capillary electrophoresis*. *Electrophoresis*, 2002, **23(17)**: 2888-2893.
- [70] Zemann, A.J., Schnell, E., Volgger, D., Bonn, G.K., *Contactless Conductivity Detection for Capillary Electrophoresis*. *Anal. Chem.*, 1998, **70**: 563-567.
- [71] Fracassi, J.A., Silva, D., Lago, D., *An oscillometric detector for capillary electrophoresis*. *Anal. Chem.*, 1998, **70(20)**: 4339-4343.
- [72] Kubáň, P., Hauser, P.C., *Fundamental aspects of contactless conductivity detection for capillary electrophoresis. Part I: Frequency behavior and cell geometry*. *Electrophoresis*, 2004, **25**: 3387-3397.
- [73] Rengel, Z., Römheld, V. *Root exudation and Fe uptake and transport in wheat genotypes differing in tolerance to Zn deficiency*. *Plant and Soil*, 2000, **222**: 25-34.
- [74] Loqué, D., Ludewig, U., Yuan, L., von Wiren, N., *Tonoplast aquaporins AtTIP2;1 and AtTIP2;3 facilitate NH<sub>3</sub> transport into the vacuole*. *Plant Physiol.*, 2005, **137**: 671-680.
- [75] Tanyanyiwa, J., Schweizer, K., Hauser, P.C., *High-voltage contactless conductivity detection of underivatized amino acids in capillary electrophoresis*. *Electrophoresis*, 2003, **24(12-13)**: 2119-2124.
- [76] Alpert, A.J., *Hydrophilic-interaction chromatography for the separation of peptides, nucleic acids and other polar compounds*. *J. Chromatogr.*, 1990, **499**: 177-196.
- [77] Murakami, T., Ise, K., Hayakawa, M., Kamei, S., Takagi, S., *Stabilities of metal complexes of mugineic acid and their specific affinities for iron(III)*. *Chem. Lett.*, 1989, 2137-2140.

- [78] Anderegg, G., Ripperger, H., *Correlation between metal complex formation and biological activity of nicotianamine analogues*. J. Chem. Soc. Chem. Commun., 1989, 647-650.
- [79] Frost, A.E., Freedman, H.H., Westerback, S.J., Martell, A.E., *Chelate tendencies of N, N'-ethylenebis-[2-(o-hydroxyphenyl)] glycine*. J. Am. Chem. Soc., 1958, **80**: 530-536.
- [80] Ahrland, S., Dahlgren Å., Persson, I., *Stabilities and hydrolysis of some iron(III) and manganese(II) complexes with chelating ligands*. Acta. Agric. Scand., 1990, **40**: 101-111.
- [81] Obrador, A., Novillo, J., Alvarez, J.M., *Mobility and Availability to Plants of Two Zinc Sources Applied to a Calcareous Soil*. Soil Sci. Soc. Am. J., 2003, **67**: 564-572.
- [82] Lucena, J.J., *Synthetic Iron Chelates to Correct Iron Deficiency in Plants, Iron Nutrition in Plants and Rhizospheric Microorganisms*, edited by Larry L. Barton and Javier Abadia, 103-128.
- [83] Nayyar, V.K., Arora, C.L., Kataki, P.K., *Management of Soil Micronutrient Deficiencies in the Rice-Wheat Cropping System*, 2001, **4**: 87-131.
- [84] Wik, R.M., Fisher, P.R., Kopsell, D.A., Argo, W.R., *Iron form and concentration affect nutrition of container-grown Pelargonium and Calibrachoa*. HortScience, 2006, **41(1)**: 244-251.
- [85] Hernández-Apaolaza, L., Barak, P., Lucena, J.J., *Chromatographic determination of commercial Fe(III)-chelates of EDTA, EDDHA and EDDHMA*. J. Chromatogr. A, 1997, **789(1-2)**: 453-460.
- [86] Smith, R.M., Martel, A.E., *Critical Stability Constants*. Plenum Press: New York, 1989, **Vols.1-6**.
- [87] Hider, R.C., Yoshimura, E., Khodr, H., von Wirén, N., *Competition or complementation: the iron-chelating abilities of nicotianamine and phytosiderophores*. New Phytologist., 2004, **164**: 204-208.
- [88] Yunta, F., Garcia-Marco, S., Lucena, J.J., Gomez-Gallego, M., Alcazar, R., Sierra, MA., *Chelating agents related to ethylenediamine bis(2-hydroxyphenyl)acetic acid (EDDHA): synthesis, characterization, and equilibrium studies of the free ligands and their Mg<sup>2+</sup>, Ca<sup>2+</sup>, Cu<sup>2+</sup>, and Fe<sup>3+</sup> chelates*. Inorg Chem., 2003, **42**: 5412-5421.
- [89] Sugiura, Y., Tanaka, H., Mino, Y., Ishida, T., Ota, N., Inoue, M., Nomote, K., Yoshioka, H., Takemoto, T., *Structure, Properties, and Transport Mechanism*

- of Iron(III) Complex of Mugineic Acid, a Possible Phytosiderophore*. J. Am. Chem. Soc., 1981. **103**: 6979-6982.
- [90] Liu, Y.J., Foote, R.S., Culbertson, C.T., Jacobson, S.C., Ramsey, R.S., Ramsey, J.M., *Electrophoretic separation of proteins on microchips*. J. Microcol., 2000, **12**: 407-411.
- [91] Gong, B.Y., Ho, J.W., *Effect of zwitterionic surfactants on the separation of proteins by capillary electrophoresis*. Electrophoresis, 1997, **18**: 732-735.
- [92] Wei, W., Jiu, H.X., *Application of dodecyldimethyl (2-hydroxy-3-sulfopropyl) ammonium in wall modification for capillary electrophoresis separation of proteins*. Electrophoresis, 2005, **26**: 586-592.
- [93] Mori, M., Hu, W.Z., Hasebe, K., Tanaka, S., Tanaka, K., *Use of phosphobetaine-type zwitterionic surfactant for the determination of alkali and alkaline earth metal ions and ammonium ion in human saliva by capillary electrophoresis*. Anal. Bioanal. Chem., 2002, **374**: 75-79.
- [94] Fillet, M., Servais, A.C., Crommen, J., *Effects of background electrolyte composition and addition of selectors on separation selectivity in nonaqueous capillary electrophoresis*. Electrophoresis, 2003, **24**: 1499-1507.
- [95] Chipperfield, J.R., *Nonaqueous Solvents*, Oxford University Press, New York 1999, 69.
- [96] Prousek, J., *Fenton reaction after a century*. Chem. Listy., 1995, **89**: 11-21.
- [97] Pierre, J.L., Fontecave, M., *Iron and activated oxygen species in biology: The basic chemistry*. Biometals, 1999. **12**: 195-199.
- [98] Pierre, J.L., Fontecave, M., Crichton, R.R., *Chemistry for an essential biological process: the reduction of ferric iron*. BioMetals, 2002, **15**: 341-346.
- [99] Engelmann, M.D., Bobier, R.T., Hiatt, T., Cheng, I.F., *Variability of the Fenton reaction characteristics of the EDTA, DTPA, and citrate complexes of iron*. BioMetals, 2003, **16**: 519-527.
- [100] Boukhalfa, H., Crumbliss, A.L., *Chemical aspects of siderophore mediated iron transport*. BioMetals, 2002. **15**: 325-339.
- [101] Comporti, M., Signorini, C., Buonocore, G., Ciccoli, L., *Iron release, oxidative stress and erythrocyte ageing*. Free Radic. Biol. Med., 2002, **32**: 568-576.
- [102] Joshua, H., *Determination of aflatoxins by reversed-phase HPLC with*

- post-column in-line photochemical derivatization and fluorescence detection.* J. Chrom. A, 1993, **654**: 247-254.
- [103] Bellec, G., Cauvin, J.M., Salaun, M.C., Le Calveè, K., Dreèano, Y., Goureèrou, H., Meènez, J.F., Berthou, F., *Analysis of N-nitrosamines by high-performance liquid chromatography with post-column photohydrolysis and colorimetric detection.* J. Chromatogr., 1996, **727(1)**: 83-92.
- [104] Miles, C.J., *Determination of national survey of pesticides analytes in ground water by liquid chromatography with postcolumn reaction detection.* J. Chromatogr., 1992, **592**: 283-290.
- [105] Di, Pietra, A.M., Gotti, R., Andrisano, V., Cavrini, V., *Application of high-performance liquid chromatography with diode-array detection and on-line post-column photochemical derivatization to the determination of analgesics.* J. Chromatogr., 1996, **729**: 355-361.
- [106] Birks, J.W., (Ed.), *Chemiluminescence and Photochemical Reaction Detection in Chromatography*, VCH, New York, 1989.
- [107] Birks, J.W., Frei, R.W., *Photochemical Reaction Detection in HPLC*, Trends in Anal. Chem., 1982. **1**: 361-367.
- [108] Perez-Ruiz, T., Martinez-Lozano, C., Tomas, V., Martin, J., *High-performance liquid chromatographic separation and quantification of citric, lactic, malic, oxalic and tartaric acids using a post-column photochemical reaction and chemiluminescence detection.* J. Chromatogr. A, 2004, **1026**: 57-64.
- [109] Mawatari, K., Mashiko, S., Watanabe, M., Nakagomi, K., *Fluorometric Determination of Khellin in Human Urine and Serum by High-Performance Liquid Chromatography Using Postcolumn Photoirradiation.* Anal. Sci., 2003, **19**: 1071-1073.
- [110] Bocchini, P., Andalo, C., Pozzi, R., Galletti, G.C., Antonelli, A., *Determination of diallyl thiosulfinate (allicin) in garlic (Allium sativum L.) by high-performance liquid chromatography with a post-column photochemical reactor.* Anal. Chim. Acta., 2001, **441**: 37-43.
- [111] Milofsky, R., Ward, J., Shaw, H., Klundt, I., *Post-column photochemical reaction detection in liquid chromatography based on photosensitized generation of singlet molecular oxygen: Study of reaction parameters and application to the determination of polychlorinated biphenyls.* Chromatographia, 2000, **51(3-4)**: 205-211.



- [112] Blau, K., Halket, J.M. (Editors), *Handbook of Derivatives for Chromatography, 2nd Ed.*, John Wiley and Sons, New York, 1993.
- [113] Dickson, J., Odom, M., Ducheneaux, F., Murray, J., Milofsky, R.E., *Coupling Photochemical Reaction Detection Based on Singlet Oxygen Sensitization to Capillary Electrochromatography*. *Anal. Chem.*, 2000, **72**: 3038-3042.
- [114] Tao, L., Thompson, J.E., Kennedy, R.T., *Optically gated capillary electrophoresis of ophthalaldehyde/beta-mercaptoethanol derivatives of amino acids for chemical monitoring*. *Anal. Chem.*, 1998, **70(19)**: 4015-4022.
- [115] Kakkar, P., Dos, B., Vishwanathan, P.N., *A modified spectrophotometric assay of superoxide dismutase*. *Ind. J. Biochem. Biophys.*, 1984, **21**: 130-32.
- [116] Schaich, K.M., Borg, D.C., *Fenton reactions in lipid phases*. *Lipids*, 1988, **23(6)**: 570-579.
- [117] Stadtman, E.R., Berlett, B.S., *Fenton chemistry. Amino acid oxidation*. *J Biol Chem.*, 1991, **266(26)**: 17201-11.
- [118] Winterbourn, C.C., *Comparison of superoxide with other reducing agents in the biological production of hydroxyl radicals*. *Biochem. J.*, 1979. **182(2)**: 625-628.
- [119] Tien, M., Bucher, J.R., Aust, S.D., *Thiol-dependent lipid peroxidation*, *Biochem. Biophys. Res. Commun.*, 1982, **107**: 279-285.
- [120] Langford, C.H., Carey, J.H., *The Charge Transfer Photochemistry of the Hexaaquoiron(III) Ion, the Chloropentaaquoiron(III) Ion, and the  $\mu$ -Dihydroxo Dimer Explored with tert-Butyl Alcohol Scavenging*. *J. Chem.*, 1975, **53**: 2430-2435.
- [121] Balzani, V., Carassiti, V., *Photochemistry of Coordination Compounds*. Academic Press, London, 1970
- [122] Baxendale, J.H., Bridge, N.K., *Photoreduction of Ferric Compounds in Aqueous Solution*. *J. Phys. Chem.* 1955. **59**: 783-788.
- [123] Carey, J.H., Langford, C.H., *Outer sphere oxidation of alcohol and formic acid by charge transfer excited states of iron (III) species*. *Can. J. Chem.*, 1975, **53**: 2436-2440.
- [124] Carey, J.H., Oliver, B.G., *The photoreduction of hexaaquoiron(III) perchlorate in the presence of tertiary aliphatic alcohols. The effect of added copper*. *Can. J. Chem.*, 1977, **55**: 1207-1212.

- [125] Carey, J.H., Casgrove, E.G., Oliver, B.G., *The photolysis of hexaquoiron(III) perchlorate in the presence of ethylene glycol*. *Can. J. Chem.*, 1977, **55**: 625-629.
- [126] Vepřek-Šiška, J., Luňák, S., *Photocatalytic effects of trace metals evidence against a free radical chain mechanism in sulfite autoxidation*. *React. Kinet. Catal. Lett.*, 1978, **8**: 483-487.
- [127] Bozzi, A., Yuranova, T., Mielczarski, J.A., Kiwi, J., *Evidence for immobilized photo-Fenton degradation of organic compounds on structured silica surfaces involving Fe recycling*. *New J. Chem.*, 2004, **28**: 519-526.
- [128] Zuo, Y.G., *Kinetics of photochemical chemical cycling of iron coupled with organic-substances in cloud and fog droplets*. *Geochim. Cosmochim. Acta.*, 1995, **59(15)**: 3123-3130.
- [129] Leon, L.E., Rois, A., Luque de Castro, M.D., Valcarcel M., *Use of photochemical reactions in flow injection: determination of oxalate in urine*. *Analyst*, 1990, **115(12)**: 1549-1552.
- [130] Kuyper, C., Milofsky, R., *Recent development in chemiluminescence and photochemical reaction detection for capillary electrophoresis*. *Trends Anal. Chem.*, 2001, **20**: 232-240.
- [131] Concha-Herrera, V., Torres-Lapasio, J.R., Vivo-Truyols, G., *Chromatographic Determination of Thiols After Pre-column Derivatization with o-Phthalaldehyde and Isoleucine*. *J. Liq. Chrom. Relat. Tech.*, 2006, **29(17)**: 2521-2536.
- [132] Piraud, M., Vianey-Saban, C., Bourdin, C., Acquaviva-Bourdain, C., Boyer, S., Elfakir, C., Bouchu, D., *A new reversed-phase liquid chromatographic/tandem mass spectrometric method for analysis of underivatized amino acids: evaluation for the diagnosis and the management of inherited disorders of amino acid metabolism*. *Rapid Commun. Mass Spectrom.*, 2005, **19**: 3287-3297.
- [133] Silva, M.F., Chipre L.F., Raba J., *Amino acids characterization by reversed-phase liquid chromatography. Partial least-squares modeling of their transport properties*. *Chromatographia*, 2001, **53(7-8)**: 392-400.
- [134] Corradini, D., Grego, S., Liburdi, K., *A Combined Approach Employing Soxhlet Extraction and Linear Gradient Elution Reversed-Phase HPLC for the Fingerprinting of Soil Organic Matter According to Hydrophobicity*. *Chromatographia*, 2006, **63(13)**: 11-16.
- [135] Cawthray, G.R., *Improved reversed-phase liquid chromatography method for*

- the analysis of low-molecular-mass organic acids in plant root exudates.* J. Chromatogr. A, 2003, **1011**: 233-240.
- [136] Vial, J., Hennion, M.C., Fernandez-Alba, A., *Use of porous graphitic carbon coupled with mass detection for the analysis of polar phenolic compounds by liquid chromatography.* J. Chromatogr. A, 2001, **937(1-2)**: 21-29.
- [137] Torres-Lapasio, J.R., Roses, M., Bosch, E., *Interpretive optimisation strategy applied to the isocratic separation of phenols by reversed-phase liquid chromatography with acetonitrile-water and methanol-water mobile phases.* J. Chromatogr. A, 2000, **886(1-2)**: 31-46.
- [138] Jiang, W., Fischer, G., Girmay, J., Irgum, K., *Zwitterionic Stationary Phase with Covalently Bonded Phosphorylcholine Type Polymer Grafts and its Applicability to Separation of Peptides in the Hydrophilic Interaction liquid chromatography mode.* J. Chromatogr. A, 2006, **1127**: 82-91.
- [139] Tolstikov, V.V., Fiehn, O., *Analysis of highly polar compounds of plant origin: Combination of hydrophilic interaction chromatography and electrospray ion trap mass spectrometry.* Anal. Biochem., 2002, **301**: 298-307.
- [140] Schlichtherle-Cerny, H., Affolter, M., Cerny, C., *Hydrophilic interaction liquid chromatography coupled to electrospray mass spectrometry of small polar compounds in food analysis.* Anal. Chem., 2003, **75**: 2349-2354.
- [141] Strege, M.A., Stevenson, S., Lawrence, S.M., *Mixed-mode anion-cation exchange/hydrophilic interaction liquid chromatography-electrospray mass spectrometry as an alternative to reversed phase for small molecule drug discovery.* Anal. Chem., 2000, **72**: 4629-4633.
- [142] Litowski, J.R., Semchuk, P.D., Mant, C.T., Hodges, R.S., *Hydrophilic interaction/cation-exchange chromatography for the purification of synthetic peptides from closely related impurities: serine side-chain acetylated peptides.* J. Pept. Res., 1999, **54**: 1-11.
- [143] Ouerdane, L., Mari, S., Czernic, P., Lebrun, M., Lobinsky, R., *Speciation of non-covalent nickel species in plant tissue extracts by electrospray Q-TOFMS/MS after their isolation by 2D size exclusion-hydrophilic interaction LC (SEC-HILIC) monitored by ICP-MS.* J. Anal. At. Spectrom., 2006, **21(7)**: 676-683.
- [144] Zheng, J., Ohata, M., Furuta, N., *Reversed-phase liquid chromatography with mixed ion-pair reagents coupled with ICP-MS for the direct speciation analysis of selenium compounds in human urine.* J. Anal. At. Spectrom., 2002, **17**: 730-735.

- [145] Lucena, J.J., Barak, P., Hernández-Apaolaza, L., *Isocratic ion-pair high-performance liquid chromatographic method for determination of various iron(III) chelates*. J. Chromatogr. A, 1996, **727**: 253-264.
- [146] Rigas, P.G., Arvanitis, S.J., Pietrzyk, D.J., *Ion interaction chromatographic separation of amino acids using a basic-tetraalkylammonium salt mobile phase*. J. Liq. Chromatogr., 1987, **10**: 2891-2910.
- [147] Saurina, J., Hernandez-Cassou, S., *Determination of amino acids by ion-pair liquid chromatography with post-column derivatization using 1,2-naphthoquinone-4-sulfonate*. J. Chromatogr., 1994, **676**: 311-319.
- [148] Yokoyama, Y., Amaki, T., Horikoshi, S., Sato, H., *Optimum combination of reversed-phase column type and mobile-phase composition for gradient elution ion-pair chromatography of amino acids*. Anal. Sci., 1997, **13**: 963-967.
- [149] Whitehead, K., Hedges, J.I., *Analysis of mycosporine-like amino acids (MAAs) in plankton by liquid chromatography electrospray-ionization mass spectrometry*. Mar. Chem., 2002, **80**: 27-39.
- [150] Kotiaho, T., Eberlin, M.N., Vainiotalo, P., Kostianen, R., *Electrospray Mass and Tandem Mass Spectrometry Identification of Ozone Oxidation Products of Amino Acids and Small Peptides*. J. Am. Soc. Mass Spectrom., 2000, **11**: 526-535.
- [151] Soga, T., Kakazu, Y., Robert, M., Tomita, M., Nishioka, T., *Qualitative and quantitative analysis of amino acids by capillary electrophoresis: Electrospray ionization tandem mass spectrometry*. Electrophoresis, 2004, **25**: 1964-1972.
- [152] Klampfl, C.W., Ahrer, W., *Determination of free amino acids in infant food by capillary zone electrophoresis with mass spectrometric detection*. Electrophoresis, 2001, **22(8)**: 1579-1584.
- [153] Hagberg, J., *Analysis of low-molecular-mass organic acids using capillary zone electrophoresis-electrospray ionization mass spectrometry*. J. Chromatogr. A, 2003, **988**: 127-133.
- [154] Dabek-Zlotorzynska, E., Aranda-Rodriguez, R., Graham, L., *Capillary electrophoresis determinative and GC-MS confirmatory method for water-soluble organic acids in airborne particulate matter and vehicle emission*. J. Sep. Sci., 2005, **28(13)**: 1520-1528.
- [155] Knust, U., Erben, G., Spiegelhalder, B., Bartsch, H., Owen, R.W., *Identification*

- and quantitation of phenolic compounds in faecal matrix by capillary gas chromatography and nano-electrospray mass spectrometry.* Rapid Commun. Mass Spectrom., 2006, **20**: 3119-3129.
- [156] Montoro, P., Piacente, S., Oleszek, W., Pizza, C., *Liquid chromatography/tandem mass spectrometry of unusual phenols from Yucca schidigera bark: comparison with other analytical techniques.* J. Mass Spectrom., 2004, **39**: 1131-1138.
- [157] Gledhill, M., *Electrospray ionization-mass spectrometry of hydroxamate siderophores.* Analyst, 2001, **126**: 1359-1362.
- [158] Spasojevic, I., Boukhalfa, H., Stevens, R.D., Crumbliss, A.L., *Aqueous Solution Speciation of Fe(III) Complexes with Di-Hydroxamate Siderophores Alcaligin and Rhodotorulic Acid and Synthetic Analogues Using Electrospray Ionization Mass Spectrometry (ESI-MS).* Inorg. Chem., 2001, **40**: 49-58.
- [159] Neubert, H., Hider, R.C., Cowan, D.A., *Speciation of Fe(III)-chelate complexes by electrospray ionization ion trap and laser desorption/ionization Fourier transform ion cyclotron resonance mass spectrometry.* Rapid Commun. Mass Spectrom., 2002, **16**: 1556-1561.
- [160] Budimir, N., Fournier, F., Bailly, T., Burgada, R., Tabet, J.C., *Study of metal complexes of a tripodal hydroxypyridinone ligand by electrospray tandem mass spectrometry.* Rapid Commun. Mass Spectrom., 2005, **19**: 1822-1828.
- [161] Weber, G., von Wirén, N., Hayen, H., *Analysis of iron(II)/iron(III) phytosiderophore complexes by nano-electrospray ionization Fourier transform ion cyclotron resonance mass spectrometry.* Rapid Commun. Mass Spectrom., 2006, **20**: 973-980.
- [162] Krokhin, O.V., Kuzina, O.V., Hoshino, H., Shpigun, O.A., Yotsuyanagi, T., *Potential of ethylenediaminedi (o-hydroxyphenylacetic acid) and N,N'-bis (hydroxybenzyl) ethylenediamine-N,N'-diacetic acid for the determination of metal ions by capillary electrophoresis.* J. Chromatogr. A, 2000, **890**: 363-369.
- [163] Jiang, W., Irgum, K., *Tentacle-type Zwitterionic Stationary Phase, Prepared by Surface Initiated Graft Polymerization of 3- [N,N-dimethyl-N-(methacryloyloxy-ethyl) ammonium] propanesulfonate Through Peroxide Groups Tethered on Porous Silica.* Anal. Chem., 2002, **74**: 4682-4687.
- [164] Roessner, U., Luedemann, A., Brust, D., Fiehn, O., Linke, T., Willmitzer, L., Fernie, A.R., *Metabolic profiling allows comprehensive phenotyping of genetically or environmentally modified plant systems.* Plant Cell, 2001, **13**: 11-29.

**7 Index of Abbreviations**

2-D NMR	two dimensional nuclear magnetic resonance
AC	alternating current
ACN	acetonitrile
APCI	Atmospheric Pressure Chemical Ionization
API	Atmospheric Pressure Ionization
Arg	Arginine
Asp	Aspartic acid
BGEs	background electrolytes
C	cell capacitance in F
$C_0$	stray capacitance in F
$C^4D$	capacitively coupled contactless conductivity detector
CE	capillary electrophoresis
CE-MS	capillary electrophoresis – mass spectrometry
CFIA	capillary flow injection analysis
CGE	capillary gel electrophoresis
CI	chemical ionization
CID	collision induced dissociation
cIEF	capillary isoelectric focusing
cITP	capillary isotachopheresis
CZE	capillary zone electrophoresis
d	capillary diameter in $\mu\text{m}$
DAD	diode array detector
DC	direct current
DMA	2'-deoxymugineic acid
DSB	dodecyldimethyl (2-hydroxy-3-sulfopropyl) ammonium, named dodecyl sulfobetaine
E	electric field
EDDHA	ethylenediaminedi( <i>o</i> -hydroxy- <i>p</i> -methylphenylacetic) acid
EDTA	ethylenediaminetetraacetic acid
EOF	electroosmotic flow
<i>epi</i> -HMA	<i>epi</i> -hydroxymugineic acid
EI	Electron Impact
ESI	Electrospray Ionization
f	frequency in Hz
$F_E$	Electric force
$F_F$	Frictional force
FAB	Fast Atom Bombardment
FD/FI	Field Desorption / Field Ionization
FMOC	9-fluorenylmethoxycarbonyl
FIA	flow injection analysis
FTICR	Fourier-transform ion-cyclotron resonance
FWTH	full width at half maximum
GC-MS	gas chromatography – mass spectrometry

Glu	glutamic acid
Gln	glutamine
HEPES	Hydroxy-(5Z,8Z,11Z,13E,17Z)-eicosapentaenoic acid
HMA	hydroxymugineic acid
HILIC	Hydrophilic interaction liquid chromatography
His	histidine
HPLC	high-performance liquid chromatography
i	current in A
ICP-MS	inductively coupled plasma mass spectrometry
IEC	ion-exchange chromatography
IPC	ion pair chromatography
IP-RPLC	Ion pair – reversed phase liquid chromatography
j	imaginary unit
KO	knock out
l	effective capillary length (to the detector)
L	total capillary length in cm
LC-MS	Liquid chromatography-mass spectrometry
LMW	low-molecular-weight
LOD	limit of detection
Lys	Lysine
m/z	mass to charge ratio
MA	mugineic acid
MALDI	Matrix Assisted Laser Desorption Ionization
MES	2-morpholinoethanesulfonic acid
MEKC	micellar electrokinetic capillary chromatography
MOPSO	3-(N-Morpholino)-2-hydroxypropanesulfonic Acid
MS	mass spectrometry
NA	nicotianamine
NAAT	Nicotianamine aminotransferase
NACE	nonaqueous capillary electrophoresis
NAS	Nicotianamine synthase
NPLC	normal phase liquid chromatography
OE	overexpressor
OPA	o-phthaldialdehyde
P	injection pressure in mbar
PAH	polycyclic aromatic hydrocarbon
PCRD	photochemical reaction detection
PM	plasma membrane
PITC	phenylisothiocyanate
PS	phytosiderophores
q	effective charge
Q	ion charge
QIT	quadrupole ion traps
r	ion radius
R <sub>f</sub>	feedback resistor value on the pick-up amplifier in $\Omega$

R	cell resistance in $\Omega$
RF	radio frequency
RIC	Reconstructed ion chromatogram
RPLC	reversed-phase liquid chromatography
S/N	signal-to-noise ratio
SEC	size-exclusion chromatography
SIM	selected ion monitor
SPE	Solid phase extraction
t	time
TBA	tetrabutyl ammonium
TIC	total ion chromatogram
TLC	thin-layer chromatography
TOF	time-of-flight
Tris	2-amino-2-hydroxymethyl-1,3-propanediol
TSI	Thermospray Ionization
TR	transporter
TXRF	total reflection x-ray fluorescence
V	applied voltage
v	ion velocity
$v_{EOF}$	velocity
$V_{out}$	output voltage in V
$V_{out}$	output voltage in V
$V_{in}$	input voltage in V
WT	wild type
ZIC	zwitterionic
ZIC-HILIC	zwitterionic hydrophilic interaction liquid chromatography
ZIC-MPC	zwitterionic 2-methacryloyloxyethyl phosphorylcholine hydrophilic interaction liquid chromatography
$\epsilon$	dielectric constant
$\zeta_{ion}$	zeta potential of the analyte ion
$\zeta_{wall}$	zeta potential at the capillary wall
$\eta$	viscosity of the fluid in cP
$\mu_a$	apparent mobility
$\mu_e$	electrophoretic mobility
$\mu_{EOF}$	EOF "mobility" (= mobility of neutral substances)
$\mu_{normalized}$	the mobility of the solute ion in the solvent mixture normalized to the mobility in solvent A
$\mu_{solventA}$	the mobility of the solvent A



## Appendix

Chemicals	Purity	Purchase
2-mopholinoethanesulfo nic acid monohydrate (MES)	≥ 99.5 %	Carl Roth (Karlsruhe, Germany)
2-amino-2-hydroxymethy l-1,3-propandiol (TRIS)	Buffer pure, ≥ 99.9 %	Carl Roth (Karlsruhe, Germany)
Acetic acid solution	100 %	Merck KGaA (Darmstadt, Germany)
Acetonitrile	LC–MS grade	Carl Roth (Karlsruhe, Germany)
Ammonium acetate	≥ 98 %	Merck KGaA (Darmstadt, Germany)
Ammonium hydroxid solution	25 % in water	Fluka Chemie AG (Buchs, Switzerland)
Arginine	≥ 98.5%	Carl Roth (Karlsruhe, Germany)
Aspartic acid	≥ 98.5 %	Carl Roth (Karlsruhe, Germany)
Boric acid	Buffer pure, ≥ 99 %	Carl Roth (Karlsruhe, Germany)
Citric acid	≥ 99.5 %, p.a., ACS, water free	Carl Roth (Karlsruhe, Germany)
Copper(II) acetate	GR for analysis	Merck KGaA (Darmstadt, Germany).
Ethylenediaminetetra acetic acid (EDTA)	GR for analysis	Merck (Darmstadt, Germany)
Ethylenediamine- <i>N,N'</i> -bi s( <i>o</i> -hydroxyphenyl) acetic acid (EDDHA)	86.3 %	Complete Green Co. (El Segundo, CA, USA)
Glutaminic acid	≥ 99 %	Carl Roth (Karlsruhe, Germany)
Gluconic acid solution 50% in water	for synthesis	Merck KGaA (Darmstadt, Germany)
HEPES	Buffer pure, ≥ 98 %	Carl Roth (Karlsruhe, Germany)
Histidine	≥ 98.5 %	Carl Roth (Karlsruhe, Germany)
Hydrochloric acid solution	37 %	Carl Roth (Karlsruhe, Germany)

---

Iron(II) chloride tetrahydrate	GR for analysis	Merck KGaA (Darmstadt, Germany).
Lysine	≥ 97 %	Carl Roth (Karlsruhe, Germany)
MOPSO	Buffer pure, ≥ 98 %	Carl Roth (Karlsruhe, Germany)
Nickel(II)-chloride hexahydrate	GR for analysis	Merck KGaA (Darmstadt, Germany).
Serine	≥ 98.5 %	Carl Roth (Karlsruhe, Germany)
Sodium acetate	GR for analysis	Merck KGaA (Darmstadt, Germany)
Sodium dihydrogen phosphate monohydrate	GR for analysis	Merck KGaA (Darmstadt, Germany).
Stock solution of iron(III)	10 mg/mL diluted in HCl	Merck KGaA (Darmstadt, Germany).
Stock solution NaOH	1M	Carl Roth (Karlsruhe, Germany)
Taurine	puriss. p.a.	Fluka Chemie AG (Buchs, Switzerland)
Tetrabutyl ammonium acetate	~ 95 %	Merck (Darmstadt, Germany).
Tributylamine solution	For synthesis	Merck Schuchardt OHG (Hohenbrunn, Germany)
Ultrapure water	For analysis	Synergy 185 water purification system (Millipore, Schwalbach, Germany)
Zinc acetate dihydrate	GR for analysis	Merck KGaA (Darmstadt, Germany).

### **Lebenslauf**

Name	Yue Xuan
Geburtstag	29.08.1978
Geburtsort	ShenYang, V.R.China
Familienstand	Ledig
Staatsangehörigkeit	Chinesisch

---

### **Ausbildung**

Sep 1985 - Jun 1997	Grundschule und Gymnasium mit Abitur in China
Sep 1997 - Jun 2001	Studium der Chemie an der LiaoNing Normal University, DaLian, China. Abschluß: Bachelor of Science in Chemistry
Okt 2001 - Apr 2004	Studium der Chemie an der Free Berlin University, Berlin, Germany Abschluß: Master of Science in Chemistry
Mai 2004 - Apr 2007	PhD Dissertation am Institute for analytical sciences (ISAS) in Dortmund

---

### **Publikationen**

**Yue Xuan, G. Weber, A. Manz,** Construction and analytical application of an on-column photo reactor for improved detection of iron-species as plant metabolites in capillary flow injection and capillary electrophoresis, *Journal of Chromatography A*, 1130 (2006) 212 – 218.

**Yue Xuan, E.B. Scheuermann, A.R. Meda, H. Hayen, N. Von Wirén, G. Weber,** Separation and Identification of Phytosiderophores and their metal complexes in plants by zwitterionic hydrophilic interaction liquid chromatography coupled to electrospray-ionization mass spectrometry, *Journal of Chromatography A*, 1136 (2006) 73 – 81.

**Yue Xuan, E.B. Scheuermann, A.R. Meda, P. Jacob, N. Von Wirén, G. Weber,** CE of phytosiderophores and related metal species in plants, *Electrophoresis*, 28 (2007) 3507 – 3519.

---

### **Poster**

**Yue Xuan, G. Weber, N. von Wirén, A. Manz,** Separation and Identification of Phytosiderophores and their metal complexes by zwitterionic hydrophilic interaction liquid chromatography (ZIC-HILIC) with ESI-MS, and direct Nanospray FTICR-MS, 17<sup>th</sup> International Mass Spectrometry Conference, Prague, Czech Republic 27.08.2006 – 01.09.2006.

---

### **Presentation**

**Yue Xuan, G. Weber, A. Manz.,** Construction and analytical application of an on-column photo reactor for improved detection of iron-species as plant metabolites in capillary flow injection and capillary electrophoresis, 20<sup>th</sup> International Symposium on Microscale Bioseparations, Amsterdam, the Netherlands 22.01.2006 – 26.01.2006.

---

### Acknowledgements

I would like to express my gratitude to all those who gave me the possibility to complete this thesis.

Firstly, I would like to express my most sincere acknowledgements to my supervisors, Prof. Dr. Andreas Manz and PD. Dr. Jörg Ingo Baumbach. Prof. Manz offered me the opportunity to work on this interesting project at Institute for Analytical Sciences (ISAS) and supervised my PhD work for the first two and half years. PD. Dr. Jörg Ingo Baumbach supervised me for the final half year of my PhD and instructively corrected this dissertation. Prof. Micheal Spiteller is sincerely appreciated by me for being my PhD exam consultant and gave me useful suggestions of my dissertation. Thanks to my PhD mentor, Dr. Günther Weber. In this three-year-PhD studying process, I have been learning a lot from Günther. He did the first time correction of this dissertation.

Special thanks to Dr. Peter Jacob, who generously offered me the photo reactor and gave me many precious literatures. Peter also corrected my CE and Photo Reactor chapters. He is not only a colleague, but also a kindly and helpful friend for me. Thanks to Dr. Jürgen Nolte for all the precious suggestions for my HPLC-MS chapter. To Dr. Heiko Hayen, I wish to appreciate him for fruitful discussion of mass spectrometer and making my CE experiments at University Münster possible. Thanks to Prof. Dr. Uwe Karst and Tobias Revermann, they generously offered me their CE instrument so that I can work on my last part of CE measurements at University Münster. Mrs. Gudrun Kauenberg is sincerely appreciated for showing me some important laboratory techniques and being a wonderful colleague for me. Thanks to Mr. von Bohlen for the TXRF measurements. Thanks to our cooperation group, Prof. Nicolaus von Wiren's group at Hohenheim University, they prepared the plant samples. And thanks to DFG for the financial support.

Finally, I would like to thank my family. They are my spiritual support. Without their understanding, I would never have this opportunity to study abroad and have so many wonderful experiences in Germany. I thank my very special friend, ChiaYu, who understands and supports me all the time. Whatever I achieve today is closely connected by all the love they give me.